

**Development of Practical Fluorination Methods and
Selective C–H Borylation of Methane**

by

Sydonie Dannielle Schimler

A dissertation submitted in partial fulfillment
of the requirements for the degree of
Doctor of Philosophy
(Chemistry)
in the University of Michigan
2017

Doctoral Committee:

Professor Melanie S. Sanford, Chair
Assistant Professor Matthew B. Soellner
Professor Nathaniel Szymczak
Professor John P. Wolfe

Sydonie D. Schimler

schimles@umich.edu

ORCID iD: 0000-0002-7170-1643

© Sydonie D. Schimler
2017

To Watson

ACKNOWLEDGEMENTS

I have been fortunate to have had the opportunity to work with so many great and supportive people during my graduate school career at the University of Michigan. Thank you first and foremost to my advisor Prof. Melanie Sanford. Thank you for giving me the opportunity to work on so many diverse projects throughout my graduate school career. Thank you for being supportive and for all your encouragement throughout the years. I have learned so much from you that I hope to carry through the rest of my career and life. Despite my apparent lack of enthusiasm and excitement at times, it truly has been a great experience, and it would not have been the same without you as an advisor.

I would like to thank my dissertation committee Prof. John Wolfe, Prof. Nathaniel Szymczak, and Prof. Matthew Soellner. Thank you for all your suggestions and feedback from my candidacy, data meeting, and defense. Prof. Wolfe, thank you for the opportunity to rotate in your lab during my first year in graduate school. Prof. Szymczak, thank you for the opportunity to teach Chem 482; I've learned so much about how to manage and design an undergraduate lab from this experience. I would also like to thank Prof. Nagorny for being my first rotation advisor the summer before I started graduate school.

Additionally, I would like to thank all the support staff for making sure the chemistry department runs smoothly. I would like to acknowledge everyone in the administrative and business offices especially Liz Oxford. I would especially like to acknowledge, Eugenio Alvarado and Chris Kojiro for NMR support and Jim Windak and Paul Lennon for mass spectroscopy support. I would also like to thank Andrew Higgs and Kate Dyki for making sure our lab has run smoothly for the past few years.

The Dow project has been an essential part of my graduate career. I am grateful for all of the opportunities it has given me and all of the people I got to work with on it. Yingda was my mentor when I officially joined the lab. He taught me so much about fluorination chemistry that I still value to this day. Laura and Sarah were so kind and excellent at being overly enthusiastic during our Dow meetings that I don't think I would

have gotten through them without you. Megan, thank you for working with me on the fluorosulfonate project, making sure I didn't die while using sulfuryl fluoride, and for being under enthusiastic with me. Thank you for being a great coworker and a good friend (I guess).

Our collaborators at Dow have been very important for my development as a chemist. From monthly meetings that forced me to talk about my work even though I was uncomfortable to making me think critically about the importance of my chemistry, the insight from Patrick Hanley, Matt Jansma, Yang Cheng, Jim Ringer, Robert Froese, and John Anderson has shaped how I think about chemistry. I would especially like to thank Doug Bland. Thank you so much for your patience, encouragement, and suggestions throughout the last four years. Your management of the Dow collaboration has been fantastic and you've always gone above and beyond to make this collaboration a productive experience.

To the other members of fluorination subgroup (Naoko, Joe, Katarina, Matt, Christian, Cristina, Michael, Devin, James), thank you for all your questions and insight during our weekly meetings. Special thanks to James for never being afraid to ask the questions that no one else would and for numerous suggestions and questions that made me think more critically about my experiments.

The methane project allowed me to diversify my skills beyond fluorination chemistry and has proven invaluable for my time spent in graduate school and for the future. Amanda, thank you for all your help and encouragement on this project. I joined the project knowing little about C-H functionalization, high pressure reactions, and organometallic synthesis, and despite how busy you were your last few months here, you were willing to provide me with so much help. Thanks to Danielle for your help with Raman spectroscopy; we will always share our mutual hatred to ethane. To Prof. Matzger, thank you for the late nights/early weekend mornings that you spent determining the concentrations of ethane and methane. Mark, thank you for continuously discussing methane chemistry with me and for your enthusiasm for the project.

Thank you to my numerous deskmates Yingda, Joe, Łukasz, Anna, and Koen. Thank you for productive (and sometimes not so productive) conversations about chemistry and everything else. My baymates throughout the years have helped keep me

sane. Special thanks to Rachel, Naoko, and Joe, for your help and support through my candidacy exam and for helping calm me down during that stressful time. To my fellow fifth years, Ian, Nicole, Nomaan, and Pablo, you have been an excellent and talented group to tackle candidacy, data meetings, ORP, and everything else with. I would like to acknowledge Devin, Megan, Katarina, James, Courtney, and Mark for reading through chapters of this thesis.

To all the past and current members of the Sanford lab, thank you for all your questions, support, and insight over the years. You have all been an excellent group to work with, learn from, and develop as a chemist. Thank you for the help and encouragement throughout the years; I could not have asked for a better group to be a part of.

It would be remiss if I did not acknowledge those outside of the University of Michigan chemistry department who have influenced and supported me throughout my graduate school years. I would like to thank my undergraduate advisor Prof. Stefan Debbert for instilling a love of organic chemistry in me. I would like to thank my family and friends for support and encouragement. I would like to especially thank my cat Watson for constant love and support even through the roughest times.

TABLE OF CONTENTS

DEDICATION	ii
ACKNOWLEDGEMENTS	iii
LIST OF SCHEMES	x
LIST OF FIGURES	xii
LIST OF TABLES	xv
LIST OF IMAGES	xvi
ABSTRACT	xvii
CHAPTER 1. Introduction	1
1.1. Significance of Aryl Fluorides	1
1.2. Traditional Methods for the Synthesis of Aryl Fluorides	2
1.3. Transition Metal-Mediated and -Catalyzed Aromatic Fluorination	4
1.3.1. Copper-Mediated and -Catalyzed Fluorination	5
1.3.2. Palladium-Catalyzed Fluorination of Aryl Triflates	6
1.4. Deoxyfluorination of Phenols	7
1.5. References	8
CHAPTER 2. Room Temperature S_NAr Fluorination of Aryl Chlorides and Nitroarenes with Tetramethylammonium Fluoride	12
2.1. Background	12
2.2. Initial Results and Optimization	14
2.3. Effect of Leaving Group on S _N Ar Fluorination	19
2.4. Substrate Scope	24
2.5. Conclusion	27
2.6. Outlook	27
2.7. Experimental Details and Characterization	29
2.7.1. General Information	29

2.7.2. Materials and Methods	30
2.7.3. General Procedures for Fluorination Reactions	31
2.7.4. Product Synthesis and Characterization	34
2.8. References	44

CHAPTER 3. Nucleophilic Deoxyfluorination of Phenols via Sulfonate

Intermediates	47
3.1. Background	47
3.2. Initial Results and Comparison of Electrophiles	50
3.3. Substrate Scope	55
3.4. Mechanistic Investigations	60
3.5. Investigation of Other Sulfonate Electrophiles	68
3.6. Conclusions	73
3.7. Outlook	74
3.8. Experimental Details and Characterization	74
3.8.1. General Information	74
3.8.2. Materials and Methods	75
3.8.3. Synthesis of Aryl Fluorosulfonates	78
3.8.4. Synthesis of Phenols	88
3.8.5. Synthesis of Aryl Triflates	93
3.8.6. Synthesis of Aryl Nonafates	96
3.8.7. Synthesis of Diaryl Sulfates	98
3.8.8. General Procedures	101
3.8.9. Computational Details	123
3.9. References	125

CHAPTER 4. Copper-Mediated and -Catalyzed Fluorination with Nucleophilic Fluoride

Fluoride	130
4.1. Background	130
4.2. Initial Results and Optimization	134
4.3. Substrate Scope	143
4.4. Proposed Mechanism and Attempts at Copper-Catalyzed Fluorination of Aryl Trifluoroborates	146

4.5. Copper-Catalyzed Fluorination of Aryl Halides via a Directed Approach.....	149
4.6. Conclusion	155
4.7. Outlook.....	156
4.8. Experimental Details and Characterization	160
4.8.1. General Information.....	160
4.8.2. Materials and Methods	160
4.8.3. General Procedures for Copper-Mediated and -Catalyzed Fluorination .	162
4.8.4. Product Synthesis and Characterization.....	167
4.9. References.....	180
 CHAPTER 5. Copper-Mediated Functionalization of Aryl Trifluoroborates	183
5.1. Background	183
5.2. Reaction Optimization	185
5.3. Nucleophile and Substrate Scope	187
5.4. Mechanistic Considerations	193
5.5. Conclusion and Outlook	196
5.6. Experimental Details and Characterization	197
5.6.1. General Information.....	197
5.6.2. Materials and Methods	198
5.6.3. General Procedures for Copper-Mediated Functionalization of Aryl Trifluoroborates	199
5.7. References.....	221
 CHAPTER 6. Metal-Catalyzed Selective Borylation of Methane and Ethane.....	224
6.1. Background	224
6.2. Initial Studies and Optimization with Cp [*] Rh(η ⁴ -C ₆ Me ₆)	229
6.3. Evaluation of Catalysts.....	232
6.4. Evaluation of Diboron Reagents.....	239
6.5. Conclusion	244
6.6. Outlook.....	244
6.7. Experimental Details	245
6.7.1. General Information.....	245

6.7.2. Materials and Methods	246
6.7.3. Catalyst Synthesis	248
6.7.4. Reactor Descriptions	249
6.7.5. General Procedures for C–H Borylation Reactions	252
6.7.6. Determining Concentration of Methane and Ethane	259
6.8. References	263

LIST OF SCHEMES

Scheme 1.1: Balz-Schiemann Reaction	2
Scheme 1.2. S _N Ar Fluorination of Aryl Chlorides	3
Scheme 1.3. S _N Ar Fluorination Using <i>in situ</i> Generated Anhydrous TBAF*	4
Scheme 1.4. Acyl Azolium Fluorides for S _N Ar Fluorination	4
Scheme 1.5. Copper-Catalyzed Fluorination of Macrocyclic System Through a Defined Cu ^{III} Intermediate	5
Scheme 1.6. Copper-Mediated Electrophilic Fluorination	6
Scheme 1.7. Copper-Mediated Nucleophilic Fluorination of Aryl Iodides	6
Scheme 1.8. Pd-Catalyzed Fluorination of Aryl Triflates.....	7
Scheme 1.9. A. Deoxyfluorination of Phenols. B. Proposed Mechanism.....	8
Scheme 2.1. Traditional S _N Ar Fluorination	12
Scheme 2.2. Anhydrous Fluoride Sources for Room Temperature S _N Ar Fluorination ..	13
Scheme 2.3. <i>in Situ</i> Generation of NMe ₄ F (anh) from Phenoxides and Sulfuryl Fluoride	29
Scheme 3.1. Classical S _N Ar Fluorination Reaction.....	48
Scheme 3.2. Deoxyfluorination with PhenoFluor	48
Scheme 3.3. Pd-Catalyzed Fluorination of Aryl Triflates.....	49
Scheme 3.4. S _N Ar Fluorination of Aryl Fluorosulfonates.....	49
Scheme 3.5. Possible Mechanism for the Formation of 14-F	65
Scheme 3.6. Effect of Exogenous SO ₂ F ₂ on the Fluorination Reaction of 3-sulfate	68
Scheme 4.1. Examples of Copper-Mediated Electrophilic Aromatic Fluorination	131
Scheme 4.2. Copper-Catalyzed Fluorination of Macrocyclic System through a Defined Cu ^{III} Intermediate	132
Scheme 4.3. Copper-Mediated Nucleophilic Fluorination of Aryl Iodides	132
Scheme 4.4. Directed Copper-Catalyzed Fluorination with AgF	133

Scheme 4.5. Proposed Cu-Mediated Fluorination with Nucleophilic Fluoride.....	134
Scheme 4.6. Cu-Mediated Fluorination of Alkyl Trifluoroborates with KF	146
Scheme 4.7. Proposed Mechanism for the Cu(OTf) ₂ -Mediated Fluorination	147
Scheme 4.8. Mechanism Proposed for the Cu-Catalyzed Directed Fluorination	149
Scheme 4.9. Mass Balance of Cu-Catalyzed Fluorination with NMe ₄ F	153
Scheme 4.10. Substrates for Cu-Catalyzed Fluorination	155
Scheme 5.1. Cu-Mediated Ullmann Coupling	183
Scheme 5.2. Chan-Lam-Evans Cu-Catalyzed Coupling Reaction	184
Scheme 5.3. Potential Mechanism for the Cu(OTf) ₂ -Mediated Functionalization	196
Scheme 6.1. Shilov Electrophilic Activation of Methane with Pt ^{II} Catalyst	225
Scheme 6.2. Pt-Catalyzed Conversion of Methane to Protected Methyl Ester	226
Scheme 6.3. Ag-Catalyzed C–C Bond Formation Between Methane and Carbene ...	226
Scheme 6.4. Transition Metal Catalyzed C–H Borylation of Alkanes.....	227
Scheme 6.5. Benzylic C–H Borylation of Toluene	228
Scheme 6.6. C–H Borylation of Methane Developed by Mindiola and Coworkers	245

LIST OF FIGURES

Figure 1.1. Representative Examples of Agrochemicals and Pharmaceuticals Containing an Aryl Fluoride	2
Figure 2.1. Time Studies for the Fluorination of 1 at Different Concentrations	19
Figure 2.2. Reaction Profiles for the Reactions of 3a-e with NMe ₄ F (anh) to Form 4 ...	21
Figure 2.3. Reaction Profiles for the Reactions of 5a-e with NMe ₄ F (anh) to Form 6 ..	23
Figure 2.4. Scope of Chloropicolates for S _N Ar Fluorination with NMe ₄ F (anh).....	25
Figure 2.5. Chloroquinoline, Chloroisoquinoline, and Chloropyridazine Substrates	25
Figure 2.6. Scope of Substituted 2-Chloropyridines for S _N Ar Fluorination with NMe ₄ F	26
Figure 2.7. Scope of Simple Arenes for S _N Ar Fluorination with NMe ₄ F (anh).....	27
Figure 3.1. Reaction Profiles for the Conversion of 1-X to 1-F at 80 °C.....	52
Figure 3.2. Substrate Scope for the Fluorination of Aryl Fluorosulfonates with NMe ₄ F	56
Figure 3.3. Direct Conversion of Phenols for Aryl Fluorides	58
Figure 3.4. Energy Diagrams for the Reaction of 1-Cl and 1-OFs with Fluoride	60
Figure 3.5. Hammett Plot for the Fluorination of Aryl Fluorosulfonates	61
Figure 3.6. ¹⁹ F NMR Spectra of Reaction of 14-OFs at 25 °C	62
Figure 3.7. Reaction Profile of the Fluorination of 14-OFs with NMe ₄ F	63
Figure 3.8. Reaction Profile of the Fluorination of 14-sulfate with NMe ₄ F	64
Figure 3.9. Fluorination of 14-sulfate after 10 Minutes at 80 °C.....	65
Figure 3.10. Initial Rates for Fluorination of Diaryl Sulfate Substrates at 80 °C.....	67
Figure 3.11. Reaction Profiles of Sulfonate Electrophiles of 1 with NMe ₄ F to Form 1-F	70
Figure 3.12. Initial Rates of Fluorination of Aryl Fluorosulfonates versus Aryl Triflates for Electronically Different Substrates	71
Figure 3.13. Substrate Scope for the Fluorination of Aryl Triflates Compared to Aryl Fluorosulfonates.....	72
Figure 3.14. Hammett Plot for Fluorination of Aryl Triflates	73

Figure 4.1. Reaction Profiles for the Fluorination of 1 with Alkali Metal Fluorides	136
Figure 4.2. Reaction Profiles for the Fluorination of 1 at Various Temperatures	137
Figure 4.3. Ligands for the Cu(OTf) ₂ -Mediated Fluorination of 1	140
Figure 4.4. Alkyne Ligands for the Cu(OTf) ₂ -Mediated Fluorination of 1	142
Figure 4.5. Substrate Scope of Cu(OTf) ₂ -Mediated Fluorination of Aryl Trifluoroborates with Potassium Fluoride	145
Figure 4.6. Cu-Mediated Fluorination of Aryl Stannanes	156
Figure 4.7. Cu-Mediated Radiofluorination of Aryl Boronate Esters	157
Figure 4.8. Cu-Mediated Fluorination of Aryl Boronate Esters	158
Figure 4.9. Cu-Mediated Radiofluorination of Aryl Boronic Acids	159
Figure 4.10. Cu-Mediated Radiofluorination of Aryl Stannanes	159
Figure 5.1. Scope of Cu(OTf) ₂ -Mediated Coupling with Carboxylate Nucleophiles	188
Figure 5.2. Scope of Cu(OTf) ₂ -Mediated Coupling with Sodium Pivalate	189
Figure 5.3. Scope of Oxygen Nucleophiles for Cu(OTf) ₂ -Mediated Coupling with 1 ...	190
Figure 5.4. Cu(OTf) ₂ -Mediated Halogenation	191
Figure 5.5. Nitrogen Nucleophiles for the Cu(OTf) ₂ -Mediated Functionalization	192
Figure 5.6. Cu(OTf) ₂ -Mediated Azidation of (Hetero)Aryl Trifluoroborates	193
Figure 5.7. Cu(OTf) ₂ -Mediated Cyanation of 1	193
Figure 5.8. Equivalents of KN ₃ and NaOPiv versus Yield of 29 and 6	195
Figure 6.1. Challenges Associated with the C–H Functionalization of Methane	225
Figure 6.2. Reactivity and Selectivity Challenges of Methane C–H Borylation	228
Figure 6.3. ¹ H NMR Spectra of ¹³ CH ₄ Labelling Experiment	234
Figure 6.4. Initial Rates for the C–H Borylation of Cyclohexane with Catalysts 1 and 2	237
Figure 6.5. Initial Rates for the C–H Borylation of CH ₃ Bpin with Catalysts 1 and 2 ...	238
Figure 6.6. Reaction Profiles with Ru Catalyst 3 with B ₂ pin ₂ and B ₂ pnd ₂	243
Figure 6.7. GCMS of ¹³ CH ₄ Labelling Experiment with Catalyst 2	253
Figure 6.8. Mole Ratio versus Pressure at 298 K for Methane in Cyclohexane	260
Figure 6.9. Mole Ratio versus Pressure at 298 K for Ethane in Cyclohexane	262

LIST OF TABLES

Table 2.1. S _N Ar Fluorination of 1 with NMe ₄ F (anh).....	14
Table 2.2. Effect of Water and Sources of NMe ₄ F on the S _N Ar Fluorination of 1	15
Table 2.3. NMe ₄ F (anh) as a Phase Transfer Reagent for S _N Ar Fluorination of 1	17
Table 2.4. Solvents for the S _N Ar Fluorination of 1	18
Table 2.5. Comparison of Reactions of 3a-e with NMe ₄ F (anh) and CsF	20
Table 2.6. Comparison of Reactions of 5a-e with NMe ₄ F (anh) and CsF)	22
Table 3.1. Fluorination of Different Aryl Electrophiles with NMe ₄ F.....	51
Table 3.2. Solvents for the Deoxyfluorination of 1-OFs	53
Table 3.3. Fluoride Sources for the Fluorination of 1-OFs	54
Table 3.4. Fluorination of Unactivated Aryl Electrophiles with NMe ₄ F	55
Table 3.5. Fluorination of Different Aryl Electrophiles with NMe ₄ F.....	59
Table 3.6. Fluorination of Aryl Fluorosulfonates Compared to Diaryl Sulfates.....	66
Table 3.7. Fluorination of Different Sulfonate Electrophiles with NMe ₄ F.....	69
Table 4.1. Copper Salts for the Nucleophilic Fluorination of 1	135
Table 4.2. Effect of Copper Counterion on the Fluorination of 1	138
Table 4.3. Solvents for the Cu(OTf) ₂ -Mediated Fluorination of 1	139
Table 4.4. Effect of Ambient Conditions on the Cu(OTf) ₂ -Mediated Fluorination of 1 .	143
Table 4.5. Oxidants for the Cu(OTf) ₂ -Mediated Fluorination of 1	148
Table 4.6. Cu-Catalyzed Fluorination of 38	150
Table 4.7. Solvents for the Cu-Catalyzed Fluorination of 38 with AgF.....	151
Table 4.8. Copper and Additive Screen for the Cu-Catalyzed Fluorination with NMe ₄ F	152
Table 4.9. Aryl Halides for Cu-Catalyzed Fluorination	154

Table 5.1. Copper-Mediated Trifluoroacetoxylation of 1 to Form 2	186
Table 5.2. Scope of Aryl Boron Reagents for Cu-Mediated Trifluoroacetoxylation	187
Table 5.3. Cu ^{II} Salts for Azidation and Pivalation of 1	194
Table 6.1. Solvent for Methane C–H Borylation Catalyzed by 1	230
Table 6.2. Optimization of Methane C–H Borylation with 1	232
Table 6.3. Impact of Catalyst Choice on the Yield and Selectivity of Methane Borylation	233
Table 6.4. C–H Borylation of Alkanes with Catalysts 1–3	235
Table 6.5. Methane and Ethane One-Pot Competition	236
Table 6.6. Ru Complexes for Methane C–H Borylation	239
Table 6.7. Methane C–H Borylation with HBpin	241
Table 6.8. Diboron Reagents for Methane C–H Borylation	242
Table 6.9. Borylation of Alkanes with Catalysts 1–3 and B ₂ pnd ₂	244
Table 6.10. Amounts of Methane and Ethane Added and Results of the Competition Reactions	256
Table 6.11. Results from Determining the Methane:Ethane Concentration Ratio under the Conditions Reported in Table 6.10	263

LIST OF IMAGES

Image 6.1. Reactor A	250
Image 6.2. Reactor B	250
Image 6.3. Reactor C	251
Image 6.4. Reactor D	251
Image 6.5. Set Up for Reaction Monitoring	258

Abstract

Fluorinated (hetero)arenes are finding increasing importance in pharmaceuticals and agrochemicals. As a result, the development of mild, inexpensive, and practical methods for the formation of aryl fluorides has been highly sought. Over the past few decades, transition metal-catalyzed methods as well as mild S_NAr fluorination methods have emerged as approaches for the generation of aryl–F bonds. Despite considerable progress in this field, current methods generally suffer from the use of expensive reagents (catalysts, fluoride sources), harsh reaction conditions, poor generality to electronically diverse substrates, and inapplicability of industrial scale processes. Chapters 2–4 of this thesis describe several approaches to overcome some of the remaining challenges in this field.

Chapter 1 describes the importance of fluorinated arenes, the remaining challenges for the formation of these bonds, and the relevant precedent for the work detailed herein.

Chapter 2 focuses on the development of a mild S_NAr fluorination method for the conversion of (hetero)aryl chlorides and nitroarenes to the (hetero)aryl fluoride using anhydrous tetramethylammonium fluoride (NMe_4F). The reagent effectively converts aryl–X ($X = Cl, Br, I, NO_2, OTf$) to aryl–F with the relative rates of reactions varying with X. These mild conditions can be used for the fluorination of electron-deficient (hetero)aromatics.

Chapter 3 details a mild deoxyfluorination method for the conversion of phenols to aryl fluorides through an aryl fluorosulfonate ($ArOFs$) intermediate. The reaction of $ArOFs$ with NMe_4F proceeds under mild conditions for many electronically diverse and functional group rich substrates. The method is then extended to a one-pot transformation of phenols to aryl fluorides with the combination of sulfuryl fluoride (SO_2F_2) and NMe_4F . Experimental and computational studies provide insight into the mechanism of the

reaction that ultimately lead to the extension of this deoxyfluorination reaction to the fluorination of aryl triflates (ArOTf).

Chapter 4 is focused on the development and optimization of a mild copper(II)-mediated fluorination reaction of aryl trifluoroborates using potassium fluoride (KF). The reaction shows a broad substrate scope including application to heteroarenes. Attempts to render the reaction catalytic in copper(II) proved challenging. A system involving directing group assistance to achieve copper-catalyzed fluorination of aryl halides was investigated but reactivity remained low.

Chapter 5 details the extension of the copper(II)-mediated fluorination reaction to the use of other nucleophiles to produce a wide array of functionalized products under ambient conditions. Weakly nucleophilic coupling partners react with aryl trifluoroborates in the presence of $\text{Cu}(\text{OTf})_2$ to form C–O, C–N, and C–halide bonds. Preliminary studies point toward the importance of copper salts bearing noncoordinating counterions for this mild reactivity.

Another outstanding challenge for synthetic chemists is the functionalization of the C–H bonds of methane. While recent progress has been made in the selective functionalization of liquid alkane C–H bonds, few of these methods have been extended to the functionalization of methane. Chapter 6 describes the development and optimization of a transition metal-catalyzed method for the C–H borylation of methane. Formation of mono-borylated methane over di-borylated methane can be tuned as a function of catalyst with a ruthenium dimer providing the highest selectivity. Furthermore, several transition metal catalysts are shown to be more selective for methane over ethane. Examination of boron reagents reveals that bis(pinacolborane) (B_2pin_2) and a diboron reagent derived from pinene were most reactive and selective in this C–H borylation reaction.

Chapter 1

Introduction

1.1. Significance of Aryl Fluorides

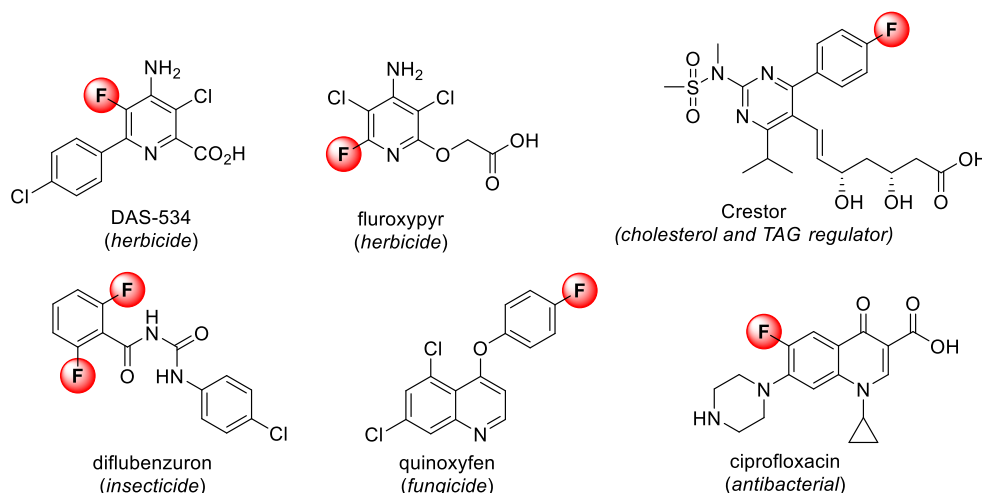
Fluorinated aromatic molecules have found increasing importance and application in agrochemicals, pharmaceuticals, and materials.¹ The addition of a fluorine atom to biologically relevant molecules can impart improved lipophilicity, efficacy, and metabolic stability.^{2,3,4} Fluorinated compounds are generally more chemically inert, thermally stable, and soluble than their nonfluorinated counterparts. As the most electronegative element, fluorine's inclusion in a molecule has profound effects on the acidity or basicity of nearby functional groups because of the σ -inductive effect of fluorine.³

Because of the dramatic effect of fluorine, currently as many as 30–40% of agrochemicals and about 20–30% of pharmaceuticals contain C–F bonds including many of the top selling pharmaceuticals (Figure 1.1).^{4,5,6} Additionally, radiofluorinated aromatic compounds are gaining wide application in the field of positron emission tomography (PET).⁷

The development of methods for the incorporation of C–F bonds into aromatic systems is a major challenge for synthetic chemists as carbon-fluorine bond formation is a difficult transformation. This is in large part due to the high electronegativity of fluorine and the high hydration energy of the fluoride anion.⁸ Harsh conditions are often required to incorporate a C–F bond which limits the functional group tolerance. Therefore, C–F bonds are often incorporated in early stages of the synthesis of complex molecules. However, there is a desire to develop methods for late stage fluorination as such transformations would enable applications to PET imaging and diversification for medicinal chemistry applications.⁷ Additionally, current methods for the incorporation of a carbon–fluorine bond are not readily amenable to kilogram scale process due to the use

of elevated temperatures, reactive (explosive) intermediates, and low yielding processes. As such, it is of high importance to develop new methodologies that can affect the desired incorporation of a carbon-fluorine bond.⁹

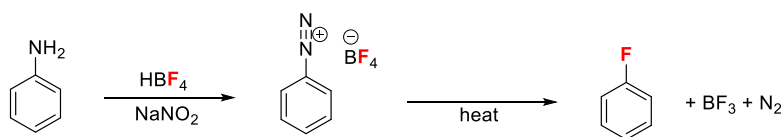
Figure 1.1. Representative Examples of Agrochemicals and Pharmaceuticals Containing an Aryl Fluoride



1.2. Traditional Methods for the Synthesis of Aryl Fluorides

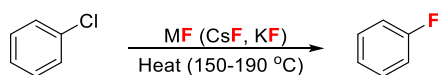
Two fluorination methods are most prevalent for application to industrial scale processes: the Balz-Schiemann reaction and halogen exchange (Halex) processes.¹⁰ The Balz-Schiemann reaction involves the formation of aryl fluorides from anilines through an aromatic diazonium tetrafluoroborate intermediate (Scheme 1.1).¹¹ Thermal or photochemical decomposition of an aryl diazonium tetrafluoroborate results in the desired aryl fluoride, where BF_4^- acts as the nucleophilic fluoride source.¹² An advantage of this method is that it can be used for the fluorination of electronically diverse aryl diazonium tetrafluoroborates.¹³ However, the forcing reaction conditions (typically $>100^\circ\text{C}$) and formation of a potentially explosive intermediate are not ideal.

Scheme 1.1. Balz-Schiemann Reaction



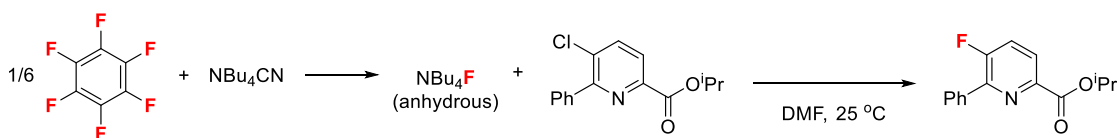
The halogen exchange process (S_NAr fluorination) is a widely-used method for the synthesis of aryl fluorides from aryl chlorides (Scheme 1.2).¹⁴ This method involves the reaction of an electron-deficient (hetero)aryl chloride with a nucleophilic fluoride source, such as spray-dried potassium fluoride (KF), to furnish the desired (hetero)aryl fluoride. However, due to the poor solubility of alkali metal fluoride salts in organic solvents, forcing conditions ($>100\text{ }^{\circ}\text{C}$) and additives such as phase transfer reagents¹⁵ are required to increase the efficiency of S_NAr fluorination processes. Furthermore, the scope of S_NAr fluorination is limited, as electron-withdrawing groups are necessary to activate (hetero)aryl chlorides for the reaction due to stabilization of a charged Meisenheimer intermediate. Competing regioisomer formation is another limitation of this reaction.¹⁶ Fluorodenitration reactions are an alternative to S_NAr fluorination reactions of aryl chlorides but still suffer from the same limitations,¹⁷ as well as byproduct formation due to competing S_NAr reactions associated with the displaced NO_2^- anion.^{17,18}

Scheme 1.2. S_NAr Fluorination of Aryl Chlorides



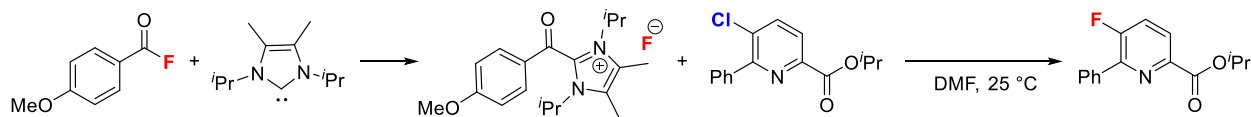
Recent work on S_NAr fluorination reactions has focused on the identification of milder conditions to induce the desired fluorination reaction. Milder conditions can minimize side product formation and potentially increase the functional group tolerance of the reaction. To achieve mild reaction conditions, the identification of a more organic soluble fluoride sources is important. In 2006, DiMagno reported the use of *in situ* generated anhydrous tetrabutylammonium fluoride (TBAF^*)¹⁹ for the room temperature S_NAr fluorination of (hetero)aryl chlorides.²⁰ In 2014, the Sanford group reported an extension of this work to the fluorination of biologically relevant heteroaryl chlorides (Scheme 1.3).²¹ The mild reaction conditions (room temperature) mitigate the production of undesired side products. This method, while a notable example of mild S_NAr fluorination, suffers from the use of toxic and expensive reagents and the instability of the fluoride source to heat.²²

Scheme 1.3. S_NAr Fluorination Using *in situ* Generated Anhydrous TBAF*



To overcome the limitations of TBAF*, Sanford and coworkers have reported the *in situ* generation of anhydrous fluoride from the combination of acid fluorides and *N*-heterocyclic carbenes (NHCs) (Scheme 1.4).²³ While the fluorination reaction occurred at room temperature, the reaction was plagued by expensive reagents (NHC) and side products that were challenging to separate from the desired product. Other soluble fluoride sources have been reported but often suffer from limited applicability to S_NAr fluorination due to the highly basic nature of the naked fluoride anion.^{24,25,26,27,28} Therefore, there is still a need for the identification of a soluble, anhydrous fluoride source to promote the desired S_NAr fluorination under mild conditions.

Scheme 1.4. Acyl Azolium Fluorides for S_NAr Fluorination



Chapter 2 of this thesis is focused on the use of anhydrous tetramethylammonium fluoride (NMe₄F) for the room temperature S_NAr fluorination of (hetero)aryl chlorides and nitroarenes.²⁹

1.3. Transition Metal-Mediated and -Catalyzed Aromatic Fluorination

Many of the challenges associated with S_NAr fluorination could potentially be overcome using a transition metal to either mediate or catalyze the fluorination reaction.³⁰ Over the past several years, several transition metal-catalyzed or -mediated methods have been developed for C–F bond formation. These methods are predominated by the use of palladium^{31,32,33,34} or silver^{35,36,37} catalysts to induce the desired bond formation using electrophilic fluorine. While these methods overcome some of the challenges of traditional methods of fluorination, they suffer from the use of expensive electrophilic

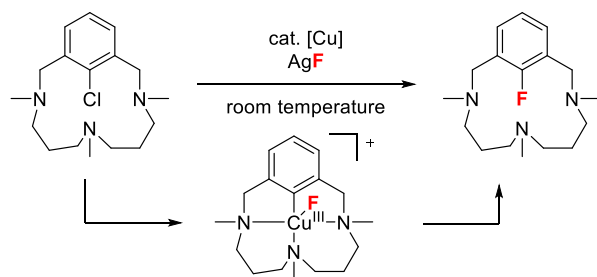
fluoride sources and transition metal catalysts that limit their applicability of large scale applications.

1.3.1. Copper-Mediated and -Catalyzed Fluorination

The use of copper to mediate or catalyze fluorination reactions offers an attractive alternative to the use of expensive palladium complexes. However, early developments of copper-mediated transformations suffer from the use of stoichiometric CuF_2 , forcing conditions (150–550 °C), and low yields of the fluorinated product.^{38,39} Furthermore, not much was understood about these reactions and the nature of the active (aryl)Cu(F) was unknown, making optimization challenging.

In a seminal report in 2011, Ribas and coworkers reported the first example of aryl–F bond forming reductive elimination from a well-defined aryl– Cu^{III} complex at room temperature (Scheme 1.5).⁴⁰ Furthermore, it was demonstrated that copper-catalyzed fluorination was possible on a macrocyclic scaffold. This model study relied on a highly coordinating macrocyclic scaffold to stabilize the aryl– Cu^{III} –F species,^{40,41} and was not shown to have generality to the copper-catalyzed fluorination of simpler arenes.

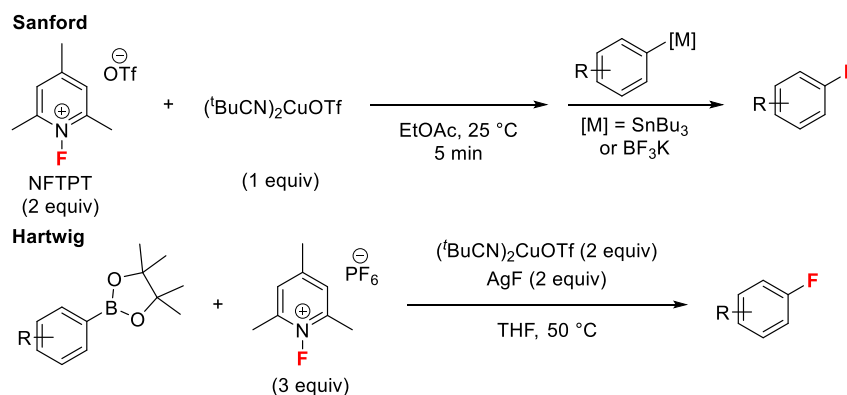
Scheme 1.5. Copper-Catalyzed Fluorination of Macrocyclic System Through a Defined Cu^{III} Intermediate



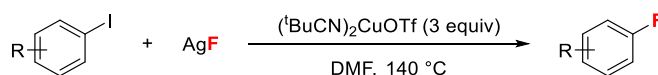
Drawing from this seminal work, the past few years have witnessed a surge in the use of copper to both mediate and catalyze fluorination reactions.^{42,43,44} Electrophilic fluorination of aryl boron reagents and aryl stannanes using superstoichiometric copper was reported independently by the Hartwig group⁴⁵ and the Sanford group⁴⁶ (Scheme 1.6). This fluorination method occurred under mild conditions and exhibited broad functional group tolerance; however, the use of expensive electrophilic fluorinating

reagents precludes the implementation of this chemistry on large scale. The Hartwig group reported the copper-mediated fluorination of aryl iodides using silver fluoride (Scheme 1.7).⁴⁷ However, the rigorously dry and harsh conditions (140 °C) and strong basicity of the fluoride anion limited the functional group tolerance of this method.

Scheme 1.6. Copper-Mediated Electrophilic Fluorination



Scheme 1.7. Copper-Mediated Nucleophilic Fluorination of Aryl Iodides



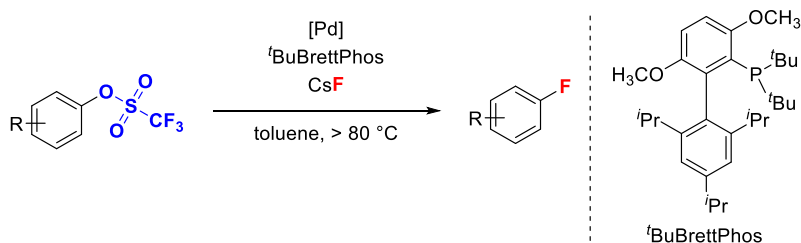
Despite recent advances in the field of copper-mediated and -catalyzed fluorination, current methods rely on elevated temperatures and/or electrophilic fluoride sources that limit the substrate scope and potential applicability to large scale processes. Chapter 4 describes a mild copper-mediated nucleophilic fluorination method of aryl trifluoroborates using potassium fluoride⁴⁸ and attempts to extend this and related systems to copper-catalyzed fluorination. Additionally, Chapter 5 extends this methodology to the copper-mediated functionalization of aryl trifluoroborates using a variety of weakly nucleophilic coupling partners under ambient conditions.⁴⁹

1.3.2. Palladium-Catalyzed Fluorination of Aryl Triflates

In 2009, the Buchwald group demonstrated the use of nucleophilic fluoride (CsF) for the fluorination of aryl triflates using palladium catalysis (Scheme 1.8).⁵⁰ They later extended this methodology to the palladium-catalyzed fluorination of aryl iodides and

bromides.⁵¹ Aryl triflates are attractive electrophiles for this transformation due to the availability of phenols as starting materials.⁵² However, the expensive cost of the Pd catalyst and ligand necessary for the transformation preclude use of this reaction on large scale.

Scheme 1.8. Pd-Catalyzed Fluorination of Aryl Triflates

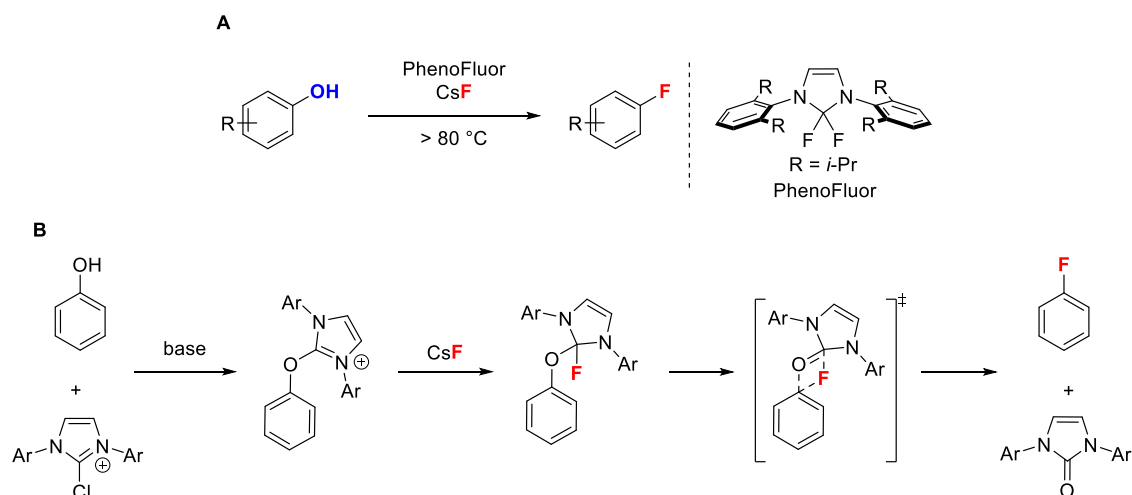


1.4. Deoxyfluorination of Phenols

The use of phenols and phenolic derivatives for fluorination reactions are attractive alternatives to the use of aryl halides as they are sustainable starting materials for the generation of aryl fluorides.⁵² Buchwald⁵⁰ and Larhed⁵³ developed methods for the conversion of phenolic derivatives to aryl fluorides using palladium catalysis, but a more ideal transformation would exclude the use of a transition metal catalyst.

In 2011, Ritter and coworkers reported the conversion of phenols to aryl fluorides using PhenoFluor and CsF (Scheme 1.9-A).⁵⁴ This fluorination method was demonstrated on a wide substrate scope, ranging from electron-deficient to electron-rich substrates, producing high yields of the desired fluorinated product. Investigation of the mechanism of the reaction led the authors to conclude that the deoxyfluorination reaction proceeds through a concerted mechanism, without the formation of a highly charged intermediate (Scheme 1.9-B).⁵⁵ The absence of a negatively charged intermediate is likely responsible for the electronically diverse substrate scope as the intermediate would not need to be stabilized by strongly electron-withdrawing groups. However, the expense of PhenoFluor and CsF limits the applicability to large scale processes.

Scheme 1.9. A. Deoxyfluorination of Phenols. B. Proposed Mechanism



Chapter 3 describes the metal-free fluorination of phenolic derivatives (aryl fluorosulfonates, aryl triflates, aryl nonaflates, and phenols). The substrate scope of the transformation is discussed as well as preliminary investigations into the mechanism of the reaction.⁵⁶

1.5. References

- (1) (a) Jeschke, P. *Pest Manag. Sci.* **2010**, 66, 10–27. (b) Kirk, K. L. *Org. Process Res. Dev.* **2008**, 12, 305–321.
- (2) Purser, S.; Moore, P. R.; Swallow, S.; Gouverneur, V. *Chem. Soc. Rev.* **2008**, 37, 320–330.
- (3) (a) Chambers, R. D. *Fluorine in Organic Chemistry*. Blackwell Publishing, Oxford, England, 2000. (b) Morgenthaler, M.; Schweizer, E.; Hoffmann-Röder, A.; Benini, F.; Martin, R. E.; Jaeschke, G.; Wagner, B.; Fischer, H.; Bendels, S.; Zimmerli, D.; Schneider, J.; Diederich, F.; Kansy, M.; Müller, K. *ChemMedChem* **2007**, 2, 1100–1115.
- (4) (a) Thayer, A. M. *Chem. Eng. News* **2006**, 84, 15–24. (b) Müller, K.; Faeh, C.; Diederich, F. *Science* **2007**, 317, 1881–1886.
- (5) Zhou, Y.; Wang, J.; Gu, Z.; Wang, S.; Zhu, W.; Aceña, J. L.; Soloshonok, V. A.; Izawa, K.; Liu, H. *Chem. Rev.* **2016**, 116, 422–518.
- (6) (a) Fujiwara, T.; O'Hagan, D. *J. Fluorine Chem.* **2014**, 167, 16–29. (b) Theodoridis, G. Fluorine-Containing Agrochemicals: An Overview of Recent Developments. In *Advances in Fluorine Science*; Tressaud, A., Ed.; Elsevier: New York, 2006; pp 121–175.
- (7) (a) Brooks, A. F.; Topczewski, J. J.; Ichiishi, N.; Sanford, M. S.; Scott, P. J. H. *Chem. Sci.* **2014**, 5, 4545–4553. (b) Ametamey, S. M.; Honer, M.; Schubiger, P.

- A. *Chem. Rev.* **2008**, *108*, 1501–1516. (c) Cai, L.; Lu, S.; Pike, V. W. *Eur. J. Org. Chem.* **2008**, 2853–2873.
- (8) (a) Emsley, J. *Chem. Soc. Rev.* **1980**, *9*, 91–124. (b) Liang, T.; Neumann, C. N.; Ritter, T. *Angew. Chem., Int. Ed.* **2013**, *52*, 8214–8264.
 - (9) (a) Furuya, T.; Kamlet, A. S.; Ritter, T. *Nature* **2011**, *473*, 470–477. (b) Furuya, T.; Kuttruff, C. A.; Ritter, T. *Curr. Opin. Drug Discov. Dev.* **2008**, *11*, 803–819.
 - (10) Langlois, B.; Gilbert, L.; Forat, G. Fluorination of aromatic compounds by halogen exchange with fluoride anions (“halex” reaction). In *Industrial Chemistry Library*; Jean-Roger, D., Serge, R.; Eds.; Elsevier: New York, 1996; pp 244–292.
 - (11) (a) Balz, G.; Schiemann, G. *Ber. Dtsch. Ges.* **1927**, *60*, 1186–1190. (b) Swain, C. G.; Rogers, R. J. *J. Am. Chem. Soc.* **1975**, *97*, 799–800.
 - (12) Furuya, T.; Klein, J. E. M. N.; Ritter, T. *Synthesis* **2010**, *11*, 1804–1821.
 - (13) Laali, K. K.; Gettwert, V. J. *J. Fluorine Chem.* **2001**, *107*, 31–34.
 - (14) (a) Gottlieb, H. B. *J. Am. Chem. Soc.* **1936**, *58*, 532–533. (b) Finger, G. C.; Kruse, C. W. *J. Am. Chem. Soc.* **1956**, *78*, 6034–6037.
 - (15) Allen, L. J.; Lee, S. H.; Cheng, Y.; Hanley, P. S.; Muhuhi, J. M.; Kane, E.; Powers, S. L.; Anderson, J. E.; Bell, B. M.; Roth, G. A.; Sanford, M. S.; Bland, D. C. *Org. Process Res. Dev.* **2014**, *18*, 1045–1054.
 - (16) Grushin, V. V.; Marshall, W. J. *Organometallics* **2008**, *27*, 4825–4828.
 - (17) (a) Adams, D. J.; Clark, J. H. *Chem. Soc. Rev.* **1999**, *28*, 225–231. (b) Boechat, N.; Clark, J. H. *J. Chem. Soc., Chem. Commun.* **1993**, 921–922.
 - (18) Adams, D. J.; Clark, J. H.; McFarland, H.; Nightingale, D. J. *J. Fluorine Chem.* **1999**, *94*, 51–55.
 - (19) Sun, H.; DiMagno, S. G. *J. Am. Chem. Soc.* **2005**, *127*, 2050–2051.
 - (20) Sun, H.; DiMagno, S. G. *Angew. Chem., Int. Ed.* **2006**, *45*, 2720–2725.
 - (21) Allen, L. J.; Muhuhi, J. M.; Bland, D. C.; Merzel, R.; Sanford, M. S. *J. Org. Chem.* **2014**, *79*, 5827–5833.
 - (22) Dermeik, S.; Sasson, Y. *J. Org. Chem.* **1989**, *54*, 4827–4829.
 - (23) Ryan, S. J.; Schimmler, S. D.; Bland, D. C.; Sanford, M. S. *Org. Lett.* **2015**, *17*, 1866–1869.
 - (24) Chambers, R. D.; Holmes, T. F.; Korn, S. R.; Sanford, G. *J. Chem. Soc., Chem. Commun.* **1993**, 855–856.
 - (25) (a) Schwesinger, R.; Link, R.; Wenzl, P.; Kossek, S. *Chem. Eur. J.* **2006**, *12*, 438–445. (b) Bolli, C.; Gellhaar, J.; Jenne, C.; Keßler, M.; Scherer, H.; Seeger, H.; Uzun, R. *Dalton Trans.* **2014**, *43*, 4326–4334.
 - (26) Christe, K. O.; Wilson, W. W.; Wilson, R. D.; Bau, R.; Feng, J. *J. Am. Chem. Soc.* **1990**, *112*, 7619–7625.
 - (27) Adams, D. J.; Clark, J. H.; Nightingale, D. J. *Tetrahedron* **1999**, *55*, 7725–7738.
 - (28) Mu, X.; Liu, G. *Org. Chem. Front.* **2014**, *1*, 430–433.
 - (29) Schimmler, S. D.; Ryan, S. J.; Bland, D. C.; Anderson, J. E.; Sanford, M. S. *J. Org. Chem.* **2015**, *80*, 12137–12145.
 - (30) (a) Grushin, V. V. *Acc. Chem. Res.* **2010**, *43*, 160–171. (b) Brown, J. M.; Gouverneur, V. *Angew. Chem. Int. Ed.* **2009**, *48*, 8610–8614.
 - (31) (a) Lee, E.; Kamlet, A. S.; Powers, D. C.; Neumann, C. N.; Boursalian, G. B.; Furuya, T.; Choi, D. C.; Hooker, J. M.; Ritter, T. *Science* **2011**, *334*, 639–642. (b) Brandt, J. R.; Lee, E.; Boursalian, G. B.; Ritter, T. *Chem. Sci.* **2014**, *5*, 169–179.

- (32) (a) Furuya, T.; Kaiser, N. M.; Ritter, T. *Angew. Chem. Int. Ed.* **2008**, *47*, 5993–5996. (b) Mazzotti, A. R.; Campbell, M. G.; Tang, P.; Murphy, J. M.; Ritter, T. *J. Am. Chem. Soc.* **2013**, *135*, 14012–14015.
- (33) (a) Lou, S.-J.; Xu, D.-Q.; Xu, Z.-Y. *Angew. Chem. Int. Ed.* **2014**, *53*, 10330–10335. (b) Lou, S.-J.; Xu, D.-Q.; Xia, A.-B.; Wang, Y.-F.; Liu, Y.-K.; Du, X.-H.; Xu, S.-Y. *Chem. Commun.* **2013**, *49*, 6218–6220.
- (34) (a) Grushin, V. V. *Chem. Eur. J.* **2002**, *8*, 1007–1014. (b) Yandulov, D. V.; Tran, N. T. *J. Am. Chem. Soc.* **2007**, *129*, 1342–1358.
- (35) (a) Furuya, T.; Strom, A. E.; Ritter, T. *J. Am. Chem. Soc.* **2009**, *131*, 1662–1663. (b) Tang, P.; Furuya, T.; Ritter, T. *J. Am. Chem. Soc.* **2010**, *132*, 12150–12154.
- (36) (a) Furuya, T.; Ritter, T. *Org. Lett.* **2009**, *11*, 2860–2863. (b) Dubbaka, S. R.; Narreddula, V. R.; Gadde, S.; Mathew, T. *Tetrahedron* **2014**, *70*, 9676–9681.
- (37) Tang, P.; Ritter, T. *Tetrahedron* **2011**, *67*, 4449–4454.
- (38) Subramanian, M. A.; Manzer, L. E. *Science* **2002**, *297*, 1665.
- (39) Grushin, V. V. Process for preparing fluoroarenes from haloarenes. US Patent 7202388, April 10, 2007.
- (40) Casitas, A.; Canta, M.; Solà, M.; Costas, M.; Ribas, X. *J. Am. Chem. Soc.* **2011**, *133*, 19386–19392.
- (41) Yao, B.; Wang, Z.-L.; Zhang, H.; Wang, D.-X.; Zhao, L.; Wang, M.-X. *J. Org. Chem.* **2012**, *77*, 3336–3340.
- (42) Truong, T.; Klimovica, K.; Daugulis, O. *J. Am. Chem. Soc.* **2013**, *135*, 9342–9345.
- (43) Mu, X.; Zhang, H.; Chen, P.; Liu, G. *Chem. Sci.* **2014**, *5*, 275–280.
- (44) Ichiishi, N.; Canty, A. J.; Yates, B. F.; Sanford, M. S. *Org. Lett.* **2014**, *16*, 3224–3227.
- (45) Fier, P. S.; Luo, J.; Hartwig, J. F. *J. Am. Chem. Soc.* **2013**, *135*, 2552–2559.
- (46) Ye, Y.; Sanford, M. S. *J. Am. Chem. Soc.* **2013**, *135*, 4648–4651.
- (47) Fier, P. S.; Hartwig, J. F. *J. Am. Chem. Soc.* **2012**, *134*, 10795–10798.
- (48) Ye, Y.; Schimler, S. D.; Hanley, P. S.; Sanford, M. S. *J. Am. Chem. Soc.* **2013**, *135*, 16292–16295.
- (49) Schimler, S. D.; Sanford, M. S. *Synlett* **2016**, *27*, 2279–2284.
- (50) (a) Watson, D. A.; Su, M.; Teverovskiy, G.; Zhang, Y.; García-Fortanet, J.; Kinzel, T.; Buchwald, S. L. *Science* **2009**, *325*, 1661–1664. (b) Maimone, T. J.; Milner, P. J.; Kinzel, T.; Zhang, Y.; Takase, M. K.; Buchwald, S. L. *J. Am. Chem. Soc.* **2011**, *133*, 18106–18109. (c) Noël, T.; Maimone, T. J.; Buchwald, S. L. *Angew. Chem. Int. Ed.* **2011**, *50*, 8900–8903. (d) Lee, H. G.; Milner, P. J.; Buchwald, S. L. *Org. Lett.* **2013**, *15*, 5602–5605. (e) Milner, P. J.; Kinzel, T.; Zhang, Y.; Buchwald, S. L. *J. Am. Chem. Soc.* **2014**, *136*, 15757–15766.
- (51) Lee, H. G.; Milner, P. J.; Buchwald, S. L. *J. Am. Chem. Soc.* **2014**, *136*, 3792–3795.
- (52) *The Chemistry of Phenols*; Rappoport, Z., Ed.; John Wiley & Sons Ltd.: Chichester, 2003.
- (53) Wannberg, J.; Wallinder, C.; Ünlüsoy, M.; Sköld, C.; Larhed, M. *J. Org. Chem.* **2013**, *78*, 4184–4189.
- (54) (a) Tang, P.; Wang, W.; Ritter, T. *J. Am. Chem. Soc.* **2011**, *133*, 11842–11844. (b) Fujimoto, T.; Becker, F.; Ritter, T. *Org. Process Res. Dev.* **2014**, *18*, 1041–1044. (c) Fujimoto, T.; Ritter, T. *Org. Lett.* **2015**, *17*, 544–547.

- (55) Neumann, C. N.; Hooker, J. M.; Ritter, T. *Nature* **2016**, *534*, 369–373.
- (56) Schimler, S. D.; Cismesia, M. A.; Hanley, P. S.; Froese, R. D. J.; Jansma, M. J.; Bland, D. C.; Sanford, M. S. *J. Am. Chem. Soc.* **2017**, *139*, 1452–1455.

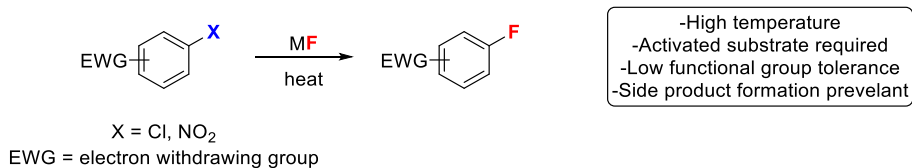
CHAPTER 2

Room Temperature S_NAr Fluorination of Aryl Chlorides and Nitroarenes with Tetramethylammonium Fluoride¹

2.1 Background

Fluorinated (hetero)arenes are finding increasing importance and application in agrochemical, pharmaceutical, and materials chemistry.² Despite their importance, there are few selective and mild methods for the formation of (hetero)aryl C–F bonds. One of the most common methods for the industrial preparation of (hetero)aryl fluorides is nucleophilic aromatic fluorination (S_NAr fluorination; Scheme 2.1).³ This method involves the reaction of an electron-deficient (hetero)aryl chloride or nitroarene with a nucleophilic fluoride source to furnish the desired (hetero)aryl fluoride. These reactions typically employ anhydrous alkali metal fluoride salts as the fluoride source, which exhibit poor solubility in organic solvents. As a result, forcing conditions (elevated temperature, long reaction times) are necessary for high conversion of the starting material, which often limits functional group tolerance and promotes side product formation.³

Scheme 2.1. Traditional S_NAr Fluorination

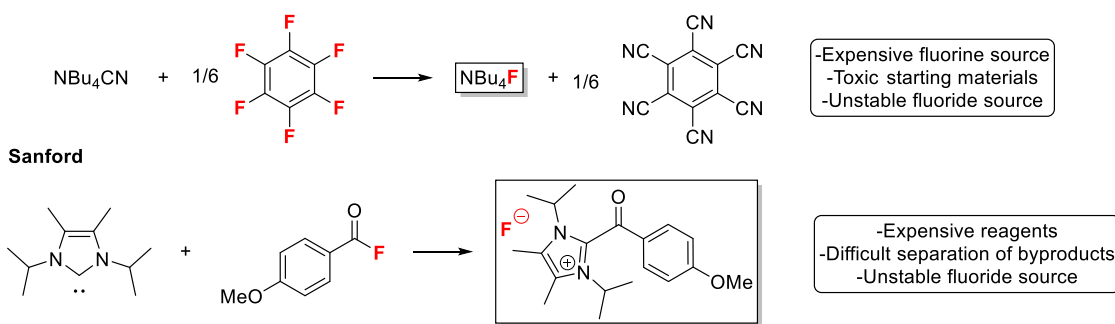


Recent research has focused on soluble anhydrous fluoride reagents as alternatives to the traditional alkali metal fluoride salts. These more soluble fluoride sources can often enable S_NAr fluorination reactions to proceed under milder reaction

conditions (in some cases even room temperature). Recently, our lab and others have reported methods for the *in situ* generation of anhydrous fluoride sources for room temperature S_NAr fluorination (Scheme 2.2).^{4,5,6} While these methods allow mild fluorination conditions, they suffer from limitations including the requirement for expensive and toxic stoichiometric reagents, which precludes the implementation of these methods to industrial scale processes.

Scheme 2.2. Anhydrous Fluoride Sources for Room Temperature S_NAr Fluorination

DiMagno, Sanford



To address this challenge, alternative anhydrous fluoride sources that might be more practical for industrial implementation were sought. An attractive alternative is anhydrous (anh) tetramethylammonium fluoride (NMe_4F), a commercially available fluoride source that can be prepared from inexpensive precursors.⁷ NMe_4F has been previously reported for the fluorination of unactivated aryl bromides via benzyne intermediates⁸ as well as for S_NAr fluorodenitration reactions.⁹ However, these reactions require elevated temperatures (≥ 60 °C) and result in the formation of side products (regioisomers as well as aryl ethers and phenols).^{3a,9} There are very few examples for the use of NMe_4F (anh) for the S_NAr fluorination of aryl chlorides, and the scope of these reactions has not extensively been explored.¹⁰

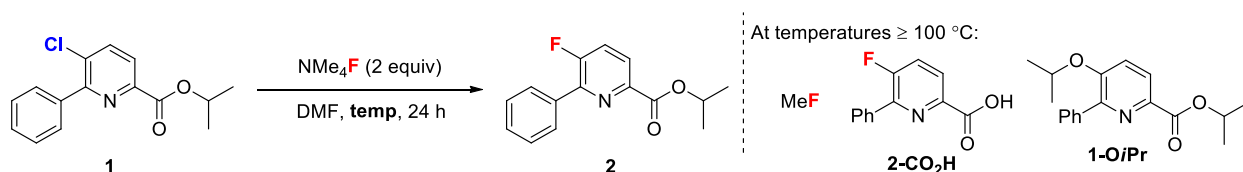
This chapter discusses the use of anhydrous NMe_4F for the room temperature S_NAr fluorination of (hetero)aryl chlorides and nitroarenes. The effect of leaving group on the rate of reaction is explored, and the reactivity of different aryl (pseudo)halides with NMe_4F and CsF are compared. Finally, the applicability of this method is demonstrated

on industrially relevant chloropicolinate as well as other electron-deficient (hetero)aromatic substrates.

2.2 Initial Results and Optimization

Our initial investigations focused on using NMe₄F for the S_NAr fluorination of 5-chloropicolinate **1**, a structural motif found in many Dow AgroSciences products.¹¹ This transformation was initially examined at 140 °C (elevated temperatures consistent with those commonly employed in S_NAr fluorination reactions).^{3,12} As shown in Table 2.1, the reaction of **1** with 2 equiv of NMe₄F (anh) at 140 °C afforded 66% yield of **2**, with complete conversion of **1** (Table 2.1, entry 1). Analysis by ¹⁹F NMR spectroscopy and GCMS showed that the major side products of the reaction are the carboxylic acid **2**-CO₂H, the isopropyl ether **1**-iPrO, and methyl fluoride (MeF).

Table 2.1. S_NAr Fluorination of **1** with NMe₄F (anh)^a



entry	equiv of NMe ₄ F	temperature	% conversion	% yield ^b
1	2	140 °C	100	66
2	2	100 °C	100	73
3	2	60 °C	100	85
4	2	40 °C	100	95
5	2	25 °C	100	99
6	1	25 °C	80	80

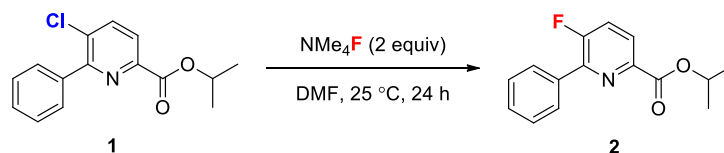
^aConditions: Substrate **1** (0.1 mmol) and anhydrous NMe₄F were stirred in DMF (0.2 M) for 24 h at the noted temperature. ^bYields determined by ¹⁹F NMR spectroscopy using 1,3,5-trifluorobenzene as standard.

It was hypothesized that lowering the temperature of the reaction might limit competing side product formation (Table 2.1, entries 2–5). Indeed, a trend was observed of increasing product yield as temperature was decreased. At room temperature, complete conversion of **1** to give quantitative yield of **2** was observed (entry 5). Furthermore, with only 1 equiv of NMe₄F, this S_NAr fluorination proceeded to afford 80% yield of **2** at room temperature, with the mass balance being unreacted starting material

(entry 6). These results demonstrate that anhydrous NMe₄F affords comparable reactivity to that of the previously reported anhydrous NBu₄F (>99% of **2**)⁵ and acyl azolium fluoride (>99% of **2**)⁶ reagents.

Initial studies focused on the use of strictly anhydrous conditions for the S_NAr fluorination reaction with anhydrous NMe₄F. The use of NMe₄F•4H₂O under conditions analogous to those in Table 2.1 afforded none of the desired fluorinated product (Table 2.2, entry 1). Attempts to dry hydrated NMe₄F (azeotropic drying with benzene, drying at 110 °C under vacuum, addition of drying reagents such as MgSO₄) did not prove fruitful, as no product was observed by ¹⁹F NMR spectroscopic analysis under these conditions. To more systematically explore the effect of H₂O on the fluorination, various quantities of water were added to reactions with anh NMe₄F as the fluoride source (Table 2.2, entries 2–5). The addition of 1 equiv of water resulted in an approximately 25% reduction in the yield (from 99% to 76%, entry 3). Furthermore, the addition of ≥2 equiv of water resulted in complete shutdown of the reaction, with bifluoride (HF₂⁻) being the major species detected by ¹⁹F NMR spectroscopic analysis.

Table 2.2. Effect of Water and Sources of NMe₄F on the S_NAr Fluorination of **1**^a

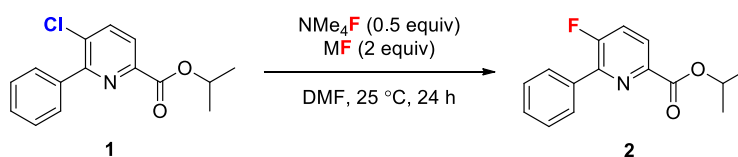


entry	NMe ₄ F source	equiv. of additional H ₂ O	% yield ^b
1	NMe ₄ F•4H ₂ O	0	<1
2	anh NMe ₄ F	0	99
3	anh NMe ₄ F	1	76
4	anh NMe ₄ F	2	1
5	anh NMe ₄ F	5	<1
6	NMe ₄ Cl + KF	0	<1
7	synthesized NMe ₄ F ^c	0	27
8	synthesized NMe ₄ F ^d	0	67

^aConditions: Substrate **1** (0.1 mmol) and anhydrous NMe₄F (0.2 mmol) were stirred in DMF (anhydrous or anhydrous with added water; 0.2 M) for 24 h at 25 °C. ^bYields determined by ¹⁹F NMR spectroscopy using 1,3,5-trifluorobenzene as standard. ^cDried under vacuum at 110 °C for 24 hours. ^dDried under vacuum at 130 °C for 7 days.

The synthesis of anhydrous NMe₄F was also investigated. Attempts to generate anh NMe₄F *in situ* from the reaction of anh NMe₄Cl and KF provided none of the desired fluorinated product (Table 2.2, entry 6). As such, the *ex situ* synthesis and drying of NMe₄F was explored. NMe₄Cl and KF were combined in a 1:1 ratio in methanol according to a literature procedure.^{7b} KCl precipitated from the solution and was removed by filtration. After removal of MeOH by rotary evaporation, the resulting solid was dried at 110 °C under vacuum for 24 h. This *ex situ* synthesized and dried NMe₄F afforded 27% yield in the fluorination of substrate **1** (Table 2.2, entry 7). Bifluoride was observed by ¹⁹F NMR spectroscopic analysis in this reaction, implicating the presence of residual protic solvent. Increasing the time and temperature that the synthesized NMe₄F was dried under vacuum (7 days at 130 °C instead of 1 day at 110 °C) had a beneficial effect on the yield of the reaction (67% yield; entry 8), but bifluoride was still detected. While the yields obtained using the synthesized NMe₄F were not the same as those obtained using commercial anhydrous NMe₄F, it is still encouraging that the active fluorinating reagent can be prepared from inexpensive reagents¹³ and dried in our lab.

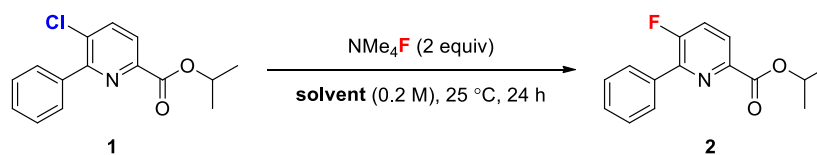
Another approach to using low cost reagents in this transformation would be to use a combination of an alkali metal fluoride salt and NMe₄F (anh) as a phase transfer reagent.¹² The S_NAr fluorination of **1** was run with substoichiometric amounts of anhydrous NMe₄F and various alkali metal fluoride salts (Table 2.3). With only 0.5 equiv of anhydrous NMe₄F, the S_NAr fluorination reaction only afforded 37% of the desired fluorinated product (entry 1). The use of a variety of alkali metal fluoride salts had little to no effect on the reaction, with every fluoride salt examined giving comparable yields to using 0.5 equiv of NMe₄F alone (entries 2–5). Under the conditions tested, anhydrous NMe₄F did not act as a phase transfer reagent to bring the poorly metal fluoride salts into solution. This may be a result of the limited solubility of anhydrous NMe₄F, which is only slightly soluble in DMF.

Table 2.3. NMe₄F (anh) as a Phase Transfer Reagent for S_NAr Fluorination of **1**^a

entry	MF	% yield ^b
1	none	37
2	KF	35
3	NaF	43
4	CsF	32
5	LiF	43

^aConditions: Substrate **1** (0.1 mmol), anhydrous NMe₄F (0.05 mmol), and alkali metal fluoride (0.2 mmol) were stirred in DMF (0.2 M) for 24 h at 25 °C. ^bYields determined by ¹⁹F NMR spectroscopy using 1,3,5-trifluorobenzene as standard.

Other solvents were explored for the S_NAr fluorination of **1** (Table 2.4). From an industrial and sustainability perspective, *N,N*-dimethylformamide (DMF) is not an ideal solvent choice.¹⁴ Acetonitrile (CH₃CN) and sulfolane are potentially attractive replacements for DMF. However, the use of sulfolane resulted in a greatly diminished yield of **2** (entry 2); furthermore, none of the desired fluorinated product was detected when the reaction was conducted in acetonitrile (entry 3). Anhydrous NMe₄F has been shown to deprotonate CH₃CN,⁷ and it is possible that this deprotonation outcompetes the desired fluorination reaction. Potentially consistent with this hypothesis, bifluoride was detected in the crude reaction mixture by ¹⁹F NMR spectroscopic analysis. The use of dimethyl sulfoxide (DMSO), dimethylacetamide (DMAc), and *N*-methyl-2-pyrrolidone (NMP) all led to reduced yields of the desired fluorinated product (entries 4–6). Furthermore, bifluoride was observed in all the reactions, suggesting the possibility of either solvent deprotonation or the presence of trace quantities of water in the solvents. Like CH₃CN, DMSO is known to be deprotonated by NMe₄F (anh); this might be a reason for the low yield of fluorinated product **2**.^{9a,b} The mass balance of the reactions in different solvents is unreacted starting material **2** and ether product **1-OⁱPr**.

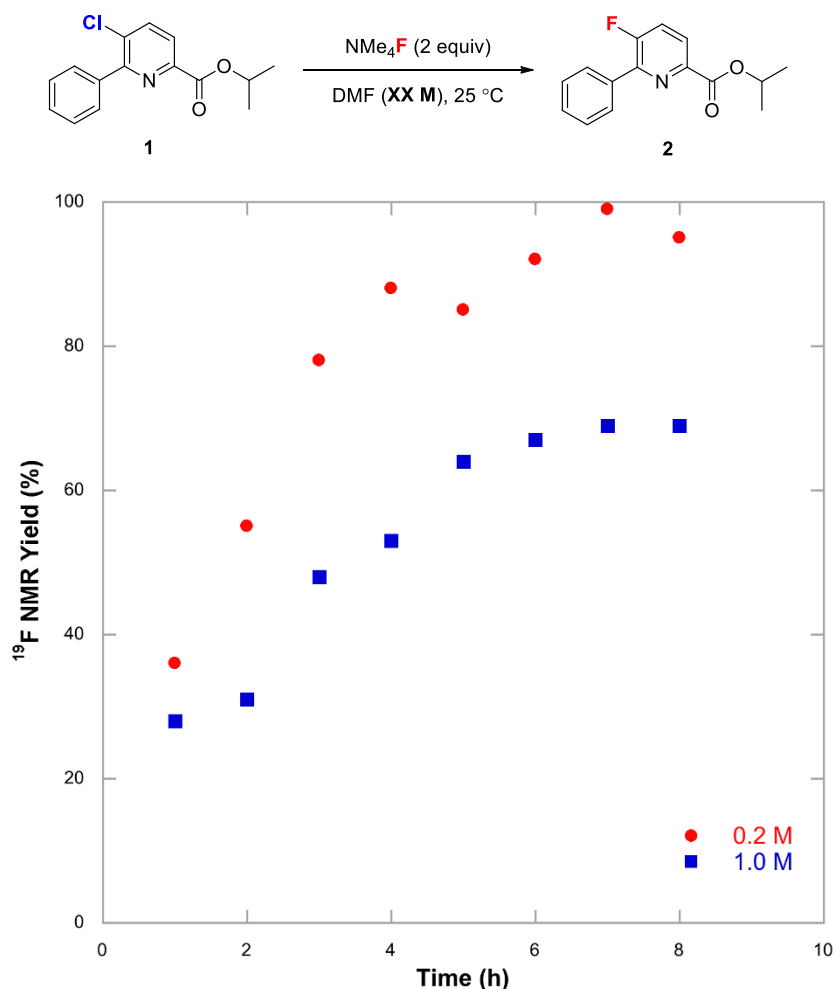
Table 2.4. Solvents for the S_NAr Fluorination of **1**^a

entry	solvent	% yield ^b
1	DMF	99
2	sulfolane	32
3	CH ₃ CN	<1
4	DMSO	26
5	DMAc	23
6	NMP	16
7	DMF (0.5 M)	93
8	DMF (1.0 M)	93

^aConditions: Substrate **1** (0.1 mmol) and anhydrous NMe₄F (0.2 mmol) were stirred in solvent for 24 h at 25 °C. ^bYields determined by ¹⁹F NMR spectroscopy using 1,3,5-trifluorobenzene as standard.

The effect of concentration on the S_NAr fluorination reaction was also explored. When the reaction was run at a higher concentration (0.5 or 1.0 M), the yield of **1** was comparable to that obtained when a concentration of 0.2 M was employed (Table 2.4, entries 7 and 8). Examination of the rates of reaction reveal that reactivity slows as concentration increases (Figure 2.1). At 0.2 M, the S_NAr fluorination of **1** was complete (>99% conversion) within 8 h, while the more concentrated reaction (1.0 M) required 11 h to reach completion.

Figure 2.1. Time Studies for the Fluorination of **1** at Different Concentrations^a



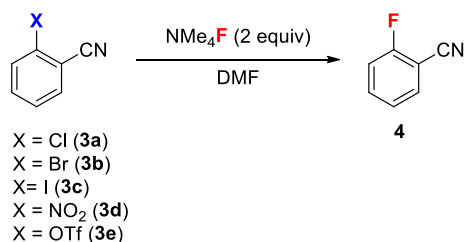
^aConditions: Substrate **1** (0.1 mmol) and anhydrous NMe₄F (0.2 mmol) were stirred in DMF for the noted time at 25 °C. Yields determined by ¹⁹F NMR spectroscopy using 1,3,5-trifluorobenzene as standard.

2.3. Effect of Leaving Group on S_NAr Fluorination

Next, the impact of the identity of the leaving group was examined, using our best conditions (2 equiv of NMe₄F (anh) in DMF (0.2 M) at 25 °C for 24 h). A first study focused on the S_NAr fluorination of a series of 2-substituted benzonitrile substrates with Cl, Br, I, NO₂, and OTf as leaving groups (**3a-e**). As shown in Table 2.5, compounds **3a-e** reacted with NMe₄F (anh) at room temperature to afford product **4** in 2–95% yield after 48 h. When the temperature of the reaction was increased to 80 °C, the reactions proceeded much more quickly, and **3a-d** were converted to **4** in 88–97% yield after only 3 h (entries 1–4). In contrast, aryl triflate **3e** showed minimal reactivity at 80 °C (entry 5), even at prolonged

reaction times (no improvement in yield after 48 h). Interestingly, aryl iodides and aryl bromides have previously been regarded as poor substrates for S_NAr fluorination reactions.¹⁵ This study shows that the reactivity of these aryl halides with NMe₄F (anh) is comparable to that of more traditional S_NAr substrates (i.e. aryl chlorides).

Table 2.5. Comparison of Reactions of **3a-e** with NMe₄F (anh) and CsF

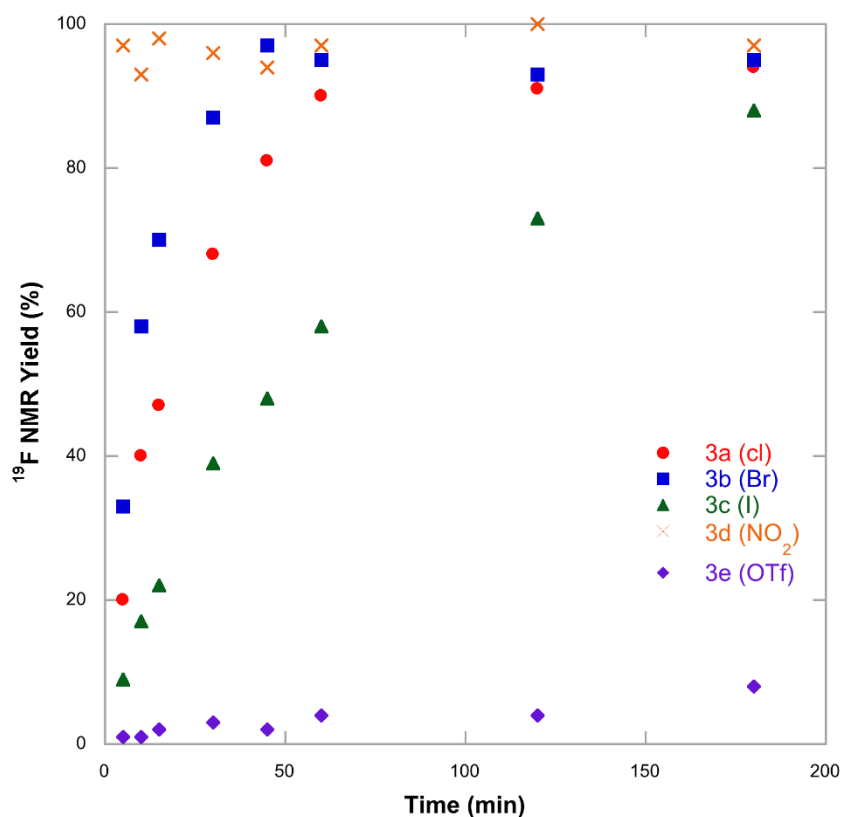


entry	substrate	% yield		
		48 h, 25 °C ^a	3 h, 80 °C ^b	CsF, 140 °C ^c
1	3a	32	94	52
2	3b	48	95	49
3	3c	8	88	22
4	3d	95	97	73
5	3e	2	8	73

^aConditions: Substrate (0.1 mmol) and anhydrous NMe₄F (0.2 mmol) stirred in DMF (0.2 M) at 25 °C for 48 h. ^bConditions: Substrate (0.1 mmol) and anhydrous NMe₄F (0.2 mmol) stirred in DMF (0.2 M) at 80 °C for 3 h. ^cConditions: Substrate (0.1 mmol) and CsF (0.2 mmol) stirred in DMF (0.2 M) at 140 °C for 24 h. All yields were determined by ¹⁹F NMR spectroscopy using 1,3,5-trifluorobenzene as an internal standard.

To obtain more insight into the relative rates of S_NAr fluorination of substrates **3a-e**, time studies were conducted at 80 °C (Figure 2.2).¹⁶ The relative rates of reaction for these substrates are: NO₂ >> Br > Cl > I >> OTf. 2-Nitrobenzonitrile **3d** afforded nearly quantitative yield of the desired fluorinated product **4** in just 5 min at 80 °C while the halide substrates **3a-c** afforded quantitative conversion within 3 h under analogous conditions. On the contrary, 2-cyanophenyl triflate **3e** reacted very slowly and provided fluorinated product **4** in very low yield after 3 h.

Figure 2.2. Reaction Profiles for the Reactions of **3a-e** with NMe₄F (anh) to Form **4**^a



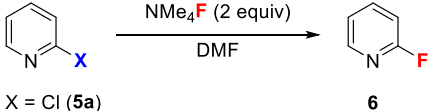
^aConditions: Substrate (0.1 mmol) and anhydrous NMe₄F (0.2 mmol) stirred in DMF (0.2 M) at 80 °C for the given time. All yields were determined by ¹⁹F NMR spectroscopy using 1,3,5-trifluorobenzene as an internal standard and represent an average of three individual runs.

The reactions of **3a-e** with NMe₄F (anh) were also compared to those with CsF, a classical reagent for S_NAr fluorination reactions.³ The use of CsF at 80 °C resulted in <5% product formation for all the tested substrates. At 140 °C, the aryl halides reacted with CsF to afford modest yield of **4** (22–52%, Table 2.5, entries 1–3). The trend here is comparable to those previously noted in the literature, where aryl iodides are the least reactive (22%) in comparison to aryl chlorides (52%).³ This contrasts the trend that is observed with anh NMe₄F, where bromoarene **3b** is most reactive. In all reactions that use aryl halides as substrates, unreacted starting material remains after 24 h. The fluorodenitration of **3d** with CsF at 140 °C afforded the desired fluorinated product **4** in 73% yield; the conversion of **3d**, however, was quantitative. By GCMS analysis of the crude reaction mixture, aryl ether side products were formed. These are common side

products of fluorodenitration reactions due to competing reactivity of the nitrite leaving group.⁹ Surprisingly, 2-cyanophenyl triflate **3e** afforded 73% of **4** (compared to 8% with NMe₄F at 80 °C).^A In general, the highest yields of **4** were obtained using NMe₄F (anh) under relatively mild reaction conditions (25 or 80 °C). These results highlight the advantage of NMe₄F (anh) over more traditional S_NAr fluorination with CsF.

An analogous set of studies was conducted with 2-substituted pyridines **5a-e**. Similar to our results with 2-substituted-benzonitrile substrates, 2-pyridyl halides **5a-c** provided the fluorinated product **6** in modest to high yield using NMe₄F (anh) at 80 °C (Table 2.6, entries 1–3). 2-Nitropyridine **5d** also reacted to afford high yield (98%) of **6**. In contrast to 2-cyanophenyl triflate **3e**, pyridine-2-yl triflate **5e** provided modest yield (43%) of the fluorinated product using NMe₄F (anh) under relatively mild conditions.

Table 2.6. Comparison of Reactions of **5a–e** with NMe₄F (anh) and CsF



X = Cl (**5a**)
X = Br (**5b**)
X = I (**5c**)
X = NO₂ (**5d**)
X = OTf (**5e**)

entry	substrate	% yield	
		4 h, 80 °C ^a	CsF, 140 °C ^b
1	5a	72	9
2	5b	96	17
3	5c	91	19
4	5d	98	100
5	5e	43	87

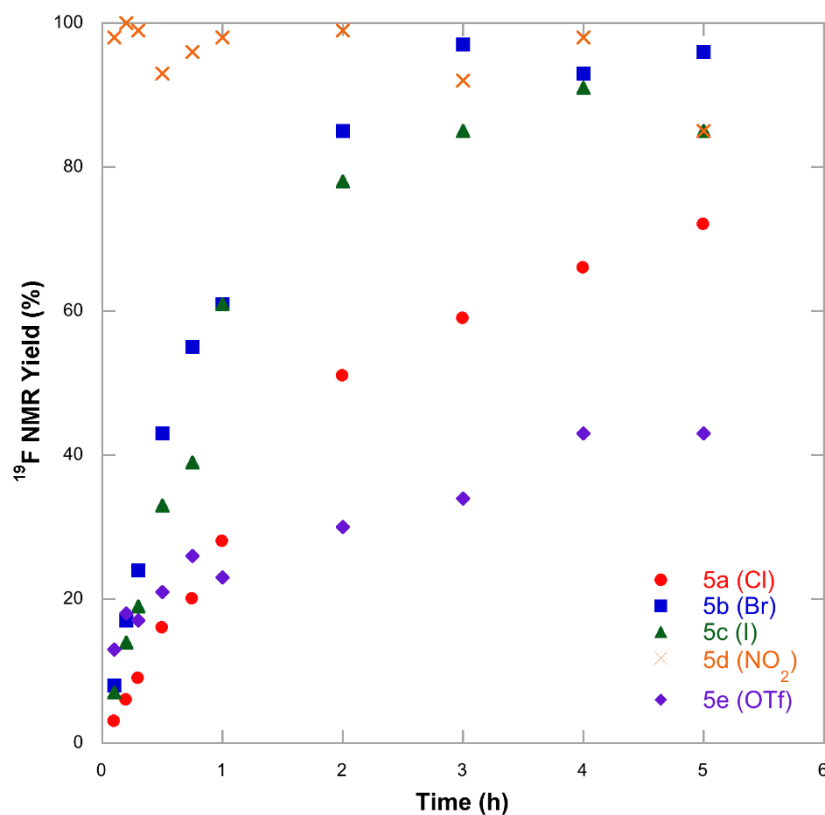
^aConditions: Substrate (0.1 mmol) and anhydrous NMe₄F (0.2 mmol) stirred in DMF (0.2 M) at 80 °C for 4 h. ^bConditions: Substrate (0.1 mmol) and CsF (0.2 mmol) stirred in DMF (0.2 M) at 140 °C for 24 h. All yields were determined by ¹⁹F NMR spectroscopy using 1,3,5-trifluorobenzene as an internal standard.

Time studies were undertaken for the reactions of **5a–e** with NMe₄F (anh) at 80 °C (Figure 2.3). Using 2-substituted pyridines, the impact of leaving group on reaction rate differed slightly from that of the 2-substituted-benzonitriles **3a–e**, with the order of

^A For a detailed study of the reactivity of aryl triflates for S_NAr fluorination reactions, see Chapter 3.

reactivity being $\text{NO}_2 \gg \text{Br} \approx \text{I} > \text{Cl} > \text{OTf}$. The initial rate of triflate **5e** is comparable to that of (hetero)aryl bromide **5b**; however, the reaction stalls after only 20 min. A similar time study as a function of leaving group has been reported for the $\text{S}_{\text{N}}\text{Ar}$ radiofluorination of 2-substituted pyridines with K^{18}F .^{16d} Similar to our findings, this radiofluorination study showed that 2-nitropyridine and 2-bromopyridine reacted faster than other 2-halopyridines. Overall, one key finding from these time studies is that the leaving group effect on the rate of reaction is substrate dependent. Additionally, the fluoride source has an impact on the reactivity of different substrates, as different trends were observed when CsF was used in place of NMe_4F .

Figure 2.3. Reaction Profiles for the Reactions of **5a–e** with NMe_4F (anh) to Form **6^a**



^aConditions: Substrate (0.1 mmol) and anhydrous NMe_4F (0.2 mmol) stirred in DMF (0.2 M) at 80 °C for the given time. All yields were determined by ^{19}F NMR spectroscopy using 1,3,5-trifluorobenzene as an internal standard and represent an average of three individual runs.

The reactions of **5a-e** with NMe₄F (anh) were also compared to reactions with CsF at 140 °C (Table 2.6). 2-Halopyridines **5a-c** showed minimal reactivity (9–19% yield) with CsF, even at elevated temperatures (entries 1–3). 2-Nitropyridine **5d** afforded comparable results with NMe₄F (anh) and CsF (entry 4). Interestingly, pyridine-2-yl triflate **5e** provided a much improved yield with CsF at 140 °C relative to NMe₄F (anh) (entry 5), providing a higher yield under these conditions than any of the 2-halopyridines. This result is similar to that observed with the use of 2-cyanophenyl triflate **3e**, where CsF at elevated temperatures provided a much improved yield relative to NMe₄F (anh). These data suggest that (hetero)aryl triflates could be good substrates for S_NAr fluorination reactions utilizing CsF at elevated temperatures.^B

2.4. Substrate Scope

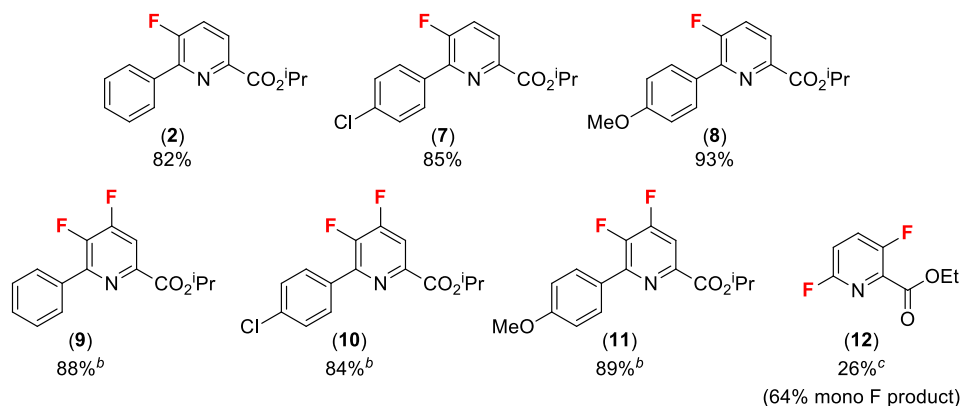
The substrate scope of S_NAr fluorination with NMe₄F reaction was next explored. As shown in Figure 2.4, a variety of monochloropicolines and dichloropicolines reacted with NMe₄F (anh) at room temperature to afford the corresponding mono- and difluorinated products **2** and **7–11** in good to excellent isolated yield. The transformation of the dichloropicolines required only 1.5 equiv of NMe₄F (anh) per chloride to proceed in high yields to the difluorinated products **9–11**. The fluorination of **2** was also conducted on 10.11 g and afforded a comparable yield to that conducted on 138.0 mg scale (82% vs 85%).^C Methoxy- and chloro-substituents in unactivated positions were compatible with these reaction conditions (**7–8**, **10–11**). The fluorination of dichloropicoline **12** was more challenging. At room temperature, only 26% of the difluorinated product was observed, with 64% monofluorination (replacement of the chloride at the 6-position) produced in the reaction. A variety of conditions were explored (temperature, time, equiv of NMe₄F (anh)), but the yield of the difluorinated product **12** did not improve, and a mixture of mono- and difluorination was always formed. This result is in stark contrast to the fluorination of the chlorinated precursor of **12** with anhydrous tetrabutylammonium fluoride (TBAF*), where

^B For a detailed study of the reactivity of aryl triflates for S_NAr fluorination reactions, see Chapter 3.

^C Scale up S_NAr fluorination reaction of **1** performed by Dr. Douglas Bland (The Dow Chemical Company).

the reaction proceeded in high yield to give the desired difluorinated product (77% yield determined by ^{19}F NMR spectroscopic analysis).⁵

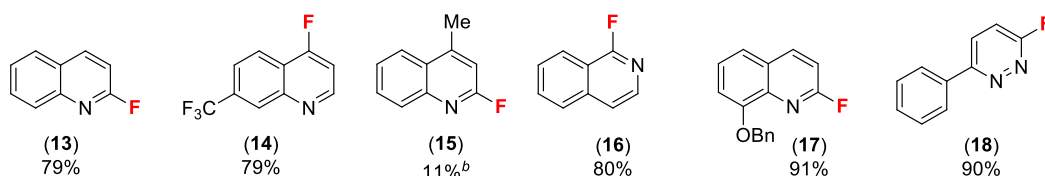
Figure 2.4. Scope of Chloropicolinates for $\text{S}_{\text{N}}\text{Ar}$ Fluorination with NMe_4F (anh)^a



^aConditions: Anhydrous NMe_4F (2 equiv) and substrate (1 equiv) were stirred in anhydrous DMF at 25 °C for 24 h. ^b3 equivalents of NMe_4F (anh) were used. ^cYield determined by ^{19}F NMR spectroscopic analysis of the crude reaction mixture using 1,3,5-trifluorobenzene as a standard.

Chloroquinoline, chloroisoquinoline, and chloropyridazine substrates underwent room temperature fluorination to form **13–18** in low to excellent yield (Figure 2.5). Quinoline **15** precursor was a poor substrate for the $\text{S}_{\text{N}}\text{Ar}$ fluorination reaction. It was hypothesized to not be electron-deficient enough to enable the fluorination to proceed in high yield. Increasing the temperature of the reaction to 80 °C did not improve the yield of the reaction. The high yielding synthesis of 8-(benzyloxy)-2-fluoroquinoline **17** is noteworthy, as the radiolabeled counterpart has been used for the PET imaging of amyloid plaques.¹⁷

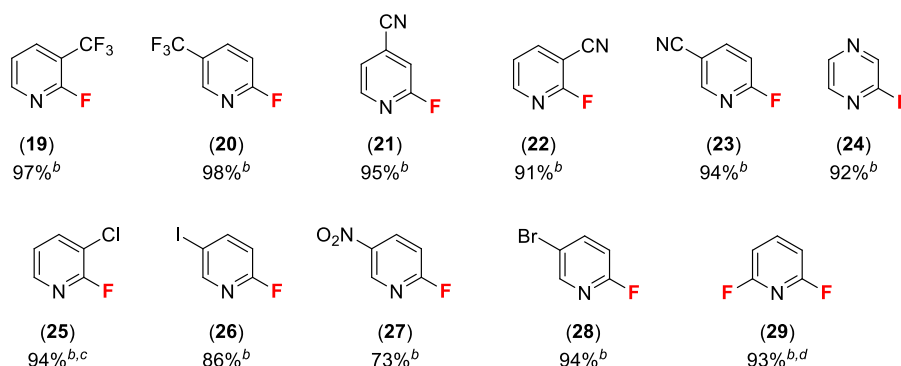
Figure 2.5. Chloroquinoline, Chloroisoquinoline, and Chloropyridazine Substrates^a



^aConditions: Anhydrous NMe_4F (2 equiv) and substrate (1 equiv) were stirred in anhydrous DMF at 25 °C for 24 h. ^bYield determined by ^{19}F NMR spectroscopic analysis of the crude reaction mixture using 1,3,5-trifluorobenzene as a standard.

A series of substituted 2-chloropyridines were next investigated for room temperature S_NAr fluorination with NMe₄F (anh) (Figure 2.6). Trifluoromethyl- and cyano-substituents were demonstrated to be compatible with the reaction conditions (**19–23**). Halides and nitro substituents in less activated positions on the pyridine ring were well tolerated, even in the presence of excess NMe₄F (anh) (**25–28**). Fluoropyrazine **24** was obtained in high yield under the mild reaction conditions. As with the dichloropyridines, 2,6-difluoropyridine **29** was obtained in high yield, requiring only 3 equiv of NMe₄F (anh).

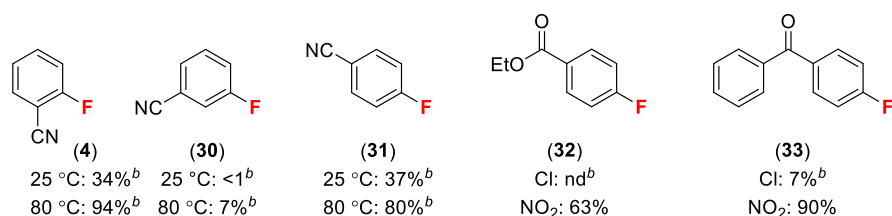
Figure 2.6. Scope of Substituted 2-Chloropyridines for S_NAr Fluorination with NMe₄F^a



^aConditions: Anhydrous NMe₄F (2 equiv) and substrate (1 equiv) were stirred in anhydrous DMF at 25 °C for 24 h. ^bYield determined by ¹⁹F NMR spectroscopic analysis of the crude reaction mixture using 1,3,5-trifluorobenzene as a standard. ^cThe corresponding nitroarene was used as the substrate. ^d3 equivalents of NMe₄F (anh) was used.

Aryl chlorides were also examined for the S_NAr fluorination reaction using NMe₄F (anh) (Figure 2.7). At room temperature, reaction of benzonitrile substrates proceeded in low yield (products **4** and **30–31** <1–32%), but when the temperature was increased, the yield improved (7–94%). S_NAr fluorination with NMe₄F (anh) produced 2- and 4-fluorobenzonitrile (**4** and **31**) in excellent yields. On the other hand, 3-fluorobenzonitrile **30** is formed in very low yield. These results are consistent with previous reports demonstrating that electron-withdrawing groups in the *meta*-position do not activate aryl rings for S_NAr fluorination.^{4a} Both ethyl 4-chlorobenzoate and 4-chlorobenzophenone were not sufficiently activated for the S_NAr fluorination reaction, providing only low yields of the desired product at room temperature with NMe₄F (anh). Use of the nitro analogs provided high yields of the fluorinated products at room temperature (**32** and **33**).

Figure 2.7. Scope of Simple Arenes for S_NAr Fluorination with NMe₄F (anh)^a



^aConditions: Anhydrous NMe₄F (2 equiv) and substrate (1 equiv) were stirred in anhydrous DMF at 25 °C for 24 h. ^bYield determined by ¹⁹F NMR spectroscopic analysis of the crude reaction mixture using 1,3,5-trifluorobenzene as a standard.

2.5. Conclusion

Anhydrous tetramethylammonium fluoride (NMe₄F) was found to be a useful reagent for mild S_NAr fluorination reactions. A diverse array of activated (electron-deficient) (hetero)aryl halides and nitroarenes reacted with NMe₄F (anh) at temperatures between 25 and 80 °C (for less activated substrates). Identity of the leaving group had an impact on the rate of the fluorination reaction, with aryl bromides and nitroarenes generally resulting in faster rates of reaction and higher yields. However, the rate of reaction was also dependent on the choice of substrate, as differences were observed between the rates of fluorination of aryl and heteroaryl substrates with different leaving groups. The yields with NMe₄F (anh) under mild conditions (25–80 °C) were directly compared to more traditional S_NAr fluorination reactions conducted with CsF at 140 °C. In many cases, the use of NMe₄F (anh) was superior to the use of CsF under more forcing conditions. An interesting exception is (hetero)aryl triflates, which react poorly with NMe₄F (anh) but reasonably well with CsF at elevated temperatures. In addition, the mild conditions of reactions with NMe₄F (anh) led to minimal byproduct formation while the harsher conditions required for fluorination with CsF in some cases led to undesired side products. Overall, this method for room temperature S_NAr fluorination with NMe₄F (anh) provides an attractive alternative to more traditional routes for fluorination.

2.6. Outlook

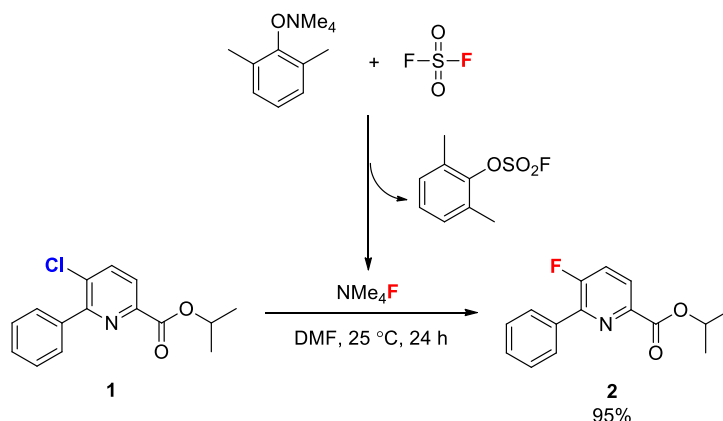
The work described in this chapter has the potential to have far reaching implications in industrial scale processes for fluorination. The use of NMe₄F (anh) was shown to enable the high yielding fluorination of chloropicolates, which are common

motifs in many agrochemicals.¹¹ Additionally, the reaction was demonstrated to be readily scalable, providing comparable yields on scales ranging from 27 mg to 10 g. The mild reaction conditions employed limit the formation of undesired side products, and in many cases, the fluorinated product can be easily isolated from the tetramethylammonium salts produced in the reaction by simple aqueous work up and column chromatography.

While NMe₄F (anh) is a more attractive alternative to other anhydrous fluoride sources, it has some drawbacks. While the reagents to synthesize NMe₄F (anh) are inexpensive, commercial NMe₄F (anh) from a single vendor (Sigma Aldrich) was found to be effective for achieving high yields of fluorinated products. Use of the tetrahydrate (NMe₄F•4H₂O) or NMe₄F that was synthesized and dried, afforded no desired reaction or lower yields, respectively. Furthermore, the presence of water in the reaction was shown to attenuate reactivity. Commercially available anhydrous NMe₄F is rather expensive¹³ and often not readily available.¹⁸ Therefore, to increase the practicality of the use of this S_NAr fluorination on larger scale, it will be essential to develop more effective methods for the synthesis and drying of NMe₄F. Alternatively, developing ways to generate anhydrous NMe₄F *in situ* might also help to overcome these issues.

Recently, our lab developed a method for the *in situ* generation of anhydrous NMe₄F from tetramethylammonium phenoxides and sulfuryl fluoride (SO₂F₂), both inexpensive commodity chemicals.¹⁹ Phenoxides were shown to react with sulfuryl fluoride to form anhydrous NMe₄F, which can then be used for the room temperature S_NAr fluorination of **1** (Scheme 2.3). This method precludes the necessity to generate NMe₄F in methanol (or other protic solvents) followed by rigorous drying to ensure sufficiently anhydrous material to effect the transformation. However, one disadvantage of this approach is that the byproducts of the reaction (aryl fluorosulfonate, diaryl sulfate) can be challenging to remove by column chromatography. Nonetheless, this is an attractive approach for the *in situ* generation of anhydrous NMe₄F for mild S_NAr fluorination reactions.

Scheme 2.3. *in Situ* Generation of NMe₄F (anh) from Phenoxides and Sulfuryl Fluoride



The findings concerning the rate of reaction as a function of leaving group have potential implications for application to positron emission tomography (PET). Faster reaction times are required for applications in PET due to the short half-life of [¹⁸F].²⁰ It is possible that other halide leaving groups (Br, I) might be better suited for the faster reaction times required for radiofluorination. Furthermore, we demonstrated that the rate of reaction increases with increasing temperature and modest yields of fluorinated products can be obtained in a relatively short amount of time.

2.7. Experimental Details and Characterization

2.7.1. General Information

NMR spectra were obtained on a 400 MHz (400.52 MHz for ¹H; 376.87 MHz for ¹⁹F; 100.71 MHz for ¹³C), a 500 MHz (500.01 MHz for ¹H; 125.75 MHz for ¹³C; 470.56 MHz for ¹⁹F), a 700 MHz (699.76 MHz for ¹H; 175.95 MHz for ¹³C), or a 500 MHz (499.90 MHz for ¹H; 125.70 for ¹³C) NMR spectrometer. ¹H and ¹³C chemical shifts are reported in parts per million (ppm) relative to residual solvent peaks (CDCl₃; ¹H δ 7.26 ppm; ¹³C δ 77.16 ppm). ¹⁹F NMR spectra are referenced based on the internal standard 1,3,5-trifluorobenzene, which appears at −108.33 ppm. Multiplicities are reported as follows: singlet (s), doublet (d), triplet (t), quartet (q), multiplet (m), doublet of doublets (dd), doublet of triplets (dt). Coupling constants (*J*) are reported in Hz. For GCMS analysis, the products were separated on a crossbond 5% diphenyl-95% dimethyl polysiloxane column (30 m length by 0.25 mm ID, 0.25 μm df). Helium was employed as the carrier gas, with

a constant column flow of 1.5 mL/min. The injector temperature was held constant at 250 °C. The GC oven temperature program for low molecular weight compounds was as follows: 32 °C hold 5 min, ramp 15 °C/min to 250 °C, and hold for 1.5 min. The GC oven temperature program for medium molecular weight compounds was as follows: 60 °C, hold for 4 minutes, ramp 15 °C/min to 250 °C. Melting points are uncorrected. High-resolution mass spectra were recorded on a Magnetic Sector mass spectrometer.

2.7.2. Materials and Methods

Commercial reagents were used as received unless otherwise noted. Anhydrous tetramethylammonium fluoride, spray dried potassium fluoride, sulfolane, 2-nitropyridine, 2-hydroxypyridine, 4-chloro-7-(trifluoromethyl)quinoline, 3-chloro-6-phenylpyridazine, 2-chloro-5-nitropyridine, 1-chloroisoquinoline, and 4-chlorobenzonitrile were obtained from Sigma Aldrich. Anhydrous *N,N*-dimethylformamide 99.8% (DMF), acetonitrile (anhydrous), dimethyl sulfoxide (anhydrous), *N*-methyl-2-pyrrolidone (NMP), 2-chlorobenzonitrile, phosphorous (V) oxide, 2-chloro-4-methylquinoline, potassium carbonate, 2-chloro-3-(trifluoromethyl)pyridine, 2-bromopyridine, 2-chloro-5-cyanopyridine, ethyl 4-nitrobenzoate, and 2-chloro-3-cyanopyridine were obtained from Alfa Aesar. Tetramethylammonium chloride was purchased from Acros and dried under vacuum at 60 °C prior to use. Tetramethylammonium fluoride tetrahydrate, dimethylacetamide, 2-chloropyridine, 2-iodopyridine, phosphorus oxychloride, 4-nitrobenzophenone, and 2,6-dichloropyridine were purchased from Acros. 3-Chlorobenzonitrile and 2,8-quinolinediol were purchased from Ark Pharm. Methanol, sodium fluoride, pentanes, hexanes, ethyl acetate, diethyl ether, and dichloromethane were purchased from Fisher Scientific. Cesium fluoride was purchased from Chemetall. Lithium fluoride was purchased from J. T. Baker. 2-Nitrobenzonitrile and 2-chloroquinoline were purchased from TCI America. 2-Cyanophenol and benzyl bromide were purchased from Fluka. Triflic anhydride and 2-chloro-5-iodopyridine were purchased from Oakwood Chemicals. 1,3,5-Trifluorobenzene, 2-chloro-4-cyanopyridine, 2-bromobenzonitrile, 2-iodobenzonitrile, and 2-chloropyrazine were purchased from Matrix. 2-Chloro-5-bromopyridine and 2-nitro-3-chloropyridine were purchased from Chem-Imprex International. Isopropyl chloroarylpicolinates were prepared using previously described

methods by The Dow Chemical Company.⁵ 2-Cyanophenyl trifluoromethanesulfonate and pyridine-2-yl trifluoromethanesulfonate were prepared using literature procedures²¹ and dried over P₂O₅ prior to use. 8-(Benzyloxy)-2-chloroquinoline were prepared using literature procedures¹⁷ and dried over P₂O₅ prior to use.

2.7.3. General Procedures for Fluorination Reactions

Experimental Details for Fluorination Reactions Reported in Table 2.1. In a drybox, substrate **1** (0.1 mmol, 1.0 equiv) and anhydrous tetramethylammonium fluoride (NMe₄F) were weighed into a 4 mL vial equipped with a micro stirbar. DMF (0.5 mL) was added, and the reaction vial was sealed with a Teflon-lined cap, removed from the drybox, and stirred at the designated temperature for 24 h. The reaction was then cooled to room temperature, diluted with dichloromethane (2.5 mL), and an internal standard (1, 3, 5-trifluorobenzene, 100 μ L of a 0.5 M solution in toluene) was added. An aliquot was removed for analysis by ¹⁹F NMR spectroscopy and GCMS.

Experimental Details for the Wet Reactions Reported in Table 2.2. A solution of anhydrous DMF (2 mL) and deionized water that was sparged with N₂ was prepared in a Schlenk flask and sparged with N₂ for 15 minutes. The Schlenk tube was then pumped into a drybox. In a drybox, substrate **1** (0.1 mmol, 1.0 equiv) and anhydrous NMe₄F (0.2 mmol, 2.0 equiv) were weighed into a 4 mL vial equipped with a micro stirbar. The water-DMF solution was then added (0.5 mL), and the reaction vial was sealed with a Teflon-lined cap, removed from the drybox, and stirred at room temperature for 24 h. The reaction was then diluted with dichloromethane (2.5 mL), and an internal standard (1, 3, 5-trifluorobenzene, 100 μ L of a 0.5 M solution in toluene) was added. An aliquot was removed for analysis by ¹⁹F NMR spectroscopy and GCMS.

Experimental Details for the Use of NMe₄F as a Phase Transfer Reagent Reported in Table 2.3. In a drybox, substrate **1** (0.1 mmol, 1.0 equiv), anhydrous NMe₄F (0.05 mmol, 0.5 equiv), and alkali metal fluoride (0.2 mmol, 2.0 equiv) were weighed into a 4 mL vial equipped with a micro stirbar. DMF (0.5 mL) was added, and the reaction vial was sealed with a Teflon-lined cap, removed from the drybox, and stirred at room temperature for 24

h. The reaction was diluted with dichloromethane (2.5 mL), and an internal standard (1, 3, 5-trifluorobenzene, 100 μ L of a 0.5 M solution in toluene) was added. An aliquot was removed for analysis by ^{19}F NMR spectroscopy.

Experimental Details for the Solvent Screen Reported in Table 2.4. In a drybox, substrate **1** (0.1 mmol, 1.0 equiv) and anh NMe₄F (0.2 mmol, 2.0 equiv) were weighed into a 4 mL vial equipped with a micro stirbar. Anhydrous solvent (0.5 mL) was added, and the reaction vial was sealed with a Teflon-lined cap, removed from the drybox, and stirred at room temperature for 24 h. The reaction was diluted with dichloromethane (2.5 mL), and an internal standard (1, 3, 5-trifluorobenzene, 100 μ L of a 0.5 M solution in toluene) was added. An aliquot was removed for analysis by ^{19}F NMR spectroscopy and GCMS.

Experimental Details for the Concentration Time Studies Reported in Figure 2.1. In a drybox, substrate **1** (0.1 mmol, 1.0 equiv) and anh NMe₄F (0.2 mmol, 2.0 equiv) were weighed into a 4 mL vial equipped with a micro stirbar. DMF was added, and the reaction vial was sealed with a Teflon-lined cap, removed from the drybox, and stirred at room temperature for the designated time. The reaction was then diluted with dichloromethane (2.5 mL), and an internal standard (1, 3, 5-trifluorobenzene, 100 μ L of a 0.5 M solution in toluene) was added. An aliquot was removed for analysis by ^{19}F NMR spectroscopy and GCMS.

Experimental Details for the Fluorination of 2-Substituted Benzonitrile Substrates Reported in Table 2.5 and Table 2.6. For reactions with anhydrous NMe₄F: In a drybox, substrate **3a–e** or **5a–e** (0.1 mmol, 1.0 equiv) and anh NMe₄F (0.2 mmol, 2 equiv) were weighed into a 4 mL vial equipped with a micro stirbar. DMF (0.5 mL) was added, and the reaction vial was sealed with a Teflon-lined cap, removed from the drybox, and stirred at the given temperature for the given time. The reactions were cooled to room temperature, diluted with dichloromethane (2.5 mL), and an internal standard (1, 3, 5-trifluorobenzene, 100 μ L of a 0.5 M solution in toluene) was added. An aliquot was removed for analysis by ^{19}F NMR spectroscopy and GCMS.

For reactions with CsF: In a drybox, substrate **3a–e** or **5a–e** (0.1 mmol, 1.0 equiv) and CsF (0.2 mmol, 2 equiv) were weighed into a 4 mL vial equipped with a micro stirbar. DMF (0.5 mL) was added, and the reaction vial was sealed with a Teflon-lined cap, removed from the drybox, and stirred at 140 °C for 24 h. The reactions were cooled to room temperature, diluted with dichloromethane (2.5 mL), and an internal standard (1, 3, 5-trifluorobenzene, 100 μ L of a 0.5 M solution in toluene) was added. An aliquot was removed for analysis by ^{19}F NMR spectroscopy and GCMS.

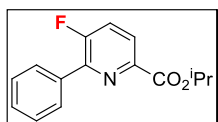
Experimental Details for the Reaction Profiles Reported in Figures 2.2 and 2.3. In a drybox, substrate **3a–e** or **5a–e** (0.1 mmol, 1.0 equiv) and anh NMe₄F (0.2 mmol, 2 equiv) were weighed into a 4 mL vial equipped with a micro stirbar. DMF (0.5 mL) was added, and the reaction vial was sealed with a Teflon-lined cap, removed from the drybox, and stirred at 80 °C for the given time. The reactions were cooled in liquid N₂, diluted with dichloromethane (2.5 mL), and an internal standard (1, 3, 5-trifluorobenzene, 100 μ L of a 0.5 M solution in toluene) was added. An aliquot was removed for analysis by ^{19}F NMR spectroscopy.

General Procedure for Isolated Yields Reported in Figures 2.4–2.7. In a drybox, anh NMe₄F (93 mg, 1 mmol, 2 equiv) and the appropriate aryl chloride or nitroarene substrate (0.5 mmol, 1 equiv) were weighed into a 4 mL vial equipped with a micro stirbar. DMF (2.5 mL) was added, and the reaction vial was sealed with a Teflon-lined cap, removed from the drybox and stirred at room temperature for 24 h. The reaction was then diluted with dichloromethane (15 mL) and transferred to a separatory funnel. The organic layer was washed with water (3 \times 25 mL) and brine (1 \times 25 mL), dried over MgSO₄, and concentrated in vacuo. The crude mixture was purified by flash column chromatography on silica gel using gradients of hexanes and either diethyl ether or ethyl acetate as eluent.

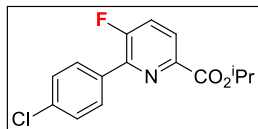
General Procedure for NMR Yields Reported in Figures 2.4–2.7. In a drybox, anh NMe₄F (18.6 mg, 0.2 mmol, 2 equiv) and the appropriate aryl chloride or nitroarene substrate (0.1 mmol, 1 equiv) were weighed into a 4 mL vial equipped with a micro stirbar. DMF (0.5 mL) was added, and the reaction vial was sealed with a Teflon-lined cap, removed from

the drybox and stirred at room temperature unless otherwise noted for 24 h. The reaction was diluted with dichloromethane and an internal standard (1, 3, 5-trifluorobenzene, 100 μ L of a 0.5 M solution in toluene) was added. An aliquot was removed for analysis by ^{19}F NMR spectroscopy and GCMS.

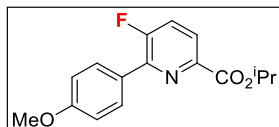
2.7.4. Product Synthesis and Characterization



Isopropyl 5-fluoro-6-phenylpicolinate (2). The general procedure was followed using *isopropyl 5-chloro-6-phenylpicolinate (1)* (137.5 mg, 0.5 mmol, 1.0 equiv), providing **2** as a colorless oil (106.0 mg, 82% yield, $R_f = 0.61$ in 70% hexanes/30% Et_2O). ^1H , $^{13}\text{C}\{^1\text{H}\}$, and ^{19}F NMR experimental data match those reported in the literature.⁵ HRMS ESI⁺ (m/z): $[\text{M} + \text{H}]^+$ calcd for $\text{C}_{15}\text{H}_{15}\text{FNO}_2$ 260.1081; found 260.1080. The yield reported in the Figure 2.4 (82%) represents an average of two runs [82% and 81%].

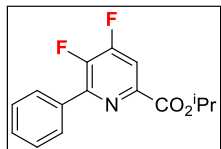


Isopropyl 5-fluoro-6-(p-chlorophenyl)picolinate (7). The general procedure was followed using *isopropyl 5-chloro-6-(p-chlorophenyl)picolinate* (154.5 mg, 0.5 mmol, 1.0 equiv), providing **7** as a white solid (122.0 mg, 83% yield, $R_f = 0.59$ in 70% hexanes/30% Et_2O , mp = 73–76 $^\circ\text{C}$). ^1H , $^{13}\text{C}\{^1\text{H}\}$, and ^{19}F NMR experimental data match those reported in the literature.⁶ HRMS ESI⁺ (m/z): $[\text{M} + \text{H}]^+$ calcd for $\text{C}_{15}\text{H}_{14}\text{ClFNO}_2$ 294.0692; found 294.0689. The yield reported in Figure 2.4 (85%) represents an average of two runs [83% and 87%].

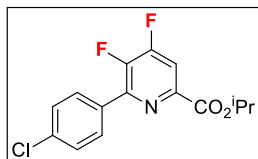


Isopropyl 5-fluoro-6-(p-methoxyphenyl)picolinate (8). The general procedure was followed using *isopropyl 5-chloro-6-(p-methoxyphenyl)picolinate* (152.5 mg, 0.5 mmol, 1.0 equiv), providing **8** as a white solid (138.0 mg, 96% yield, $R_f = 0.38$ in 70%

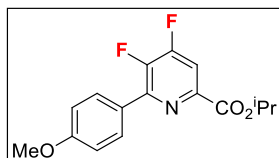
hexanes/30% Et₂O, mp = 46–48 °C). ¹H, ¹³C{¹H}, and ¹⁹F NMR experimental data match those reported in the literature.⁶ HRMS ESI⁺ (*m/z*): [M + H]⁺ calcd for C₁₆H₁₇FNO₃ 290.1187; found 290.1185. The yield reported in Figure 2.4 (93%) represents an average of two runs [96% and 90%].



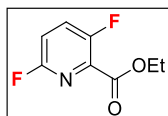
Isopropyl 4,5-difluoro-6-phenylpicolinate (9). The general procedure was followed using *isopropyl 4,5-dichloro-6-phenylpicolinate* (154.5 mg, 0.5 mmol, 1.0 equiv) and anhydrous NMe₄F (140.0 mg, 1.5 mmol, 3.0 equiv), providing **9** as a colorless oil (121.0 mg, 87% yield, R_f = 0.64 in 70% hexanes/30% Et₂O). ¹H, ¹³C{¹H}, and ¹⁹F NMR experimental data match those reported in the literature.⁵ HRMS ESI⁺ (*m/z*): [M + H]⁺ calcd for C₁₅H₁₄F₂NO₂ 278.0987; found 278.0986. The yield reported in Figure 2.4 (88%) represents an average of two runs [87% and 88%].



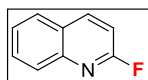
Isopropyl 4,5-difluoro-6-(p-chlorophenyl)picolinate (10). The general procedure was followed using *isopropyl 4,5-dichloro-6-(p-chlorophenyl)picolinate* (171.5 mg, 0.5 mmol, 1.0 equiv) and anhydrous NMe₄F (140.0 mg, 1.5 mmol, 3.0 equiv), providing **10** as a white solid (138.0 mg, 89% yield, R_f = 0.69 in 70% hexanes/30% Et₂O, mp = 74–76 °C). ¹H, ¹³C{¹H}, and ¹⁹F NMR experimental data match those reported in the literature.⁵ HRMS ESI⁺ (*m/z*): [M + H]⁺ calcd for C₁₅H₁₃ClF₂NO₂ 312.0597; found 312.0597. The yield reported in Figure 2.4 (84%) represents an average of two runs [89% and 79%].



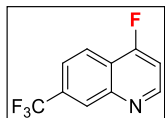
Isopropyl 4,5-difluoro-6-(*p*-methoxyphenyl)picolinate (**11**). The general procedure was followed using isopropyl 4,5-dichloro-6-(*p*-methoxyphenyl)picolinate (179.5 mg, 0.5 mmol, 1.0 equiv) and anhydrous NMe_4F (140 mg, 1.5 mmol, 3.0 equiv), providing **11** as a white solid (136.0 mg, 89% yield, $R_f = 0.61$ in 70% hexanes/30% Et_2O , mp = 37–38 °C). ^1H , $^{13}\text{C}\{^1\text{H}\}$, and ^{19}F NMR experimental data match those reported in the literature.⁵ HRMS ESI⁺ (m/z): $[\text{M} + \text{H}]^+$ calcd for $\text{C}_{16}\text{H}_{16}\text{F}_2\text{NO}_3$ 308.1093; found 308.1091. The yield reported in Figure 2.4 (89%) represents an average of two runs [89% and 88%].



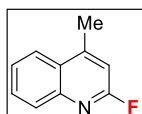
Ethyl 3,6-difluoropicolinate (**12**). The general procedure was followed using ethyl 3,6-dichloropicolinate (21.9 mg, 0.1 mmol, 1.0 equiv) providing a mixture of **12** in 26% yield and ethyl 3-chloro-6-fluoropicolinate in 64% yield as determined by ^{19}F NMR spectroscopic analysis of the crude reaction mixture. The product **12** showed a ^{19}F NMR signals at –67 (1F) and –124 (1F) ppm in DCM (lit. –69.4 (1F), –122.5 (1F) ppm in CDCl_3).⁵ The monofluorinated product shows a ^{19}F NMR signal at –70.6 ppm.



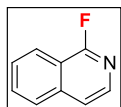
2-Fluoroquinoline (**13**). The general procedure was followed using 2-chloroquinoline (82.0 mg, 0.5 mmol, 1.0 equiv), providing **13** as a colorless oil (56.0 mg, 77% yield, $R_f = 0.51$ in 70% hexanes/30% Et_2O). ^1H , $^{13}\text{C}\{^1\text{H}\}$, and ^{19}F NMR experimental data match those reported in the literature.⁵ HRMS ESI⁺ (m/z): $[\text{M} + \text{H}]^+$ calcd for $\text{C}_9\text{H}_7\text{FN}$ 148.0557; found 148.0555. The yield reported in Figure 2.5 (79%) represents an average of two runs [77% and 80%].



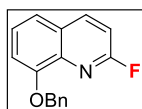
4-Fluoro-7-(trifluoromethyl)quinoline (**14**). The general procedure was followed using 4-chloro-7-(trifluoromethyl)quinoline (115.5 mg, 0.5 mmol, 1.0 equiv), providing **14** as a white solid (88.0 mg, 82% yield, R_f = 0.38 in 70% hexanes/30% Et₂O, mp = 84–86 °C). ¹H, ¹³C{¹H}, and ¹⁹F NMR experimental data match those reported in the literature.⁵ HRMS ESI⁺ (m/z): [M + H]⁺ calcd for C₁₀H₆F₄N 216.0431; found 216.0430. The yield reported in Figure 2.5 (79%) represents an average of two runs [82% and 75%].



2-Fluoro-4-methylquinoline (**15**). The general procedure was followed using 2-chloro-4-methylquinoline (17.7 mg, 0.1 mmol, 1.0 equiv), providing **15** in 11% yield as determined by ¹⁹F NMR spectroscopic analysis of the crude reaction mixture. The product showed a ¹⁹F NMR signals at –64.5 (1F) ppm in DCM (lit. –63.8 (1F) ppm in CDCl₃).²²

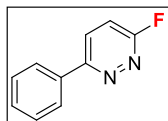


1-Fluoroisoquinoline (**16**). The general procedure was followed using 1-chloroisoquinoline (81.5 mg, 0.5 mmol, 1.0 equiv), providing **16** as a colorless oil (59.0 mg, 80% yield, R_f = 0.53 in 70% hexanes/30% Et₂O). ¹H, ¹³C{¹H}, and ¹⁹F NMR experimental data match those reported in the literature.⁶ HRMS ESI⁺ (m/z): [M + H]⁺ calcd for C₉H₇FN 148.0557; found 148.0555. The yield reported in Figure 2.5 (78%) represents an average of two runs [80% and 76%].

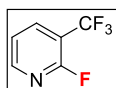


8-(Benzyloxy)-2-fluoroquinoline (**17**). The general procedure was followed using 8-(benzyloxy)-2-chloroquinoline (134.5 mg, 0.1 mmol, 1.0 equiv), providing **17** as a white

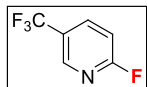
solid (120.0 mg, 95% yield, $R_f = 0.38$ in 70% hexanes/30% Et₂O, mp = 67–69 °C). ¹H and ¹⁹F NMR experimental data match those reported in the literature. ¹⁷c ¹³C{¹H} NMR (125.75 MHz, CDCl₃): δ 161.5 (d, $J = 242$ Hz), 153.4, 142.0 (d, $J = 9.5$ Hz), 138.7, 137.6 (d, $J = 15.3$ Hz), 136.8, 128.6, 128.0 (d, $J = 1.9$ Hz), 127.0, 126.9, 126.1 (d, $J = 2.9$ Hz), 119.6, 111.6, 110.6 (d, $J = 42.9$ Hz), 70.7. HRMS ESI⁺ (m/z): [M + H]⁺ calcd for C₁₆H₁₃FNO, 254.0976; found 254.0975. The yield reported in Figure 2.5 (91%) represents an average of two runs [95% and 86%].



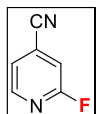
3-Fluoro-6-phenylpyridazine (**18**). The general procedure was followed using 3-chloro-6-phenylpyridazine (95.3 mg, 0.5 mmol, 1.0 equiv), providing **18** as a white solid (79.0 mg, 91% yield, $R_f = 0.38$ in 70% hexanes/30% Et₂O, mp = 129–131 °C). ¹H NMR (500 MHz, CDCl₃): δ 8.01–7.98 (multiple peaks, 3H), 7.53–7.49 (multiple peaks, 3H), 7.29 (dd, $J = 9.5, 2.0$ Hz, 1H). ¹³C{¹H} NMR (175.95 MHz, CDCl₃): δ 166.7 (d, $J = 245$ Hz), 159.2 (d, $J = 3.5$ Hz), 135.1 (d, $J = 2.1$ Hz), 130.2, 129.5 (d, $J = 7.6$ Hz), 129.0, 127.0, 116.1 (d, $J = 33.4$ Hz). ¹⁹F NMR (100 MHz, CDCl₃): –84.8 (d, $J = 1.5$ Hz). IR (cm^{–1}): 1584, 1556, 1450, 1427, 1278, 1108, 852, 778, 739. HRMS ESI⁺ (m/z): [M + H]⁺ calcd for C₁₀H₇FN₂, 175.0666; found 175.0663. The yield reported in Figure 2.5 (90%) represents an average of two runs [91% and 88%].



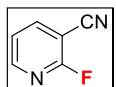
2-Fluoro-3-(trifluoromethyl)pyridine (**19**). The general procedure was followed using 2-chloro-3-(trifluoromethyl)pyridine (18.1 mg, 0.1 mmol, 1.0 equiv), providing **19** in 100% yield as determined by ¹⁹F NMR spectroscopic analysis of the crude reaction mixture. The product showed a ¹⁹F NMR signals at –63.42 (3F) and –68.06 (1F) ppm in DCM (lit. –60.62 (3F), –63.01 (1F) ppm in DMSO).^{4a} The identity of the product was further confirmed by GCMS analysis ($m/z = 165$). The yield reported in Figure 2.6 (97%) represents an average of two runs [100% and 94%].



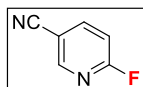
2-Fluoro-5-(trifluoromethyl)pyridine (**20**). The general procedure was followed using 2-chloro-5-(trifluoromethyl)pyridine (18.1 mg, 0.1 mmol, 1.0 equiv), providing **20** in 95% yield as determined by ^{19}F NMR spectroscopic analysis of the crude reaction mixture. The product showed ^{19}F NMR signals at -62.68 (3F) and -63.51 (1F) ppm in DCM (lit. -60.62 (3F), -63.01 (1F) ppm in DMSO).^{4a} The identity of the product was further confirmed by GCMS analysis ($m/z = 165$). The yield reported in Figure 2.6 (98%) represents an average of two runs [95% and 100%].



2-Fluoro-4-cyanopyridine (**21**). The general procedure was followed using 2-chloro-4-cyanopyridine (13.8 mg, 0.1 mmol, 1.0 equiv), providing **21** in 100% yield as determined by ^{19}F NMR spectroscopic analysis of the crude reaction mixture. The ^{19}F NMR spectral data matched that of an authentic sample (Synthonix, s, -64.94 ppm). The identity of the product was further confirmed by GCMS analysis ($m/z = 122$). The yield reported in Figure 2.6 (95%) represents an average of two runs [100% and 89%].



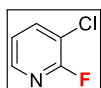
2-Fluoro-3-cyanopyridine (**22**). The general procedure was followed using 2-chloro-3-cyanopyridine (13.8 mg, 0.1 mmol, 1.0 equiv), providing **22** in 93% yield as determined by ^{19}F NMR spectroscopic analysis of the crude reaction mixture. The product showed a ^{19}F NMR signal at -62.66 ppm in DCM (lit. -60.0 ppm in CDCl_3).²³ The identity of the product was further confirmed by GCMS analysis ($m/z = 122$). The yield reported in Figure 2.6 (91%) represents an average of two runs [93% and 88%].



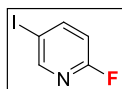
2-Fluoro-5-cyanopyridine (**23**). The general procedure was followed using 2-chloro-5-cyanopyridine (13.8 mg, 0.1 mmol, 1.0 equiv), providing **23** in 87% yield as determined by ^{19}F NMR spectroscopic analysis of the crude reaction mixture. The ^{19}F NMR spectral data matched that of an authentic sample (Matrix Scientific, s, -59.41 ppm). The identity of the product was further confirmed by GCMS analysis ($m/z = 122$). The yield reported in the Figure 2.6 (94%) represents an average of two runs [87% and 100%].



2-Fluoropyrazine (**24**). The general procedure was followed using 2-chloropyrazine (11.4 mg, 0.1 mmol, 1.0 equiv), providing **24** in 99% yield as determined by ^{19}F NMR spectroscopic analysis of the crude reaction mixture. The product showed a ^{19}F NMR signal at -81.00 ppm in DCM (lit. -80.4 ppm in DMSO).^{4a} The identity of the product was further confirmed by GCMS analysis ($m/z = 98$). The yield reported in Figure 2.6 (92%) represents an average of two runs [99% and 84%].

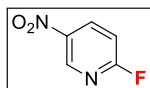


2-Fluoro-3-chloropyridine (**25**). The general procedure was followed using 2-nitro-3-chloropyridine (15.8 mg, 0.1 mmol, 1.0 equiv), providing **25** in 94% yield as determined by ^{19}F NMR spectroscopic analysis of the crude reaction mixture. The product showed a ^{19}F NMR signal at -72.54 ppm in DCM (lit. -73.03 ppm in DMSO).^{4a} The identity of the product was further confirmed by GCMS analysis ($m/z = 131$). The yield reported in Figure 2.6 (94%) represents an average of two runs [94% and 94%].

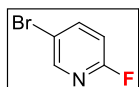


2-Fluoro-5-iodopyridine (**26**). The general procedure was followed using 2-chloro-5-iodopyridine (23.9 mg, 0.1 mmol, 1.0 equiv), providing **26** in 85% yield as determined by

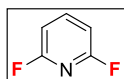
^{19}F NMR spectroscopic analysis of the crude reaction mixture. The ^{19}F NMR spectral data matched that of an authentic sample (Sigma Aldrich, m, -71.28 ppm). The identity of the product was further confirmed by GCMS analysis ($m/z = 223$). The yield reported in Figure 2.6 (86%) represents an average of two runs [85% and 87%].



2-Fluoro-5-nitropyridine (**27**). The general procedure was followed using 2-chloro-5-nitropyridine (15.8 mg, 0.1 mmol, 1.0 equiv), providing **27** in 70% yield as determined by ^{19}F NMR spectroscopic analysis of the crude reaction mixture. The ^{19}F NMR spectral data matched that of an authentic sample (Oakwood Chemicals, s, -59.14 ppm). The identity of the product was further confirmed by GCMS analysis ($m/z = 142$). The yield reported in Figure 2.6 (73%) represents an average of two runs [70% and 76%].

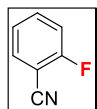


2-Fluoro-5-bromopyridine (**28**). The general procedure was followed using 2-chloro-5-bromopyridine (19.1 mg, 0.1 mmol, 1.0 equiv), providing **28** in 100% yield as determined by ^{19}F NMR spectroscopic analysis of the crude reaction mixture. The ^{19}F NMR spectral data matched that of an authentic sample (Oakwood Products, s, -71.69 ppm). The identity of the product was further confirmed by GCMS analysis ($m/z = 175$). The yield reported in Figure 2.6 (94%) represents an average of two runs [100% and 88%].



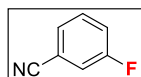
2,6-Difluoropyridine (**29**). The general procedure was followed using 2,6-dichloropyridine (14.7 mg, 0.1 mmol, 1.0 equiv) and anhydrous NMe_4F (27.9 mg, 0.3 mmol, 3.0 equiv), providing **29** in 91% yield as determined by ^{19}F NMR spectroscopic analysis of the crude reaction mixture. The ^{19}F NMR spectral data matched that of an authentic sample (Alfa Aesar, m, -68.91 ppm). The identity of the product was further confirmed by GCMS analysis ($m/z =$

115). The yield reported in Figure 2.6 (93%) represents an average of two runs [91% and 95%].



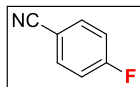
2-Fluorobenzonitrile (**4**). The general procedure was followed using 2-chlorobenzonitrile (13.7 mg, 0.1 mmol, 1.0 equiv) at room temperature, providing **4** in 34% yield as determined by ^{19}F NMR spectroscopic analysis of the crude reaction mixture. The ^{19}F NMR spectral data matched that of an authentic sample (Ark Pharm, m, -108.02 ppm). The identity of the product was further confirmed by GCMS analysis ($m/z = 121$). The yield reported in Figure 2.7 (34%) represents an average of two runs [34% and 33%].

The general procedure was followed using 2-chlorobenzonitrile (13.7 mg, 0.1 mmol, 1.0 equiv) at $80\text{ }^{\circ}\text{C}$, providing **4** in 98% yield as determined by ^{19}F NMR spectroscopic analysis of the crude reaction mixture. The ^{19}F NMR spectral data matched that of an authentic sample (Ark Pharm, m, -108.02 ppm). The identity of the product was further confirmed by GCMS analysis ($m/z = 121$). The yield reported in Figure 2.7 (94%) represents an average of three runs [98%, 83% and 100%].



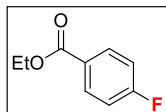
3-Fluorobenzonitrile (**30**). The general procedure was followed using 3-chlorobenzonitrile (13.7 mg, 0.1 mmol, 1.0 equiv) at room temperature, providing **30** in $<1\%$ yield as determined by ^{19}F NMR spectroscopic analysis of the crude reaction mixture. The yield reported in Figure 2.7 ($<1\%$) represents an average of two runs [$<1\%$ and $<1\%$].

The general procedure was followed using 3-benzonitrile (13.7 mg, 0.1 mmol, 1.0 equiv) at $80\text{ }^{\circ}\text{C}$, providing **30** in 6% yield as determined by ^{19}F NMR spectroscopic analysis of the crude reaction mixture. The ^{19}F NMR spectral data matched that of an authentic sample (Oakwood Chemicals, m, -111.18 ppm). The identity of the product was further confirmed by GCMS analysis ($m/z = 121$). The yield reported in Figure 2.7 (7%) represents an average of two runs [6% and 7%].



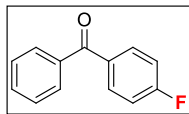
4-Fluorobenzonitrile (**31**). The general procedure was followed using 4-chlorobenzonitrile (13.7 mg, 0.1 mmol, 1.0 equiv) at room temperature, providing **31** in 35% yield as determined by ^{19}F NMR spectroscopic analysis of the crude reaction mixture. The ^{19}F NMR spectral data matched that of an authentic sample (Oakwood Chemicals, m, -103.89 ppm). The identity of the product was further confirmed by GCMS analysis ($m/z = 121$). The yield reported in Figure 2.7 (37%) represents an average of two runs [35% and 38%].

The general procedure was followed using 4-chlorobenzonitrile (13.7 mg, 0.1 mmol, 1.0 equiv) at $80\text{ }^{\circ}\text{C}$, providing **31** in 79% yield as determined by ^{19}F NMR spectroscopic analysis of the crude reaction mixture. The ^{19}F NMR spectral data matched that of an authentic sample (Oakwood Chemicals, m, -103.89 ppm). The identity of the product was further confirmed by GCMS analysis ($m/z = 121$). The yield reported in Figure 2.7 (80%) represents an average of two runs [79% and 81%].



Ethyl 4-Fluorobenzoate (**32**). The general procedure was followed using ethyl 4-chlorobenzoate (18.4 mg, 0.5 mmol, 1.0 equiv). No product was observed by ^{19}F NMR spectroscopic analysis.

The general procedure was followed using ethyl 4-nitrobenzoate (97.5 mg, 0.5 mmol, 1.0 equiv), providing **32** as a colorless oil (51.0 mg, 61% yield, $R_f = 0.58$ in 90% hexanes/10% EtOAc). ^1H , $^{13}\text{C}\{^1\text{H}\}$, and ^{19}F NMR experimental data match those reported in the literature.⁶ HRMS ESI⁺ (m/z): $[\text{M}]^+$ calcd for $\text{C}_9\text{H}_9\text{FO}_2$ 168.0587; found 168.0584. The yield reported in Figure 2.7 (63%) represents an average of two runs [61% and 65%].



4-Fluorobenzophenone (**33**). The general procedure was followed using 4-chlorobenzophenone (21.6 mg, 0.5 mmol, 1.0 equiv), providing **33** in 5% yield as determined by ^{19}F NMR spectroscopic analysis of the crude reaction mixture.

The general procedure was followed using 4-nitrobenzophenone (113.6 mg, 0.5 mmol, 1.0 equiv), providing **33** as a white solid (89.0 mg, 89% yield, R_f = 0.54 in 90% hexanes/10% EtOAc, mp = 47–48 °C). ^1H , $^{13}\text{C}\{^1\text{H}\}$, and ^{19}F NMR experimental data match those reported in the literature.⁵ HRMS ESI⁺ (m/z): $[\text{M} + \text{H}]^+$ calcd for $\text{C}_{13}\text{H}_{10}\text{FO}$ 201.0710; found 201.0708. The yield reported in Figure 2.7 (90%) represents an average of two runs [89% and 90%].

2.8. References

- (1) Adapted with permission from: Schimler, S. D.; Ryan, S. J.; Bland, D. C.; Anderson, J. E.; Sanford, M. S. *J. Org. Chem.* **2015**, *80*, 12137–12145. ©
- (2) (a) Wang, J.; Sánchez-Roselló, M.; Aceña, J. L.; del Pozo, C.; Sorochinsky, A. E.; Fustero, S.; Soloshonok, V. A.; Liu, H. *Chem. Rev.* **2014**, *114*, 2432–2506. (b) Jeschke, P. *Pest Manage. Sci.* **2010**, *66*, 10–27. (c) Purser, S.; Moore, P. R.; Swallow, S.; Gouverneur, V. *Chem. Soc. Rev.* **2008**, *37*, 320–330. (d) Müller, K.; Faeh, C.; Diederich, F. *Science* **2007**, *317*, 1881–1886. (e) Kirk, K. L. *Org. Process Res. Dev.* **2008**, *12*, 305–321.
- (3) (a) Adams, D. J.; Clark, J. H. *Chem. Soc. Rev.* **1999**, *28*, 225–231. (b) Langlois, B.; Gilbert, L.; Forat, G. Fluorination of aromatic compounds by halogen exchange with fluoride anions (“halex” reaction). In *Industrial Chemistry Library*; Jean-Roger, D., Serge, R., Eds.; Elsevier: New York, 1996; pp 244–292. (c) Champagne, P. A.; Desroches, J.; Hamel, J.-D.; Vandamme, M.; Paquin, J.-F. *Chem. Rev.* **2015**, *115*, 9073–9174. (d) Clark, J. H.; Wails, D.; Bastock, T. W. *Aromatic Fluorination*; CRC Press, Boca Raton, FL, 1996.
- (4) (a) Sun, H.; DiMagno, S. G. *Angew. Chem., Int. Ed.* **2006**, *45*, 2720–2725. (b) Sun, H.; DiMagno, S. G. *J. Am. Chem. Soc.* **2005**, *127*, 2050–2051. (c) DiMagno, S. G.; Sun, H. Anhydrous Fluoride Salts and Reagents and Methods for Their Production. Patent US20060089514A1, April 27, 2006.
- (5) Allen, L. J.; Muhuhi, J. M.; Bland, D. C.; Merzel, R.; Sanford, M. S. *J. Org. Chem.* **2014**, *79*, 5827–5833.
- (6) Ryan, S. J.; Schimler, S. D.; Bland, D. C.; Sanford, M. S. *Org. Lett.* **2015**, *17*, 1866–1869.

- (7) (a) Dermeik, S.; Sasson, Y. *J. Org. Chem.* **1989**, *54*, 4827–4828. (b) Tunder, F.; Siegel, B. *J. Inorg. Nucl. Chem.* **1963**, *25*, 1097–1098. (c) Christie, K. O.; Wilson, W. W.; Wilson, R. D.; Bau, R.; Feng, J. *J. Am. Chem. Soc.* **1990**, *112*, 7619–7625. (d) Christie, K. O.; Wilson, W. W. Anhydrous, chloride- and bifluoride-free tetramethylammonium fluoride. Patent EP0457966A1, November 27, 1991. (e) Urban, G.; Dötzer, R. Method of producing onium fluorides selected from the group consisting of nitrogen, antimony, boron, and arsenic. Patent US3388131A1, June 11, 1968.
- (8) Grushin, V. V.; Marshall, W. J. *Organometallics* **2008**, *27*, 4825–4828.
- (9) (a) Adams, D. J.; Clark, J. H.; McFarland, H.; Nightingale, D. J. *J. Fluorine Chem.* **1999**, *94*, 51–55. (b) Adams, D. J.; Clark, J. H.; Nightingale, D. J. *Tetrahedron* **1999**, *55*, 7725–7738. (c) Adams, D. J.; Clark, J. H.; McFarland, H. *J. Fluorine Chem.* **1998**, *92*, 127–129. (d) Boechat, N.; Clark, J. H. *J. Chem. Soc., Chem. Commun.* **1993**, 921–922. (e) Clark, J. H.; Wails, D. *J. Fluorine Chem.* **1995**, *70*, 201–205. (f) Clark, J. H.; Wails, D. *Tetrahedron Lett.* **1993**, *34*, 3901–3902. (g) Clark, J. H.; Wails, D.; Jones, C. W.; Smith, H.; Boechat, N.; Mayer, L. U.; Mendonca, J. S. *J. Chem. Res.* **1994**, 478. (h) Maggini, M.; Passudetti, M.; Gonzales-Trueba, G.; Prato, M.; Quintily, U.; Scorrano, G. *J. Org. Chem.* **1991**, *56*, 6406–6411.
- (10) (a) Filatov, A. A.; Boiko, V. N.; Yagupolskii, Y. L. *J. Fluorine Chem.* **2012**, *143*, 123–129. (b) Smyth, T.; Carey, A. *Tetrahedron* **1995**, *51*, 8901–8914.
- (11) (a) Eckelbarger, J. D.; Epp, J. B.; Schmitzer, P. R.; Siddall, T. L. 3-Alkenyl-6-halo-4-aminopicolinates and their use as herbicides. US 20120190548 A1, July 26, 2012. (b) Whiteker, G. T.; Arndt, K. E.; Renga, J. M.; Yuanming, Z.; Lowe, C. T.; Siddall, T. L.; Podhorez, D. E.; Roth, G. A.; West, S. P.; Arndt, C. Process for the preparation of 4-amino-5-fluoro-3-halo-6-(substituted)picolinates. US 20120190860, July 26, 2012. (c) Yerkes, C. N.; Lowe, C. T.; Eckelbarger, J. D.; Epp, J. B.; Guentenspberger, K. A.; Siddall, T. L.; Schmitzer, P. R. Arylalkyl esters of 4-amino-6-(substitutedphenyl)picolinates and 6-amino-2-(substitutedphenyl)-4-pyrimidinecarboxylates and their use as selective herbicides for crops. US 20150025238 A1, January 22, 2015. (d) Eckelbarger, J. D.; Epp, J. B.; Schmitzer, P. R. 6-Amino-2-substituted-5-vinylsilylpyrimidine-4-carboxylic acids and esters and 4-amino-6-substituted-3-vinylsilylpyridine-2-carboxylic acids and esters as herbicides. US 20120190549 A1, July 26, 2012. (e) Epp, J. B.; Schmitzer, P. R.; Balko, T. W.; Ruiz, J. M.; Yerkes, C. N.; Siddall, T. L.; Lo, W. C. 2-Substituted-6-amino-5-alkyl, alkenyl or alkynyl-4-pyrimidinecarboxylic acids and 6-substituted-4-amino-3-alkyl, alkenyl and alkynyl picolinic acids and their use as herbicides. US 20090088322 A1, April 2, 2009. (f) Walsh, T. A.; Hicks, G.; Honma, M.; Davies, J. P. Resistance to auxinic herbicides. US 20070220629 A1, September 20, 2007.
- (12) Allen, L. J.; Lee, S. H.; Cheng, Y.; Hanley, P. S.; Muhuhi, J. M.; Kane, E.; Powers, S. L.; Anderson, J. E.; Bell, B. M.; Roth, G. A.; Sanford, M. S.; Bland, D. C. *Org. Process Res. Dev.* **2014**, *18*, 1045–1054.
- (13) Based on the largest available quantity from Sigma Aldrich, NMe₄Cl (reagent grade, 97%) is \$20.23/mol, KF (ACS reagent, ≥ 99.0%) is \$4.33/mol. Anhydrous NMe₄F from Sigma Aldrich is \$5234.47/mol.

- (14) (a) Alfonsi, K.; Colberg, J.; Dunn, P. J.; Fevig, T.; Jennings, S.; Johnson, T. A.; Kleine, H. P.; Knight, C.; Nagy, M. A.; Perry, D. A.; Stefaniak, M. *Green Chem.* **2008**, *10*, 31–36. (b) Prat, D.; Pardigon, O.; Flemming, H.-W.; Letestu, S.; Ducandas, V.; Isnard, P.; Guntrum, E.; Senac, T.; Ruisseau, S.; Cruiani, P.; Hosek, P. *Org. Process Res. Dev.* **2013**, *17*, 1517–1525.
- (15) (a) Furuya, T.; Klein, J. E. M. N.; Ritter, T. *Synthesis* **2010**, *11*, 1804–1821. (b) Miller, J. *Aromatic Nucleophilic Substitution*; Elsevier: London, 1968. (c) Terrier, F. *Modern Nucleophilic Aromatic Substitution*; Wiley-VCH: Weinheim, Germany, 2013.
- (16) For examples of rate studies in the radiofluorination of aryl halides and nitroarenes, see: (a) Karamkam, M.; Hinnen, F.; Berrehouma, M.; Hlavacek, C.; Vaufrey, F.; Halldin, C.; McCarron, J. A.; Pike, V. W.; Dollé, F. *Bioorg. Med. Chem.* **2003**, *11*, 2769–2782. (b) Al-Labadi, A.; Zeller, K.-P.; Machulla, H.-J.; *J. Radioanal. Nucl. Chem.* **2006**, *270*, 313–318. (c) Guo, M.; Alagille, D.; Tamagnan, G.; Price, R. R.; Baldwin, R. M. *Appl. Radiat. Isot.* **2008**, *66*, 1396–1402. (d) Dolci, L.; Dollé, F.; Jubeau, S.; Vaufrey, F.; Crouzel, C. *J. Labelled Compd. Radiopharm.* **1999**, *42*, 975–985.
- (17) (a) Hicken, E. J.; Marmsater, F. P.; Munson, M. C.; Schlachter, S. T.; Robinson, J. E.; Allen, S.; Burgess, L. E.; DeLisle, R. K.; Rizzi, J. P.; Topalov, G. T.; Zhao, Q.; Hicks, J. M.; Kallan, N. C.; Tarlton, E.; Allen, A.; Callejo, M.; Cox, A.; Rana, S.; Klopfenstein, N.; Woessner, R.; Lyssikatos, J. P. *ACS Med. Chem. Lett.* **2014**, *5*, 78–83. (b) Duncan, K. W.; Chesworth, R.; Boriack-Sjodin, P. A.; Munchhof, M. J.; Jin, L. Prmt5 inhibitors containing a dihydro- or tetrahydroisoquinoline and uses thereof. Patent WO2014100730A1, June 26, 2014. (c) Vasdev, N.; Cao, P.; van Oosten, E. M.; Wilson, A. A.; Houle, S.; Hao, G.; Sun, X.; Slavine, N.; Alhasan, M.; Antich, P. P.; Bonte, F. J.; Kulkarni, P. *MedChemComm* **2012**, *3*, 1228–1230.
- (18) Per the Sigma Aldrich website, at the time of writing, the estimated ship day for a 1 or 5 gram bottle of anhydrous NMe₄F is May 28, 2017.
- (19) Cismesia, M. A.; Ryan, S. J.; Bland, D. C.; Sanford, M. S. *J. Org. Chem.* **2017**, *82*, 5020–2026.
- (20) (a) Brooks, A. F.; Topczewski, J. J.; Ichiishi, N.; Sanford, M. S.; Scott, P. J. H. *Chem. Sci.* **2014**, *5*, 4545–4553. (b) Ametamey, S. M.; Honer, M.; Schubiger, P. A. *Chem. Rev.* **2008**, *108*, 1501–1516.
- (21) (a) Qin, L.; Ren, X.; Lu, Y.; Li, Y. Zhou, J. *Angew. Chem., Int. Ed.* **2012**, *51*, 5915–5919. (b) Xu, X.-H.; Wang, X.; Liu, G.-K.; Tokunaga, E.; Shibata, N. *Org. Lett.* **2012**, *14*, 2544–2547.
- (22) Shestopalov, A. M.; Fedorov, A. E.; Rodinovskaya, L. A.; Shestopalov, A. A.; Gakh, A. A. *Tetrahedron Lett.* **2009**, *50*, 5257–5259.
- (23) Umemoto, T.; Tomizawa, G. *J. Org. Chem.* **1989**, *54*, 1726–1731.

CHAPTER 3

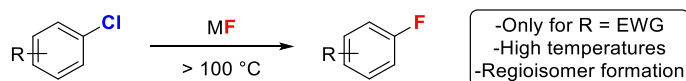
Nucleophilic Deoxyfluorination of Phenols via Sulfonate Intermediates¹

3.1 Background

(Hetero)aryl fluorides are common components of many pharmaceuticals and agrochemicals.² Despite the importance of (hetero)aryl fluorides in many chemistry disciplines, there are few mild, general, and selective methods for the construction of C(sp²)-F bonds specifically in aromatic systems. From a cost and practicality standpoint, the ideal C-F bond forming reaction would involve the reaction of a nucleophilic fluoride source with a readily available and accessible (hetero)aryl electrophile. Furthermore, this transformation should be applicable to a wide scope of electronically diverse substrates under mild conditions without the use of expensive transition metal catalysts or stoichiometric additives.

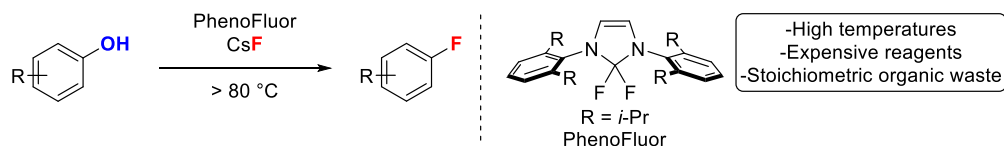
Industrially, S_NAr fluorination is one of the most common fluorination reactions.³ These reactions involve the transformation of an aryl chloride or a nitroarene to an aryl fluoride typically using an alkali metal fluoride (Scheme 3.1). However, this transformation required harsh reaction conditions (>100 °C) to drive the reaction, largely due to the insolubility of alkali metal fluoride salts in organic solvents.⁴ These harsh conditions often lead to limited functional group tolerance and regioisomer formation.^{5,6} Additionally, the scope of S_NAr fluorination reactions is limited to substrates bearing strongly electron-withdrawing groups in activating positions of the aromatic system. Since aryl chlorides and nitroarenes rarely occur naturally, these functionalities must be preinstalled to perform the S_NAr fluorination reaction. This leads to additional steps and added waste to the overall transformation to create a C-F bond.

Scheme 3.1. Classical S_NAr Fluorination Reaction



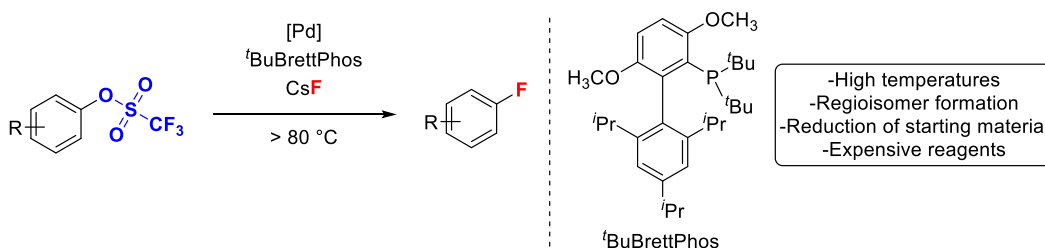
Phenols offer more sustainable starting materials for the generation of aryl fluorides as many are readily available from biomass.⁷ Significant effort has been made recently to develop fluorination methods that use phenols or phenolic derivatives as viable substrates. Ritter and coworkers have developed the reagent PhenoFluor to mediate the deoxyfluorination of phenols (Scheme 3.2).^{8,9} This deoxyfluorination reaction relies on the use of stoichiometric PhenoFluor and excess CsF to induce the desired fluorination. The expense of both PhenoFluor¹⁰ and CsF¹¹ limit the application of this chemistry for industrial scale processes. In addition, harsh reaction conditions (>80 °C) are required and stoichiometric organic waste is produced in these reactions that must be separated from the desired fluorinated product.

Scheme 3.2. Deoxyfluorination with PhenoFluor



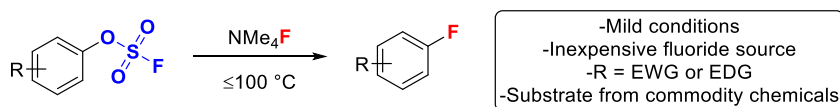
Buchwald and coworkers have reported the conversion of aryl triflates to aryl fluorides via palladium catalysis (Scheme 3.3).^{12,13} This methodology relies on the use of an expensive Pd catalyst and ligand (^tBuBrettPhos) to induce the transformation. Harsh conditions are required which lead to side product formation, including regioisomers and reduced starting material, which are difficult to separate from the desired fluorinated product. The cost of the Pd catalyst, ligand, and CsF prohibit the use of this methodology on large scale.

Scheme 3.3. Pd-Catalyzed Fluorination of Aryl Triflates



While there has been much recent development in the creation of new aryl fluorination methods, none of these methods meet all the criteria for an ideal fluorination reaction. They all suffer from at least one major limitation with respect to harsh reaction conditions, limited substrate scope, the formation of inseparable side products, and/or the use of expensive reagents and catalysts. The development of a mild fluorination reaction using phenolic derivatives as starting materials is highly sought after. Herein, we report that aryl fluorosulfonates (ArOFs) can be converted to aryl fluorides under mild conditions. These reactions utilize tetramethylammonium fluoride (NMe₄F) as an inexpensive nucleophilic fluoride source without the need for a transition metal catalyst or an expensive stoichiometric reagent (Scheme 3.4).^{14,15} Importantly, aryl fluorosulfonates are easily accessed by reaction of phenols with sulfuryl fluoride (SO₂F₂), a commodity chemical that is widely used as an insecticide.

Scheme 3.4. S_NAr Fluorination of Aryl Fluorosulfonates



This chapter discusses the development of a nucleophilic deoxyfluorination reaction via aryl fluorosulfonate intermediates using anhydrous tetramethylammonium fluoride (NMe₄F). The reactivity of aryl fluorosulfonates is compared to other aryl electrophiles traditionally used for S_NAr fluorination reactions, and the substrate scope of this transformation is explored. Mechanistic studies, both computational and experimental, were conducted to better understand the high reactivity of these electrophiles. Based on our mechanistic studies, the use of other sulfate electrophiles for

this deoxyfluorination method was examined, and aryl triflates were identified as promising alternatives that exhibit similar reactivity to aryl fluorosulfonates.

3.2. Initial Results and Comparison of Electrophiles

The reactivity of aryl fluorosulfonates toward nucleophilic fluorination with NMe₄F was examined to analyze their reactivity with respect to other more traditional S_NAr fluorination electrophiles (Table 3.1). 4-Cyanophenyl sulfofluoridate (**1-OFs**) was selected as the test substrate, as the *para*-cyano substituent is a strongly activating group for S_NAr fluorination reactions.^{5a} Initial studies demonstrated that **1-OFs** reacts with 2 equivalents of NMe₄F at room temperature within 24 h, affording the corresponding aryl fluoride **1-F** in 92% yield (entry 1). When the corresponding aryl chloride **1-Cl** was used as the electrophile in the S_NAr fluorination reaction, only 35% of the desired fluorinated product was obtained at room temperature; elevated temperatures (80 °C) resulted in higher yields that were comparable to those obtained with **1-OFs** (entry 2). The analogous reaction with nitroarene **1-NO₂** compares favorably with that of **1-OFs**; but when the reaction is heated to 80 °C for an extended time (24 h), the yield of **1-F** from **1-NO₂** erodes to 57% (entry 3). This is a result of reaction of the fluorinated product with the displaced NO₂[−] anion;^{5b,16} diaryl ether was observed by GCMS analysis of the crude reaction mixture. The examination of other sulfonate electrophiles (**1-OTf**, **1-OMs**, and **1-OTs**) afforded low yields of **1-F** (entries 4–6). For aryl triflate **1-OTf**, the yield of the reaction did improve with elevated temperatures but only modestly (entry 4).

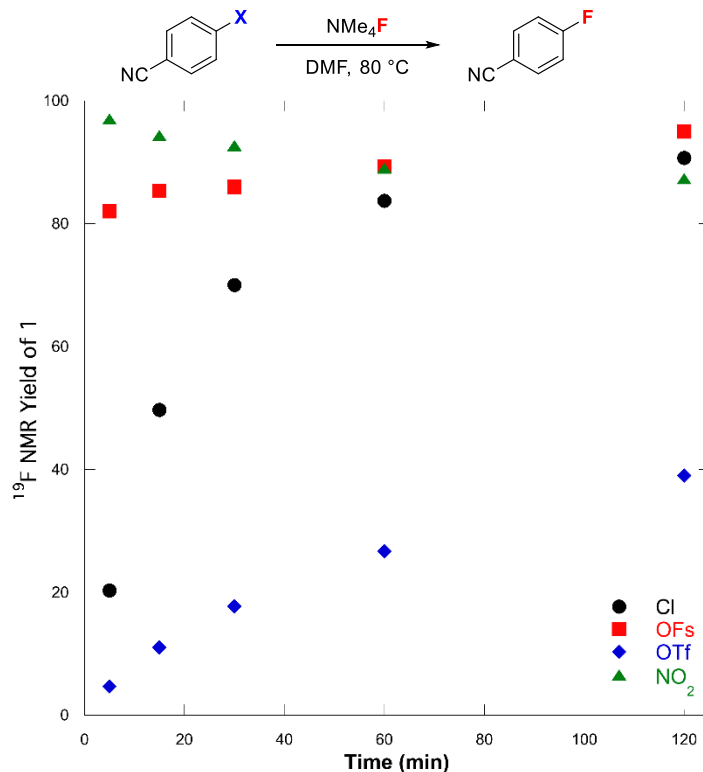
Table 3.1. Fluorination of Different Aryl Electrophiles with NMe₄F^a

entry	X	% yield ^b	
		25 °C	80 °C
1	-OSO ₂ F (1-OFs)	92	92
2	-Cl (1-Cl)	35	91
3	-NO ₂ (1-NO₂)	88	57
4	-OSO ₂ CF ₃ (1-OTf)	10	66
5	-OSO ₂ CH ₃ (1-OMs)	<1	<1
6	-OSO ₂ C ₆ H ₄ CH ₃ (1-OTs)	<1	<1
7	-OH (1-OH)	<1	<1

^aConditions: Substrate (0.1 mmol, 1.0 equiv) and NMe₄F (0.2 mmol, 2.0 equiv) stirred in anhydrous DMF (0.2M) at the designated temperature for 24 h. ^bYields were determined by ¹⁹F NMR spectroscopy of the crude reaction mixture using 1,3,5-trifluorobenzene as an internal standard. Crude reactions were analyzed by GCMS.

Time studies were conducted to examine the relative rates of the reaction of **1-X** with NMe₄F at 80 °C (Figure 3.1). The reaction of **1-OFs** with NMe₄F proceeds significantly faster than that of the corresponding aryl chloride **1-Cl**. Aryl triflate **1-OTf** reacted very slowly under the reaction conditions, affording only 39% of **1-F** in 2 h at 80 °C. While nitroarene **1-NO₂** reacts faster than **1-OFs**, the product yield erodes with time due to side reactions with NO₂⁻ leaving group.^{5b,16} These studies suggest that **1-OFs** is a superior electrophile for this S_NAr fluorination reaction with respect to its fast reactivity and stability of the resulting anion leaving group (⁻OSO₂F).

Figure 3.1. Reaction Profiles for the Conversion of **1-X** to **1-F** at 80 °C^a



^aConditions: Substrate (0.1 mmol, 1.0 equiv) and NMe₄F (0.2 mmol, 2.0 equiv) stirred in DMF at 80 °C for the given time. Yields were determined by ¹⁹F NMR spectroscopy with 1,3,5-trifluorobenzene as an internal standard.

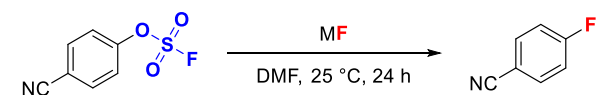
Various solvents were evaluated for the fluorination reaction of aryl fluorosulfonate **1-OFs** (Table 3.2). Use of amide solvents including *N,N*-dimethylformamide (DMF), *N*-methyl-2-pyrrolidone (NMP), and 1,3-dimethyl-2-imidazolidinone (DMI), afforded modest to high yields of the desired fluorinated product (entries 1–3). Dimethyl sulfoxide (DMSO), another solvent frequently used for S_NAr fluorination reactions, could be used to afford modest yields of **1-F** (entry 4). Interestingly, use of acetonitrile (CH₃CN) afforded modest yield of the fluorinated product. Anhydrous NMe₄F is known to deprotonate CH₃CN,¹⁷ yielding bifluoride (HF₂[−]) which is inactive for S_NAr fluorination reactions. However, in this deoxyfluorination reaction, this deprotonation appears to occur more slowly than the desired fluorination reaction. Less polar solvents such as tetrahydrofuran (THF) afford modest yields of **1-F** (entry 6), but the nonpolar solvent toluene afforded very low yields of the desired product.¹⁸ This is likely due to the low solubility of NMe₄F in nonpolar solvents such as toluene.

Table 3.2. Solvents for the Deoxyfluorination of **1-OFs**^a

entry	solvent	% yield ^b
1	DMF	92
2	NMP	87
3	DMI	77
4	DMSO	78
5	CH ₃ CN	76
6	THF	73
7	Toluene	3

^aConditions: **1-OFs** (0.1 mmol, 1.0 equiv) and NMe₄F (0.2 mmol, 2.0 equiv) stirred in anhydrous solvent (0.2M) at 25 °C for 24 h. ^bYields were determined by ¹⁹F NMR spectroscopy of the crude reaction mixture using 1,3,5-trifluorobenzene as an internal standard.

Different fluoride sources were also examined for the deoxyfluorination reaction of **1-OFs** (Table 3.3). Soluble fluoride sources such as cobaltocenium fluoride (Cp₂CoF)¹⁹ and *in situ*-generated anhydrous tetrabutylammonium fluoride (TBAF*)^{20,21} provided lower yields than anhydrous NMe₄F (entries 1–3). While poorly soluble alkali metal fluoride salts did not affect the fluorination reaction at room temperature, the use of elevated temperatures (140 °C) resulted in modest yields when potassium fluoride (KF) and cesium fluoride (CsF) were used (entries 4–7). The addition of a phase transfer reagent to fluorination reactions utilizing KF resulted in higher yields of **1-F** (entry 8). Anhydrous conditions and reagents were required for the deoxyfluorination reaction; the use of NMe₄F • H₂O resulted in no desired product formation; by GCMS, starting material was consumed and phenol and a diaryl sulfate byproduct were observed.

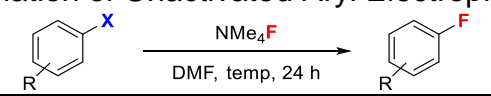
Table 3.3. Fluoride Sources for the Fluorination of **1-OFs**^a


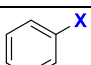
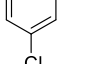
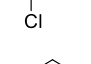
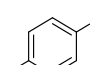
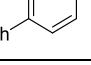
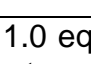
entry	MF	% yield ^b
1	NMe ₄ F	92
2	Cp ₂ CoF	77
3	TBAF*	40
4	CsF	76 ^c
5	NaF	<1 ^c
6	LiF	<1 ^c
7	KF	43 ^c
8	KF + NMe ₄ Cl	71 ^c
9	NMe ₄ F • H ₂ O	<1

^aConditions: **1-OFs** (0.1 mmol, 1.0 equiv) and MF (0.2 mmol, 2.0 equiv) stirred in DMF (0.2M) at 25 °C for 24 h. ^bYields were determined by ¹⁹F NMR spectroscopy of the crude reaction mixture using 1,3,5-trifluorobenzene as an internal standard. ^c140 °C.

Next, less activated substrates were examined for the nucleophilic fluorination reaction (Table 3.4) such as 3-chlorophenyl-substituted electrophiles (**2-OFs**, **2-Cl**, and **2-NO₂**). These substrates are expected to be less reactive for S_NAr fluorination reactions due to chloro substituents being less activating than cyano groups and *meta* substitution does not activate the aromatic system in the same manner.^{5,20b} As expected, **2-Cl** and **2-NO₂** exhibit low reactivity in the S_NAr fluorination reaction, affording low yields of **2-F** (2% and 15%, respectively) after 24 h at 80 °C (entries 2–3). In contrast, **2-OFs** afforded 67% yield of **2-F** under analogous conditions (entry 1).

The electron-neutral (1,1'-biphenyl)-4-substituted electrophiles were examined as well. While reactivity of **3-OFs** was low at room temperature, remarkably, **3-OFs** reacted with NMe₄F to afford **3-F** in 85% yield over 24 h at 100 °C (entry 4). In contrast, minimal reactivity was observed for **3-Cl** (<1%) and **3-NO₂** (6%). These results demonstrate the possibility of high yielding transition metal free nucleophilic fluorination of electronically diverse aryl fluorosulfonates, which is in marked contrast to reactions of aryl chlorides and nitroarenes.

Table 3.4. Fluorination of Unactivated Aryl Electrophiles with NMe₄F^a


entry	substrate	X	% yield ^b
1		OFs (2-OFs) ^c	67
2		Cl (2-Cl) ^c	2
3		NO ₂ (2-NO₂) ^c	15
4		OFs (3-OFs) ^d	85
5		Cl (3-Cl) ^d	<1
6		NO ₂ (3-NO₂) ^d	6

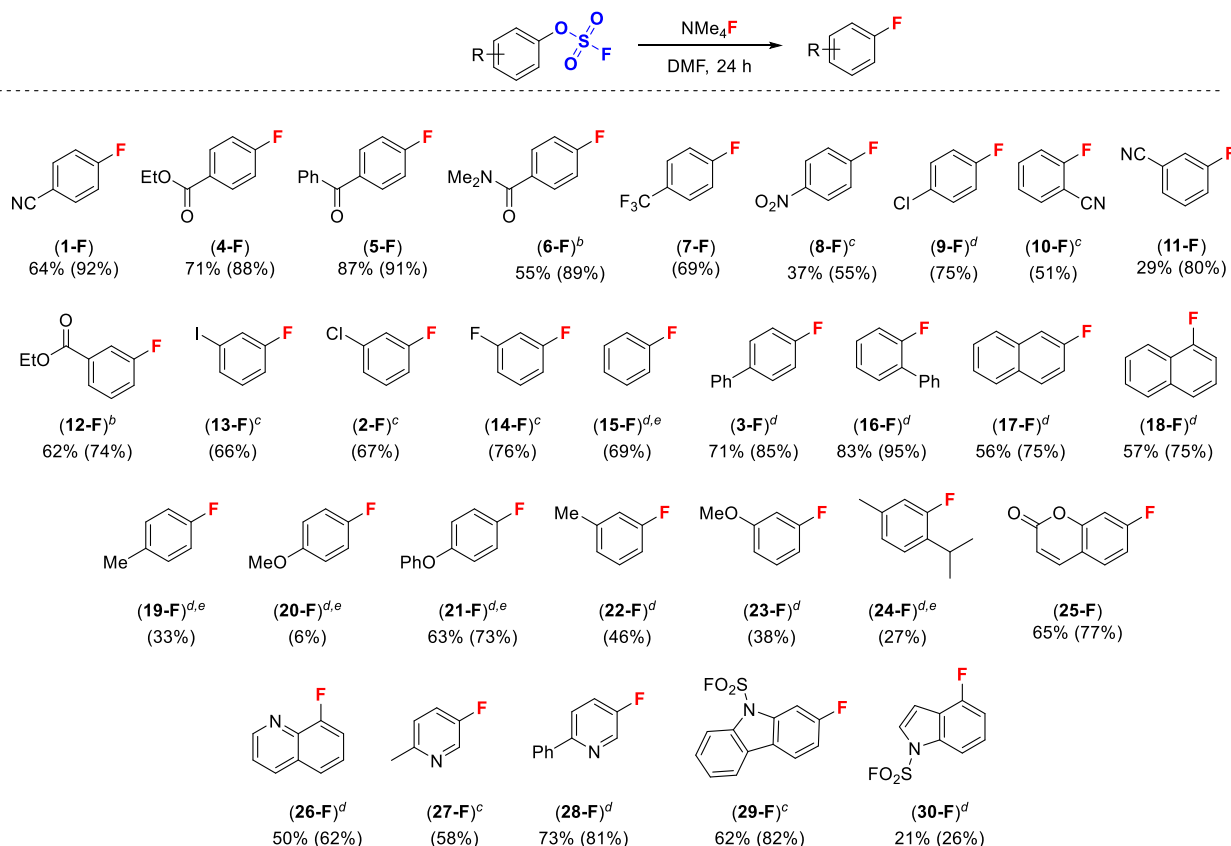
^aCondition: Substrate (0.1 mmol, 1.0 equiv) and NMe₄F (0.2 mmol, 2.0 equiv) stirred in DMF (0.2 M) at the given temperature for 24 h. ^bYields were determined by ¹⁹F NMR spectroscopy with 1,3,5-trifluorobenzene as internal standard. ^c80 °C. ^d100 °C.

3.3. Substrate Scope

The results in Tables 3.1 and 3.4 demonstrate the feasibility of the high yielding nucleophilic fluorination of electronically diverse aryl fluorosulfonates with NMe₄F. With this in mind, the scope and limitations of the fluorination reaction was investigated (Figure 3.2). Aryl fluorosulfonates bearing *para*- or *ortho*-electron-withdrawing substituents reacted with NMe₄F, typically at room temperature, to afford **1-F**, **4–10-F** in modest to excellent yields. These substrates demonstrate the compatibility of this fluorination method with nonenolizable esters, ketones, and amides (**4–6-F**). Notably, –OFs reacts selectively in the presence of other potential leaving groups including –NO₂ (to form **8-F**) and –Cl (to form **9-F**). In reactions with these substituents, 1,4-difluorobenzene (formed from displacement of –OFs and –NO₂/–Cl) is not observed in the reactions, even at elevated temperatures. This indicates that both the starting materials and the products are not sufficiently electron-poor enough to facilitate the S_NAr fluorination to displace other leaving groups.^{20b} Aryl fluorosulfonates bearing electron-withdrawing substituents at the less activating *meta*-position reacted with NMe₄F at slightly elevated temperatures (60–80 °C) to afford the fluorinated products **2-F** and **11–14-F** in good yields. Under these reaction conditions, no isomeric fluorinated products were detected by ¹⁹F NMR spectroscopic analysis of the crude reaction mixture. However, for many of these substrates, regioisomers consistent with benzyne intermediates were detected when the reactions were conducted at higher temperatures (≥100 °C). The yield of these benzyne products were low (<10%). Under the mild conditions, competing benzyne formation,

which is a common side reaction in S_NAr fluorination reactions of less activated aryl electrophiles,⁶ does not occur and high yields of the desired product are selectively formed.

Figure 3.2. Substrate Scope for the Fluorination of Aryl Fluorosulfonates with NMe_4F ^a



^aConditions: Substrate (0.5 mmol, 1.0 equiv) and NMe_4F (1.0 mmol, 2.0 equiv) in DMF (0.2 M) at 25 °C for 24 h. Isolated yields reported with ^{19}F NMR yields in parentheses. ^b60 °C. ^c80 °C. ^d100 °C. ^e5.0 equiv NMe_4F .

This S_NAr fluorination method can also be applied to electron-neutral and moderately electron-rich aryl fluorosulfonates (Figure 3.2). Unsubstituted, biphenyl, and naphthyl fluorosulfonate substrates reacted with NMe_4F at 100 °C to afford the fluorinated products **3-F** and **15–18-F** in good to excellent yields. Additionally, aryl fluorosulfonates with methyl, methoxy, and phenoxy substituents underwent fluorination at 100 °C to afford fluoroarenes **19–24-F** in low to moderate yields. In some cases, fluorination of electron-rich substrates required excess NMe_4F (5 equivalents) to obtain modest yields of the product. For these electron-rich substrates, unreacted starting material remains after 24

hours at 100 °C. In some cases, a diaryl sulfate byproduct was formed as detected by GCMS. Longer reaction times and higher temperatures did not improve the reactions. While the yields in some cases were rather low, these results are exciting because the corresponding aryl chlorides and nitroarenes do not react with NMe₄F to give any detected fluorinated product (see below for more discussion).

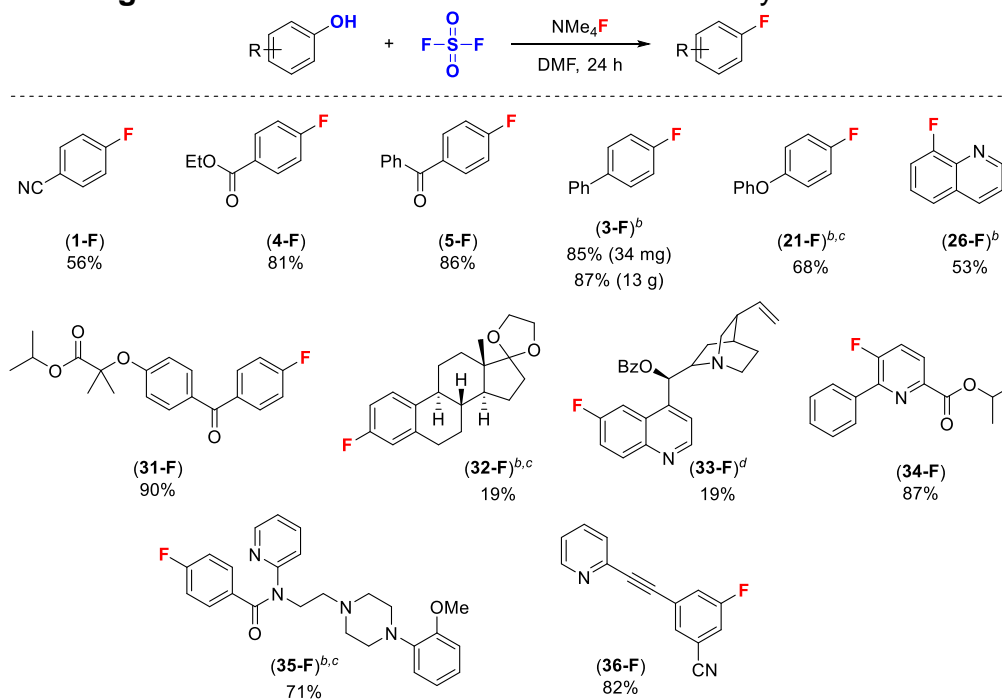
Heterocyclic fluorosulfonates, including quinolines, pyridines, carbazoles, and indoles, were also viable substrates for the fluorination reaction, affording **25–30-F** in low to good yield. For all the substrates in Figure 3.2, the only fluorinated product detected resulted from reaction at the *ipso* carbon. Overall, the results described here demonstrate that the nucleophilic fluorination of aryl fluorosulfonates proceeds with high selectivity to afford a wide range of fluoroarene products that are not accessible by classical S_NAr fluorination reactions.^{5,6,20b}

A more appealing transformation is the direct conversion of a phenol to a fluoroarene without the need for an isolated intermediate. As aryl fluorosulfonates are synthesized by the reaction of phenols with sulfuryl fluoride (SO₂F₂) in the presence of base,²² it was hypothesized that NMe₄F could act as both the base and fluorine source for the reaction. The one-pot conversion of ArOH, SO₂F₂, and NMe₄F was pursued, and this one-pot deoxyfluorination proved highly effective for electronically diverse phenol substrates and biologically relevant compounds (Figure 3.3).^{A,14,23} The yields for the one-pot fluorination procedure were comparable to those obtained from the isolated aryl fluorosulfonates. This one-pot deoxyfluorination method was scalable, and comparable yields of **3-F** were obtained on scales ranging from 34.0 mg to 13.0 g.^B This one-pot methodology demonstrates the potential applicability of this fluorination chemistry to larger scale processes.

^A Work on the one-pot conversion of phenols to fluoroarenes through an aryl fluorosulfonate intermediate was primarily done by Dr. Megan Cismesia.

^B Scale up of **3-F** was performed by Dr. Matthew Jansma (The Dow Chemical Company).

Figure 3.3. Direct Conversion of Phenols for Aryl Fluorides^a



^aConditions: Substrate (0.2 mmol, 1.0 equiv), NMe₄F (0.6 mmol, 3.0 equiv) and SO₂F₂ (0.14 M solution in anhydrous DMF; 0.4 equiv, 2.0 equiv) at 25 °C. Isolated yields are reported.

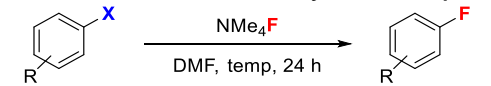
^b100 °C. ^c6.0 equiv NMe₄F. ^d4.5 equiv NMe₄F.

This one-pot fluorination method was also applied to the deoxyfluorination of a series of bioactive molecules (Figure 3.3). Fluorine-containing analogues of the hypercholesterolemia drug fenofibrate,²⁴ the steroid estrone, and the cinchona alkaloid quinine were prepared in low to excellent yields (**31–33-F**). For the latter two cases, the enolizable ketone and alcohol functional groups required protection to avoid side reactions under the basic reaction conditions. The 6-aryl picolinate ester **34-F**, a common structural motif in several herbicides,²⁵ was synthesized in excellent yield (87%).²⁶ 2'-Methoxyphenyl-(*N*-2'-pyridinyl)-*p*-fluorobenzamido-ethylpiperazine (MPPF, **35-F**), a serotonin 1A receptor ligand,²⁷ and 3-fluoro-5-(pyridine-2-ylethynyl)benzonitrile (F-PEB), a metabotropic glutamate receptor subtype 5 ligand,²⁸ were obtained in good yields from the corresponding phenols. These examples highlight the compatibility of the one-pot method with common functional groups and demonstrate the applicability of this methodology to the fluorination of structurally complex, biologically relevant compounds.

The substrate scope revealed significant differences between the reactivity of aryl fluorosulfonates compared to previous reports of S_NAr fluorination. To gain a more direct

comparison, the fluorination of several chloroarenes and nitroarenes was conducted under comparable conditions to the corresponding aryl fluorosulfonates (Table 3.5; see also Tables 3.1 and 3.4 above). For substrates with strongly electron-withdrawing groups (*p*-CO₂Et), nitroarenes outperform aryl fluorosulfonates (entries 1–3), but aryl chlorides are poorly reactive under mild conditions (room temperature). When electron-withdrawing groups are in less activating *meta*-positions, aryl fluorosulfonates are more reactive under mild conditions, providing high yields of the desired fluorinated product, while nitroarenes are poorly reactive and chloroarenes are unreactive (entries 4–6). For both electron-neutral and electron-rich substrates, aryl fluorosulfonates react with NMe₄F under more forcing conditions (100 °C, 5 equiv NMe₄F) to provide only low yields of product. The corresponding nitroarene and aryl chlorides do not react at all under these conditions (entries 7–15). These results further exemplify the utility of aryl fluorosulfonates for fluorination reactions with NMe₄F as these substrates are frequently more reactive than other classical S_NAr substrates.^{5,20b}

Table 3.5. Fluorination of Different Aryl Electrophiles with NMe₄F^a

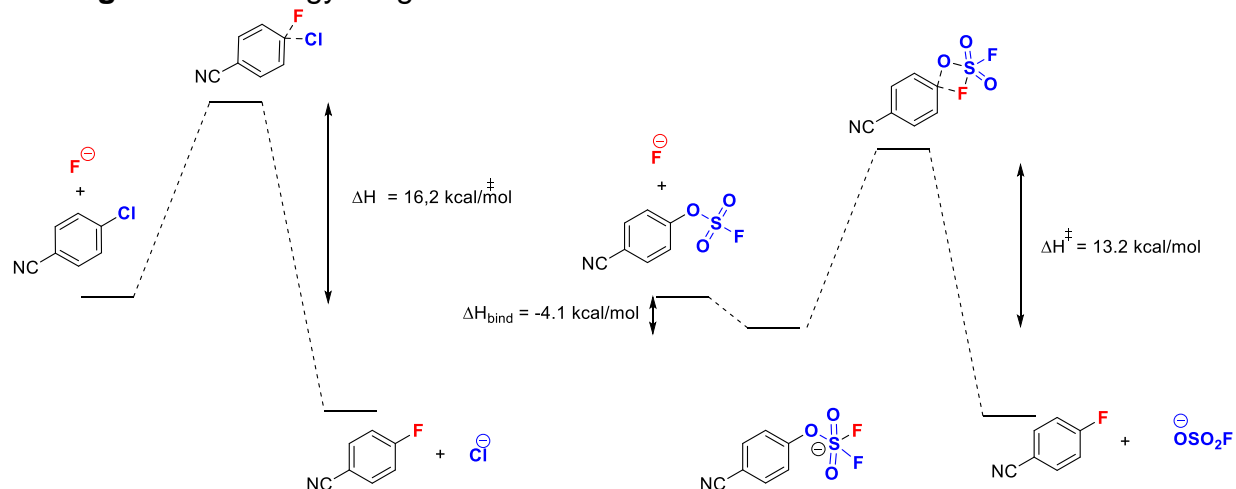
			
entry	R =	X =	% yield ^b
1	<i>p</i> -CO ₂ Et	4-OFs	88
2		4-Cl	<1
3		4-NO₂	>95
4	<i>m</i> -CN	11-OFs	80
5		11-Cl	<1
6		11-NO₂	48
7	<i>m</i> -Me ^c	22-OFs	53
8		22-Cl	<1
9		22-NO₂	<1
10	<i>p</i> -Me ^{c,d}	19-OFs	33
11		19-Cl	<1
12		19-NO₂	<1
13	<i>p</i> -OMe ^{c,d}	20-OFs	6
14		20-Cl	<1
15		20-NO₂	<1

^aConditions: Substrate (0.1 mmol, 1.0 equiv) and NMe₄F (0.2 mmol, 2.0 equiv) stirred in DMF (0.2 M) at 25 °C for 24 h. ^bYields were determined by ¹⁹F NMR spectroscopy with 1,3,5-trifluorobenzene as internal standard. ^c100 °C. ^d5.0 equiv NMe₄F.

3.4. Mechanistic Investigations

Examination of the substrate scope of the deoxyfluorination method revealed stark contrasts between this method and more traditional S_NAr fluorination reactions with aryl chlorides or nitroarenes. It was hypothesized that the deoxyfluorination reaction proceeds via a different mechanism than S_NAr fluorination of aryl chlorides. *Ab initio* calculations were conducted on the reaction of **1-OFs** and **1-Cl** with fluoride (F^-).^{C,29} As shown in Figure 3.4, for the fluorination of aryl chlorides, the conversion of **1-Cl** to the transition state proceeds with an activation energy (ΔH^\ddagger) of 16.2 kcal/mol. For **1-OFs**, these calculations reveal that the binding of fluoride to sulfur to form a pentacoordinate intermediate is enthalpically favorable ($\Delta H_{\text{bind}} = -4.1$ kcal/mol).³⁰ The conversion of this pentacoordinate intermediate to the transition state then proceeds with a ΔH^\ddagger of 13.2 kcal/mol, consistent with the faster rate for the conversion of **1-OFs** compared to that of **1-Cl** measured experimentally (Figure 3.1).

Figure 3.4. Energy Diagrams for the Reaction of **1-Cl** and **1-OFs** with Fluoride

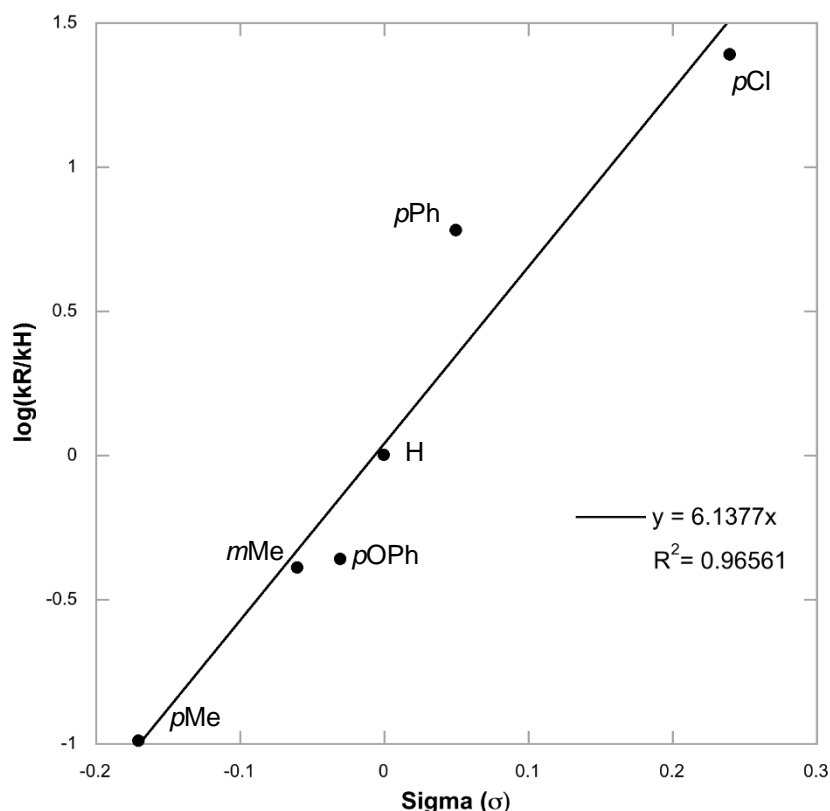


A Hammett study of the fluorination of aryl fluorosulfonates is shown in Figure 3.5. This plot shows a ρ value of ~ 6 , indicating that fluorination is significantly faster with electron-withdrawing substituents on the aromatic ring and that significant negative charge is delocalized on the aromatic ring in the transition state. This large Hammett ρ value is consistent with conventional S_NAr reactions, where typical ρ values range from 3

^C Computations were conducted by Dr. Robert Froese (The Dow Chemical Company).

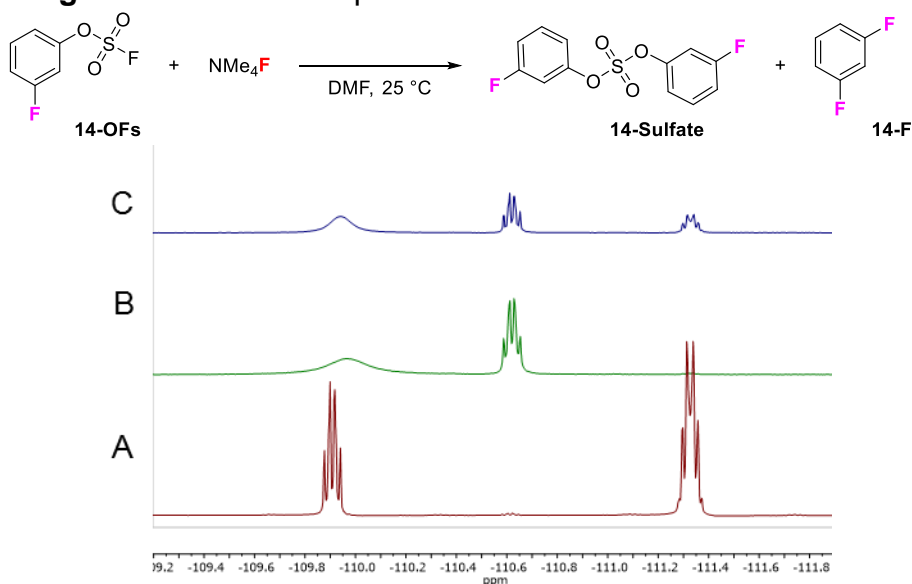
to 8.³¹ In contrast, a recent report by Ritter and coworkers suggests a concerted S_NAr reaction mechanism for the deoxyfluorination of phenols with PhenoFluor through a uronium intermediate.⁹ A smaller Hammett ρ value of 1.79 is observed indicating that there is limited delocalization of negative charge onto the aromatic substrate in the transition state of this reaction.

Figure 3.5. Hammett Plot for the Fluorination of Aryl Fluorosulfonates



To gain a better understanding of the deoxyfluorination reaction experimentally, the reaction of 3-fluorophenyl sulfofluoridate (**14-OFs**) was monitored by ¹⁹F NMR spectroscopy (Figure 3.6). At room temperature after just 30 minutes, the ¹⁹F NMR signal aromatic C–F of the starting material (**14-OFs**; –109.9 ppm) significantly broadens in the presence of 2 equivalents of NMe₄F (Figure 3.6B). A new ¹⁹F NMR signal appears quickly as well (–110.6 ppm) that is attributed to the formation of bis(3-fluorophenyl)sulfate (**14-sulfate**). After 24 h, product **14-F** is formed in low quantities (–111.4 ppm) and both the diaryl sulfate **14-sulfate** and starting material **14-OFs** remain.

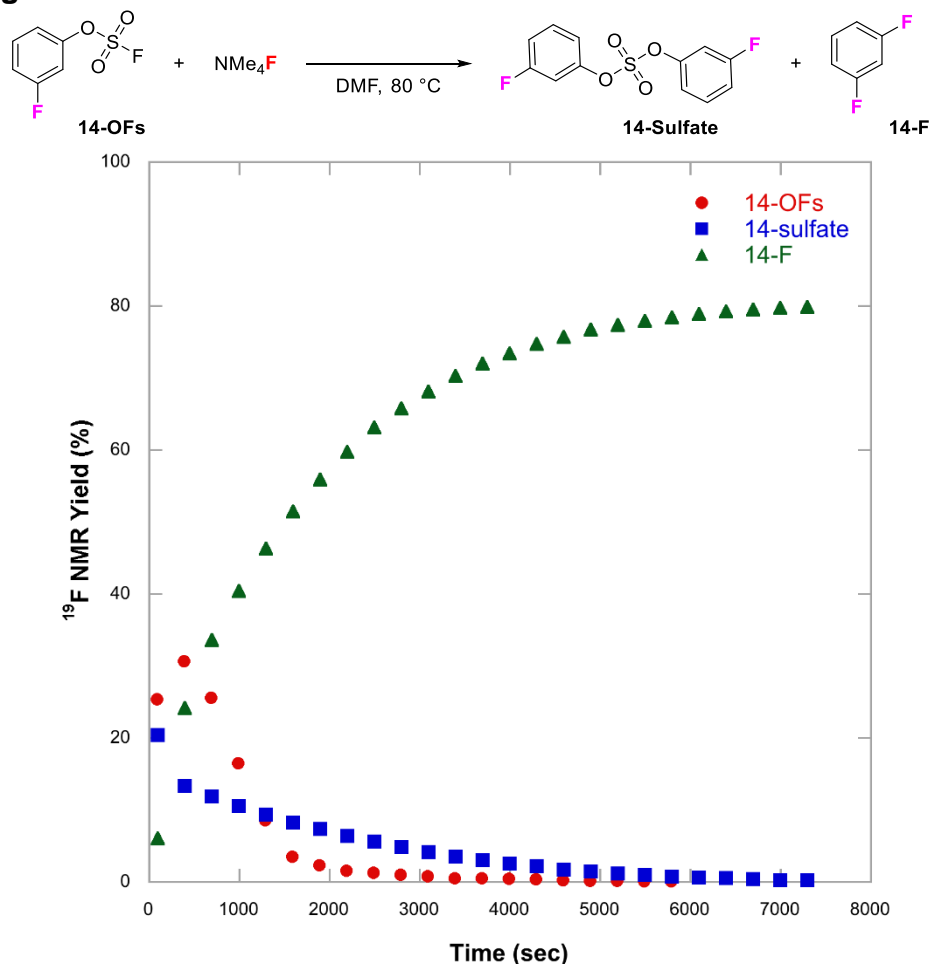
Figure 3.6. ^{19}F NMR Spectra of Reaction of **14-OFs** at 25 °C



A: ^{19}F NMR spectra of 3-fluorophenyl sulfofluoridate (**14-OFs**) and 1,3-difluorobenzene (**14-F**). B: ^{19}F NMR spectra of 3-fluorophenyl sulfofluoridate (0.1 mmol, 1.0 equiv) and NMe_4F (0.2 mmol, 2.0 equiv) in anh. DMF (0.2 M) at 25 °C at 30 min. C: ^{19}F NMR spectra of 3-fluorophenyl sulfofluoridate (0.1 mmol, 1.0 equiv) and NMe_4F (0.2 mmol, 2.0 equiv) in anh. DMF (0.2 M) at 25 °C at 24 h.

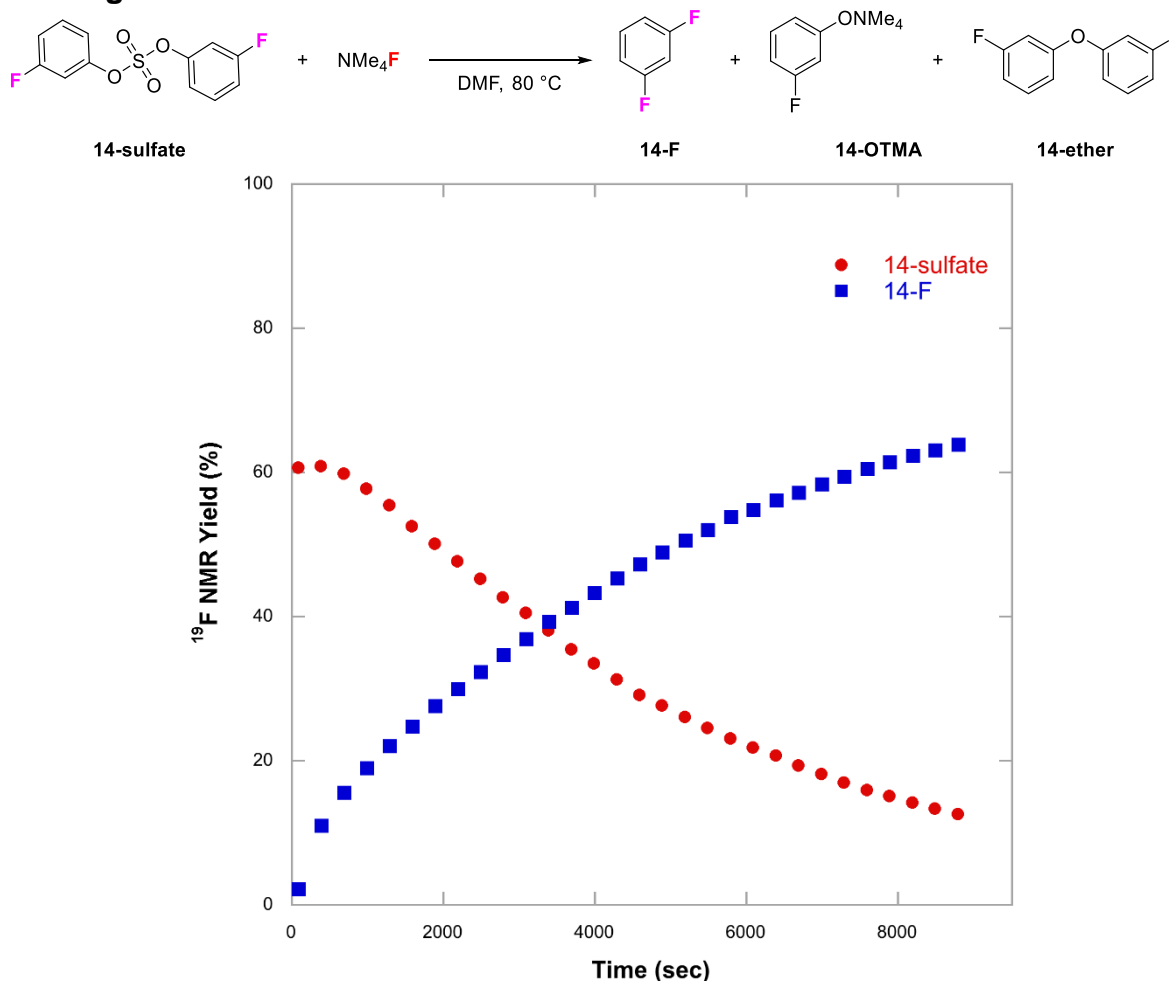
14-Sulfate forms quickly at room temperature under the fluorination reaction conditions. To investigate the fate of the diaryl sulfate (as an undesired byproduct or as an intermediate in the fluorination reaction), the fluorination of **14-F** was monitored by ^{19}F NMR spectroscopy at 80 °C (Figure 3.7). At 80 °C, the ^{19}F NMR signal corresponding to **14-OFs** broadens significantly in minutes (as is shown in Figure 3.5) and is consumed quickly. **14-Sulfate** is formed quickly and is consumed over the course of 2 h. The consumption of both **14-OFs** and **14-sulfate** suggest that both can be converted to product **14-F**. To verify this, bis(3-fluorophenyl)sulfate (**14-sulfate**) was independently synthesized and subjected to the reaction conditions and monitored by ^{19}F NMR spectroscopy at 80 °C (Figure 3.8). The reaction of **14-sulfate** is slower than the corresponding fluoroination of **14-OFs**, but product **14-F** is formed in 64% over the course of 2.5 h. Fluorination of **14-sulfate** produces many byproducts; tetramethylammonium 3-fluorophenoxide (66%, **14-OTMA**) and di(3-fluorophenyl)ether (2%, **14-ether**) are formed in addition to formation of **14-F** (see Scheme 3.5 for possible mechanism).

Figure 3.7. Reaction Profile of the Fluorination of **14-OFs** with NMe_4F^a



^aConditions: **14-OFs** (0.1 mmol, 1.0 equiv) and NMe_4F (0.2 mmol, 2.0 equiv) in anh. DMF (0.2 M) at 80 °C. ^{19}F NMR spectra collected every 5 minutes for a total of 2 hours. Yields were determined by ^{19}F NMR spectroscopy with 4-fluoroanisole as internal standard

Figure 3.8. Reaction Profile of the Fluorination of **14-sulfate** with NMe_4F^a



^aConditions: **14-sulfate** (0.1 mmol, 1.0 equiv) and NMe_4F (0.2 mmol, 2.0 equiv) in anh. DMF (0.2 M) at 80 °C. ^{19}F NMR spectra collected every 5 minutes for a total of 2.5 hours. Yields were determined by ^{19}F NMR spectroscopy with 4-fluoroanisole as internal standard.

A possible mechanism for the formation of diaryl sulfate is shown in Scheme 3.5. Aryl fluorosulfonate **14-OFs** reacts with one equivalent of NMe_4F to form a pentacoordinate sulfur intermediate **14-intermediate**. As shown by computations (Figure 3.4), this pentacoordinate sulfur intermediate can collapse to form the desired fluorinated product **14-F**. Alternatively, this intermediate can collapse to form sulfonyl fluoride (SO_2F_2) and phenoxide **14-OTMA**. This phenoxide can act as a nucleophile to attack an equivalent of starting material **14-OFs**, forming a new pentacoordinate sulfur intermediate, and collapse into **14-sulfate** and NMe_4F . This equilibrium process would explain the formation of diaryl sulfate **14-sulfate** as well as its ability to form the fluorinated product **14-F**. This

mechanism suggests that aryl fluorosulfonate **14-OFs** should be observable during the course of the fluorination reaction of **14-sulfate**. At 80 °C, the ^{19}F NMR signal for the starting material is too broad to distinguish. Therefore, in order to observe formation of **14-OFs** during the reaction, the reaction was heated to 80 °C for 10 minutes and then cooled to 25 °C prior to obtaining a ^{19}F NMR spectra of the sample (Figure 3.9). After 10 minutes at 80 °C, a ^{19}F NMR signal corresponding to **14-OFs** (−109.9 ppm) is observed in the fluorination reaction of **14-sulfate** along with formation of **14-OTMA**.

Scheme 3.5. Possible Mechanism for the Formation of **14-sulfate**

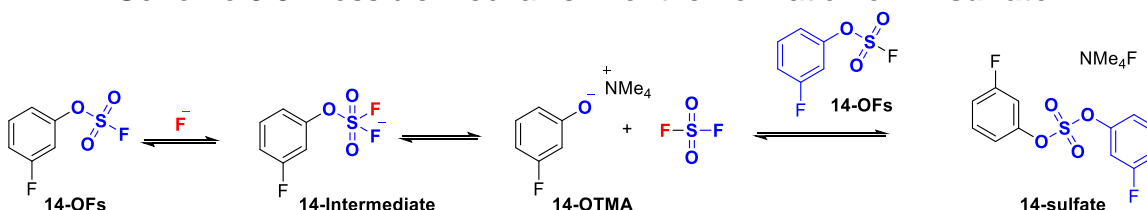
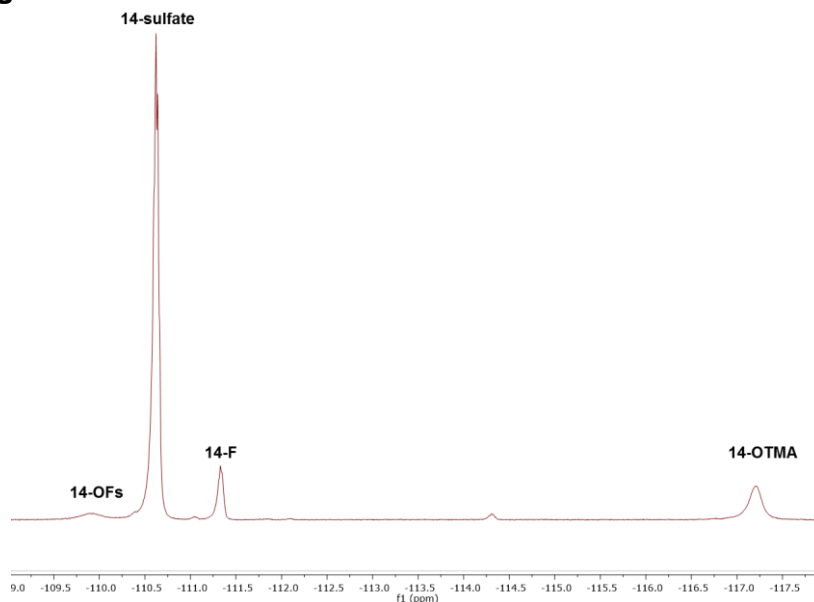


Figure 3.9. Fluorination of **14-sulfate** after 10 Minutes at 80 °C^a



^aConditions: **14-sulfate** (0.1 mmol, 1.0 equiv) and NMe_4F (0.2 mmol, 2.0 equiv) in anh. DMF (0.2 M) at 80 °C for 10 min. ^{19}F NMR spectra was collected at 25 °C.

To better understand the reactivity of diaryl sulfates, electronically diverse diaryl sulfates were examined as substrates for the fluorination reaction with NMe_4F (Table 3.6). Diaryl sulfates with electron-withdrawing substituents react at 80 °C with NMe_4F to provide modest yields of the desired fluorinated product (entries 1–2). The reactivity of diaryl

sulfates compares well to that of the corresponding aryl fluorosulfonate. Contrarily, electron-neutral and -rich diaryl sulfates react poorly with NMe_4F , affording low yields of the fluorinated product (entries 3–4). Fluorination of bis(4-phenoxyphenyl) sulfate **21-sulfate** affords only 3% of the desired fluorinated product and unreacted starting material remains after 24 h (entry 4).

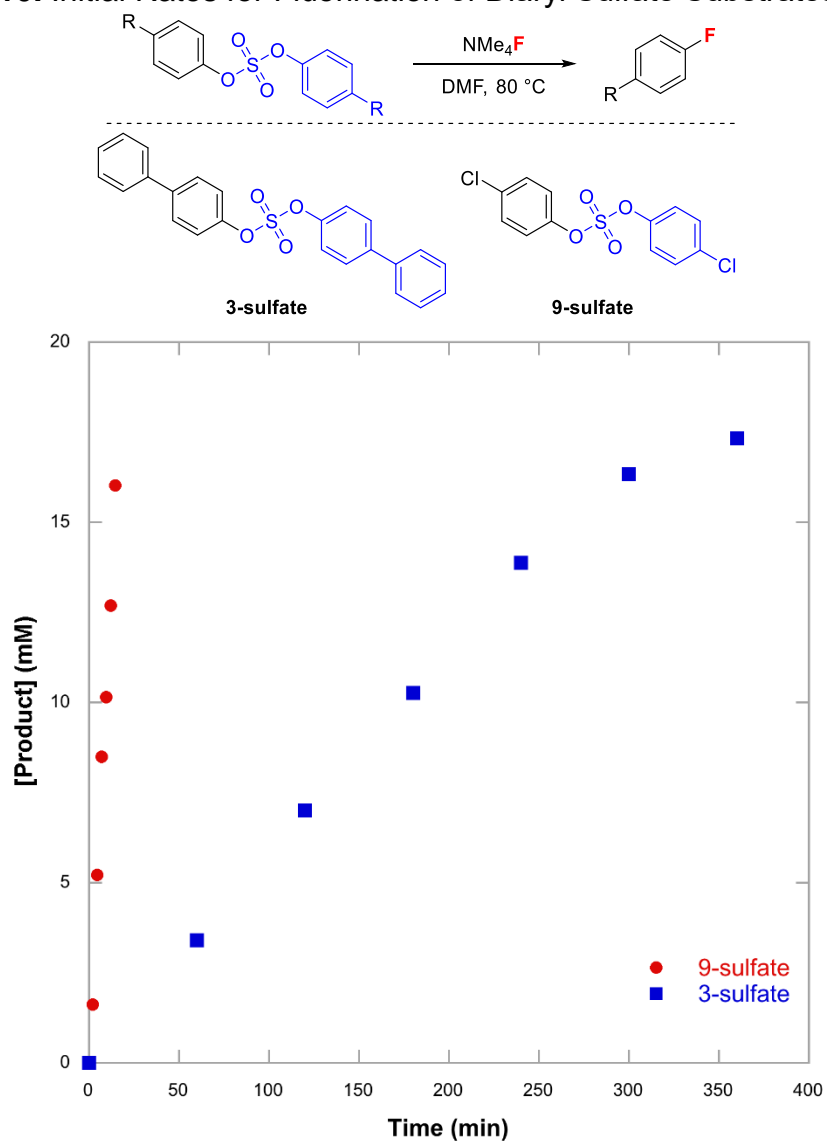
Table 3.6. Fluorination of Aryl Fluorosulfonates Compared to Diaryl Sulfates^a

entry	R =	 (OFs)	 (sulfate)
1	CN (1-X)	92	54
2	Cl (9-X)	75	70
3	Ph (3-X)	77	29
4	OPh (21-X)	29	3

^aConditions: Substrate (0.1 mmol, 1.0 equiv) and NMe_4F (0.2 mmol, 2.0 equiv) stirred in DMF (0.2 M) at 80 °C for 24 h. Yields were determined by ^{19}F NMR spectroscopy with 1,3,5-trifluorobenzene as internal standard.

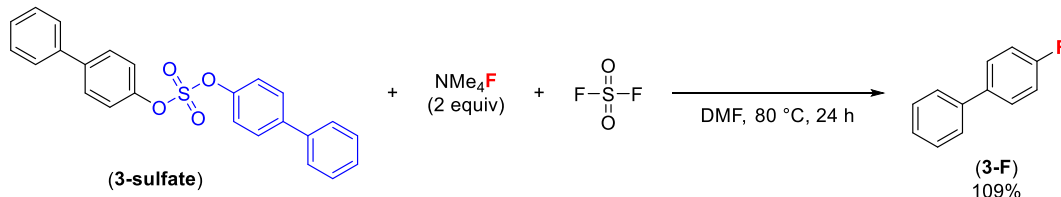
The low reactivity of the electron-neutral and -rich diaryl sulfates may in part explain the low yields of the fluorination of the corresponding aryl fluorosulfonate. The initial rates of di[(1,1'-biphenyl)-4-yl] sulfate (**3-sulfate**) and bis(4-chlorophenyl) sulfate (**9-sulfate**) were obtained at 80 °C. As shown in Figure 3.10, **3-sulfate** reacts very slowly under the reaction conditions while **9-sulfate** reacts quickly, providing ~10% of **9-F** in just 15 minutes. To improve the reactivity of electron-neutral substrates for the fluorination, the addition of exogenous SO_2F_2 to the reaction was investigated (Scheme 3.6). When di[(1,1'-biphenyl)-4-yl] sulfate (**3-sulfate**) is subjected to the standard conditions, the fluorination reaction affords only 29% of the desired fluorinated product (Table 3.6, entry 3). If exogenous SO_2F_2 (1 equiv) is added to the reaction solution, the yield greatly improves to 109% of **3-F** (Scheme 3.6). The yield of >100% is expected as the starting diaryl sulfate can form 2 equivalents of product. The experiment in Scheme 3.6 provides further support for the proposed mechanism in Scheme 3.5; the addition of SO_2F_2 pushes the reaction towards the formation of aryl fluorosulfonate **3-OFs**, from which the desired fluorination reaction can proceed.

Figure 3.10. Initial Rates for Fluorination of Diaryl Sulfate Substrates at 80 °C^a



^aConditions: Substrate (0.1 mmol, 1.0 equiv) and NMe₄F (0.2 mmol, 2.0 equiv) stirred in DMF (0.2 M) at 80 °C for the given time. Yields were determined by ¹⁹F NMR spectroscopy with 1,3,5-trifluorobenzene as internal standard.

Scheme 3.6. Effect of Exogenous SO₂F₂ on the Fluorination Reaction of **3-sulfate**^a



^aConditions: **3-sulfate** (0.05 mmol, 1.0 equiv), NMe₄F (0.1 mmol, 2.0 equiv), and SO₂F₂ (0.05 mmol, 1.0 equiv in DMF solution) stirred in DMF (0.2 M) at 80 °C for 24 h. Yields were determined by ¹⁹F NMR spectroscopy with 1,3,5-trifluorobenzene as internal standard.

3.5. Investigation of Other Sulfonate Electrophiles

While the fluorination of aryl fluorosulfonates with NMe₄F provides many advantages over the use of classic S_NAr electrophiles such as aryl chlorides, there are still some disadvantages. The formation of a diaryl sulfate intermediate reduces the yields of electron-neutral and electron-rich aryl fluorosulfonates as this byproduct is significantly less reactive for the desired fluorination reaction. Diaryl sulfate formation can be avoided using different sulfonate electrophiles where collapse of the pentacoordinate sulfur intermediate produces a less stable anion (relative to F⁻). Furthermore, while aryl fluorosulfonates offer a good alternative for industrial chemists, where access to phenols and sulfonyl fluoride offers an inexpensive alternative to the use of aryl chlorides, this methodology might have limited application in an academic or smaller scale setting where the use of SO₂F₂ is precluded by its toxicity and limited availability to academic chemists.³² Therefore, the utilization of other sulfonate electrophiles for deoxyfluorination reactions with NMe₄F is desirable.

A series of sulfonate electrophiles were investigated for the deoxyfluorination reaction with NMe₄F (Table 3.7). The reactivity of electronically diverse aryl fluorosulfonates (ArOFs) for fluorination with NMe₄F was compared to the corresponding aryl triflate (ArOTf)³³ and aryl nonaflate (ArONf).^{34,35} As shown in Table 3.7, for substrates with the strongly electron-withdrawing cyano group, **1-OFs** provided the highest yields of the desired fluorinated product; aryl triflate **1-OTf** provided only modest yields (66%) of **1-F** and byproducts including 4-cyanophenol were observed by GCMS indicating hydrolysis of the starting aryl triflate under the basic reaction conditions (entry 1). Aryl nonaflate **1-**

ONf afforded intermediate reactivity (73%). When *para*-Cl substrates are used in the fluorination reaction, the reactivity of these substrates differed from substrates with strongly electron-withdrawing groups (entry 2). For 4-chloro-substituted sulfonate electrophiles, aryl triflate **9-OTf** provided a higher yield of the desired fluorinated product than aryl fluorosulfonate **9-OFs** (85% versus 75%). This was also the case for electron-neutral and electron-rich substrates; aryl triflates provided comparable or slightly improved yields of the fluorinated product than the corresponding aryl fluorosulfonate (entries 3 and 4). This may be in part due to the lack of diaryl sulfate formation from the aryl triflate.

Table 3.7. Fluorination of Different Sulfonate Electrophiles with NMe₄F^a

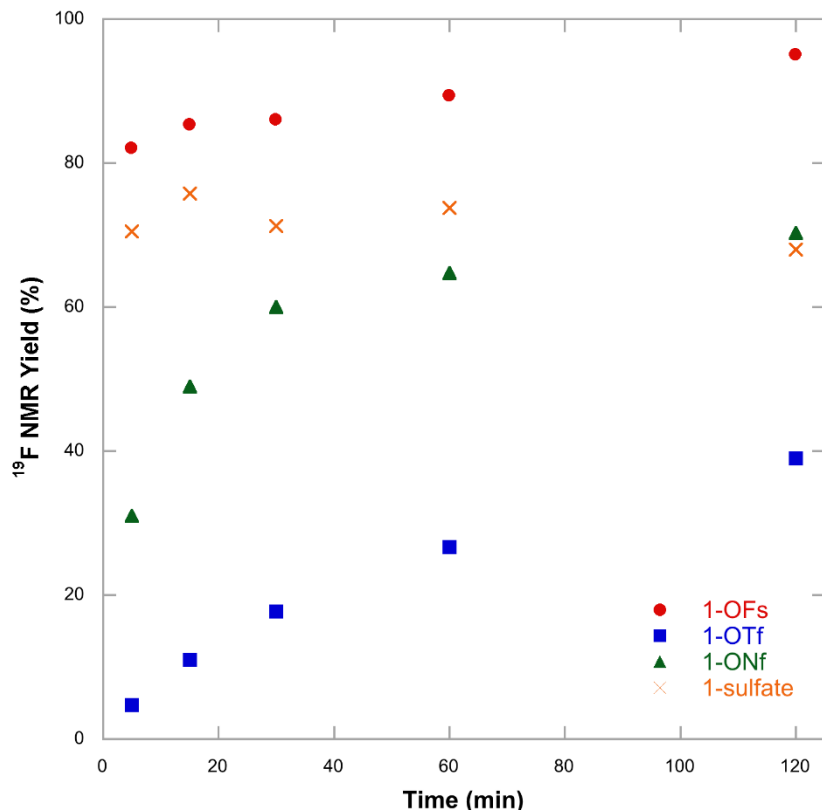
entry	R =	 (OFs)	 (OTf)	 (ONf)
1	CN (1-X)	92	66	73
2	Cl (9-X)	75	85	64
3	Ph (3-X)	77	87	53
4	OPh (21-X)	29	34	13

^aConditions: Substrate (0.1 mmol, 1.0 equiv) and NMe₄F (0.2 mmol, 2.0 equiv) stirred in DMF (0.2 M) at 80 °C for 24 h. Yields were determined by ¹⁹F NMR spectroscopy with 1,3,5-trifluorobenzene as internal standard.

To obtain more insight into the relative rates of fluorination of these different sulfonate electrophiles, time studies were conducted with 4-substituted benzonitrile substrates **1-OFs**, **1-OTf**, **1-ONf**, and **1-sulfate** (Figure 3.11). The relative rates of these substrates are: **1-OFs** > **1-sulfate** > **1-ONf** > **1-OTf**. **1-Sulfate** afforded 78% of the desired fluorinated product **1-F** in just 15 minutes at 80 °C; however, the yield of this reaction decreased by about 10% over the course of 2 hours. Additionally, when the reaction is run for 24 hours at 80 °C, the yield decreases to 54% (Table 3.6). This decrease in observed yield is indicative of the fluorinated product acting as an electrophile for subsequent reactions with *in situ* generated nucleophiles.^{5b,16} Biaryl ether products are observed by GCMS resulting from the reaction of **1-F** with phenoxide that is formed during

the course of the fluorination reaction. This side reaction can be suppressed by reducing the temperature to 25 °C (75% **1-F** after 24 h) or reducing the reaction time.

Figure 3.11. Reaction Profiles of Sulfonate Electrophiles of **1** with NMe₄F to Form **1-F**^a

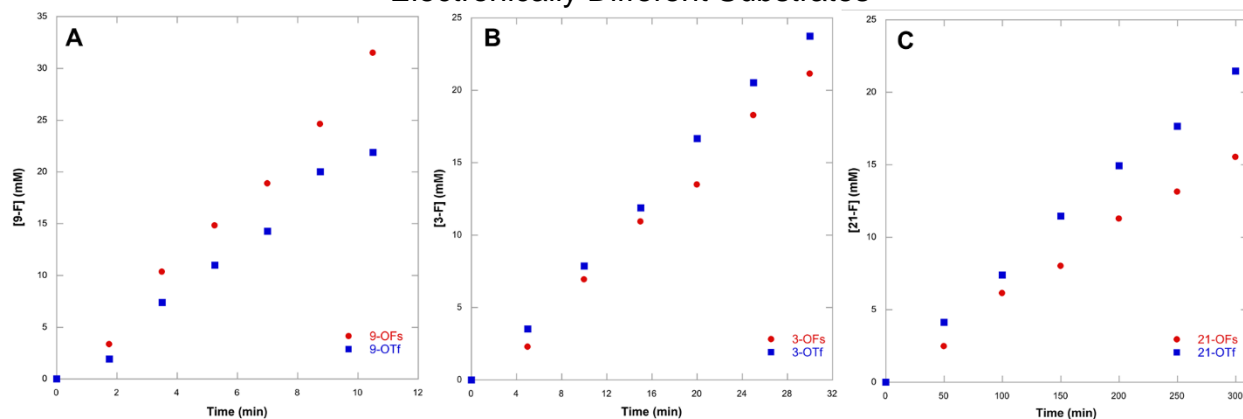


^aConditions: Substrate (0.1 mmol, 1.0 equiv) and NMe₄F (0.2 mmol, 2.0 equiv) stirred in DMF (0.2 M) at 80 °C for the given time. Yields were determined by ¹⁹F NMR spectroscopy with 1,3,5-trifluorobenzene as internal standard.

With disparities between the reactivity of aryl fluorosulfonates and aryl triflates regarding the electronic character of the substrates, rate studies were undertaken to gain a better understanding of the differences observed. For these studies, 4-chloro-substituted (**9-X**), 4-phenyl-substituted (**3-X**), and 4-phenoxy-substituted (**21-X**) aryl triflates and aryl fluorosulfonates were examined for the fluorination reaction (4-substituted benzonitrile substrates react too quickly at 80 °C to obtain meaningful kinetic data). Initial rates were obtained for this series of substrates for comparison of the differences in reactivity between the aryl fluorosulfonate and aryl triflate. As shown in Figure 3.12, electron-poor aryl fluorosulfonates react faster than the corresponding triflate (**9-X** substrates, Figure 3.12-A). As the substrates become more electron-neutral, the

reactivity of the aryl fluorosulfonate and triflate are very similar, with the aryl triflate **3-OTf** reacting slightly faster than the aryl fluorosulfonate **3-OFs** (Figure 3.12-B). Reactivity is switched for electron-rich substrates compared to electron-deficient substrates; 4-phenoxy-substituted aryl triflate **21-OTf** react faster than the corresponding aryl fluorosulfonate **21-OFs** (Figure 3.12-C). The improved reactivity of electron-rich aryl triflates may in part explain the increased yields of the desired fluorinated product. Furthermore, the formation of diaryl sulfate is avoided with this electrophile; the rate of fluorination is not necessarily outcompeted by other processes that consume starting material.

Figure 3.12. Initial Rates of Fluorination of Aryl Fluorosulfonates versus Aryl Triflates for Electronically Different Substrates

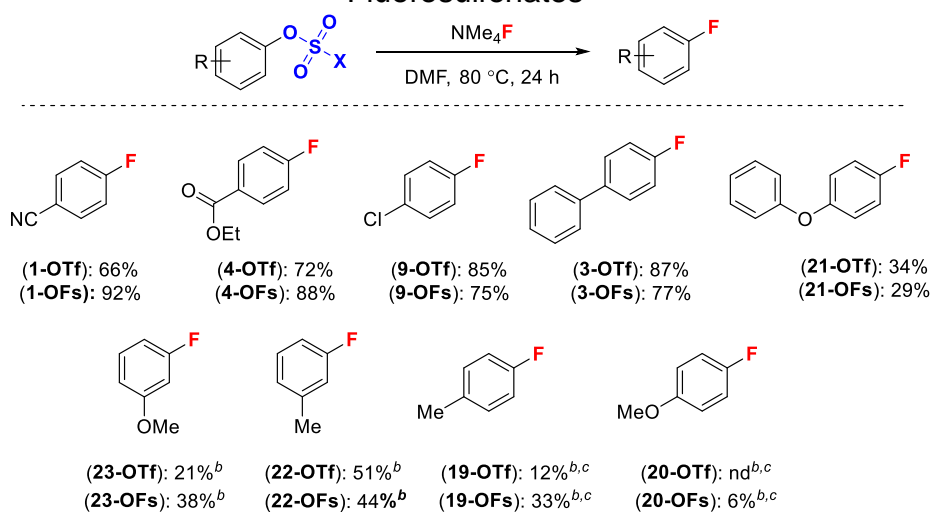


A. Initial rates for the fluorination of **9-OFs** and **9-OTf**. B. Initial rates for the fluorination of **3-OFs** and **3-OTf**. C. Initial rates for the fluorination of **21-OFs** and **21-OTf**. Conditions: Substrate (0.1 mmol, 1.0 equiv) and NMe₄F (0.2 mmol, 2.0 equiv) stirred in DMF (0.2 M) at 80 °C for the given time. Yields were determined by ¹⁹F NMR spectroscopy with 1,3,5-trifluorobenzene as internal standard.

With a better understanding of the reactivity of aryl triflates, the substrate scope for this fluorination reaction was evaluated and compared to the corresponding aryl fluorosulfonate (Figure 3.13). Aryl triflates with strongly electron-withdrawing substituents react poorly under the fluorination conditions in comparison to the aryl fluorosulfonates (**1** and **4**). This may be in part to the hydrolysis and/or fluorolysis of aryl triflates, and the improved yields with aryl fluorosulfonate substrates is a result of improved stability under the strongly basic conditions.³⁶ As the electronic nature of the arene becomes less pronounced, the difference in the yield of the fluorinated product between the aryl

fluorosulfonate and the aryl triflate becomes less apparent but with aryl triflates providing slightly higher yields (**3**, **9**, **21**, and **22**). When strongly electron-donating substituents are present on the substrates, the difference in reactivity is again more pronounced; fluorination of electron-rich aryl triflates is less efficient and lower yields are obtained relative to the corresponding aryl fluorosulfonate.

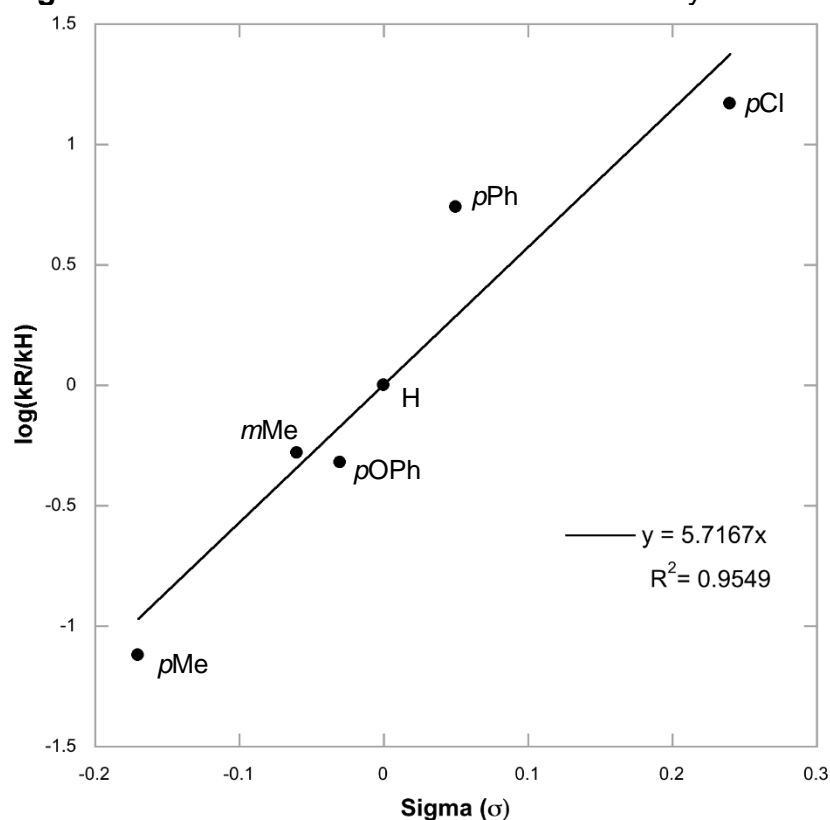
Figure 3.13. Substrate Scope for the Fluorination of Aryl Triflates Compared to Aryl Fluorosulfonates^a



^aConditions: Substrate (0.1 mmol, 1.0 equiv) and NMe₄F (0.02 mmol, 2.0 equiv) in DMF (0.2 M) at 80 °C for 24 h. Yields were determined by ¹⁹F NMR spectroscopy with 1,3,5-trifluorobenzene as internal standard. ^b100 °C. ^c5 equiv NMe₄F.

To verify that aryl triflates react similarly to aryl fluorosulfonates, a Hammett plot of the rate data for aryl triflates was made (Figure 3.14). This plot shows a ρ value of 5.7, indicating that fluorination is significantly faster with electron-withdrawing substituents on the aromatic ring and that significant negative charge is delocalized on the aromatic ring in the transition state. A similar Hammett plot was obtained for aryl fluorosulfonates (see Figure 3.5 above). These data support that the fluorination of aryl fluorosulfonates and aryl triflates proceed via a similar mechanism.

Figure 3.14. Hammett Plot for Fluorination of Aryl Triflates



3.6. Conclusions

A deoxyfluorination methodology was developed whereby phenols are converted to aryl fluorides via an aryl fluorosulfonate intermediate. The mild reaction can be applied to electronically diverse substrates, providing modest to excellent yield of the desired fluorinated product without the formation of regioisomers. Computational studies suggest that a key intermediate in the fluorination reaction is the coordination of F^- to sulfur from which a facile delivery of fluoride to the *ipso* carbon provides the desired product. This fluorination reaction offers an alternative to more traditional S_NAr fluorination and may find utility to large scale due to the inexpensive nature of the starting materials.

The transition metal free nucleophilic fluorination of aryl triflates offers an appealing alternative to the fluorination of aryl fluorosulfonates. Rate studies indicate that electron-rich aryl triflate react faster than the corresponding aryl fluorosulfonate; the slower reactivity of aryl fluorosulfonates is due to the formation of a diaryl sulfate intermediate that reacts slower in the fluorination reaction with electron-rich substrates. For substrates

with strongly electron-withdrawing groups, aryl fluorosulfonates display much improved reactivity than the aryl triflate potentially due to competing hydrolysis of the less stable aryl triflate. Computational studies and Hammett plots suggest similar mechanism for the fluorination reaction of the two sulfonate electrophiles. Since aryl triflates are more readily available to academic chemists and discovery chemists, this methodology may find utility in a development scale process, where large amounts of material are not required. For larger scale fluorination process, aryl fluorosulfonates are still a more viable option due to their synthesis from inexpensive commodity chemicals.

3.7. Outlook

It is anticipated that the research described in this chapter has the potential for far reaching application to industrial chemistry. The use of phenols and sulfuryl fluoride can offer an inexpensive alternative to the use of aryl chlorides for fluorination reactions. The use of aryl triflates to affect the same transformation offers advantages for smaller-scale applications. However, the mechanism of the reaction is still not fully understood and electron-rich substrates are low yielding. Computations suggest the formation of a pentacoordinate sulfur species as a key intermediate yet concerted S_NAr fluorination seems unlikely in light of experimental findings. A better understanding of the mechanism might help find improved conditions for electron-rich substrates.

3.8. Experimental Details and Characterization

3.8.1. General Information

NMR spectra were obtained on a Varian MR400 (400.52 MHz for 1H ; 376.87 MHz for ^{19}F ; 100.71 MHz for ^{13}C), a Varian vnmrs 500 (500.01 MHz for 1H ; 125.75 MHz for ^{13}C , and 470.56 MHz for ^{19}F), a Varian vnmrs 700 (699.76 MHz for 1H ; 175.95 MHz for ^{13}C), or a Varian Inova 500 (499.90 MHz for 1H ; 125.70 for ^{13}C) spectrometer. 1H and ^{13}C chemical shifts are reported in parts per million (ppm) relative to the residual solvent peak ($CDCl_3$: 1H : δ = 7.26 ppm, ^{13}C : δ = 77.16 ppm; $DMSO-d_6$: 1H : δ = 2.50 ppm, ^{13}C : δ = 39.52 ppm). ^{19}F NMR spectra are referenced based on the internal standard 1,3,5-trifluorobenzene, which appears at -108.33 ppm, or 4-fluoroanisole, which appears at -125.55 ppm. 1H and ^{19}F multiplicities are reported as follows: singlet (s), doublet (d), triplet

(t), quartet (q), multiplet (m), doublet of doublets (dd), doublet of triplets (dt), doublet of doublets (ddd), doublet of doublet of triplets (ddt). Coupling constants (J) are reported in Hz. GCMS analysis was performed on a Shimadzu GCMSQP2010 gas chromatograph mass spectrometer. The products were separated on a 30m length by 0.25 mm id RESTEK XTI-5 column coated with a 0.25 μ m film. Helium was employed as the carrier gas, with a constant column flow of 1.5 mL/min. The injector temperature was held constant at 250 °C. The GC oven temperature parameters are as follows: 32 °C hold for 5 min, ramp at 15 °C/min to 250 °C. Melting points were determined with a Mel-Temp 3.0 (Laboratory Devices, Inc) and are uncorrected. High resolution mass spectra were recorded on a Micromass AutoSpec Ultima Magnetic Sector mass spectrometer. Infrared spectroscopy was performed on a Perkin-Elmer Spectrum BX FT-IR spectrometer, and peaks are reported in cm^{-1} . Separations using preparatory HPLC were performed on a Varian PrepStar HPLC using a Waters μ PorasilTM 10 μ m 19x300mm silica column. All reactions utilizing sulfuryl fluoride were performed in a well-ventilated fumehood equipped with a wall mounted sulfuryl fluoride specific detector from Spectros Instruments.

3.8.2. Materials and Methods

Commercial reagents and solvents were used as received unless otherwise stated. Sulfuryl fluoride (SO_2F_2) was obtained from Synquest Laboratories. Anhydrous tetramethylammonium fluoride (NMe_4F), 8-hydroxyquinoline, 1-naphthol, 2-naphthol, Fenofibrate, spray-dried potassium fluoride, *N,N*-diisopropylethylamine, tetrabutylammonium cyanide, tetrabutylammonium difluorotriphenylsilicate (TBAT), 4-cyanophenol, 4-chlorophenol, oxalyl chloride, *p*-toluene sulfonic acid, imidazole, 4-dimethylaminopyridine (DMAP), sodium hydride (60% dispersion in mineral oil), and *m*-cresol were purchased from Sigma Aldrich. 4-Hydroxybenzophenone, 7-hydroxycoumarin, phenol, 3-methoxyphenol, acetohydroxamic acid, dimethyl sulfoxide (99.7% extra dry, anhydrous, AcroSealTM), *N,N*-dimethylformamide (99.8% extra dry, anhydrous, AcroSealTM), tetramethylammonium fluoride trihydrate, ethyl 4-hydroxybenzoate, tetrabutylammonium fluoride (1.0 M in THF), 1,1'-sulfonyldiimidazole, and boron tribromide solution (1.0 M in dichloromethane) were purchased from Acros. Tetramethylammonium chloride (NMe_4Cl) was purchased from Acros and dried at 60 °C

under vacuum overnight prior to use. Cesium fluoride was purchased from Chemetall. Lithium fluoride and potassium acetate were purchased from J. T. Baker. 4-Nitrophenol was purchased from Matheson, Coleman, and Bell, Inc. Estrone was purchased from G. D. Searle & Co. *N,N*-Dimethylformamide, anhydrous, 99.8% (DMF), triethylamine, dimethyl sulfoxide (DMSO), potassium carbonate (anhydrous), *N*-methyl-2-pyrrolidone (NMP), 1,3-dimethyl-2-imidazolidinone (DMI), acetonitrile (CH₃CN) (anhydrous), phosphorus (V) oxide, cesium carbonate, tetramethylammonium hydroxide (25% w/w aqueous solution), and 2-hydroxycarbazole were purchased from Alfa Aesar. 2-(Trimethylsilylethynyl)pyridine was purchased from Accela Chembio Inc. 1,3,5-Trifluorobenzene and 3,5-dibromobenzonitrile were purchased from Matrix Scientific. 2-Bromo-5-hydroxypyridine, perfluorodecalin, hexafluorobenzene, bis(pinacolato)diboron phenyl boronic acid, 3-fluorophenol, triflic anhydride, *tert*-butyldimethylsilyl chloride (TBSCl), perfluoro-1-butanefluorosulfonyl fluoride, 1,8-diazabicyclo[5.4.0]undec-7-ene (DBU), and bis(triphenylphosphine)palladium(II) dichloride were purchased from Oakwood Products. 4-Phenoxyphenol and 4-hydroxyindole were purchased from Chem-Impex International. Concentrated hydrochloric acid was purchased from EMD Millipore. 4-Hydroxy-*N,N*-dimethylbenzamide was purchased from Enamine. 2-Phenylphenol, 1,1'-sulfonyldiimidazole, and 4-phenylphenol were purchased from TCI America. Sodium fluoride, ethylene glycol, dichloromethane, pentane, diethyl ether, ethyl acetate, toluene, acetonitrile, hydrogen peroxide (30% in water), pyridine, and hexanes were obtained from Fisher Scientific and used as received. DMSO-*d*₆ and CDCl₃ were purchased from Cambridge Isotope Laboratories. Palladium(0) tetrakis(triphenylphosphine), copper (I) iodide, [1,1'-bis(diphenylphosphino)ferrocene] dichloropalladium(II), and cobaltocene were purchased from Strem. Ammonium hydroxide (30%) was purchased from VWR International. Tetrahydrofuran (THF) and toluene were purchased from VWR International and purified by an Innovative Technologies solvent purification system consisting of a copper catalyst, activated alumina, and molecular sieves.

P-Tolylfluorosulfonate, 4-methoxyphenyl sulfofluoridate, 4-(trifluoromethyl)phenyl sulfofluoridate, ethyl-4-((fluorosulfonyl)oxy)benzoate, 6-methylpyridin-3-yl sulfofluoridate, 3-chlorophenyl sulfofluoridate (**2-OFs**), and 2-isopropyl-5-methylphenyl sulfofluoridate were synthesized according to literature procedures.³⁷ 3-Hydroxy-5-(pyridine-2-

ylethynyl)benzonitrile was prepared according to the literature.^{9,38} Cobaltocenium fluoride (Cp₂CoF) was synthesized according to the literature procedure¹⁹ and stored in the freezer in an N₂-filled drybox. Anhydrous tetrabutylammonium fluoride and *isopropyl* 5-chloro-6-phenylpicolinate were prepared according to the literature procedure.²¹ *N*-(2-(4-(2-methoxyphenyl)piperazin-1-yl)ethyl)pyridin-2-amine was synthesized according to literature procedure.³⁹ 4-((Tertbutyldimethylsilyl)oxy)benzoic acid was prepared according to literature procedures.⁴⁰ O-Benzoylquinine was prepared according to literature procedure.⁴¹

A 1.5 wt % solution of sulfuryl fluoride in dry DMF was prepared by bubbling sulfuryl fluoride through a 100 mL AcroSeal® bottle of dry DMF for 15 min or until 1.5 g of sulfuryl fluoride was added. Excess sulfuryl fluoride was passed through a knockout pot containing an aqueous 1.0 M NaOH solution. Caution: Sulfuryl fluoride is a highly toxic gas. As such, all preparations of sulfuryl fluoride solutions were carried out in a well-ventilated fume hood and in the presence of a sulfuryl fluoride detector (Spectros Instruments).

Silica gel (6A, 40-63 µm particle size) for flash chromatography was purchased from Silicycle. Diatomaceous earth was purchased from Aqua Solutions. Magnesium sulfate (anhydrous, powder) was purchased from Avantor Performance Materials. Thin layer chromatography (TLC) was performed on Macherey-Nagel GmbH & Co. pre-coated TLC-plates SIL G-25 UV254 (0.25 mm silica gel with fluorescent indicator UV254).

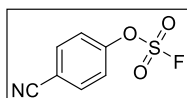
For the scale up of **3-F**, tetramethylammonium fluoride (99%), 4-phenylphenol (99.8%), anhydrous DMF (99.92%) and methyl *tert*-butyl ether (MTBE, 99%) were obtained from Sigma-Aldrich. Sulfuryl fluoride was obtained from Douglas Products (ProFume®). Dilute (1.0 N) hydrochloric acid was prepared from concentrated hydrochloric acid (12.1 N, 37.3 wt %) that was obtained from Fischer Scientific. Deionized water was taken directly from the laboratory tap immediately prior to use. All other reagents were obtained from commercial suppliers and used as received without further purification.

3.8.3. Synthesis of Aryl Fluorosulfonates

Synthesis of substrates 3-OFs, S5–6-OFs, S8–9-OFs, S15–16-OFs, and S21–23-OFs

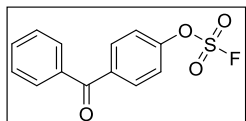
A solution of sulfuryl fluoride in 1,4-dioxane was prepared by bubbling sulfuryl fluoride through a premassed sealed bottle of anhydrous 1,4-dioxane (Acros) for 10 min. The wt % of SO₂F₂ was determined by massing the solution after preparation. These solutions were typically obtained in about 1.4–2.1 wt % of sulfuryl fluoride. To prepare the aryl fluorosulfonates, the corresponding phenol (1.0 equiv) and base (3.5 equiv) were combined in a round bottom flask equipped with a magnetic stir bar. The flask was sealed with a rubber septum, and the sulfuryl fluoride solution was added via syringe (1.6 equiv of SO₂F₂ relative to phenol). The resulting solution was stirred at room temperature for overnight. The reaction mixture was then purged with N₂ for 30 min to remove the residual SO₂F₂, and water was added. The mixture was acidified with concentrated HCl, and the product was extracted into dichloromethane. The organic layer was collected, dried over MgSO₄, filtered through a silica plug, and concentrated under vacuum. The products were purified by column chromatography on silica gel using either diethyl ether/pentane or hexanes/ethyl acetate as the eluent. All products were dried under vacuum in the presence of P₂O₅ prior to use in the fluorination reactions.

Synthesis of substrates 1-OFs, S10–13-OFs, S14-OFs, S17–18-OFs, S25–26-OFs, and S28–30-OFs. The corresponding phenol (1.0 equiv), base (3.0–3.5 equiv), and solvent (dichloromethane, ethyl acetate or acetonitrile) were combined in a round bottom flask equipped with a magnetic stir bar. The flask was capped with a rubber septum. Sulfuryl fluoride was bubbled through the reaction mixture for the specified time at room temperature. The reaction solution was then allowed to stir at room temperature overnight. The reaction was then worked up as described above.

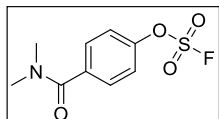


The reaction was performed using 4-cyanophenol (5.0 g, 42.0 mmol, 1.0 equiv) and triethylamine (20.0 mL, 147.0 mmol, 3.5 equiv) in dichloromethane (50.0 mL) in a 100 mL round bottom flask equipped with a magnetic stir bar. Product **1-OFs** was obtained as a

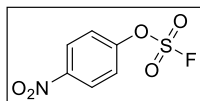
white solid (2.19 g, 26% yield, mp = 37.7–39.5 °C, R_f = 0.26 in 10% diethyl ether in pentane). The ^1H NMR (CDCl_3), ^{19}F NMR (CDCl_3), and $^{13}\text{C}\{^1\text{H}\}$ NMR (CDCl_3) spectra matched those previously reported in the literature.⁴² HRMS EI (m/z): $[\text{M}]^+$ calcd for $\text{C}_7\text{H}_4\text{FNO}_3\text{S}$, 200.9896; found, 200.9905.



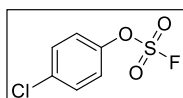
The reaction was performed using 4-hydroxybenzophenone (396.2 mg, 2.0 mmol, 1.0 equiv), triethylamine (1.0 mL, 7.0 mmol, 3.5 equiv), and 1.4 wt % SO_2F_2 in dioxane (23.0 mL, 3.2 mmol, 1.6 equiv). The product **5-OFs** was obtained as a white solid (375.2 mg, 67% yield, mp = 85.3–86.3 °C, R_f = 0.37 in 5% diethyl ether in pentane). ^1H NMR (401 MHz, CDCl_3): δ 7.94 (d, J = 8.8 Hz, 2H), 7.79 (d, J = 8.8 Hz, 2H), 7.63 (t, J = 7.6 Hz, 1H), 7.53–7.46 (multiple peaks, 4H). $^{13}\text{C}\{^1\text{H}\}$ NMR (176 MHz, CDCl_3): δ 194.6, 152.2, 137.8, 136.6, 133.0, 132.2, 129.9, 128.5, 120.9. ^{19}F NMR (376 MHz, CDCl_3): δ 38.7 (s, 1F). IR (cm^{-1}): 1647.6, 1590.3, 1453.9, 1231.7, 1139.1, 907.4, 814.6. HRMS EI (m/z): $[\text{M}]^+$ calcd for $\text{C}_{13}\text{H}_9\text{FO}_4\text{S}$, 280.0206; found, 280.0199.



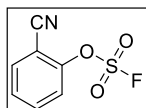
The reaction was performed using 4-hydroxy-*N,N*-dimethylbenzamide (330.0 mg, 2.0 mmol, 1.0 equiv), triethylamine (1.0 mL, 7.0 mmol, 3.5 equiv), and 1.9 wt % SO_2F_2 in dioxane (16.0 mL, 3.2 mmol, 1.6 equiv). The product **6-OFs** was obtained as a white solid (322.0 mg, 65% yield, mp = 77.4–78.5 °C, R_f = 0.33 in 2:1 ethyl acetate/hexanes). ^1H NMR (700 MHz, CDCl_3): δ 7.56 (d, J = 8.6 Hz, 2H), 7.40 (d, J = 8.6 Hz, 2H), 3.13 (s, 3H), 2.99 (s, 3H). $^{13}\text{C}\{^1\text{H}\}$ NMR (176 MHz, CDCl_3): δ 169.5, 150.3, 136.9, 129.3, 121.0, 39.5, 35.4. ^{19}F NMR (376 MHz, CDCl_3): δ 38.1 (s, 1F). IR (cm^{-1}): 1614.5, 1444.3, 1410.3, 1231.6, 1136.9, 924.3, 908.5, 808.0. HRMS electrospray (m/z): $[\text{M}+\text{H}]^+$ calcd for $\text{C}_9\text{H}_{11}\text{FNO}_4\text{S}$, 248.0387; found, 248.0394.



The reaction was performed using 4-nitrophenol (278.2 mg, 2.0 mmol, 1.0 equiv), triethylamine (1.0 mL, 7.0 mmol, 3.5 equiv), and 1.9 wt % SO₂F₂ in dioxane (16.0 mL, 3.2 mmol, 1.6 equiv). The product **8-OFs** was obtained as a pale yellow oil (338.7 mg, 77% yield, *R*_f = 0.39 in 5% diethyl ether in pentane). The ¹H NMR (CDCl₃), ¹⁹F NMR (CDCl₃), and ¹³C{¹H} NMR (CDCl₃) spectra matched those previously reported in the literature.⁴³ HRMS EI (*m/z*): [M]⁺ calcd for C₆H₄FNO₅S, 220.9794; found, 220.9798.

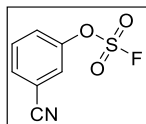


The reaction was performed using 4-chlorophenol (257.0 mg, 2.0 mmol, 1.0 equiv), triethylamine (1.0 mL, 7.0 mmol, 3.5 equiv), and 1.9 wt % SO₂F₂ in dioxane (16.0 mL, 3.2 mmol, 1.6 equiv). The product **9-OFs** was obtained as a colorless oil (315.8 mg, 75% yield, *R*_f = 0.41 in pentane). ¹H NMR (400 MHz, CDCl₃): δ 7.46 (d, *J* = 8.8 Hz, 2H), 7.30 (d, *J* = 8.8 Hz, 2H). ¹³C{¹H} NMR (126 MHz, CDCl₃): δ 148.5, 134.7, 130.7, 122.5. ¹⁹F NMR (376 MHz, CDCl₃): δ 37.6 (s, 1F). IR (cm⁻¹): 1448.4, 1232.1, 1146.2, 1093.8, 906.3. HRMS EI (*m/z*): [M]⁺ calcd for C₆H₄ClFO₃S, 209.9554; found, 209.9548.

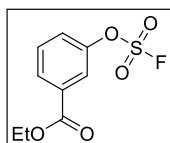


The reaction was performed using 2-cyanophenol (5.0 g, 42.0 mmol, 1.0 equiv) and potassium carbonate (12.0 g, 87.0 mmol, 2.1 equiv) in ethyl acetate (100 mL) in a 500 mL three-necked round bottom flask. SO₂F₂ was bubbled into the mixture at room temperature for 4 h, at which time GCMS analysis showed complete conversion to the desired product. The reaction mixture was purged with N₂ for 15 min to remove residual SO₂F₂, and the mixture was then filtered through a silica plug, which was washed with ethyl acetate (100 mL). The volatiles were removed under vacuum to afford product **10-OFs** as a colorless oil (8.1 g; 96% yield). ¹H NMR (400 MHz, CDCl₃): δ 7.88–7.71 (multiple peaks, 2H), 7.64–7.52 (multiple peaks, 2H). ¹³C{¹H} NMR (101 MHz, CDCl₃): δ 149.9,

135.0, 134.5, 129.2, 122.4, 113.2, 107.4. ^{19}F NMR (376 MHz, CDCl_3): δ 40.6 (s, 1F). IR (cm^{-1}): 2239.6, 1607.9, 1488.0, 1448.6, 1235.0, 1162.0, 1090.1, 905.9, 819.2, 786.5, 764.2. HRMS EI (m/z): $[\text{M}]^+$ calcd for $\text{C}_7\text{H}_4\text{FNO}_3\text{S}$, 200.9896; found, 200.9904.

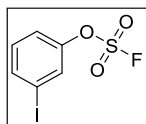


The reaction was performed using 3-cyanophenol (5.0 g, 42 mmol, 1.0 equiv) and potassium carbonate (11.6 g, 84.0 mmol, 2.1 equiv) in ethyl acetate (100 mL) in a 500 mL three-necked round bottom flask. SO_2F_2 was bubbled into the mixture at room temperature for 6 h, at which time GCMS analysis showed complete conversion to the desired product. The reaction mixture was purged with N_2 for 15 min to remove residual SO_2F_2 , and the mixture was then filtered through a silica plug, which was washed with ethyl acetate (100 mL). The volatiles were removed under vacuum to afford product **11-OFs** as a colorless oil (8.1 g, 96% yield). ^1H NMR (400 MHz, CDCl_3): δ 7.74 (m, 1H), 7.69–7.63 (multiple peaks, 3H). $^{13}\text{C}\{^1\text{H}\}$ NMR (101 MHz, CDCl_3): δ 149.6, 132.4, 131.6, 125.8, 124.8, 116.6, 114.8. ^{19}F NMR (376 MHz, CDCl_3): δ 38.8 (s, 1F). IR (cm^{-1}): 2338.3, 1579.6, 1449.7, 1432.9, 1236.9, 1206.3, 1121.6, 944.2, 846.6, 794.7, 677.2. HRMS EI (m/z): $[\text{M}]^+$ calcd for $\text{C}_7\text{H}_4\text{FNO}_3\text{S}$, 200.9896; found, 200.9903.

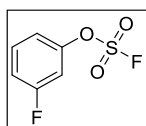


The reaction was performed using ethyl-3-hydroxybenzoate (10.4 g, 62 mmol, 1.0 equiv) and potassium carbonate (14.7 g, 125.0 mmol, 2.1 equiv) in ethyl acetate (100 mL) in a 500 mL three-necked round bottom flask. SO_2F_2 was bubbled through the solution at room temperature, and after 2 h, the bubbling was stopped, and the mixture was allowed to stir overnight. In the morning, GCMS analysis showed complete conversion to the desired product. The reaction mixture was purged with N_2 for 15 min to remove residual SO_2F_2 , and the mixture was then filtered through a silica plug, which was washed with ethyl acetate (100 mL). The volatiles were removed under vacuum to afford product **12-OFs** as a pale yellow oil (14.7 g, 95% yield). ^1H NMR (400 MHz, CDCl_3): δ 8.11 (dt, $J =$

7.3, 1.5 Hz, 1H), 8.01 (ddt, $J = 2.4, 1.6, 0.7$ Hz, 1H), 7.62–7.47 (multiple peaks, 2H), 4.42 (q, $J = 7.2$ Hz, 2H), 1.42 (t, $J = 7.2$ Hz, 3H). $^{13}\text{C}\{^1\text{H}\}$ NMR (101 MHz, CDCl_3): δ 164.5, 149.9, 133.3, 130.5, 129.7, 125.1, 122.0, 61.8, 14.2. ^{19}F NMR (376 MHz, CDCl_3): δ 38.1 (s, 1F). IR (cm^{-1}): 1721.7, 1444.2, 1263.4, 1227.7, 1155.2, 1095.2, 942.6, 817.5, 752.2. HRMS EI (m/z): $[\text{M}]^+$ calcd for $\text{C}_9\text{H}_9\text{FO}_5\text{S}$, 248.0155; found, 248.0159.

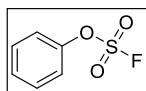


The reaction was performed using 3-iodophenol (10.0 g, 45 mmol, 1 equiv) and potassium carbonate (12.7 g, 91.0 mmol, 2.1 equiv) in ethyl acetate (100 mL) in a 500 mL three-necked round bottom flask. SO_2F_2 was bubbled through the solution at room temperature for 4 h, at which time GCMS analysis showed complete conversion to the desired product. The reaction mixture was purged with N_2 for 15 min to remove residual SO_2F_2 , and the mixture was then filtered through a silica plug, which was washed with ethyl acetate (100 mL). The volatiles were removed under vacuum to afford product **13-OFs** as a colorless oil (13.2 g, 96% yield). ^1H NMR (400 MHz, CDCl_3): δ 7.77 (d, $J = 8.5$ Hz, 1H), 7.70 (s, 1H), 7.34 (dt, $J = 8.5, 2.5$ Hz, 1H), 7.22 (m, 1H). $^{13}\text{C}\{^1\text{H}\}$ NMR (176 MHz, CDCl_3): δ 149.6, 137.9, 131.5, 130.0, 120.3, 93.9. ^{19}F NMR (376 MHz, CDCl_3): δ 38.2 (s, 1F). IR (cm^{-1}): 1573.2, 1446.8, 1230.0, 1146.3, 917.4, 818.1, 786.3, 770.4. HRMS EI (m/z): $[\text{M}]^+$ calcd for $\text{C}_6\text{H}_4\text{FIO}_3\text{S}$, 301.8910; found, 301.8911.

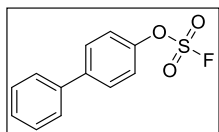


The reaction was performed using 3-fluorophenol (8.0 g, 71 mmol, 1.0 equiv) and potassium carbonate (19.7 g, 143.0 mmol, 2.1 equiv) in ethyl acetate (100 mL) in a 500 mL three-necked round bottom flask. SO_2F_2 was bubbled into the mixture at room temperature for 3 h, at which time GCMS analysis showed complete conversion to the desired product. The reaction mixture was purged with N_2 for 15 min to remove residual SO_2F_2 , and the mixture was then filtered through a silica plug, which was washed with ethyl acetate (100 mL). The volatiles were removed under vacuum to afford product **14-**

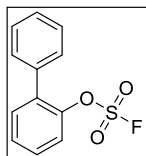
OFs as a light pink oil (11.9 g, 86% yield). ^1H NMR (400 MHz, CDCl_3): δ 7.47 (td, $J = 8.4$, 6.3 Hz, 1H), 7.20–7.15 (multiple peaks, 2H), 7.12 (m, 1H). $^{13}\text{C}\{^1\text{H}\}$ NMR (101 MHz, CDCl_3): δ 162.8 (d, $J = 251.6$ Hz), 150.1 (d, $J = 10.3$ Hz), 131.3 (d, $J = 8.8$ Hz), 116.7 (d, $J = 3.7$ Hz), 116.0 (d, $J = 21.3$ Hz), 109.4 (d, $J = 25.7$ Hz). ^{19}F NMR (376 MHz, CDCl_3): δ 38.0 (s, 1F), -107.9 (m, 1F). IR (cm^{-1}): 1602.4, 1485.9, 1446.3, 1224.0, 1103.8, 956.1, 871.7, 804.0, 778.0, 675.8. HRMS EI (m/z): $[\text{M}]^+$ calcd for $\text{C}_6\text{H}_4\text{F}_2\text{O}_3\text{S}$, 193.9849; found, 193.9858.



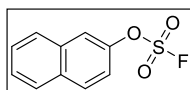
The reaction was performed using phenol (94.1 mg, 1.0 mmol, 1.0 equiv), triethylamine (0.49 mL, 3.5 mmol, 3.5 equiv), and 2.1 wt % SO_2F_2 in dioxane (7.4 mL, 1.6 mmol SO_2F_2 , 1.6 equiv). Product **15-OFs** was obtained as a colorless oil (84.8 mg, 48% yield, $R_f = 0.33$ in pentane). The ^1H NMR (CDCl_3), ^{19}F NMR (CDCl_3), and $^{13}\text{C}\{^1\text{H}\}$ NMR (CDCl_3) spectra matched those previously reported in the literature.^{43,43} HRMS EI (m/z): $[\text{M}]^+$ calcd for $\text{C}_6\text{H}_5\text{FO}_3\text{S}$, 175.9943; found, 175.9939.



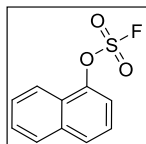
The reaction was performed using 4-phenylphenol (170.0 mg, 1.0 mmol, 1.0 equiv), triethylamine (0.49 mL, 3.5 mmol, 3.5 equiv), and 1.4 wt % SO_2F_2 in dioxane (11.5 mL, 1.6 mmol SO_2F_2 , 1.6 equiv). Product **3-OFs** was obtained as a white solid (236.8 mg, 94% yield, mp = 94.3–95.4 °C, $R_f = 0.68$ in 5% diethyl ether in pentane). The ^1H NMR (CDCl_3), ^{19}F NMR (CDCl_3), and $^{13}\text{C}\{^1\text{H}\}$ NMR (CDCl_3) spectra matched those previously reported in the literature.⁴³ HRMS EI (m/z): $[\text{M}]^+$ calcd for $\text{C}_{12}\text{H}_9\text{FO}_3\text{S}$, 252.0256; found, 252.0258.



The reaction was performed using 2-phenylphenol (340.0 mg, 2.0 mmol, 1.0 equiv), triethylamine (1.0 mL, 7.0 mmol, 3.5 equiv), and 1.4 wt % SO₂F₂ in dioxane (23.0 mL, 3.2 mmol SO₂F₂, 1.6 equiv). Product **16-OFs** was obtained as a colorless oil (261.6 mg, 52% yield, R_f = 0.64 in 5% diethyl ether in pentane). ¹H NMR (500 MHz, CDCl₃): δ 7.51–7.40 (multiple peaks, 9H). ¹³C{¹H} NMR (176 MHz, CDCl₃): δ 147.2, 135.4, 135.2, 132.0, 129.1, 129.0, 128.8, 128.6, 128.3, 121.5. ¹⁹F NMR (376 MHz, CDCl₃): δ 40.2 (s, 1F). IR (cm⁻¹): 1444.7, 1230.4, 1150.6, 1100.0, 908.5, 813.5, 780.4, 756.0, 730.7, 697.5. HRMS EI (*m/z*): [M]⁺ calcd for C₁₂H₉FO₃S, 252.0256; found, 252.0258.

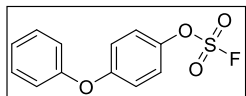


The reaction was performed using 2-naphthol (1.0 g, 6.9 mmol, 1.0 equiv) and triethylamine (3.4 mL, 24.2 mmol, 3.5 equiv) in dichloromethane (10 mL) in a 25 mL round bottom flask equipped with a magnetic stir bar. SO₂F₂ was bubbled through the reaction for 10 minutes. Product **17-OFs** was obtained as a white solid (1.37 g, 88% yield, mp = 31.2–32.5 °C, R_f = 0.81 in 5% diethyl ether in pentane). The ¹H NMR (CDCl₃), ¹⁹F NMR (CDCl₃), and ¹³C{¹H} NMR (CDCl₃) spectra matched those previously reported in the literature.⁴³ HRMS EI (*m/z*): [M]⁺ calcd for C₁₀H₇FO₃S, 226.0100; found, 226.0098.

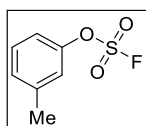


The reaction was performed using 1-naphthol (1.0 g, 6.9 mmol, 1.0 equiv) and triethylamine (3.4 mL, 24.2 mmol, 3.5 equiv) in dichloromethane (10 mL) in a 25 mL round bottom flask equipped with a magnetic stir bar. SO₂F₂ was bubbled through the reaction for 10 minutes. Product **18-OFs** was obtained as a colorless oil (1.33 g, 85% yield, R_f = 0.67 in 5% diethyl ether in pentane). The ¹H NMR (CDCl₃), ¹⁹F NMR (CDCl₃), and ¹³C{¹H} NMR (CDCl₃) spectra matched those previously reported in the literature.⁴³

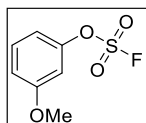
NMR (CDCl₃) spectra matched those previously reported in the literature.⁴⁴ HRMS EI (*m/z*): [M]⁺ calcd for C₁₀H₇FO₃S, 226.0100; found, 226.0101.



The reaction was performed using 4-phenoxyphenol (372.0 mg, 2.0 mmol, 1.0 equiv), triethylamine (1.0 mL, 7.0 mmol, 3.5 equiv) and 1.4 wt % SO₂F₂ in dioxane (23.0 mL, 3.2 mmol SO₂F₂, 1.6 equiv). Product **21-OFs** was obtained as a colorless oil (534.0 mg, 100% yield, R_f = 0.78 in 5% diethyl ether in pentane). ¹H NMR (500 MHz, CDCl₃): δ 7.38 (t, *J* = 8.0 Hz, 2H), 7.28 (d, *J* = 9.0 Hz, 2H), 7.18 (t, *J* = 8.0 Hz, 1H), 7.04 (d, *J* = 9.0 Hz, 4H). ¹³C{¹H} NMR (176 MHz, CDCl₃): δ 157.9, 155.9, 144.8, 130.0, 124.3, 122.2, 119.4, 118.6. ¹⁹F NMR (376 MHz, CDCl₃): δ 36.7 (s, 1F). IR (cm⁻¹): 1586.8, 1486.2, 1445.3, 1230.7, 1161.5, 1139.5, 907.9, 814.0, 690.8. HRMS EI (*m/z*): [M]⁺ calcd for C₁₂H₉FO₄S, 268.0206; found, 268.0204.

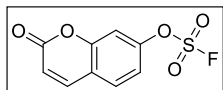


The reaction was performed using *m*-cresol (0.11 mL, 1.0 mmol, 1.0 equiv), triethylamine (0.49 mL, 3.5 mmol, 3.5 equiv), and 2.1 wt % SO₂F₂ in dioxane (7.4 mL, 1.6 mmol SO₂F₂, 1.6 equiv). Product **22-OFs** was obtained as a colorless oil (124.6 mg, 60% yield, R_f = 0.7 in pentane). ¹H NMR (500 MHz, CDCl₃): δ 7.36 (dt, *J* = 7.5, 1.5 Hz, 1H), 7.24 (d, *J* = 7.5 Hz, 1H), 7.16–7.15 (multiple peaks, 2H), 2.43 (s, 3H). ¹³C NMR (176 MHz, CDCl₃): δ 150.0, 141.0, 129.9, 129.3, 121.2, 117.7, 21.2. ¹⁹F NMR (376 MHz, CDCl₃): δ 37.5 (s, 1F). IR (cm⁻¹): 1615.9, 1444.3, 1237.7, 1212.5, 1118.0, 940.9, 855.5, 798.3, 782.7. HRMS EI (*m/z*): [M]⁺ calcd for C₇H₇FO₃S, 190.0100; found, 190.0107.

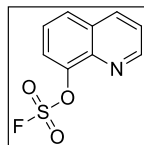


The reaction was performed using 3-methoxyphenol (0.11 mL, 1.0 mmol, 1.0 equiv), triethylamine (0.49 mL, 3.5 mmol, 3.5 equiv), and 2.1 wt % SO₂F₂ in dioxane (7.4 mL, 1.6

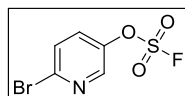
mmol SO₂F₂, 1.6 equiv). Product **23-OFs** was obtained as a colorless oil (123.8 mg, 60% yield, R_f = 0.64 in pentane). The ¹H NMR (CDCl₃), ¹⁹F NMR (CDCl₃), and ¹³C{¹H} NMR (CDCl₃) spectra matched those previously reported in the literature.⁴³ HRMS EI (*m/z*): [M]⁺ calcd for C₇H₇FO₄S, 206.0049; found, 206.0049.



The reaction was performed using 7-hydroxycoumarin (1.0 g, 6.2 mmol, 1.0 equiv) and triethylamine (3.0 mL, 21.7 mmol) in dichloromethane (10.0 mL) in a 25 mL round bottom flask equipped with a magnetic stir bar. SO₂F₂ was bubbled through the reaction for 10 minutes. Product **25-OFs** was obtained as a white solid (1.08 g, 72% yield, mp = 124.1–125.3 °C, R_f = 0.29 in 60% diethyl ether in pentane). The ¹H NMR (CDCl₃), ¹⁹F NMR (CDCl₃), and ¹³C{¹H} NMR (CDCl₃) spectra matched those previously reported in the literature.⁴³ HRMS electrospray (*m/z*): [M+H]⁺ calcd for C₉H₆FO₅S, 244.9914; found, 244.9914.

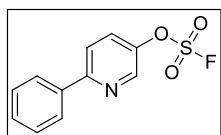


The reaction was performed using 8-hydroxyquinoline (725.0 mg, 5.0 mmol, 1.0 equiv) and *N,N*-diisopropylethylamine (2.6 mL, 15 mmol, 3.0 equiv), and acetonitrile (7.5 mL) in a 25 mL round bottom flask equipped with a magnetic stir bar. SO₂F₂ was bubbled through the reaction for 15 min. Product **26-OFs** was obtained as a white solid (482.3 mg, 42% yield, mp = 56.3–58.3 °C, R_f = 0.33 in 20% diethyl ether in pentane). The ¹H NMR (CDCl₃), ¹⁹F NMR (CDCl₃), and ¹³C{¹H} NMR (CDCl₃) spectra matched those previously reported in the literature.⁴⁵ HRMS EI (*m/z*): [M]⁺ calcd for C₉H₆FNO₃S, 227.0052; found, 227.0053.

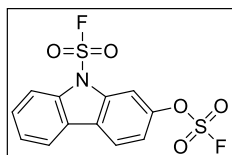


The reaction was performed using 6-bromopyridin-3-ol (864.5 mg, 5.0 mmol, 1.0 equiv) and triethylamine (1.0 mL, 7.5 mmol, 3.5 equiv) in dichloromethane (8.0 mL) in a 25 mL

round bottom flask equipped with a magnetic stir bar. SO₂F₂ was bubbled through the reaction for 15 min. The product was obtained as a white solid (990.0 mg, 78% yield, mp = 53.4–55.4 °C, R_f = 0.45 in 10% diethyl ether in pentane). The ¹H NMR (CDCl₃), ¹⁹F NMR (CDCl₃), and ¹³C{¹H} NMR (CDCl₃) spectra matched those previously reported in the literature.⁴⁵ HRMS EI (*m/z*): [M]⁺ calcd for C₅H₃BrFNO₃S, 254.9001; found, 254.9003.

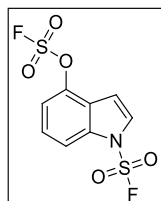


The reaction was performed using 6-bromopyridin-3-yl sulfofluoridate (255.0 mg, 1.0 mmol, 1.0 equiv), phenyl boronic acid (182.9 mg, 1.5 mmol, 1.5 equiv), Pd(PPh₃)₄ (116.0 mg, 0.01 mmol, 10 mol %), and potassium fluoride (174.0 mg, 3.0 mmol, 3.0 equiv) in toluene (10 mL) in a 20 mL vial equipped with a magnetic stir bar and capped with a Teflon-lined cap. The reaction was heated to 110 °C for 3 h and then cooled to room temperature. The reaction solution was diluted with ethyl acetate (20 mL), washed with brine, dried over MgSO₄, filtered, and concentrated. Product **28-OFs** was obtained as a white solid (195.0 mg, 77% yield, mp = 91.2–94.1 °C, R_f = 0.33 in 10% diethyl ether in pentane). The ¹H NMR (CDCl₃), ¹⁹F NMR (CDCl₃), and ¹³C{¹H} NMR (CDCl₃) spectra matched those previously reported in the literature.⁴⁵ HRMS EI (*m/z*): [M+H]⁺ calcd for C₁₁H₉FNO₃S, 254.0282; found, 254.0286.



The reaction was performed using 2-hydroxycarbazole (1.0 g, 5.5 mmol, 1.0 equiv) and *N,N*-diisopropylethylamine (2.9 mL, 16.4 mmol, 3.0 equiv) in acetonitrile (10 mL) in a 25 mL round bottom flask equipped with a magnetic stir bar. SO₂F₂ was bubbled through the reaction for 15 minutes. Product **29-OFs** was obtained as a white solid (719.7 mg, 38% yield, mp = 85.7–87.9 °C, R_f = 0.24 in 10% dichloromethane in hexanes). ¹H NMR (500 MHz, CDCl₃): δ 8.11–8.07 (multiple peaks, 3H), 8.03 (dd, *J* = 7.5, 1.0 Hz, 1H), 7.62 (td, *J* = 8.5, 1.5 Hz, 1H), 7.54 (t, *J* = 7.5 Hz, 1H), 7.51 (dd, *J* = 8.5, 1.5 Hz, 1H). ¹³C{¹H} NMR

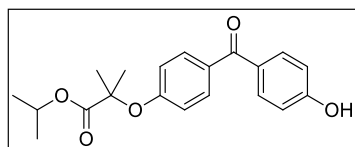
(176 MHz, CDCl₃): δ 148.9, 138.1, 137.4, 129.0, 126.3, 125.9, 124.6, 121.7, 120.7, 118.2, 114.8, 108.6. ¹⁹F NMR (376 MHz, CDCl₃): δ 53.8 (s, 1F), 38.1 (s, 1F). IR (cm⁻¹): 1454.1, 1436.2, 1223.1, 1210.8, 1111.5, 963.8, 894.8, 778.5. HRMS EI (*m/z*): [M]⁺ calcd for C₁₂H₇F₂NO₅S₂, 346.9743; found 346.9737.



The reaction was performed using 4-hydroxyindole (1.0 g, 7.5 mmol, 1.0 equiv) and *N,N*-diisopropylethylamine (3.9 mL, 22.5 mmol, 3.0 equiv) in acetonitrile (10 mL) in a 25 mL round bottom flask equipped with a magnetic stir bar. SO₂F₂ was bubbled through the reaction for 15 minutes. Product **30-OFs** was obtained as a white solid (966.9 mg, 43% yield, mp = 60.4–61.9 °C, R_f = 0.66 in 6:1 hexanes/ethyl acetate). ¹H NMR (500 MHz, CDCl₃): δ 7.96 (d, *J* = 8.0 Hz, 1H), 7.54–7.49 (multiple peaks, 2H), 7.40 (d, *J* = 8.0 Hz, 1H), 6.94 (d, *J* = 3.6 Hz, 1H). ¹³C{¹H} NMR (126 MHz, CDCl₃): δ 142.6, 136.3, 127.9, 126.8, 123.6, 117.1, 114.2, 106.6. ¹⁹F NMR (376 MHz, CDCl₃): δ 56.0 (s, 1F), 38.5 (s, 1F). IR (cm⁻¹): 1429.6, 1222.3, 1188.2, 1169.0, 1131.8, 965.8, 791.1, 750.7. HRMS EI (*m/z*): [M]⁺ calcd for C₈H₅F₂NO₅S₂, 296.9577; found, 296.9585.

3.8.4. Synthesis of Phenols

Phenols **31-OH** and **33-OH** were prepared via a modified literature procedure as described in detail below.⁴⁶

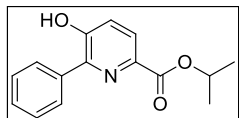


Fenofibrate (1.0 g, 2.8 mmol, 1.0 equiv), acetohydroxamic acid (624.0 mg, 8.3 mmol, 3.0 equiv), potassium carbonate (1.9 g, 13.9 mmol, 5.0 equiv), and dimethyl sulfoxide (10 mL, 0.3 M) were added to a 20 mL glass vial equipped with a magnetic stir bar. The vial was sealed with a Teflon-lined cap and heated to 80 °C for 40 h. The reaction was cooled

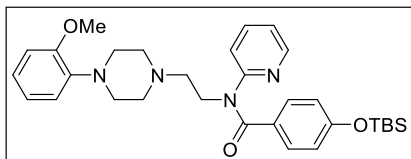
in an ice bath and then acidified slowly with 2.0 M HCl. The reaction mixture was extracted with ethyl acetate, and the organic layers were collected, dried over MgSO₄, filtered, and concentrated under vacuum. The resulting residue was purified by flash chromatography on silica gel to afford the product **31-OH** as a tan solid (438.1 mg, 46% yield, mp = 95.7–97.5 °C, R_f = 0.24 in 3:1 hexanes/EtOAc). ¹H NMR (CDCl₃, 400 MHz): δ 7.70 (dd, *J* = 8.8, 2.0 Hz, 4H), 6.88 (dd, *J* = 14.4, 8.8 Hz, 4H), 5.07 (septet, *J* = 6.3 Hz, 1H), 1.66 (s, 6H), 1.21 (d, *J* = 6.3 Hz, 6H). ¹³C{¹H} NMR (CDCl₃, 176 MHz): δ 194.80, 173.3, 159.1, 132.5, 131.7, 131.1, 130.6, 130.4, 117.2, 115.0, 79.3, 69.3, 25.3, 21.5. IR (cm⁻¹): 3278.8, 1733.9, 1718.2, 1598.2, 1560.0, 1282.4, 1147.0, 1098.8. HRMS electrospray (*m/z*): [M+H]⁺ calcd for C₂₀H₂₃O₅, 343.1540; found, 343.1541.

Estrone (2.0 g, 7.40 mmol, 1.0 equiv), *p*-toluenesulfonic acid (17.0 mg, 0.09 mmol, 0.01 equiv), ethylene glycol (2.5 mL, 44.83 mmol, 6.0 equiv), and toluene (12.5 mL, 0.6 M) were added to a round bottom flask equipped with a magnetic stir bar and a Dean-Stark trap. The reaction mixture was heated to reflux overnight. The reaction was cooled to room temperature and diluted with ethyl acetate. The organic layer was extracted with saturated sodium bicarbonate, water, and then brine. The organic layer was then collected, dried over MgSO₄, filtered, and concentrated under vacuum. The resulting residue was purified by silica flash chromatography to afford product **32-OH** as a white solid (1.78 g, 77% yield, mp = 183.5–184.1 °C, R_f = 0.11 in 5:1 pentane/ether). ¹H NMR (500 MHz, CDCl₃) δ 7.15 (d, *J* = 8.4 Hz, 1H), 6.63 (dd, *J* = 8.4, 2.6 Hz, 1H), 6.57 (d, *J* = 2.6 Hz, 1H), 5.39 (s, 1H), 4.04–3.87 (multiple peaks, 4H), 2.90–2.72 (multiple peaks, 2H), 2.31 (ddd, *J* = 11.4, 6.8, 3.9 Hz, 1H), 2.20 (m, 1H), 2.06 (ddd, *J* = 14.3, 11.7, 2.9 Hz, 1H), 1.93–1.83 (multiple peaks, 2H), 1.83–1.72 (multiple peaks, 2H), 1.64 (m, 1H), 1.55 (m, 1H), 1.51–1.28 (multiple peaks, 4H), 0.90 (s, 3H). ¹³C{¹H} NMR (126 MHz, CDCl₃) δ 153.5, 138.4, 132.8, 126.6, 119.7, 115.4, 112.8, 65.3, 64.7, 49.4, 46.3, 43.7, 39.1, 34.3, 30.9, 29.7, 27.0, 26.2.

22.5, 14.5. HRMS electrospray (m/z): $[M+H]^+$ calcd for $C_{20}H_{26}O_3$, 315.1955; found 315.1952.

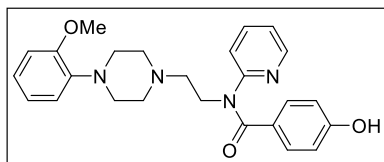


Isopropyl 5-chloro-6-phenylpicolinate (1.0 g, 3.6 mmol, 1.0 equiv), acetohydroxamic acid (820.0 mg, 10.9 mmol, 3.0 equiv), potassium carbonate (2.5 g, 18.0 mmol, 5.0 equiv), and dimethyl sulfoxide (12 mL, 0.3 M) were added to a 20 mL glass vial equipped with a magnetic stir bar. The vial was sealed with a Teflon-lined cap and heated to 80 °C for 40 h. The reaction mixture was cooled in an ice bath and then acidified slowly with 2.0 M HCl. The resulting mixture was extracted with ethyl acetate, and the organic layer was collected, dried over $MgSO_4$, filtered, and concentrated under vacuum. The resulting residue was purified by flash chromatography on silica gel to afford product **33-OH** as a yellow solid (813.5 mg, 88% yield, mp = 143.6–145.6 °C, R_f = 0.24 in 3:1 hexanes/EtOAc). 1H NMR ($CDCl_3$, 500 MHz): δ 8.00 (d, J = 8.5 Hz, 1H), 7.75 (d, J = 7.0 Hz, 2H), 7.50–7.427 (multiple peaks, 3H), 7.36 (d, J = 8.5 Hz, 1H), 6.16 (s, 1H), 5.29 (septet, J = 6.5 Hz, 1H), 1.39 (d, J = 6.5 Hz, 6H). $^{13}C\{^1H\}$ NMR ($CDCl_3$, 176 MHz): δ 164.7, 153.8, 146.6, 135.7, 129.0, 128.8, 128.2, 125.9, 123.8, 69.3, 30.9, 21.8. IR (cm^{-1}): 3301.8, 1698.3, 1572.0, 1269.7, 1208.0, 1102.7. HRMS electrospray (m/z): $[M+H]^+$ calcd for $C_{15}H_{16}NO_3$, 258.1125; found, 258.1130.



4-((*tert*-butyldimethylsilyl)oxy)benzoic acid (1.51 g, 6.0 mmol, 2.0 equiv), dichloromethane (10 mL), and dimethylformamide (5 drops) were added to a round bottom flask equipped with magnetic stir bar. The reaction was chilled in an ice bath as oxalyl chloride (0.52 mL, 6.1 mmol, 2.0 equiv) was added dropwise. The reaction was stirred cold for 1 h and at room temperature for 1 h before the dichloromethane and excess oxalyl chloride were removed under vacuum. The remaining residue was taken

up in dichloromethane (20 mL) and was slowly added to a chilled round bottom flask containing *N*-(2-(4-(2-methoxyphenyl)piperazin-1-yl)ethyl)pyridin-2-amine (957.0 mg, 3.0 mmol, 1.0 equiv), triethylamine (1.7 mL, 12 mmol, 4.0 equiv), and dichloromethane (20 mL). The reaction was stirred in the ice bath for 15 min. Water was added, and the resulting mixture was extracted with dichloromethane. The organic extracts were collected, dried over MgSO₄, filtered, and concentrated under vacuum. The resulting residue was purified by flash chromatography on silica gel to afford the product **34-OTBS** as a yellow oil (1.26 g, 73% yield, *R*_f = 0.51 in ethyl acetate).^E ¹H NMR (500 MHz, CDCl₃): δ 8.41 (d, *J* = 4.6 Hz, 1H), 7.35 (t, *J* = 7.7 Hz, 1H), 7.22 (d, *J* = 8.5 Hz, 2H), 7.02–6.92 (m, 2H), 6.91–6.78 (multiple peaks, 3H), 6.72 (d, *J* = 8.0 Hz, 1H), 6.64 (d, *J* = 8.5 Hz, 2H), 4.28 (t, *J* = 6.7 Hz, 2H), 3.82 (s, 3H), 2.92 (s, br, 4H), 2.75 (t, *J* = 6.7 Hz, 3H), 2.64 (s, br, 4H), 0.93 (s, 9H), 0.14 (s, 6H). ¹³C{¹H} NMR (126 MHz, CDCl₃): δ 170.6, 157.6, 157.0, 152.3, 148.6, 141.5, 136.91, 130.8, 129.1, 123.0, 122.9, 121.0, 120.6, 119.7, 118.2, 111.3, 56.6, 55.4, 53.4, 50.7, 45.6, 25.7, 18.3, –4.4. HRMS electrospray (*m/z*): [M+H]⁺ calcd for C₃₁H₄₂N₄O₃Si, 547.3099; found 547.3102.

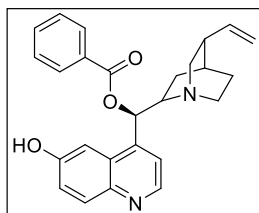


Product **34-OTBS** (416.0 mg, 7.6 mmol, 1.0 equiv) and tetrahydrofuran (7.6 mL) were added to a 20 mL glass vial equipped with magnetic stir bar. The reaction was chilled in an ice bath as a tetrabutylammonium fluoride solution (1.0 M in tetrahydrofuran, 0.9 mL, 1.2 equiv) was added dropwise. The reaction was stirred cold for 1 h and then the solvent was removed under vacuum. The remaining residue was taken up in diethyl ether and water and extracted with diethyl ether. The organic extracts were collected, dried over MgSO₄, filtered, and concentrated under vacuum. The product was purified by flash chromatography on silica gel to afford **34-OH** as a white solid (233 mg, 71% yield, mp = 61.6–62.8 °C, *R*_f = 0.39 in ethyl acetate).^F ¹H NMR (500 MHz, CDCl₃): δ 8.38 (d, *J* = 4.4 Hz, 1H), 7.37 (m, 1H), 7.12 (d, *J* = 8.5 Hz, 2H), 7.05–6.93 (multiple peaks, 2H), 6.90–6.82

^E Synthesized by Dr. Megan Cismesia.

^F Synthesized by Dr. Megan Cismesia.

(multiple peaks, 3H), 6.74 (d, $J = 8.1$ Hz, 1H), 6.52 (d, $J = 8.5$ Hz, 2H), 4.26 (t, $J = 6.8$ Hz, 2H), 3.81 (s, 3H), 2.93 (s, br, 4H), 2.74 (t, $J = 6.8$ Hz, 2H), 2.65 (s, br, 4H). $^{13}\text{C}\{^1\text{H}\}$ (126 MHz, CDCl_3): δ 171.2, 159.3, 156.6, 152.2, 148.5, 141.1, 137.3, 131.0, 126.4, 123.1, 123.0, 121.0, 118.2, 115.3, 111.3, 56.3, 55.4, 53.2, 50.4, 45.6. HRMS electrospray (m/z): $[\text{M}+\text{H}]^+$ calcd for $\text{C}_{25}\text{H}_{28}\text{N}_4\text{O}_3$, 433.2234; found 433.2235.



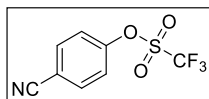
O-Benzoylcupreine (**35-OH**) was prepared using a modified literature procedure as follows.⁴¹ O-Benzoylquinine (643.0 mg, 1.50 mmol, 1.0 equiv) was dissolved in dichloromethane (30 mL, 0.05 M) under a nitrogen atmosphere and chilled in a dry ice/acetone bath. Boron tribromide (1.0 M in dichloromethane, 6.0 mL, 4.0 equiv) was added dropwise. The reaction was allowed to stir cold for 1 h before gradually being warmed to room temperature. The reaction was stirred at room temperature overnight and was then cooled in an ice bath. Ammonium hydroxide (30% aqueous, 10.0 mL) was added dropwise, and the mixture was stirred cold for 30 min. The reaction was diluted with water and extracted with dichloromethane. The organic extracts were collected, dried over MgSO_4 , filtered, and concentrated under vacuum. The product was purified by flash chromatography on silica gel to afford **35-OH** as a white solid (314.0 mg, 50% yield, mp = 211.3–212.1 °C, $R_f = 0.43$ in ethyl acetate with 2% triethylamine and 4% methanol).^G ^1H NMR (500 MHz, $\text{DMSO}-d_6$): δ 10.15 (s, 1H), 8.61 (d, $J = 4.4$ Hz, 1H), 8.07 (d, $J = 7.4$ Hz, 2H), 7.89 (d, $J = 9.1$ Hz, 1H), 7.69 (t, $J = 7.4$ Hz, 1H), 7.59–7.53 (multiple peaks, 3H), 7.51 (d, $J = 4.5$ Hz, 1H), 7.32 (dd, $J = 9.1, 2.4$ Hz, 1H), 6.44 (d, $J = 7.7$ Hz, 1H), 5.94 (m, 1H), 5.00 (dd, $J = 19.8, 13.8$ Hz, 2H), 3.49 (m, 1H), 3.09 (m, 1H), 2.88 (dd, $J = 13.5, 10.1$ Hz, 1H), 2.52 (m, 1H), 2.43 (m, 1H), 2.23 (m, 1H), 1.95 (m, 1H), 1.79 (m, 1H), 1.68 (m, 1H), 1.56 (m, 1H), 1.47 (m, 1H). $^{13}\text{C}\{^1\text{H}\}$ (126 MHz, $\text{DMSO}-d_6$): δ 165.0, 155.7, 146.6, 143.3, 143.3, 142.3, 133.8, 131.4, 129.3, 129.2, 128.9, 126.9, 121.7, 119.0, 114.4, 104.5,

^G Synthesized by Dr. Megan Cismesia.

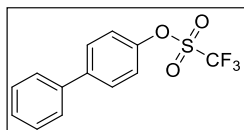
74.7, 59.3, 56.0, 41.7, 39.3, 27.3, 27.2, 24.7. HRMS electrospray (m/z): $[M+H]^+$ calcd for $C_{26}H_{26}N_2O_3$, 415.2016; found 415. 2019.

3.8.5. Synthesis of Aryl Triflates

Aryl triflates were synthesized by the literature procedure.⁴⁷ Under an N_2 atmosphere, the corresponding phenol (1.0 equiv), pyridine (1.5 equiv), and dichloromethane (0.3 M) were combined in a round bottom flask equipped with a magnetic stir bar. The round bottom flask was cooled to 0 °C in an ice bath and triflic anhydride (1.2 equiv) was added dropwise. The reaction was allowed to warm to room temperature and stirred overnight. The reaction was filtered through silica gel with hexanes. The solution was concentrated and purified by column chromatography on silica gel using gradients of either diethyl ether/pentane or hexanes/ethyl acetate as the eluent. All products were dried under vacuum in the presence of P_2O_5 prior to use in the fluorination reactions.

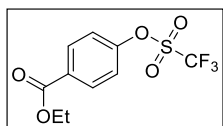


The reaction was performed using 4-cyanophenol (595.6 mg, 5.0 mmol, 1.0 equiv), pyridine (0.6 mL, 7.5 mmol, 1.5 equiv), and triflic anhydride (1.0 mL, 6.0 mmol, 1.2 equiv) in dichloromethane (15.0 mL) in a 50 mL round bottom flask equipped with a magnetic stir bar. Product **1-OTf** was obtained as a colorless oil (1.01 g, 88% yield, R_f = 0.42 in 8:1 hexanes/EtOAc). The 1H NMR ($CDCl_3$), ^{19}F NMR ($CDCl_3$), and $^{13}C\{^1H\}$ NMR ($CDCl_3$) spectra matched those previously reported in the literature.⁴⁸ HRMS EI (m/z): $[M]^+$ calcd for $C_8H_4F_3NO_3S$, 250.9864; found, 250.9862.

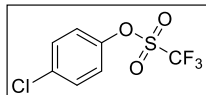


The reaction was performed using 4-phenylphenol (1.70 g, 10.0 mmol, 1.0 equiv), pyridine (1.62 mL, 20.0 mmol, 2.0 equiv), and triflic anhydride (2.03 mL, 12.0 mmol, 1.2 equiv) in dichloromethane (20.0 mL) in a 50 mL round bottom flask equipped with a magnetic stir bar. Product **3-OTf** was obtained as a white solid (2.256 g, 72% yield, mp

= 47.2–48.0 °C, R_f = 0.64 in 10:1 hexanes/EtOAc).^H The ^1H NMR (CDCl_3), ^{19}F NMR (CDCl_3), and $^{13}\text{C}\{^1\text{H}\}$ NMR (CDCl_3) spectra matched those previously reported in the literature.⁴⁸ HRMS EI (m/z): $[\text{M}]^+$ calcd $\text{C}_{13}\text{H}_9\text{F}_3\text{O}_3\text{S}$, 302.0224; found, 302.0230.



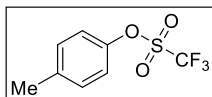
The reaction was performed using ethyl 4-hydroxybenzoate (2.5 g, 15.0 mmol, 1.0 equiv), pyridine (2.4 mL, 30.0 mmol, 2.0 equiv), and triflic anhydride (3.0 mL, 5.1 mmol, 1.2 equiv) in dichloromethane (30.0 mL) in a 100 mL round bottom flask equipped with a magnetic stir bar. Product **4-OTf** was obtained as a colorless oil (2.040 g, 45% yield, R_f = 0.38 in 10:1 hexanes/EtOAc).^I The ^1H NMR (CDCl_3) spectra matched those previously reported in the literature.⁴⁷ $^{13}\text{C}\{^1\text{H}\}$ NMR (176 MHz, CDCl_3): δ 165.1, 152.6, 132.0, 130.8, 121.5, 118.0 (q, J = 317 Hz), 61.7, 14.4. ^{19}F NMR (376 MHz, CDCl_3): δ 72.8 (s, 3F). HRMS electrospray (m/z): $[\text{M}+\text{H}]^+$ calcd $\text{C}_{10}\text{H}_{10}\text{F}_3\text{O}_5\text{S}$, 299.0196; found, 299.0196.



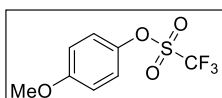
The reaction was performed using 4-chlorophenol (1.0 g, 7.8 mmol, 1.0 equiv), pyridine (0.94 mL, 11.7 mmol, 1.5 equiv), and triflic anhydride (1.57 mL, 9.3 mmol, 1.2 equiv) in dichloromethane (30.0 mL) in a 100 mL round bottom flask equipped with a magnetic stir bar. Product **9-OTf** was obtained as a colorless oil (1.31 g, 65% yield, R_f = 0.48 in pentane). The ^1H NMR (CDCl_3), ^{19}F NMR (CDCl_3), and $^{13}\text{C}\{^1\text{H}\}$ NMR (CDCl_3) spectra matched those previously reported in the literature.⁴⁹ HRMS EI (m/z): $[\text{M}]^+$ calcd $\text{C}_7\text{H}_4\text{ClF}_3\text{O}_3\text{S}$ 259.9522; found 259.9518.

^H Synthesized by Cristina García Morales.

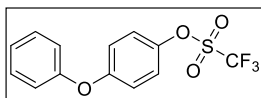
^I Synthesized by Cristina García Morales.



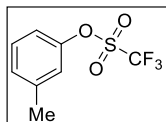
The reaction was performed using *p*-cresol (1.0 g, 9.3 mmol, 1.0 equiv), pyridine (1.1 mL, 14.0 mmol, 1.5 equiv), and triflic anhydride (1.9 mL, 11.1 mmol, 1.2 equiv) in dichloromethane (30.0 mL) in a 100 mL round bottom flask equipped with a magnetic stir bar. Product **19-OTf** was obtained as a colorless oil (2.09 g, 94% yield, R_f = 0.38 in pentane). The ^1H NMR (CDCl_3), ^{19}F NMR (CDCl_3), and $^{13}\text{C}\{^1\text{H}\}$ NMR (CDCl_3) spectra matched those previously reported in the literature.⁵⁰ HRMS EI (m/z): $[\text{M}]^+$ calcd $\text{C}_8\text{H}_7\text{F}_3\text{O}_3\text{S}$, 240.0068; found, 240.0075.



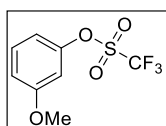
The reaction was performed using 4-methoxyphenol (620.0 mg, 5.0 mmol, 1.0 equiv), pyridine (0.6 mL, 7.5 mmol, 1.5 equiv), and triflic anhydride (1.0 mL, 6.0 mmol, 1.2 equiv) in dichloromethane (15.0 mL) in a 50 mL round bottom flask equipped with a magnetic stir bar. Product **20-OTf** was obtained as a colorless oil (1.04 g, 81% yield, R_f = 0.45 in 8:1 hexanes/EtOAc). The ^1H NMR (CDCl_3), ^{19}F NMR (CDCl_3), and $^{13}\text{C}\{^1\text{H}\}$ NMR (CDCl_3) spectra matched those previously reported in the literature.⁵¹ HRMS EI (m/z): $[\text{M}]^+$ calcd $\text{C}_8\text{H}_7\text{F}_3\text{O}_4\text{S}$, 256.0017; found, 256.0028.



The reaction was performed using 4-phenoxyphenol (500.0 mg, 2.7 mmol, 1.0 equiv), pyridine (0.32 mL, 4.0 mmol, 1.5 equiv), and triflic anhydride (0.54 mL, 3.2 mmol, 1.2 equiv) in dichloromethane (15.0 mL) in a 50 mL round bottom flask equipped with a magnetic stir bar. Product **21-OTf** was obtained as a colorless oil (751.5 mg, 88% yield, R_f = 0.25 in pentane). ^1H NMR (500 MHz, CDCl_3): δ 7.38 (t, J = 8.0 Hz, 2H), 7.21 (d, J = 9.1 Hz, 2H), 7.18 (t, J = 8.0 Hz, 1H), 7.03 (t, J = 9.1 Hz, 4H). $^{13}\text{C}\{^1\text{H}\}$ NMR (176 MHz, CDCl_3): δ 157.5, 156.2, 144.6, 130.2, 124.5, 122.8, 119.8, 119.5, 117.0 (q, J = 320 Hz). ^{19}F NMR (376 MHz, CDCl_3): δ 72.8 (s, 3F). HRMS EI (m/z): $[\text{M}]^+$ calcd $\text{C}_{13}\text{H}_9\text{F}_3\text{O}_4\text{S}$, 318.0174; found, 218.0180.



The reaction was performed using *m*-cresol (540.5 mg, 5.0 mmol, 1.0 equiv), pyridine (0.6 mL, 7.5 mmol, 1.5 equiv), and triflic anhydride (1.0 mL, 6.0 mmol, 1.2 equiv) in dichloromethane (15.0 mL) in a 50 mL round bottom flask equipped with a magnetic stir bar. Product **22-OTf** was obtained as a colorless oil (739.4 mg, 62% yield, R_f = 0.68 in 5% EtOAc in hexanes). The ^1H NMR (CDCl_3) and $^{13}\text{C}\{^1\text{H}\}$ NMR (CDCl_3) spectra matched those previously reported in the literature.⁵² ^{19}F NMR (376 MHz, CDCl_3): δ 73.0 (s, 3F). HRMS EI (m/z): $[\text{M}]^+$ calcd $\text{C}_8\text{H}_7\text{F}_3\text{O}_3\text{S}$, 240.0068; found, 240.0075.



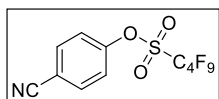
The reaction was performed using 3-methoxyphenol (500.0 mg, 4.0 mmol, 1.0 equiv), pyridine (0.5 mL, 6.0 mmol, 1.5 equiv), and triflic anhydride (0.8 mL, 4.8 mmol, 1.2 equiv) in dichloromethane (20.0 mL) in a 50 mL round bottom flask equipped with a magnetic stir bar. Product **23-OTf** was obtained as a pale yellow oil (592.9 mg, 58% yield, R_f = 0.56 in 5% diethyl ether in pentane). The ^1H NMR (CDCl_3), ^{19}F NMR (CDCl_3), and $^{13}\text{C}\{^1\text{H}\}$ NMR (CDCl_3) spectra matched those previously reported in the literature.⁴⁸ HRMS EI (m/z): $[\text{M}]^+$ calcd $\text{C}_8\text{H}_7\text{F}_3\text{O}_5\text{S}$, 256.0017; found, 256.0027.

3.8.6. Synthesis of Aryl Nonaflates

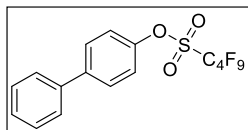
Aryl nonaflates were synthesized from literature procedures.⁵³

Synthesis of 1-ONf. A solution of phenol (1.0 equiv), 4-dimethylaminopyridine (DMAP) (0.05 equiv), and *N,N*-diisopropylethylamine (*i*Pr₂NEt) (1.2 equiv) were dissolved in dichloromethane and the solution was cooled to 0 °C in an ice bath. Perfluoro-1-butanesulfonyl fluoride (1.1 equiv) was added dropwise. The solution was allowed to warm to room temperature and stirred overnight. The solution was poured into water. The organic layer was extracted and washed with brine, dried over MgSO_4 , filtered, and concentrated. The crude material was purified by column chromatography on silica gel using gradients of hexanes/ethyl acetate as the eluent.

Synthesis of 3-ONf, 9-ONf, and 21-ONf. A round bottom flask was charged with NaH (1.3 equiv) and diethyl ether (4 mL/mmol). The flask was cooled to 0 °C in an ice bath and a solution of phenol (1.0 equiv) in diethyl ether (0.5 mL/mmol) was added dropwise. After about 15 minutes, perfluoro-1-butanesulfonyl fluoride (1.4 equiv) was added dropwise and the solution was allowed to warm to room temperature and stirred overnight. Water and diethyl ether were added to the reaction mixture and the organic layer was separated. The aqueous layer was extracted twice with diethyl ether. The combined organic layers were washed with 5% aq. NaOH and brine, dried over MgSO₄, filtered, and concentrated. The crude material was purified by column chromatography on silica gel using gradients of diethyl ether/pentane or hexanes/ethyl acetate as the eluent.

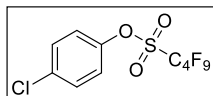


The reaction was performed using 4-cyanophenol (595.6 mg, 5.0 mmol, 1.0 equiv), DMAP (30.5 mg, 0.25 mmol, 0.05 equiv), *i*Pr₂NEt (1.0 mL, 6.0 mmol, 1.2 equiv), and perfluoro-1-butanesulfonyl fluoride (1.0 mL, 5.5 mmol, 1.1 equiv) in dichloromethane (8 mL) in a 50 mL round bottom flask. Product **1-ONf** was obtained as a white solid (1.802 mg, 90% yield, mp = 32.4–34.0 °C, *R*_f = 0.62 min 20% EtOAc in hexanes). The ¹H NMR (CDCl₃), ¹⁹F NMR (CDCl₃), and ¹³C{¹H} NMR (CDCl₃) spectra matched those previously reported in the literature.⁴⁸ HRMS EI (*m/z*): [M]⁺ calcd C₁₁H₄F₉NO₃S, 400.9768; found 400.9765.

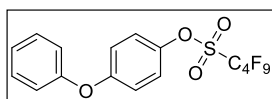


The reaction was performed using 4-phenylphenol (851.0 mg, 5.0 mmol, 1.0 equiv), NaH (260.0 mg (60% dispersion in mineral oil), 6.5 mmol, 1.3 equiv), and perfluoro-1-butanesulfonyl fluoride (1.3 mL, 7.0 mmol, 1.4 equiv) in diethyl ether (22.5 mL total) in a 50 mL round bottom flask. Product **3-ONf** was obtained as a white solid (1.785 g, 79% yield, mp = 45.5–46.7 °C, *R*_f = 0.43 in pentane). ¹H NMR (500 MHz, CDCl₃): δ 7.66–7.63 (m, 2H), 7.56–7.54 (m, 2H), 7.48–7.45 (m, 2H), 7.43–7.34 (multiple peaks, 3H). ¹³C{¹H} NMR (176 MHz, CDCl₃): δ 149.3, 141.8, 139.4, 129.1, 129.0, 128.2, 127.3, 121.7, 108.0–

118.0 (multiple peaks, 4C). ^{19}F NMR (376 MHz, CDCl_3): δ -80.6 (t, J = 9.8 Hz, 3F), -108.9 (m, 2F), -121.0 (m, 2F), -125.8 (m, 2F). HRMS EI (m/z): $[\text{M}]^+$ calcd $\text{C}_{16}\text{H}_9\text{F}_9\text{O}_3\text{S}$, 452.0129; found 452.0133.



The reaction was performed using 4-chlorophenol (642.8 mg, 5.0 mmol, 1.0 equiv), NaH (260.0 mg (60% dispersion in mineral oil), 6.5 mmol, 1.3 equiv), and perfluoro-1-butanesulfonyl fluoride (1.3 mL, 7.0 mmol, 1.4 equiv) in diethyl ether (22.5 mL total) in a 50 mL round bottom flask equipped with a magnetic stir bar. Product **9-ONf** was obtained as a colorless oil (1.438 g, 70% yield, R_f = 0.54 in pentane). The ^1H NMR (CDCl_3) and $^{13}\text{C}\{^1\text{H}\}$ NMR (CDCl_3) spectra matched those previously reported in the literature.⁵³ ^{19}F NMR (376 MHz, CDCl_3): δ 80.6 (t, J = 11.3 Hz, 3F), -108.7 (m, 2F), -120.8 (m, 2F), -125.8 (m, 2F). HRMS EI (m/z): $[\text{M}]^+$ calcd $\text{C}_{10}\text{H}_4\text{ClF}_9\text{O}_3$, 409.9426; found, 409.9420.



The reaction was performed using 4-phenoxyphenol (931.1 mg, 5.0 mmol, 1.0 equiv), NaH (260.0 mg (60% dispersion in mineral oil), 6.5 mmol, 1.3 equiv), and perfluoro-1-butanesulfonyl fluoride (1.3 mL, 7.0 mmol, 1.4 equiv) in diethyl ether (22.5 mL total) in a 50 mL round bottom flask equipped with a magnetic stir bar. Product **21-ONf** was obtained as a colorless oil (1.699 g, 73% yield, R_f = 0.64 in 10% EtOAc in hexanes). The ^1H NMR (CDCl_3), ^{19}F NMR (CDCl_3), and $^{13}\text{C}\{^1\text{H}\}$ NMR (CDCl_3) spectra matched those previously reported in the literature.⁴⁸ HRMS EI (m/z): $[\text{M}]^+$ calcd $\text{C}_{16}\text{H}_9\text{F}_9\text{O}_4\text{S}$, 468.0078; found 468.0080.

3.8.7. Synthesis of Diaryl Sulfates

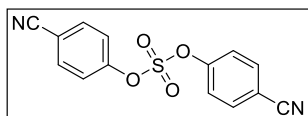
Diaryl sulfates were synthesized according to the literature procedures.^{54,55}

Synthesis of 1-sulfate. A vial was charged with aryl fluorosulfonate (1.0 equiv), aryl silyl ether (1.0 equiv), 8-diazabicyclo[5.4.0]undec-7-ene (DBU) (20 mol %), and acetonitrile (0.5 M). The vial was sealed with a Teflon-lined cap and allowed to stir at room

temperature overnight. The reaction mixture was concentrated to remove solvent. Crude product was dissolved in dichloromethane (20 mL) and extracted with water (1 x 20 mL). The organic layer was dried over MgSO₄, filtered, and concentrated. The product was recrystallized from ethyl acetate and hexanes.

Synthesis of 3-sulfate, 9-sulfate, and 21-sulfate. In an N₂-filled drybox, a vial was charged with phenol (3.0 equiv), Cs₂CO₃ (1.0 equiv), *N,N'*-sulfuryldiimidazole (1.0 equiv), and THF (3.0 M). The vial was sealed with a Teflon-lined cap and allowed to reflux overnight. The reaction solution was cooled to room temperature, filtered through Celite, and concentrated. The product was purified by column chromatography on silica gel using gradients of hexanes/ethyl acetate as eluent.

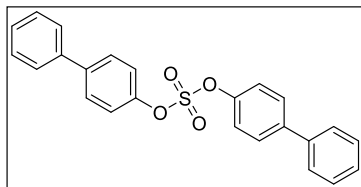
Synthesis of 14-sulfate. In an N₂-filled drybox, a vial was charged with aryl fluorosulfonate (1.0 equiv), tetramethylammonium phenoxide salt (1.0 equiv), and DMF (0.2 M). The vial was sealed with a Teflon-lined cap and allowed to stir at room temperature overnight. The reaction mixture was extracted with diethyl ether (10 mL) and water (20 mL). The organic layer was washed with water (3 x 20 mL), dried over MgSO₄, and concentrated. The product was purified by column chromatography on silica gel using gradients of pentane/diethyl ether as eluent.



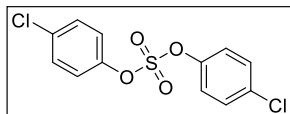
The reaction was performed using 4-cyanophenyl sulfofluoridate **1-OFs** (300.0 mg, 1.5 mmol, 1.0 equiv), 4-((*tert*-butyldimethylsilyl)oxy)benzonitrile^{56,J} (349.5 mg, 1.5 mmol, 1.0 equiv), and DBU (0.04 mL, 0.3 mmol, 20 mol %) in acetonitrile (4.0 mL) in a 20 mL vial equipped with a magnetic stir bar. Product **1-sulfate** was obtained as a crystalline white solid from recrystallization from ethyl acetate and hexanes (257.9 mg, 57% yield, mp = 152.0–154.0 °C). ¹H NMR (500 MHz, CDCl₃): δ 7.79 (d, *J* = 9.0 Hz, 4H), 7.45 (d, *J* = 9.0

^J Synthesized by Dr. Megan Cismesia.

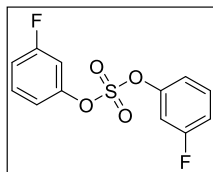
Hz, 4H). $^{13}\text{C}\{^1\text{H}\}$ NMR (176 MHz, CDCl_3): δ 152.8, 134.6, 122.1, 117.3, 112.5. HRMS EI (m/z): $[\text{M}]^+$ calcd $\text{C}_{14}\text{H}_8\text{N}_2\text{O}_4\text{S}$, 300.0205; found, 300.0203.



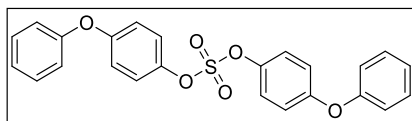
The reaction was performed using 4-phenylphenol (510.8 mg, 3.0 mmol, 3.0 equiv), Cs_2CO_3 (325.8 mg, 1.0 mmol, 1.0 equiv), and N,N' -sulfuryldiimidazole (198.2 mg, 1.0 mmol, 1.0 equiv) in THF (1.0 mL) in a 4 mL vial equipped with a magnetic stir bar. Product **3-sulfate** was obtained as a white solid (258.2 mg, 64% yield, mp = 132.6–133.8 °C, R_f = 0.41 in 5% EtOAc in hexanes). The ^1H NMR (CDCl_3) and $^{13}\text{C}\{^1\text{H}\}$ NMR (CDCl_3) spectra matched those previously reported in the literature.⁵⁴ HRMS EI (m/z): $[\text{M}]^+$ calcd $\text{C}_{24}\text{H}_{18}\text{O}_4\text{S}$, 402.0926; found, 402.0924.



The reaction was performed using 4-chlorophenol (1.93 g, 15.0 mmol, 3.0 equiv), Cs_2CO_3 (1.63 g, 5.0 mmol, 1.0 equiv), and N,N' -sulfuryldiimidazole (992.0 mg, 5.0 mmol, 1.0 equiv) in THF (5.0 mL) in a 20 mL vial equipped with a magnetic stir bar. Product **9-sulfate** was obtained as a white solid (1.04 g, 66% yield, mp = 70.0–72.0 °C, R_f = 0.66 in 10% ethyl acetate in hexanes). ^1H NMR (500 MHz, CDCl_3): δ 7.40 (d, J = 9.9 Hz, 4H), 7.25 (d, J = 9.9 Hz, 4H). $^{13}\text{C}\{^1\text{H}\}$ NMR (176 MHz, CDCl_3): δ 148.7, 133.6, 130.3, 122.6. HRMS EI (m/z): $[\text{M}]^+$ calcd $\text{C}_{12}\text{H}_8\text{Cl}_2\text{O}_4\text{S}$, 317.9520; found, 317.9520.



The reaction was performed with 3-fluorophenyl sulfonate **14-OFs** (194.0 mg, 1.0 mmol, 1.0 equiv) and tetramethylammonium 3-fluorophenoxide⁵⁷ (185.0 mg, 1.0 mmol, 1.0 equiv) in DMF (5.0 mL) in a 20 mL vial equipped with a magnetic stir bar. Product **14-sulfate** was obtained as a colorless oil (182.8 mg, 64% yield, $R_f = 0.39$ in 5% diethyl ether in pentane). ^1H NMR (500 MHz, CDCl_3): δ 7.42 (m, 2H), 7.15–7.06 (multiple peaks, 6H). $^{13}\text{C}\{^1\text{H}\}$ NMR (176 MHz, CDCl_3): δ 160.0 (d, $J = 250$ Hz), 148.0 (d, $J = 86$ Hz), 128.4 (d, $J = 9.2$ Hz), 114.2 (d, $J = 3.6$ Hz), 112.5 (d, $J = 21$ Hz), 106.8 (d, $J = 22$ Hz). ^{19}F NMR (376 MHz, CDCl_3): δ -108.6 (m, 2F). HRMS EI (m/z): $[\text{M}]^+$ calcd $\text{C}_{12}\text{H}_8\text{F}_2\text{O}_4\text{S}$, 286.011; found, 286.011.



The reaction was performed using 4-phenoxyphenol (2.79 g, 15.0 mmol, 3.0 equiv), Cs_2CO_3 (1.63 g, 5.0 mmol, 1.0 equiv), and N,N' -sulfuryldiimidazole (992.0 mg, 5.0 mmol, 1.0 equiv) in THF (5.0 mL) in a 20 mL vial equipped with a magnetic stir bar. Product **21-sulfate** was obtained as a white solid (1.82 g, 84% yield, mp = 49.7–50.8 °C, $R_f = 0.33$ in 5% ethyl acetate in hexanes). ^1H NMR (500 MHz, CDCl_3): δ 7.36 (t, $J = 7.5$ Hz, 4H), 7.27 (d, $J = 9.2$ Hz, 4H), 7.15 (t, $J = 7.5$ Hz, 2H), 7.02–7.00 (m, 8H). $^{13}\text{C}\{^1\text{H}\}$ NMR (176 MHz, CDCl_3): δ 156.7, 156.5, 146.5, 130.1, 124.2, 122.6, 119.6, 119.5. HRMS ESI⁺ (m/z): $[\text{M}+\text{Na}]^+$ calcd $\text{C}_{24}\text{H}_{18}\text{O}_6\text{SNa}$, 457.0716; found, 457.0716.

3.8.8. General Procedures

General Procedure for the Fluorination of 1-X Electrophiles with NMe_4F in Table 3.1. In an N_2 -filled drybox, substrate **1-X** (0.1 mmol, 1.0 equiv, X = OFs, OTf, Cl, NO_2 , OH, OMs, OTs) and anhydrous NMe_4F (18.6 mg, 0.2 mmol, 2.0 equiv) were weighed into a 4 mL glass vial equipped with a micro-sized magnetic stir bar. Anhydrous DMF (0.5 mL) was added, and the vial was sealed with a Teflon-lined cap. The reaction mixture was allowed

to stir at 25 °C or 80 °C for 24 h. The reaction was then diluted with dichloromethane (2.0 mL). 1,3,5-Trifluorobenzene was added as an internal standard, and the reaction was analyzed by ^{19}F NMR spectroscopy and GCMS.

General Procedure for the Reaction Profiles in Figures 3.1 and 3.11. In an N_2 -filled drybox, substrate **1-X** (0.1 mmol, 1.0 equiv, X = OFs, OTf, Cl, NO_2 , ONf, OSO_2Ar) and NMe_4F (0.2 mmol, 2.0 equiv) were weighed into a 4 mL glass vial equipped with a micro-sized magnetic stir bar. Anhydrous DMF (0.5 mL) was added, and the vial was sealed with a Teflon-lined cap. The reaction mixture was allowed to stir at 80 °C for the given time. The reaction was then cooled in an ice bath and diluted with dichloromethane (2.0 mL). 1,3,5-Trifluorobenzene was added as an internal standard, and the reaction was analyzed by ^{19}F NMR spectroscopy.

General Procedure for the Solvent Screen in Table 3.2. In an N_2 -filled drybox, **1-OFs** (20.1 mg, 0.1 mmol, 1.0 equiv) and NMe_4F (18.6 mg, 0.2 mmol, 2.0 equiv) were weighed into a 4 mL glass vial equipped with a micro-sized magnetic stir bar. Solvent (0.5 mL) was added, and the vial was sealed with a Teflon-lined cap. The reaction mixture was allowed to stir at 25 °C for 24 h. The reaction was then diluted with dichloromethane (2.0 mL). 1,3,5-Trifluorobenzene was added as an internal standard, and the reaction was analyzed by ^{19}F NMR spectroscopy.

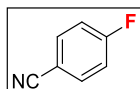
General Procedure for the Fluoride Screen in Table 3.3. In an N_2 -filled drybox, **1-OFs** (20.1 mg, 0.1 mmol, 1.0 equiv) and the fluoride source (0.2 mmol, 2.0 equiv) were weighed into a 4 mL glass vial equipped with a micro-sized magnetic stir bar. DMF (0.5 mL) was added, and the vial was sealed with a Teflon-lined cap. The reaction mixture was allowed to stir at 25 °C for 24 h. The reaction was then diluted with dichloromethane (2.0 mL). 1,3,5-Trifluorobenzene was added as an internal standard, and the reaction was analyzed by ^{19}F NMR spectroscopy.

General Procedure for the Fluorination of Different Electrophiles with NMe_4F in Table 3.4–3.5. In a N_2 -filled drybox, substrate (0.1 mmol, 1.0 equiv, X = OFs, Cl, NO_2) and NMe_4F

(18.6 mg, 0.2 mmol, 2.0 equiv or 46.5 mg, 0.5 mmol, 5.0 equiv) were weighed into a 4 mL glass vial equipped with a micro-sized magnetic stir bar. DMF (0.5 mL) was added, and the vial was sealed with a Teflon-lined cap. The reaction mixture was allowed to stir at 25 °C, 80 °C or 100 °C for 24 h. The reaction was then diluted with dichloromethane (2.0 mL). 1,3,5-Trifluorobenzene was added as an internal standard, and the reaction was analyzed by ^{19}F NMR spectroscopy and GCMS.

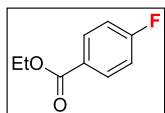
General Procedure for the Substrate Scope in Figure 3.2. For isolated compounds: In a N_2 -filled drybox, NMe_4F (93 mg, 1.0 mmol, 2.0 equiv) and the aryl fluorosulfonate substrate (0.5 mmol, 1.0 equiv) were weighed into a 4 mL glass vial equipped with a micro-sized magnetic stir bar. Anhydrous DMF (2.5 mL) was added, and the vial was sealed with a Teflon-lined cap. The reaction mixture was allowed to stir at the given temperature for 24 h. The resulting solution was diluted with diethyl ether (15 mL) and transferred to a separatory funnel. The organic layer was washed with water (4 x 20 mL) and then collected, dried over magnesium sulfate, filtered, and concentrated by rotary evaporation at 0 °C. The products were then purified by chromatography on silica gel using gradients of pentane/ diethyl ether or hexanes/ ethyl acetate as the eluent.

For NMR yields: In a N_2 -filled drybox, NMe_4F (18.6 mg, 0.2 mmol, 2 equiv) and the aryl fluorosulfonate substrate (0.1 mmol, 1 equiv) were weighed into a 4 mL glass vial equipped with a micro-sized magnetic stir bar. Anhydrous DMF (0.5 mL) was added, and the vial was sealed with a Teflon-lined cap. The reaction mixture was allowed to stir at the given temperature for 24 h. The resulting solution was diluted with dichloromethane (2 mL) and a standard (1,3,4-trifluorobenzene or 4-fluoroanisole, 100 μL of a 0.5 M solution in toluene) was added. An aliquot was removed for analysis by ^{19}F NMR spectroscopy and GCMS.

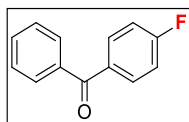


The reaction was performed using the standard conditions at room temperature with 4-cyanophenyl sulfonate **1-OFs** (100.5 mg, 0.5 mmol, 1 equiv). Product **1-F** was obtained as a white solid (37.8 mg, 62% yield, mp = 36.3–37.8 °C, R_f = 0.4 in 5% diethyl

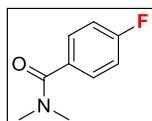
ether in pentane). The ^1H NMR (CDCl_3), ^{19}F NMR (CDCl_3), and $^{13}\text{C}\{^1\text{H}\}$ NMR (CDCl_3) spectra matched those previously reported in the literature.⁵⁸ HRMS EI (m/z): $[\text{M}]^+$ calcd for $\text{C}_7\text{H}_4\text{FN}$, 121.0328; measured, 121.0328. The isolated yield reported in Figure 3.2 is an average of two runs [62% and 66%].



The reaction was performed using the standard conditions at room temperature with ethyl-4-((fluorosulfonyl)oxy)benzoate (124.0 mg, 0.5 mmol, 1 equiv). Product **4-F** was obtained as a colorless oil (57.8 mg, 69% yield, R_f = 0.63 in 10% ethyl acetate in hexanes). The ^1H NMR (CDCl_3), ^{19}F NMR (CDCl_3), and $^{13}\text{C}\{^1\text{H}\}$ NMR (CDCl_3) spectra matched those previously reported in the literature.^{26b} HRMS EI (m/z): $[\text{M}]^+$ calcd for $\text{C}_9\text{H}_9\text{FO}_2$, 168.0587; measured, 168.0587. The isolated yield reported in Figure 3.2 is an average of two runs [69% and 73%].

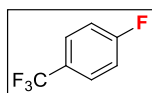


The reaction was performed using the standard conditions at room temperature with 4-benzoylphenyl sulfofluoridate **5-OFs** (140.0 mg, 0.5 mmol, 1 equiv). Product **5-F** was obtained as a white solid (89.9 mg, 90% yield, mp = 47.8–49.4 °C, R_f = 0.59 in 10% diethyl ether in pentane). The ^1H NMR (CDCl_3), ^{19}F NMR (CDCl_3), and $^{13}\text{C}\{^1\text{H}\}$ NMR (CDCl_3) spectra matched those previously reported in the literature.^{26b} HRMS EI (m/z): $[\text{M}]^+$ calcd for $\text{C}_{13}\text{H}_9\text{FO}$, 200.0637; found, 200.0646. The isolated yield reported in Figure 3.2 is an average of two runs [90% and 83%].

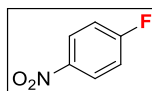


The reaction was performed using the standard conditions at 60 °C with 4-(dimethylcarbamoyl)phenyl sulfofluoridate **6-OFs** (123.5 mg, 0.5 mmol, 1 equiv). Product

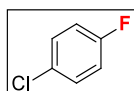
6-F was obtained as a colorless oil (47.5 mg, 57% yield, $R_f = 0.19$ in 33% hexanes in ethyl acetate). The ^1H NMR (CDCl_3), ^{19}F NMR (CDCl_3), and $^{13}\text{C}\{^1\text{H}\}$ NMR (CDCl_3) spectra matched those previously reported in the literature.^{8a} HRMS electrospray (m/z): $[\text{M}+\text{H}]^+$ calcd for $\text{C}_9\text{H}_{11}\text{FNO}$, 168.0819; found, 168.0818. The isolated yield reported in Figure 3.2 is an average of two runs [57% and 53%].



The reaction was performed using the standard conditions at room temperature with 4-trifluoromethylphenyl sulfofluoridate (24.4 mg, 0.1 mmol, 1 equiv), providing product **7-F** in 66% yield as determined by ^{19}F NMR spectroscopic analysis of the crude reaction mixture. The ^{19}F NMR spectral data matched that of an authentic sample (Oakwood Products, s, -61.6 ppm, 3F; m, -108.2 ppm, 1F). The identity of the product was further confirmed by GCMS analysis ($m/z = 164$). The yield reported in Figure 3.2 is an average of two runs [66% and 71%].

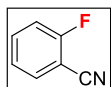


The reaction was performed using the standard conditions at $80\text{ }^\circ\text{C}$ with 4-nitrophenyl sulfofluoridate **8-OFs** (110.5 mg, 0.5 mmol, 1 equiv). Product **8-F** was obtained as a colorless oil (26.6 mg, 38% yield, $R_f = 0.58$ in 5% diethyl ether in pentane). The ^1H NMR (CDCl_3), ^{19}F NMR (CDCl_3), and $^{13}\text{C}\{^1\text{H}\}$ NMR (CDCl_3) spectra matched those previously reported in the literature.^{8a} HRMS EI (m/z): $[\text{M}]^+$ calcd for $\text{C}_6\text{H}_4\text{FNO}_2$, 141.0226; found, 141.0228. The isolated yield reported in Figure 3.2 is an average of two runs [38% and 36%].

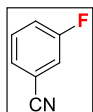


The reaction was performed using the standard conditions at $100\text{ }^\circ\text{C}$ with 4-chlorophenyl sulfofluoridate **9-OFs** (21.0 mg, 0.1 mmol, 1 equiv), providing product **9-F** in 74% yield as determined by ^{19}F NMR spectroscopic analysis of the crude reaction mixture. The ^{19}F

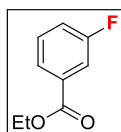
NMR spectral data matched that of an authentic sample (Oakwood Products, m, -116.7 ppm). The identity of the product was further confirmed by GCMS analysis ($m/z = 130$). The yield reported in Figure 3.2 is an average of two runs [74% and 76%].



The reaction was performed using the standard conditions at $80\text{ }^{\circ}\text{C}$ with 2-cyanophenyl sulfofluoridate **10-OFs** (20.1 mg, 0.1 mmol, 1 equiv), providing product **10-F** in 54% yield as determined by ^{19}F NMR spectroscopic analysis of the crude reaction mixture. The ^{19}F NMR spectral data matched that of an authentic sample (Ark Pharm, m, -107.4 ppm). The identity of the product was further confirmed by GCMS analysis ($m/z = 121$). The yield reported in Figure 3.2 is an average of two runs [54% and 47%].

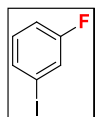


The reaction was performed using the standard conditions at room temperature with 3-cyanophenyl sulfofluoridate **11-OFs** (100.5 mg, 0.5 mmol, 1 equiv). Product **11-F** was obtained as a colorless oil (18.9 mg, 31% yield, $R_f = 0.42$ in 5% diethyl ether in pentane). The ^1H NMR (CDCl_3), ^{19}F NMR (CDCl_3), and $^{13}\text{C}\{^1\text{H}\}$ NMR (CDCl_3) spectra matched those of an authentic sample (Oakwood Products). HRMS EI (m/z): $[\text{M}]^+$ calcd for $\text{C}_7\text{H}_4\text{FN}$, 121.0328; found, 121.0328. The isolated yield reported in Figure 3.2 is an average of two runs [31% and 27%]. The low isolated yield is due to the volatility of the product ($\text{bp} = 183\text{ }^{\circ}\text{C}$). The ^{19}F NMR yield of the crude reaction mixture is 80%.

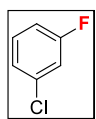


The reaction was performed using the standard conditions at $60\text{ }^{\circ}\text{C}$ with ethyl-3-((fluorosulfonyl)oxy) benzoate **12-OFs** (124.0 mg, 0.5 mmol, 1 equiv). Product **12-F** was obtained as a colorless oil (51.8 mg, 62% yield, $R_f = 0.54$ in 10% ethyl acetate in hexanes). The ^1H NMR (CDCl_3) and $^{13}\text{C}\{^1\text{H}\}$ NMR (CDCl_3) spectra matched those

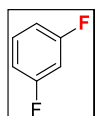
previously reported in the literature.⁵⁹ ^{19}F NMR (376 MHz, CDCl_3): δ -112.6 (m, 1F). HRMS EI (m/z): $[\text{M}]^+$ calcd for $\text{C}_9\text{H}_9\text{FO}_2$, 168.0587; found, 168.0585. The isolated yield reported in Figure 3.2 is an average of two runs [62% and 61%].



The reaction was performed using the standard conditions at 60 °C with 3-iodophenyl sulfofluoridate **13-OFs** (30.2 mg, 0.1 mmol, 1 equiv), providing product **13-F** in 66% yield as determined by ^{19}F NMR spectroscopic analysis of the crude reaction mixture. The ^{19}F NMR spectral data matched that of an authentic sample (Acros, m, -111.6 ppm). The identity of the product was further confirmed by GCMS analysis (m/z = 222). The yield reported in Figure 3.2 is an average of two runs [66% and 66%].



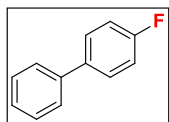
The reaction was performed using the standard conditions at 80 °C with 3-chlorophenyl sulfofluoridate (21.0 mg, 0.1 mmol, 1 equiv), providing product **2-F** in 64% yield as determined by ^{19}F NMR spectroscopic analysis of the crude reaction mixture. The ^{19}F NMR spectral data matched that of an authentic sample (Matrix Scientific, m, -111.7 ppm). The identity of the product was further confirmed by GCMS analysis (m/z = 130). The yield reported in Figure 3.2 is an average of two runs [64% and 69%].



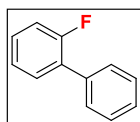
The reaction was performed using the standard conditions at 80 °C with 3-fluorophenyl sulfofluoridate **14-OFs** (19.4 mg, 0.1 mmol, 1 equiv), providing product **14-F** in 73% yield as determined by ^{19}F NMR spectroscopic analysis of the crude reaction mixture. The ^{19}F NMR spectral data matched that of an authentic sample (Matrix, m, -110.9 ppm). The yield reported in Figure 3.2 is an average of two runs [73% and 79%].



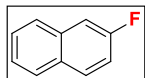
The reaction was performed at 100 °C with phenyl sulfonate **15-OFs** (17.6 mg, 0.1 mmol, 1 equiv) and NMe₄F (46.5 mg, 0.5 mmol, 5 equiv), providing product **15-F** in 67% yield as determined by ¹⁹F NMR spectroscopic analysis of the crude reaction mixture. The ¹⁹F NMR spectral data matched that of an authentic sample (Matrix, m, –114.1 ppm). The yield reported in Figure 3.2 is an average of two runs [67% and 71%].



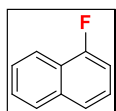
The reaction was performed using the standard conditions at 100 °C with (1,1'-biphenyl)-4-yl sulfonate **3-OFs** (126.0 mg, 0.5 mmol, 1 equiv). Product **3-F** was obtained as a white solid (65 mg, 75% yield, mp = 74.8–75.8 °C, R_f = 0.60 in pentane). The ¹H NMR (CDCl₃), ¹⁹F NMR (CDCl₃), and ¹³C{¹H} NMR (CDCl₃) spectra matched those previously reported in the literature.^{8a} HRMS EI (*m/z*): [M]⁺ calcd for C₁₂H₉F, 172.0688; found, 172.0684. The isolated yield reported in Figure 3.2 is an average of two runs [75% and 67%].



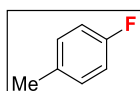
The reaction was performed using the standard conditions at 100 °C with (1,1'-biphenyl)-2-yl sulfonate **16-OFs** (126.0 mg, 0.5 mmol, 1 equiv). Product **16-F** was obtained as a white solid (71.2 mg, 83% yield, mp = 73.9–75.5 °C, R_f = 0.66 in pentane). The ¹H NMR (CDCl₃), ¹⁹F NMR (CDCl₃), and ¹³C{¹H} NMR (CDCl₃) spectra matched those previously reported in the literature.^{8c} HRMS EI (*m/z*): [M]⁺ calcd for C₁₂H₉F, 172.0688; found, 172.0685. The isolated yield reported in Figure 3.2 is an average of two runs [83% and 82%].



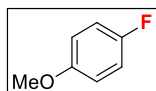
The reaction was performed using the standard conditions at 100 °C with naphthalen-2-yl sulfofluoridate **17-OFs** (113.0 mg, 0.5 mmol, 1.0 equiv). Product **17-F** was obtained as a colorless oil (38.3 mg, 52% yield, R_f = 0.72 in pentane). The ^1H NMR (CDCl_3), ^{19}F NMR (CDCl_3), and $^{13}\text{C}\{^1\text{H}\}$ NMR (CDCl_3) spectra matched those previously reported in the literature.⁶⁰ HRMS EI (m/z): $[\text{M}]^+$ calcd for $\text{C}_{10}\text{H}_7\text{F}$, 146.0532; found, 146.0533. The isolated yield reported in Figure 3.2 is an average of two runs [52% and 60%].



The reaction was performed using the standard conditions at 100 °C with naphthalen-1-yl sulfofluoridate **18-OFs** (113.0 mg, 0.5 mmol, 1.0 equiv). Product **18-F** was obtained as a colorless oil (41.9 mg, 57% yield, R_f = 0.71 in pentane). The ^1H NMR (CDCl_3), ^{19}F NMR (CDCl_3), and $^{13}\text{C}\{^1\text{H}\}$ NMR (CDCl_3) spectra matched those previously reported in the literature.⁶¹ HRMS EI (m/z): $[\text{M}]^+$ calcd for $\text{C}_{10}\text{H}_7\text{F}$, 146.0532; found, 146.0528. The isolated yield reported in Figure 3.2 is an average of two runs [57% and 57%].

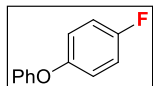


The reaction was performed at 100 °C with *p*-tolylfluorosulfonate (19.0 mg, 0.1 mmol, 1 equiv) and NMe_4F (46.5 mg, 0.5 mmol, 5 equiv), providing product **19-F** in 36% yield as determined by ^{19}F NMR spectroscopic analysis of the crude reaction mixture. The ^{19}F NMR spectral data matched that of an authentic sample (Matrix Scientific, m , -119.5 ppm). The identity of the product was further confirmed by GCMS analysis (m/z = 110). The yield reported in Figure 3.2 is an average of two runs [36% and 30%].

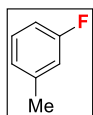


The reaction was performed at 100 °C with 4-methoxyphenyl sulfofluoridate (20.6 mg, 0.1 mmol, 1 equiv) and NMe_4F (46.5 mg, 0.5 mmol, 5 equiv), providing product **20-F** in 6%

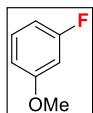
yield as determined by ^{19}F NMR spectroscopic analysis of the crude reaction mixture. The ^{19}F NMR spectral data matched that of an authentic sample (Acros, m, -125.5 ppm). The identity of the product was further confirmed by GCMS analysis ($m/z = 126$). The yield reported in Figure 3.2 is an average of two runs [6% and 5%].



The reaction was performed at $100\text{ }^{\circ}\text{C}$ with 4-phenoxyphenyl sulfonate **21-OFs** (134.0 mg, 0.5 mmol, 1 equiv) and NMe_4F (232.5 mg, 2.5 mmol, 5 equiv). Product **21-F** was obtained as a colorless oil (58.0 mg, 62% yield, $R_f = 0.57$ in pentane). The ^1H NMR (CDCl_3), ^{19}F NMR (CDCl_3), and $^{13}\text{C}\{^1\text{H}\}$ NMR (CDCl_3) spectra matched those previously reported in the literature.^{8c} HRMS EI (m/z): $[\text{M}]^+$ calcd for $\text{C}_{12}\text{H}_9\text{FO}$, 188.0637; found, 188.0637. The isolated yield reported in Figure 3.2 is an average of two runs [62% and 63%].

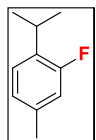


The reaction was performed using the standard conditions at $100\text{ }^{\circ}\text{C}$ with *m*-tolylfluorosulfonate **22-OFs** (19.0 mg, 0.1 mmol, 1 equiv) providing product **22-F** in 46% yield as determined by ^{19}F NMR spectroscopic analysis of the crude reaction mixture. The ^{19}F NMR spectral data matched that of an authentic sample (Matrix, m, -115.2 ppm). The yield reported in Figure 3.2 is an average of two runs [46% and 46%].

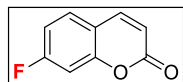


The reaction was performed using the standard conditions at $100\text{ }^{\circ}\text{C}$ with 3-methoxyphenyl sulfonate **23-OFs** (20.6 mg, 0.1 mmol, 1 equiv), providing product **23-F** in 39% yield as determined by ^{19}F NMR spectroscopic analysis of the crude reaction mixture. The ^{19}F NMR spectral data matched that of an authentic sample (Sigma Aldrich,

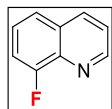
m, -112.9 ppm). The identity of the product was further confirmed by GCMS analysis ($m/z = 126$). The yield reported in Figure 3.2 is an average of two runs [39% and 37%].



The reaction was performed at $100\text{ }^{\circ}\text{C}$ with 2-isopropyl-5-methylphenyl sulfonate (23.2 mg, 0.1 mmol, 1 equiv) and NMe_4F (46.5 mg, 0.5 mmol, 5 equiv), providing product **24-F** in 24% yield as determined by ^{19}F NMR spectroscopic analysis of the crude reaction mixture (m, -121.3 ppm). The identity of the product was further confirmed by GCMS analysis ($m/z = 152$). The yield reported in Figure 3.2 is an average of two runs [24% and 29%].

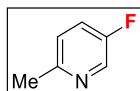


The reaction was performed using the standard conditions at room temperature with 2-oxo-2H-chromen-7-yl sulfonate **25-OFs** (122.0 mg, 0.5 mmol, 1 equiv). Product **25-F** was obtained as a white solid (54.4 mg, 66% yield, mp = $148.1\text{--}150.3\text{ }^{\circ}\text{C}$, $R_f = 0.63$ in 60% diethyl ether in pentane). ^1H NMR (700 MHz, CDCl_3): δ 7.68 (d, $J = 9.5$ Hz, 1H), 7.47 (dd, $J = 8.5, 6.0$ Hz, 1H), 7.08–6.97 (multiple peaks, 2H), 6.36 (d, $J = 9.5$ Hz, 1H). $^{13}\text{C}\{^1\text{H}\}$ NMR (176 MHz, CDCl_3): δ 166.20 (d, $J = 252$ Hz), 160.17, 155.27 (d, $J = 13$ Hz), 142.84 (d, $J = 1$ Hz), 129.43 (d, $J = 10.4$ Hz), 115.54 (d, $J = 2.5$ Hz), 115.41 (d, $J = 3.1$ Hz), 112.59 (d, $J = 22.7$ Hz), 104.55 (d, $J = 25.3$ Hz). ^{19}F NMR (100 MHz, CDCl_3): -105.09 (m, 1F). IR (cm^{-1}): 3086.1, 1720.8, 1698.5, 1623.7, 1504.0, 1400.7, 1118.4, 842.5. HRMS electrospray (m/z): $[\text{M}+\text{H}]^+$ calcd for $\text{C}_9\text{H}_5\text{FO}_2$, 165.0346; found, 165.0343. The isolated yield reported in Figure 3.2 is an average of two runs [66% and 64%].

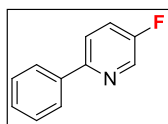


The reaction was performed using the standard conditions at $100\text{ }^{\circ}\text{C}$ with quinolin-8-yl sulfonate **26-OFs** (113.5 mg, 0.5 mmol, 1 equiv). Product **26-F** was obtained as a

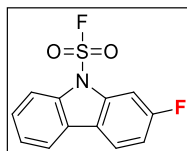
colorless oil (35.4 mg, 48% yield, $R_f = 0.29$ in 40% diethyl ether in pentane). The ^1H NMR (CDCl_3), ^{19}F NMR (CDCl_3), and $^{13}\text{C}\{^1\text{H}\}$ NMR (CDCl_3) spectra matched those previously reported in the literature.^{8c} HRMS EI (m/z): $[\text{M}]^+$ calcd for $\text{C}_9\text{H}_6\text{FN}$, 147.0484; found, 147.0480. The isolated yield reported in Figure 3.2 is an average of two runs [48% and 51%].



The reaction was performed using the standard conditions at 100 °C with 6-methylpyridin-3-yl sulfofluoridate (19.1 mg, 0.1 mmol, 1 equiv), providing product **27-F** in 57% yield as determined by ^{19}F NMR spectroscopic analysis of the crude reaction mixture. The ^{19}F NMR spectral data matched that of an authentic sample (Ark Pharm, m, -133.5 ppm). The identity of the product was further confirmed by GCMS analysis ($m/z = 111$). The yield reported in Figure 3.2 is an average of two runs [57% and 59%].

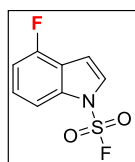


The reaction was performed using the standard conditions at 100 °C with 6-phenylpyridin-3-yl fluorosulfate **28-OFs** (126.5 mg, 0.5 mmol, 1 equiv). Product **28-F** was obtained as a white solid (62.3 mg, 72% yield, mp = 42.8–44.9 °C, $R_f = 0.44$ in 5% diethyl ether in pentane). The ^1H NMR (CDCl_3) and $^{13}\text{C}\{^1\text{H}\}$ NMR (CDCl_3) spectra matched those previously reported in the literature.⁶² ^{19}F NMR (100 MHz, CDCl_3): -129.8 (m, 1F). HRMS electrospray (m/z): $[\text{M}+\text{H}]^+$ calcd for $\text{C}_{11}\text{H}_9\text{FN}$, 174.0714; found, 174.0712. The isolated yield reported in Figure 3.2 is an average of two runs [72% and 73%].



The reaction was performed using the standard conditions at 80 °C with 9-(fluorosulfonyl)-9H-carbazol-2-yl sulfofluoridate **29-OFs** (173.5 mg, 0.5 mmol, 1.0 equiv). Product **29-F**

was obtained as a white solid (79.9 mg, 60% yield, mp = 63.4–65.5 °C, R_f = 0.67 in 10% dichloromethane in hexanes). ^1H NMR (CDCl_3 , 500 MHz): δ 8.01 (d, J = 8.0 Hz, 1H), 7.93–7.89 (multiple peaks, 2H), 7.78 (dd, J = 9.5, 2.5 Hz, 1H), 7.53–7.45 (multiple peaks, 2H), 7.20 (td, J = 8.5, 2.0 Hz, 1H). $^{13}\text{C}\{^1\text{H}\}$ NMR (CDCl_3 , 176 MHz): δ 162.4 (d, J = 246 Hz), 137.8 (d, J = 1.8 Hz), 137.7 (d, J = 1.6 Hz), 137.6 (t, J = 1.9 Hz), 127.6, 125.5 (d, J = 7.4 Hz), 122.3 (d, J = 2.3 Hz), 121.3 (d, J = 9.9 Hz), 120.0, 114.6, 113.2 (d, J = 23.6 Hz), 102.8 (d, J = 29.6 Hz). ^{19}F NMR (CDCl_3 , 376 MHz): δ 52.7 (s, 1F), –110.6 (m, 1F). IR (cm^{-1}): 1599.2, 1439.5, 1417.8, 1234.9, 1199.7, 1145.9, 1013.4, 960.1, 772.2, 756.5. HRMS EI (m/z): $[\text{M}]^+$ calcd for $\text{C}_{12}\text{H}_7\text{F}_2\text{NO}_2\text{S}$, 267.0166; found, 267.0161. The isolated yield reported in Figure 3.2 is an average of two runs [60% and 63%].

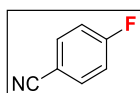


The reaction was performed using the standard conditions but at 100 °C with 1-(fluorosulfonyl)-1*H*-indol-4-yl sulfofluoridate **30-OFs** (148.5 mg, 0.5 mmol, 1.0 equiv). Product **30-F** was obtained as a colorless oil (21.2 mg, 20% yield, R_f = 0.5 in pentane). ^1H NMR (CDCl_3 , 400 MHz): δ 7.70 (d, J = 8.4 Hz, 1H), 7.44–7.34 (multiple peaks, 2H), 7.07 (t, J = 8.4 Hz, 1H), 6.91 (d, J = 3.6 Hz, 1H). $^{13}\text{C}\{^1\text{H}\}$ NMR (CDCl_3 , 126 MHz): δ 155.0 (d, J = 251 MHz), 136.7 (d, J = 8.9 MHz), 127.0 (d, J = 14.0 MHz), 126.1 (d, J = 2.3 MHz), 119.6 (d, J = 23.1 MHz), 110.5 (d, J = 18.4 MHz), 109.7 (d, J = 4.2 MHz), 106.7 (d, J = 1.6 MHz). ^{19}F NMR (CDCl_3 , 376 MHz): δ 54.8 (s, 1F), –119.9 (m, 1F). IR (cm^{-1}): 1588.9, 1488.0, 1452.9, 1441.8, 1224.4, 1201.0, 1132.1, 1033.4, 783.0, 742.1. HRMS EI (m/z): $[\text{M}]^+$ calcd for $\text{C}_8\text{H}_5\text{F}_2\text{NO}_2\text{S}$, 217.0009; found, 217.0003. The isolated yield reported in Figure 3.2 is an average of two runs [20% and 22%].

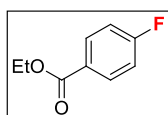
General Procedure for the One-Pot Deoxyfluorination of Phenols in Figure 3.3.^K In an N_2 -filled glovebox, NMe_4F (0.6–1.2 mmol, 3–6 equiv) and the appropriate phenol (0.2 mmol, 1 equiv) were weighed into a 4 mL glass vial equipped with a magnetic stir bar. The

^K Reactions performed and products isolated by Dr. Megan Cismesia, except for **36-F**.

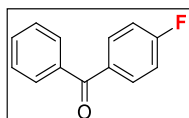
sulfuryl fluoride solution in DMF (2.9 mL, 0.4 mmol, 2 equiv) was added, and the vial was sealed with a Teflon-lined cap. The reaction mixture was allowed to stir at the given temperature for 24 h. The resulting solution was diluted with diethyl ether or dichloromethane (10 mL). The organic layer was washed with water (4–8 x 10 mL), collected, dried over MgSO₄, filtered, and the solvent was removed by rotary evaporation. The crude reaction mixture was purified by chromatography on silica gel using gradients of pentane/ diethyl ether unless noted otherwise.



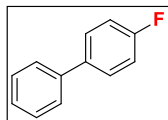
The reaction was performed using the standard conditions at room temperature with 4-cyanophenol (23.8 mg, 0.2 mmol, 1 equiv) and NMe₄F (56.1 mg, 0.6 mmol, 3.0 equiv). Product **1-F** was obtained as a white solid (13.0 mg, 54% yield). The isolated yield reported in Figure 3.3 is an average of two runs [54% and 57%].



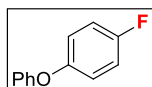
The reaction was performed using the standard conditions at room temperature with ethyl 4-hydroxybenzoate (33.2 mg, 0.2 mmol, 1 equiv) and NMe₄F (56.3 mg, 0.6 mmol, 3.0 equiv). Product **4-F** was obtained as a colorless oil (28.9 mg, 86% yield). The isolated yield reported in Figure 3.3 is an average of three runs [86%, 85% and 73%].



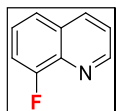
The reaction was performed using the standard conditions at room temperature with 4-hydroxybenzophenone (39.6 mg, 0.2 mmol, 1 equiv) and NMe₄F (56.2 mg, 0.6 mmol, 3.0 equiv). Product **5-F** was obtained as a white solid (34.4 mg, 86% yield). The isolated yield reported in Figure 3.3 is an average of four runs [86%, 95%, 89% and 73%].



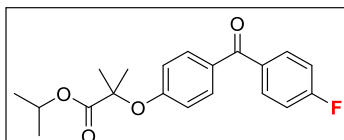
The reaction was performed using the standard conditions at 100 °C with 4-phenylphenol (33.9 mg, 0.2 mmol, 1 equiv) and NMe₄F (56.0 mg, 0.6 mmol, 3.0 equiv). Product **3-F** was obtained as a white solid (28.7 mg, 84% yield). The isolated yield reported in Figure 3.3 is an average of two runs [84% and 86%].



The reaction was performed at 100 °C with 4-phenoxyphenol (37.2 mg, 0.2 mmol, 1 equiv) and NMe₄F (112.0 mg, 1.2 mmol, 6.0 equiv). Product **21-F** was obtained as a colorless oil (26.4 mg, 70% yield). The isolated yield reported in Figure 3.3 is an average of two runs [70% and 66%].

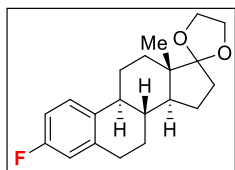


The reaction was performed using the standard conditions at 100 °C with 8-hydroxyquinoline (29.1 mg, 0.2 mmol, 1 equiv) and NMe₄F (56.0 mg, 0.6 mmol, 3.0 equiv). Product **26-F** was obtained as a colorless oil (17.0 mg, 58% yield). The isolated yield reported in Figure 3.3 is an average of three runs [58%, 57% and 45%].

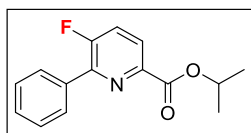


The reaction was performed using the standard conditions at room temperature with **31-OH** (68.7 mg, 0.2 mmol, 1 equiv) and NMe₄F (55.9 mg, 0.6 mmol, 3.0 equiv). Product **31-F** was obtained as a white solid (64.0 mg, 93% yield, mp = 66.7–67.7 °C, R_f = 0.41 in 5:1 pentane/ether). ¹H NMR (500 MHz, CDCl₃): δ 7.78 (dd, *J* = 8.6, 5.5 Hz, 2H), 7.72 (d, *J* = 8.7 Hz, 2H), 7.13 (t, *J* = 8.6 Hz, 2H), 6.86 (d, *J* = 8.7 Hz, 2H), 5.08 (heptet, *J* = 6.2 Hz, 1H), 1.65 (s, 6H), 1.19 (d, *J* = 6.2 Hz, 6H). ¹³C{¹H} NMR (126 MHz, CDCl₃): δ 194.2,

173.2, 165.2 (d, $J = 253.2$ Hz), 159.7, 134.4 (d, $J = 3.3$ Hz), 132.4 (d, $J = 9.1$ Hz), 132.0, 130.6, 117.3, 115.4 (d, $J = 21.8$ Hz), 79.5, 69.4, 25.5, 21.6. ^{19}F NMR (470 MHz, CDCl_3): δ -106.8 (m, 1F). HRMS electrospray (m/z): $[\text{M}+\text{H}]^+$ calcd for $\text{C}_{20}\text{H}_{21}\text{FO}_4$, 345.1497; found 345.1502. The isolated yield reported in Figure 3.3 is an average of two runs [93% and 86%].

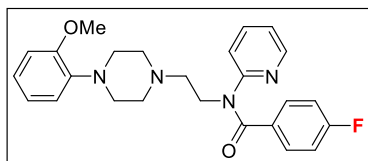


The reaction was performed using the standard conditions at 100 °C with **32-OH** (63.2 mg, 0.2 mmol, 1 equiv) and NMe_4F (111.8 mg, 1.2 mmol, 6.0 equiv). Product **32-F** was obtained as a white solid (11.5 mg, 18% yield, mp = 60.7–62.4 °C, $R_f = 0.58$ in 5:1 pentane/ether). ^1H NMR (500 MHz, CDCl_3): δ 7.23 (dd, $J = 8.4, 6.1$ Hz, 1H), 6.82 (td, $J = 8.5, 2.6$ Hz, 1H), 6.77 (dd, $J = 9.6, 2.3$ Hz, 1H), 4.01–3.86 (multiple peaks, 4H), 2.94–2.75 (multiple peaks, 2H), 2.32 (m, 1H), 2.23 (m, 1H), 2.03 (m, 1H), 1.96–1.71 (multiple peaks, 4H), 1.65 (m, 1H), 1.59–1.28 (multiple peaks, 5H), 0.89 (s, 4H). $^{13}\text{C}\{^1\text{H}\}$ NMR (126 MHz, CDCl_3): δ 161.0 (d, $J = 243.6$ Hz), 139.1 (d, $J = 6.9$ Hz), 136.1 (d, $J = 2.8$ Hz), 126.9 (d, $J = 7.9$ Hz), 119.5, 115.2 (d, $J = 20.0$ Hz), 112.4 (d, $J = 20.8$ Hz), 65.4, 64.7, 49.5, 46.2, 43.8, 39.0, 34.4, 30.8, 29.8 (d, $J = 1.3$ Hz), 26.9, 26.3, 22.5, 14.5. ^{19}F NMR (470 MHz, CDCl_3): δ -118.7 (m, 1F). HRMS electrospray (m/z): $[\text{M}+\text{H}]^+$ calcd for $\text{C}_{20}\text{H}_{25}\text{FO}_2$, 317.1911; found 317.1910. The isolated yield reported in Figure 3.3 is an average of two runs [18% and 19%].

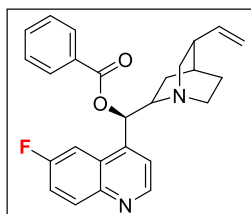


The reaction was performed using the standard conditions at room temperature with **33-OH** (51.9 mg, 0.2 mmol, 1 equiv) and NMe_4F (55.9 mg, 0.6 mmol, 3.0 equiv). Product **33-F** was obtained as a clear oil (45.1 mg, 86% yield, $R_f = 0.49$ in 5:1 pentane/ether). ^1H NMR (CDCl_3), ^{19}F NMR (CDCl_3), and $^{13}\text{C}\{^1\text{H}\}$ NMR (CDCl_3) spectra match those previously reported in the literature.²¹ HRMS electrospray (m/z): $[\text{M}+\text{H}]^+$ calcd for

$C_{15}H_{14}FNO_2$, 260.1081; found 260.1083. The isolated yield reported in Figure 3.3 is an average of two runs [86% and 88%].

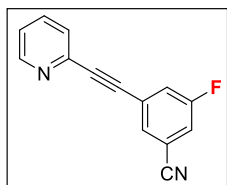


The reaction was performed at 100 °C with **34-OH** (86.2 mg, 0.2 mmol, 1.0 equiv) and NMe_4F (111.5 mg, 1.2 mmol, 6.0 equiv). Product **34-F** was obtained as a brown oil (56.0 mg, 65% yield, $R_f = 0.43$ in ethyl acetate). 1H NMR (500 MHz, $CDCl_3$): δ 8.41 (d, $J = 4.5$ Hz, 1H), 7.40 (t, $J = 7.6$ Hz, 1H), 7.36–7.28 (multiple peaks, 2H), 7.02 (m, 1H), 6.96 (t, $J = 7.4$ Hz, 1H), 6.92–6.78 (multiple peaks, 5H), 6.74 (d, $J = 8.0$ Hz, 1H), 4.27 (t, $J = 6.6$ Hz, 2H), 3.82 (s, 3H), 2.91 (s, br, 4H), 2.74 (t, $J = 6.6$ Hz, 2H), 2.63 (s, br, 4H). $^{13}C\{^1H\}$ NMR (126 MHz, $CDCl_3$): δ 169.6, 163.6 (d, $J = 251.0$ Hz), 156.6, 152.3, 148.8, 141.4, 137.2, 132.3 (d, $J = 3.2$ Hz), 131.1 (d, $J = 8.7$ Hz), 122.9, 122.9, 121.0, 121.0, 118.1, 115.1 (d, $J = 21.8$ Hz), 111.2, 56.4, 55.4, 53.4, 50.7, 45.7. ^{19}F NMR (470 MHz, $CDCl_3$): δ –109.36 (m, 1F). HRMS EI (m/z): $[M+H]^+$ calcd for $C_{25}H_{27}N_4FO_2$, 435.2191; found 435.2188. The isolated yield reported in Figure 3.3 is an average of two runs [65% and 76%].



The reaction was performed using the standard conditions at room temperature with *O*-benzoylcupreine (82.8 mg, 0.2 mmol, 1 equiv) and NMe_4F (83.8 mg, 0.9 mmol, 4.5 equiv). Product **35-F** was purified by HPLC to yield a white solid (15.4 mg, 19% yield, mp = 35.9–36.2 °C, $R_f = 0.50$ in dichloromethane with 10% methanol). 1H NMR (500 MHz, $CDCl_3$): δ 8.84 (d, $J = 4.5$ Hz, 1H), 8.13 (dd, $J = 9.2, 5.7$ Hz, 1H), 8.08 (d, $J = 7.4$ Hz, 2H), 7.95 (dd, $J = 10.3, 2.6$ Hz, 1H), 7.60 (t, $J = 7.4$ Hz, 1H), 7.53–7.44 (multiple peaks, 4H), 6.60 (d, $J = 7.4$ Hz, 1H), 5.85 (m, 1H), 5.12–4.95 (multiple peaks, 2H), 3.50 (m, 1H), 3.19 (m, 1H), 3.06 (dd, $J = 13.8, 10.1$ Hz, 1H), 2.75–2.56 (multiple peaks, 2H), 2.30 (m, 1H), 2.01 (m,

1H), 1.99 (m, 1H), 1.77 (m, 1H), 1.65 (dd, $J = 13.5, 7.5$ Hz, 1H), 1.58 (m, 1H). $^{13}\text{C}\{^1\text{H}\}$ NMR (126 MHz, CDCl_3): δ 165.7, 160.8 (d, $J = 248.2$ Hz), 149.4 (d, $J = 2.5$ Hz), 146.0, 145.2 (d, $J = 5.8$ Hz), 141.8, 133.7, 133.1 (d, $J = 9.4$ Hz), 129.8, 129.7, 128.8, 126.9 (d, $J = 9.6$ Hz), 119.7 (d, $J = 26.0$ Hz), 119.6, 114.8, 107.4 (d, $J = 23.3$ Hz), 74.9, 60.0, 56.8, 42.5, 39.8, 28.0, 27.7, 25.0. ^{19}F NMR (377 MHz, CDCl_3): δ -111.33 (m, 1F). HRMS EI (m/z): $[\text{M}+\text{H}]^+$ calcd for $\text{C}_{25}\text{H}_{25}\text{N}_2\text{FO}_2$, 417.1973; found 417.1978. The isolated yield reported in Figure 3.3 is an average of two runs [19% and 18%].



The reaction was performed using the standard conditions at 80 °C with hydroxy-5-(pyridine-2-ylethynyl)benzonitrile (11.0 mg, 0.05 mmol, 1.0 equiv) and NMe_4F (14.0 mg, 0.15 mmol, 3.0 equiv). Product **36-F** was obtained as a white solid (9.0 mg, 81% yield, mp = 94.7–95.6 °C, $R_f = 0.15$ in 15% ethyl acetate in hexanes). ^1H NMR (CDCl_3), ^{19}F NMR (CDCl_3), and $^{13}\text{C}\{^1\text{H}\}$ NMR (CDCl_3) spectra match those previously reported in the literature.^{38,63} HRMS EI (m/z): $[\text{M}+\text{H}]^+$ calcd for $\text{C}_{14}\text{H}_7\text{FN}_2$, 223.0666; found, 223.0669. The isolated yield reported in Figure 3.3 is an average of two runs [81% and 83%].

General Procedure for the Room Temperature ^{19}F NMR Studies in Figure 3.6. In an N_2 -filled drybox, a screw-cap NMR tube was charged with **14-OFs** (19.4 mg, 0.1 mmol, 1.0 equiv), NMe_4F (9.3 mg, 0.1 mmol, 1.0 equiv), and anh. DMF (0.5 mL). The NMR tube was sealed with a Teflon-lined cap. After 30 minutes, a ^{19}F NMR spectra was acquired. The NMR tube was allowed to sit at room temperature for 24 hours and a ^{19}F NMR spectra was acquired. A truncated ^{19}F NMR spectra is shown in Figure 3.5. 4-Fluoroanisole was used as an internal standard. For comparison, an NMR tube was prepared with **14-OFs** and **14-F** and ^{19}F NMR spectra was acquired.

General Procedure for the ^{19}F NMR Spectra Monitoring Shown in Figures 3.7–3.8. In an N_2 -filled drybox, a screw-cap NMR tube was charged with **14-OFs** or **14-sulfate** (0.1

mmol, 1.0 equiv), NMe₄F (18.6 mg, 0.2 mmol, 2.0 equiv), and DMF (0.5 mL). The NMR tube was sealed with a Teflon-lined cap and removed from the drybox. The NMR tube was then placed into an NMR spectrometer that had been pre-heated to 80 °C. The fluorination reaction of **14-OFs** or **14-sulfate** to form **14-F** was monitored by ¹⁹F NMR spectroscopy at 80 °C. Yield versus time plots were acquired by integration of the ¹⁹F signals of **14-OFs**, **14-sulfate**, and **14-F** relative to internal standard (4-fluoroanisole).

General Procedure for the ¹⁹F NMR Study in Figure 3.9. In an N₂-filled drybox, a screw-cap NMR tube was charged with **14-sulfate** (28.6 mg, 0.1 mmol, 1.0 equiv), NMe₄F (18.6 mg, 0.2 mmol, 2.0 equiv), and DMF (0.5 mL). The NMR tube was sealed with a Teflon-lined cap and removed from the drybox. The NMR tube was placed into a pre-heated oil bath at 80 °C such that the solution was immersed in the heated oil. After 10 minutes, the NMR tube was removed from the oil bath, flash frozen in liquid N₂, and warmed to room temperature to acquire a ¹⁹F NMR spectra. A truncated ¹⁹F NMR spectra is shown in Figure 3.8. 4-Fluoroanisole was used as an internal standard.

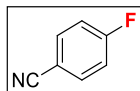
General Procedure for the Fluorination of Aryl Fluorosulfonates, Triflates, Nonaflates, and Diaryl Sulfates in Tables 3.6–3.7. In a N₂-filled drybox, substrate (0.1 mmol, 1.0 equiv) and NMe₄F (18.6 mg, 0.2 mmol, 2.0 equiv or 46.5 mg, 0.5 mmol, 5.0 equiv) were weighed into a 4 mL glass vial equipped with a micro-sized magnetic stir bar. DMF (0.5 mL) was added, and the vial was sealed with a Teflon-lined cap. The reaction mixture was allowed to stir at 80 °C for 24 h. The reaction was then diluted with dichloromethane (2.0 mL). 1,3,5-Trifluorobenzene was added as an internal standard, and the reaction was analyzed by ¹⁹F NMR spectroscopy and GCMS. For reactions with diaryl sulfates, yield was determined based on 0.1 mmol of starting material producing a maximum of 0.2 mmol fluorinated product.

General Procedure for the Initial Rate Studies in Figures 3.5, 3.11–3.12, and 3.14. In a N₂-filled drybox, substrate (0.1 mmol, 1.0 equiv) and NMe₄F (18.6 mg, 0.2 mmol, 2.0 equiv) were weighed into a 4 mL vial equipped with a magnetic stir bar. DMF (0.5 mL) was added, and the vial was sealed with a Teflon-lined cap. The vial was removed from

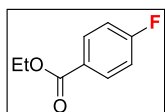
the drybox and heated to 80 °C on a pre-heated aluminum heat block. After the desired reaction time (measured by a timer), the reaction was flash frozen in a liquid N₂ bath. The reaction was then warmed to room temperature and diluted with dichloromethane (2.0 mL). 1,3,5-Trifluorobenzene was added as an internal standard, and the reaction was analyzed by ¹⁹F NMR spectroscopy. Yields and concentrations of product are reported as an average of three independent vial reactions. Concentration versus time data were collected from the integration of the ¹⁹F NMR signals of product versus internal standard (1,3,5-trifluorobenzene). The rate constant for each experiment was determined by a linear fit of the growth of fluorinated product. A plot of Hammett values,⁶⁴ σ , versus log (k_R/k_H) showed a linear correlation.

General Procedure for the Effect of Exogenous SO₂F₂ on Reaction of 3-sulfate in Scheme 3.6. In a N₂-filled drybox, **3-sulfate** (20.1 mg, 0.05 mmol, 1.0 equiv) and NMe₄F (9.3 mg, 0.1 mmol, 2.0 equiv) were weighed into a 4 mL vial equipped with a magnetic stir bar. A solution of SO₂F₂ in anhydrous DMF (0.36 mL of 0.14M solution, 0.05 mmol, 1.0 equiv) was added, and the vial was quickly sealed with a Teflon-lined cap. The reaction was heated at 80 °C for 24 hours. The reaction was cooled to room temperature and diluted with dichloromethane (2.0 mL). 1,3,5-Trifluorobenzene was added as an internal standard, and the reaction was analyzed by ¹⁹F NMR spectroscopy.

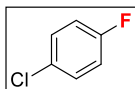
General Procedure for the Substrate Scope in Figure 3.13. In a N₂-filled drybox, NMe₄F (18.6 mg, 0.2 mmol, 2 equiv) and the aryl triflate substrate (0.1 mmol, 1 equiv) were weighed into a 4 mL glass vial equipped with a micro-sized magnetic stir bar. DMF (0.5 mL) was added, and the vial was sealed with a Teflon-lined cap. The reaction mixture was allowed to stir at the given temperature for 24 h. The resulting solution was diluted with dichloromethane (2 mL) and a standard (1,3,4-trifluorobenzene or 4-fluoroanisole, 100 μ L of a 0.5 M solution in toluene) was added. An aliquot was removed for analysis by ¹⁹F NMR spectroscopy and GCMS.



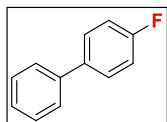
The reaction was performed using the standard conditions at 80 °C with 4-cyanophenyl trifluoromethanesulfonate **1-OTf** (25.1 mg, 0.1 mmol, 1 equiv), providing product **1-F** in 65% yield as determined by ^{19}F NMR spectroscopic analysis of the crude reaction mixture. The ^{19}F NMR spectral data matched that of an authentic sample (Oakwood Chemicals, m, -103.89 ppm). The identity of the product was further confirmed by GCMS analysis ($m/z = 121$). The yield reported in Figure 3.13 is an average of two runs [65% and 66%].



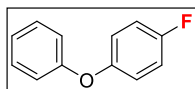
The reaction was performed using the standard conditions at 80 °C with ethyl 4-(((trifluoromethyl)sulfonyl)oxy)benzoate (29.8 mg, 0.1 mmol, 1.0 equiv), providing product **4-F** in 79% yield as determined by ^{19}F NMR spectroscopic analysis of the crude reaction mixture. The product showed a ^{19}F NMR signals at -107.3 ppm in DCM (lit. -106.1 ppm in CDCl_3).^{26b} The identity of the product was further confirmed by GCMS analysis ($m/z = 168$). The yield reported in Figure 3.13 is an average of two runs [79% and 65%].



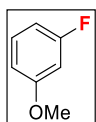
The reaction was performed using the standard conditions at 80 °C with 4-chlorophenyl trifluoromethanesulfonate (26.0 mg, 0.1 mmol, 1.0 equiv), providing product **9-F** in 85% yield as determined by ^{19}F NMR spectroscopic analysis of the crude reaction mixture. The ^{19}F NMR spectral data matched that of an authentic sample (Oakwood Products, m, -116.7 ppm). The identity of the product was further confirmed by GCMS analysis ($m/z = 130$). The yield reported in Figure 3.13 is an average of two runs [85% and 85%].



The reaction was performed using the standard conditions at 80 °C with [1,1'-biphenyl]-4-yl trifluoromethanesulfonate (30.2 mg, 0.1 mmol, 1.0 equiv), providing **3-F** in 86% yield as determined by ^{19}F NMR spectroscopic analysis of the crude reaction mixture. The ^{19}F NMR spectral data matched that of an authentic sample (Matrix, m, -116.7 ppm). The identity of the product was further confirmed by GCMS analysis ($m/z = 172$). The yield reported in Figure 3.13 is an average of two runs [86% and 87%].



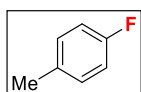
The reaction was performed using the standard conditions at 80 °C with 4-phenoxyphenyl trifluoromethanesulfonate (31.8 mg, 0.1 mmol, 1.0 equiv), providing **21-F** in 33% yield as determined by ^{19}F NMR spectroscopic analysis of the crude reaction mixture. The product showed a ^{19}F NMR signals at -121.1 ppm in DCM (lit. -120.1 ppm in CDCl_3).⁶⁵ The identity of the product was further confirmed by GCMS analysis ($m/z = 188$). The yield reported in Figure 3.13 is an average of two runs [33% and 34%].



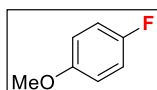
The reaction was performed using the standard conditions at 100 °C with 3-methoxyphenyl trifluoromethanesulfonate (25.6 mg, 0.1 mmol, 1.0 equiv), providing **23-F** in 22% yield as determined by ^{19}F NMR spectroscopic analysis of the crude reaction mixture. The ^{19}F NMR spectral data matched that of an authentic sample (Sigma Aldrich, m, -112.9 ppm). The identity of the product was further confirmed by GCMS analysis ($m/z = 126$). The yield reported in Figure 3.13 is an average of two runs [22% and 19%].



The reaction was performed using the standard conditions at 100 °C with *m*-tolyl trifluoromethanesulfonate (24.0 mg, 0.1 mmol, 1.0 equiv), providing **22-F** in 43% yield as determined by ^{19}F NMR spectroscopic analysis of the crude reaction mixture. The ^{19}F NMR spectral data matched that of an authentic sample (Matrix, m, -115.2 ppm). The yield reported in Figure 3.13 is an average of two runs [43% and 46%].



The reaction was performed at 100 °C with *p*-tolyl trifluoromethanesulfonate (24.0 mg, 0.1 mmol, 1.0 equiv) and NMe_4F (46.5 mg, 0.5 mmol, 5.0 equiv), providing product **19-F** in 23% yield as determined by ^{19}F NMR spectroscopic analysis of the crude reaction mixture. The ^{19}F NMR spectral data matched that of an authentic sample (Matrix Scientific, m, -119.5 ppm). The identity of the product was further confirmed by GCMS analysis ($m/z = 110$). The yield reported in Figure 3.13 is an average of two runs [12% and 12%].



The reaction was performed at 100 °C with 4-methoxyphenyl trifluoromethanesulfonate (25.6 mg, 0.1 mmol, 1.0 equiv) and NMe_4F (46.5 mg, 0.5 mmol, 5.0 equiv), providing none of the desired product **20-F** as determined by ^{19}F NMR spectroscopic analysis of the crude reaction mixture.

3.8.9. Computational Details

Computations were performed by Dr. Robert Froese at The Dow Chemical Company.

Density functional theory (DFT) and *ab initio* methods were used within the Gaussian09 program.⁶⁶ Recently, a modified G3 method was developed for $\text{S}_{\text{N}}\text{Ar}$

reactions.⁶⁷ That method is briefly described below. The molecules are small enough to utilize high level *ab initio* methods like the G3 suite of program.⁶⁸ However, it was uncovered that the without diffuse functions the anionic transition states would not optimize. The standard procedure for G3MP2B3 included a B3LYP/6-31G* optimization and an extrapolative single point procedure, with the key parameters being:

$$E\{G3MP2B3\} = E\{QCISD(T)/6-31G^*\} + \Delta E\{MP2\},$$

$$\text{where } \Delta E\{MP2\} = E\{MP2/6-311++g(2df,2p)\} - E\{MP2/6-31G^*\}$$

However, the transition states would not optimize with the 6-31G* basis set and the MP2 basis set correction term was very large, once again due to the lack of diffuse functions in the QCISD(T)/6-31G* term. A new G3MP2B3 method was developed where initially, the geometries were optimized with the B3LYP⁶⁹ method and the 6-311+G** basis set.⁷⁰ These optimizations included the PCM continuum solvation mode⁷¹ in DMF (dielectric constant $\epsilon = 37$). Single points were done with conventional methods:

$$E\{G3^*\} = E\{QCISD(T)/6-31+G^*\} + \Delta E\{MP2^*\},$$

$$\text{where } \Delta E\{MP2^*\} = E\{MP2/6-311++g(2df,2p)\} - E\{MP2/6-31+G^*\}$$

Enthalpic corrections were added on from the B3LYP/6-311+G** optimization/frequencies.

$$H\{G3^*\} = E\{G3^*\} + H\{B3LYP/6-311+G^{**}\} - E\{B3LYP/6-311+G^{**}\}$$

These enthalpies, G3* H, are the values quoted in this work. While free energies would also be desirable, the entropies associated with ions are often complicated due to solvent orientation, so enthalpies are used instead. Since similar entropies would be expected for a bimolecular reaction of F⁻ with different substrates, it would be expected that the relative ordering of substrate activation enthalpies would be the same as the activation free energies.

Computations were carried out on the X-Ar-Cl and X-Ar-OSO₂F substrates, where X = CN, CF₃, H, Me, and OMe. The Halex reactions of substituting Cl with F were found to proceed through a concerted TS with lengthened C–F and shortened C–Cl bond. Details of this type of structure have been described previously.⁶⁷ Reactions of the

fluorosulfonate substrates can proceed through an anionic X-Ar-OSO₂F₂ intermediate. This intermediate can deliver the fluoride to the carbon and eliminate OSO₂F⁻ in a concerted fashion. While the structure of the key fluorosulfonate TS (Figure 2B, Figure S2) depicts an F–S interaction, it is important to note that this distance is long at 2.61–2.62 Å for all five transition states. However, when an intrinsic reaction coordinate (IRC) calculation is run from the TS, one direction leads to product while the other direction leads to the pentacoordinate X-Ar-OSO₂F₂ intermediate.

3.9. References

- (1) Adapted with permission from: Schimler, S. D.; Cismesia, M. A.; Hanley, P. S.; Froese, R. D. J.; Jansma, M. J.; Bland, D. C.; Sanford, M. S. *J. Am. Chem. Soc.* **2017**, *139*, 1452–1455. ©American Chemical Society
- (2) (a) Thayer, A. M. *Chem. Eng. News* **2006**, *84*, 15–24. (b) Zhou, Y.; Wang, J.; Gu, Z.; Wang, S.; Zhu, W.; Aceña, J. L.; Soloshonok, V. A.; Izawa, K.; Liu, H. *Chem. Rev.* **2016**, *116*, 422–518. (c) Purser, S.; Moore, P. R.; Swallow, S.; Gouverneur, V. *Chem. Soc. Rev.* **2008**, *37*, 320–330.
- (3) (a) Finger, G. C.; Kruse, C. W. *J. Am. Chem. Soc.* **1956**, *78*, 6034–6037. (b) Gottlieb, H. B. *J. Am. Chem. Soc.* **1936**, *58*, 532–533. (c) Langlois, B.; Gilbert, L.; Forat, G. Fluorination of aromatic compounds by halogen exchange with fluoride anion (“halex” reaction). In *Industrial Chemistry Library*; Jean-Roger, D.; Serge, R., Eds.; Elsevier: New York, 1996; pp 244–292.
- (4) Wynn, D. A.; Roth, M. M.; Pollard, B. D. *Talanta* **1984**, *31*, 1036–1040.
- (5) (a) Clark, J. H.; Wails, D.; Bastock, T. W. *Aromatic Fluorination*. CRC Press: Boca Raton, FL, 1996. (b) Adams, D. J.; Clark, J. H. *Chem. Soc. Rev.* **1999**, *28*, 225–231.
- (6) Grushin, V. V.; Marshall, W. J. *Organometallics* **2008**, *27*, 4825–4828.
- (7) *The Chemistry of Phenols*; Rappoport, Z., Ed.; John Wiley & Sons Ltd.: Chichester, 2003.
- (8) (a) Tang, P.; Wang, W.; Ritter, T. *J. Am. Chem. Soc.* **2011**, *133*, 11482–11484. (b) Fujimoto, T.; Becker, F.; Ritter, T. *Org. Process Res. Dev.* **2014**, *18*, 1041–1044. (c) Fujimoto, T.; Ritter, T. *Org. Lett.* **2015**, *17*, 544–547.
- (9) Neumann, C. N.; Hooker, J. M.; Ritter, T. *Nature* **2016**, *534*, 369–373.
- (10) Based on the largest available quantity from Ark Pharm, PhenoFluor is \$157,834.60/mol. PhenoFluor Mix (\$283.00/1g) and PhenoFluor solution (0.1M in toluene; \$309.00/10mL) are available from Sigma Aldrich.
- (11) Based on the largest available quantity from Sigma Aldrich, CsF is \$212.66/mol.
- (12) (a) Watson, D. A.; Su, M.; Teverovskiy, G.; Zhang, Y.; García-Fortanet, J.; Kinzel, T.; Buchwald, S. L. *Science* **2009**, *325*, 1661–1664. (b) Lee, H. G.; Milner, P. J.; Buchwald, S. L. *Org. Lett.* **2013**, *15*, 5602–5606. (c) Maimone, T. J.; Milner, P. J.; Kinzel, T.; Zhang, Y.; Takase, M. K.; Buchwald, S. L. *J. Am. Chem. Soc.* **2011**,

- 133, 18106–18109. (d) Noël, T.; Maimone, T. J.; Buchwald, S. L. *Angew. Chem. Int. Ed.* **2011**, *50*, 8900–8903.
- (13) Milner, P. J.; Kinzel, T.; Zhang, Y.; Buchwald, S. L. *J. Am. Chem. Soc.* **2014**, *136*, 15757–15776.
- (14) For reactions of phenols with SOF₄ to form aryl fluorides in low yields, see: Cramer, R.; Coffman, D. D. *J. Org. Chem.* **1961**, *26*, 4164–4165.
- (15) Schimler, S. D.; Ryan, S. J.; Bland, D. C.; Anderson, J. E.; Sanford, M. S. *J. Org. Chem.* **2015**, *80*, 12137–12145.
- (16) Boechat, N.; Clark, J. H. *J. Chem. Soc., Chem. Commun.* **1993**, 921–922.
- (17) Christe, K. O.; Wilson, W. W.; Wilson, R. D.; Bau, R.; Feng, J. *J. Am. Chem. Soc.* **1990**, *112*, 7619–7625.
- (18) Toluene is used as a solvent for the Pd-catalyzed fluorination of aryl triflates with CsF. See ref 12–13.
- (19) Bennett, B. K.; Harrison, R. G.; Richmond, T. G. *J. Am. Chem. Soc.* **1994**, *116*, 11165–11166.
- (20) (a) Sun, H.; DiMagno, S. G. *J. Am. Chem. Soc.* **2005**, *127*, 2050–2051. (b) Sun, H.; DiMagno, S. G. *Angew. Chem. Int. Ed.* **2006**, *45*, 2720–2725.
- (21) Allen, L. J.; Muhuhi, J. M.; Bland, D. C.; Merzel, R.; Sanford, M. S. *J. Org. Chem.* **2014**, *79*, 5827–5833.
- (22) Hedayatullah, M.; Guy, A.; Denivelle, L. C. *Acad. Sc. Paris* **1974**, *278*, 57.
- (23) The α -fluorination of fluorosulfuric acid esters using SO₂F₂ has been previously disclosed: Ishii, A.; Yasumoto, M. Method for producing fluorosulfuric acid ester. Patent US20110201825, August 18, 2011.
- (24) Keating, G. M. *Am. J. Cardiovasc. Drugs* **2011**, *11*, 227–247.
- (25) (a) Eckelbarger, J. D.; Epp, J. B.; Schmitzer, P. R.; Siddall, T. L. 3-Alkenyl-6-halo-4-aminopicolinates and their use as herbicides. US 20120190548 A1, July 26, 2012. (b) Whiteker, G. T.; Arndt, K. E.; Renga, J. M.; Yuanming, Z.; Lowe, C. T.; Siddall, T. L.; Podhorez, D. E.; Roth, G. A.; West, S. P.; Arndt, C. Process for the preparation of 4-amino-5-fluoro-3-halo-6-(substituted)picolinates. US 20120190860, July 26, 2012. (c) Yerkes, C. N.; Lowe, C. T.; Eckelbarger, J. D.; Epp, J. B.; Guentenspberger, K. A.; Siddall, T. L.; Schmitzer, P. R. Arylalkyl esters of 4-amino-6-(substitutedphenyl)picolinates and 6-amino-2-(substitutedphenyl)-4-pyrimidinecarboxylates and their use as selective herbicides for crops. US 20150025238 A1, January 22, 2015. (d) Eckelbarger, J. D.; Epp, J. B.; Schmitzer, P. R. 6-Amino-2-substituted-5-vinylsilylpyrimidine-4-carboxylic acids and esters and 4-amino-6-substituted-3-vinylsilylpyridine-2-carboxylic acids and esters as herbicides. US 20120190549 A1, July 26, 2012. (e) Epp, J. B.; Schmitzer, P. R.; Balko, T. W.; Ruiz, J. M.; Yerkes, C. N.; Siddall, T. L.; Lo, W. C. 2-Substituted-6-amino-5-alkyl, alkenyl or alkynyl-4-pyrimidinecarboxylic acids and 6-substituted-4-amino-3-alkyl, alkenyl and alkynyl picolinic acids and their use as herbicides. US 20090088322 A1, April 2, 2009. (f) Walsh, T. A.; Hicks, G.; Honma, M.; Davies, J. P. Resistance to auxinic herbicides. US 20070220629 A1, September 20, 2007.
- (26) For comparisons to the fluorination of the corresponding chloropicolinate, see ref 15, 21, and: (a) Allen, L. J.; Lee, S. H.; Cheng, Y.; Hanley, P. S.; Muhuhi, J. M.; Kane, E.; Powers, S. L.; Anderson, J. E.; Bell, B. M.; Roth, G. A.; Sanford, M. S.

- Bland, D. C. *Org. Process Res. Dev.* **2014**, *18*, 1045–1054. (b) Ryan, S. J.; Schimler, S. D.; Bland, D. C.; Sanford, M. S. *Org. Lett.* **2015**, *17*, 1866–1869.
- (27) Le Bars, D.; Lemaire, C.; Ginovart, N.; Plenevaux, A.; Aerts, J.; Brihay, C.; Hassoun, W.; Leviel, V.; Mekhsian, P.; Weissmann, D.; Pujol, J. F.; Luxen, A.; Comar, D. *Nucl. Med. Biol.* **1998**, *25*, 343–350.
- (28) (a) Hamill, T. G.; Krause, S.; Ryan, C.; Bonnefous, C.; Govek, S.; Seiders, T. J.; Cosford, N. D.; Roppe, J.; Kamenecka, T.; Patel, S.; Gibson, R. E.; Sanabria, S.; Riffel, K.; Eng, W.; King, C.; Yang, X.; Green, M. D.; O'Malley, S. S.; Hargreaves, R.; Burns, H. D. *Synapse* **2005**, *56*, 205–216. (b) Wang, J.-Q.; Tueckmantel, W.; Zhu, A.; Pellegrino, D.; Brownell, A.-L. *Synapse* **2007**, *61*, 951–961. (c) Lim, K.; Labaree, D.; Li, S.; Huang, Y. *Appl. Radiat. Isot.* **2014**, *94*, 349–354. (d) Liang, S. H.; Yokell, D. L.; Jackson, R. N.; Rice, P. A.; Callahan, R.; Johnson, K.; Alagille, D.; Tamagnan, G.; Collier, T. L.; Vasdev, N. *MedChemComm* **2014**, *5*, 432–435. (e) Stephenson, N. A.; Holland, J. P.; Kassenbrock, A.; Yokell, D. L.; Livni, E.; Liang, S. H.; Vasdev, N. *J. Nucl. Med.* **2015**, *56*, 489–492.
- (29) Calculations were carried out with a modified G3MP2B3 method and PCM solvation model in DMF. See: Froese, R. D. J.; Whiteker, G. T.; Peterson, T. H.; Arriola, D. J.; Renga, J. R.; Shearer, J. W. *J. Org. Chem.* **2016**, *81*, 10672–10682.
- (30) Hohenstein, C.; Kadzimirsz, D.; Ludwig, R.; Kornath, A. *Chem.-Eur. J.* **2011**, *17*, 925–929.
- (31) (a) Fry, S. E.; Pienta, N. J. *J. Am. Chem. Soc.* **1985**, *107*, 6399–6400. (b) Miller, J. *Aromatic Nucleophilic Substitution*; Elsevier: New York, 1968.
- (32) Sulfuryl fluoride is commercially available from SynQuest Laboratories in the United States for \$690.00/100g (\$704.21/mol).
- (33) Aryl triflates have previously been used as substrates for palladium-catalyzed fluorination with CsF, see refs 12 and 13.
- (34) The fluorination of primary and secondary alcohols using *n*-perfluorobutanesulfonyl fluoride has been previously reported: Bennua-Skalmowski, B.; Vorbrüggen, H. *Tetrahedron Lett.* **1995**, *36*, 2611–2614.
- (35) Aryl nonaflates have previously been used as substrates for palladium-catalyzed fluorination with CsF: Wannberg, J.; Wallinder, C.; Ünlüsoy, M.; Sköld, C.; Larhed, M. *J. Org. Chem.* **2013**, *78*, 4184–4189.
- (36) So, C. M.; Kwong, F. Y. *Chem. Soc. Rev.* **2011**, *40*, 4963–4972.
- (37) Hanley, P. S.; Ober, M. S.; Krasovskiy, A. L.; Whiteker, G. T.; Kruper, W. J. *ACS Catal.* **2015**, *5*, 5041–5046.
- (38) Mossine, A. V.; Brooks, A. F.; Makaravage, K. J.; Miller, J. M.; Ischiishi, N.; Sanford, M. S.; Scott, P. J. H. *Org. Lett.* **2015**, *17*, 5780–5783.
- (39) Zhuang, Z.-P.; Kung, M.-P.; Kung, H. F. *J. Med. Chem.* **1994**, *37*, 1406–1407.
- (40) Suzuki, M.; Khosrowabadi Kotyk, J. F.; Khan, S. I.; Rubin, Y. *J. Am. Chem. Soc.* **2016**, *138*, 5939–5956.
- (41) Shi, M.; Lei, Z.-Y.; Zhao, M.-X.; Shi, J.-W. *Tetrahedron Lett.* **2007**, *48*, 5743–5746.
- (42) Liang, Q.; Xing, P.; Huang, Z.; Dong, J.; Sharpless, K. B.; Li, X.; Jiang, B. *Org. Lett.* **2015**, *17*, 1942–1945.
- (43) Dong, J.; K. B. Sharpless, K. B. Sulfur (VI) fluoride compounds and methods for the preparation thereof. Patent WO 2015188120 A1, June 5, 2015.
- (44) Roth, G. P.; Fuller, C. E. *J. Org. Chem.* **1991**, *56*, 3493–3496.

- (45) Zhang, E.; Tang, J.; Li, S.; Wu, P.; Moses, J. E.; Sharpless, K. B. *Chem. Eur. J.* **2016**, *22*, 5692–5697.
- (46) Fier, P. S.; Maloney, K. M. *Org. Lett.* **2016**, *18*, 2244–2247.
- (47) Qin, L.; Ren, X.; Lu, Y.; Li, Y. Zhou, J. *Angew. Chem., Int. Ed.* **2012**, *51*, 5915–5919.
- (48) Dürr, A. B.; Yin, G.; Kalvet, I.; Napoly, F.; Schoenebeck, F. *Chem. Sci.* **2016**, *7*, 1076–1081.
- (49) Murai, N.; Yonaga, M.; Tanaka, K. *Org. Lett.* **2012**, *14*, 1278–1281.
- (50) Kale, A. P.; Pawar, G. G.; Kapur, M. *Org. Lett.* **2012**, *14*, 1808–1811.
- (51) (a) Kendall, A. J.; Salazar, C. A.; Martino, P. F.; Tyler, D. R. *Organometallics* **2014**, *33*, 6171–6178. (b) Joseph, J. T.; Sajith, A. M.; Ningegowda, R. C.; Shashikanth, A. *Adv. Synth. Catal.* **2017**, *359*, 419–425.
- (52) Lee, D.-Y.; Hartwig, J. F. *Org. Lett.* **2005**, *7*, 1169–1172.
- (53) Anderson, K. W.; Mendez-Perez, M.; Priego, J.; Buchwald, S. L. *J. Org. Chem.* **2003**, *68*, 9563–9573.
- (54) Guan, B.-T.; Lu, X.-Y.; Zheng, Y.; Yu, D.-G.; Wu, T.; Li, K.-L.; Li, B.-J.; Shi, Z.-J. *Org. Lett.* **2010**, *12*, 396–399.
- (55) Dong, J.; Sharpless, K. B.; Kwisnek, L.; Oakdale, J. S.; Fokin, V. V. *Angew. Chem. Int. Ed.* **2014**, *53*, 9466–9470.
- (56) Chesnut, R. W.; Cesati, R. R.; Cutler, C. S.; Pluth, S. L.; Katzenellenbogen, J. A. *Organometallics* **1998**, *17*, 4889–4896.
- (57) Pérez-Temprano, M. H.; Racowski, J. M.; Kampf, J. W.; Sanford, M. S. *J. Am. Chem. Soc.* **2014**, *136*, 4097–4100.
- (58) Enthaler, S.; Weidauer, M. *Catal. Lett.* **2011**, *141*, 1079–1085.
- (59) Liang, A.; Han, S.; Wang, L.; Li, J.; Zou, D.; Wu, Y.; Wu, Y. *Adv. Synth. Catal.* **2015**, *357*, 3104–3108.
- (60) Ye, Y.; Sanford, M. S. *J. Am. Chem. Soc.* **2013**, *135*, 4648–4651.
- (61) Furuya, T.; Ritter, T. *Org. Lett.* **2009**, *11*, 2860–2863.
- (62) Liu, C.; Yang, W. *Chem. Commun.* **2009**, 6267–6269.
- (63) Alagille, D.; DeCosta, H.; Chen, Y.; Hemstapat, K.; Rodriguez, A.; Baldwin, R. M.; Conn, J. P.; Tamagnan, G. D. *Bioorg. Med. Chem. Lett.* **2011**, *21*, 3243–3247.
- (64) Ritchie, C. D.; Sager, W. F. *Prog. Phys. Org. Chem.* **1964**, *2*, 323–400.
- (65) Schimmler, S. D.; Cismesia, M. A.; Hanley, P. S.; Froese, R. D. J.; Jansma, M. J.; Bland, D. C.; Sanford, M. S. *J. Am. Chem. Soc.* **2017**, *139*, 1452–1455.
- (66) Frisch, M. J.; Trucks, G. W.; Schlegel, H. B.; Scuseria, G. E.; Robb, M. A.; Cheeseman, J. R.; Scalmani, G.; Barone, V.; Mennucci, B.; Petersson, G. A.; Nakatsuji, H.; Caricato, M.; Li, X.; Hratchian, H. P.; Izmaylov, A. F.; Bloino, J.; Zheng, G.; Sonnenberg, J. L.; Hada, M.; Ehara, M.; Toyota, K.; Fukuda, R.; Hasegawa, J.; Ishida, M.; Nakajima, T.; Honda, Y.; Kitao, O.; Nakai, H.; Vreven, T.; Montgomery, J. A., Jr.; Peralta, J. E.; Ogliaro, F.; Bearpark, M.; Heyd, J. J.; Brothers, E.; Kudin, K. N.; Staroverov, V. N.; Keith, T.; Kobayashi, R.; Normand, J.; Raghavachari, K.; Rendell, A.; Burant, J. C.; Iyengar, S. S.; Tomasi, J.; Cossi, M.; Rega, N.; Millam, J. M.; Klene, M.; Knox, J. E.; Cross, J. B.; Bakken, V.; Adamo, C.; Jaramillo, J.; Gomperts, R.; Stratmann, R. E.; Yazyev, O.; Austin, A. J.; Cammi, R.; Pomelli, C.; Ochterski, J. W.; Martin, R. L.; Morokuma, K.; Zakrzewski, V. G.; Voth, G. A.; Salvador, P.; Dannenberg, J. J.; Dapprich, S.; Daniels, A. D.; Farkas,

- O.; Foresman, J. B.; Ortiz, J. V.; Cioslowski, J.; Fox, D. J. *Gaussian 09, Revision D.01*; Gaussian, Inc., Wallingford CT, 2013.
- (67) Froese, R. D. J.; Whiteker, G. T.; Peterson, T. H.; Arriola, D. J.; Renga, J. R.; Shearer, J. W. *J. Org. Chem.* **2016**, *81*, 10672–10682.
- (68) Curtiss, L. A.; Redfern, P. C.; Raghavachari, K.; Rassolov, V.; Pople, J. A. *J. Chem. Phys.* **1999**, *110*, 4703–4709.
- (69) (a) Becke, A. D. *J. Chem. Phys.* **1993**, *98*, 5648–5652. (b) Lee, C.; Yang, W.; Parr, R. G. *Phys. Rev B* **1988**, *37*, 785–789. (c) Miehlich, B.; Savin, A.; Stoll, H.; Preuss, H. *Chem. Phys. Lett.* **1989**, *157*, 200–206.
- (70) (a) Ditchfield, R.; Hehre, W. J.; Pople, J. A. *J. Chem. Phys.* **1971**, *54*, 724–728. (b) Hehre, W. J.; Ditchfield, R.; Pople, J. A. *J. Chem. Phys.* **1972**, *56*, 2257–2261. (c) Gordon, M. S. *Chem. Phys. Lett.* **1980**, *76*, 163–168. (d) McLean, A. D.; Chandler, G. S. *J. Chem. Phys.* **1980**, *72*, 5639–5648. (e) Krishnan, R.; Binkley, J. S.; Seeger, R.; Pople, J. A. *J. Chem. Phys.* **1980**, *72*, 650–654.
- (71) (a) Miertus, S.; Scrocco, E.; Tomasi, J. *J. Chem. Phys.* **1981**, *55*, 117–122. (b) Tomasi, J.; Mennucci, B.; Cancès, E. *J. Mol. Struct. (Theochem)* **1999**, *464*, 211–226 and references therein.

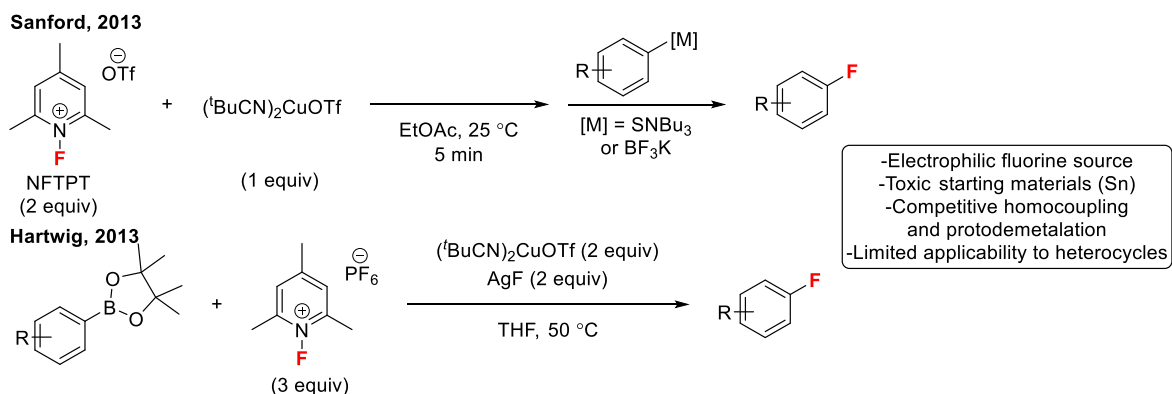
CHAPTER 4

Copper-Mediated and -Catalyzed Fluorination with Nucleophilic Fluoride¹

4.1 Background

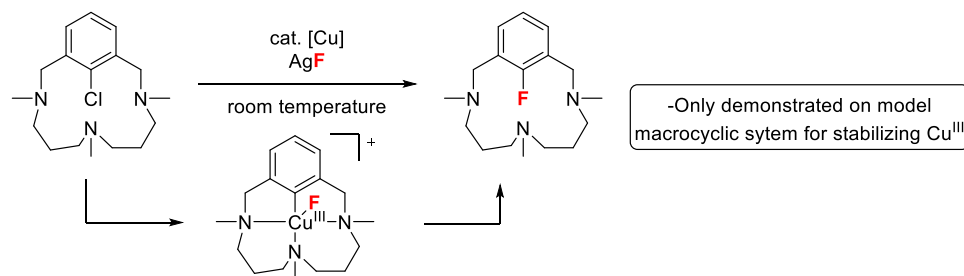
The use of copper to promote aromatic fluorination reactions is an attractive alternative to palladium- or silver-catalyzed fluorination methods as it is an earth-abundant metal. However, despite recent progress in the field of copper-mediated or -catalyzed aryl fluorination reactions, there are still many limitations to the current protocols. One approach for copper-mediated fluorination is the use of electrophilic fluorine sources (F^+). Our group reported the copper-mediated fluorination of aryl stannanes and aryl trifluoroborates using the electrophilic fluorinating reagent *N*-fluoro-2,4,6-trimethylpyridinium triflates (NFTPT) under mild reaction conditions (Scheme 4.1).² Simultaneously, the Hartwig group reported the copper-mediated electrophilic fluorination of aryl boronate esters (ArBPin) using similar conditions.³ Both reports demonstrated mild reaction conditions and broad substrate scope, but each had their limitations. Electrophilic fluorine sources are not ideal as they are expensive⁴ and have low applicability to positron emission tomography (PET) applications as their ^{18}F analogues are available in lower specific activity.⁵

Scheme 4.1. Examples of Copper-Mediated Electrophilic Aromatic Fluorination



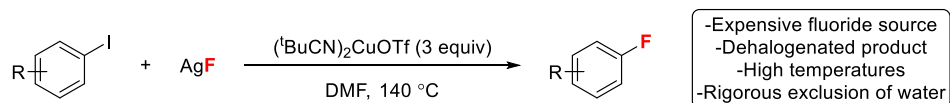
In contrast, nucleophilic fluorine sources (F^-) are more abundant, less expensive, and their ^{18}F analogues are readily accessible making them more desirable for large scale applications and PET imaging applications.⁶ In 2011, Ribas and coworkers reported the fluorination of a macrocyclic model system from a discrete Cu^{III} species and nucleophilic fluoride sources.⁷ Furthermore, they demonstrated that the conversion of an aryl halide (Cl, Br, I) to an aryl fluoride using catalytic copper was feasible (Scheme 4.2). This seminal work proved that every step in the catalytic cycle for the conversion of aryl-X to aryl fluoride was possible under mild conditions using nucleophilic fluoride such as potassium fluoride (KF). However, Ribas and coworkers only demonstrated this proof of concept on a specific model that was constructed specifically to stabilize a high valent Cu^{III} species; they did not translate this work to more general substrates. Additionally, Wang and coworkers reported the copper-mediated fluorination of a related macrocyclic system using KF.⁸ However, the transformation required elevated temperatures (refluxing acetonitrile), provided only modest yields of the fluorinated product, and could not be rendered catalytic.

Scheme 4.2. Copper-Catalyzed Fluorination of Macrocyclic System through a Defined Cu^{III} Intermediate



Based on the precedent of Ribas, the Hartwig group demonstrated the copper-mediated fluorination of aryl iodides using silver fluoride (Scheme 4.3).⁹ They demonstrated that electronically diverse aryl iodides can be converted to aryl fluorides in moderate to high yield. However, silver fluoride (AgF) is prohibitively expensive for use on large scale fluorination reactions.¹⁰ Other limitations include the need for stoichiometric copper, high reaction temperatures, side product formation (protodeiodinated arene), and the rigorous exclusion of water was essential for high yields.

Scheme 4.3. Copper-Mediated Nucleophilic Fluorination of Aryl Iodides



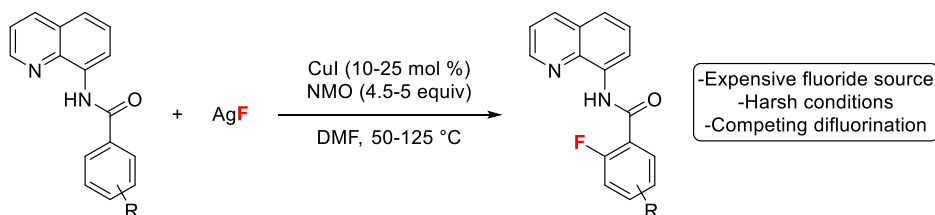
Copper(II) fluoride (CuF₂) has been reported to both induce the desired fluorination reaction of simple arenes and unactivated aryl halides as well as act as the fluoride source. Initial reports by Subramanian and Manzer used CuF₂ to convert benzene to fluorobenzene.¹¹ The heterogenous CuF₂ was regenerated from CuO₂ with HF and O₂. However, extremely harsh conditions were employed (450–550 °C), and the reaction was low yielding (~30%). Subsequently, Grushin reported the fluorination of unactivated aryl bromide and iodides using CuF₂ and *N,N,N',N'*-tetramethylethylenediamine (TMEDA) as a ligand.¹² The conditions were very harsh, required rigorously dry conditions, and yields of the desired fluorinated products were not reported.

Although copper-mediated electrophilic and nucleophilic fluorination of arenes is a significant advancement, a more desirable transformation would render copper catalytic.

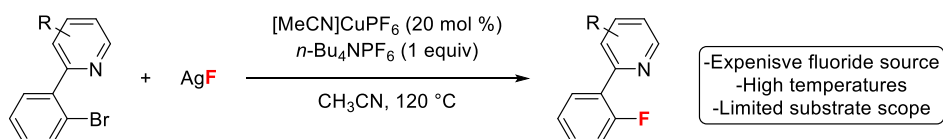
Daugulis and coworkers reported the directing group-assisted fluorination of arene C–H bonds catalyzed by CuI (Scheme 4.4).¹³ The authors utilized an aminoquinoline directing group to achieve copper-catalyzed C–H fluorination with AgF in moderate to high yields. However, the conditions were harsh and had to be tuned to avoid difluorination. Liu and coworkers reported the copper-catalyzed fluorination of 2-pyridyl aryl bromides using AgF (Scheme 4.4).¹⁴ The authors utilize a pyridyl substituent to both direct the oxidative addition and to stabilize the Cu^I species preventing its oxidation by AgF. While the reaction was demonstrated to be tolerant of a variety of functional groups, the harsh conditions, use of AgF, and need for the pyridyl substituents limited the application of this methodology to more general aryl bromides.

Scheme 4.4. Directed Copper-Catalyzed Fluorination with AgF

Daugulis, 2013

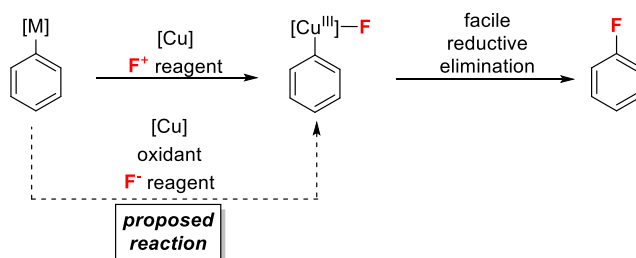


Liu, 2014



To address many of the remaining challenges of copper-mediated and -catalyzed fluorination, it is desirable to develop a mild fluorination method utilizing nucleophilic fluoride sources (ideally, potassium fluoride). Expanding on the use of electrophilic fluorination methods employing copper, it was hypothesized that the use of a copper salt, an oxidant, and a fluoride source could be used to access a Cu^{III} intermediate that would be prone to facile reductive elimination to afford the desired aryl fluoride (Scheme 4.5).¹⁵

Scheme 4.5. Proposed Cu-Mediated Fluorination with Nucleophilic Fluoride



In this chapter, the development of copper-mediated and -catalyzed fluorination reactions using nucleophilic fluoride sources is discussed. A mild and general copper-mediated fluorination reaction of aryl trifluoroborates with potassium fluoride (KF) was developed. Attempts to render the transformation catalytic in copper have been unsuccessful. Finally, a method for the directed copper-catalyzed fluorination of aryl halides was developed, albeit in low reactivity.

4.2. Initial Results and Optimization^A

The copper-mediated electrophilic fluorination of aryl trifluoroborates was inspiration for initial studies using nucleophilic fluoride.² It was envisioned that silver fluoride could replace the F^+ source and act as both an oxidant and fluoride source for the nucleophilic fluorination of aryl trifluoroborates. As an extrapolation from the reported conditions, the reaction of aryl trifluoroborate **1** with 4 equiv of $(t\text{BuCN})_2\text{Cu}(\text{OTf})$ and 4 equiv of AgF in acetonitrile (CH_3CN) at 60 °C provided none of the fluorinated product **2** (Table 4.1, entry 1). Copper salts were next evaluated, and while most copper sources provided no detectable product, the use of $\text{Cu}(\text{OTf})_2$ provided a modest yield of **2** (57%) in 20 h at 60 °C (entry 4). Other non-redox active metal fluoride salts were next evaluated as controls for this fluorination reaction. Surprisingly, the use of KF in place of AgF provided higher yield of **2** (70%) under otherwise analogous conditions (entry 6). Other alkali metal fluoride sources (NaF, CsF) provided comparable yields (entries 7–8).

To gain an understanding of the effect of counterion of these F^- salts on the rate of reaction, reaction profiles for these three-promising alkali metal fluoride sources (KF,

^A Part of the work in this section was done in collaboration with Dr. Yingda Ye. Dr. Ye's contributions include initial findings related to the use of KF for fluorination, copper screens, and fluoride screens (Table 4.1).

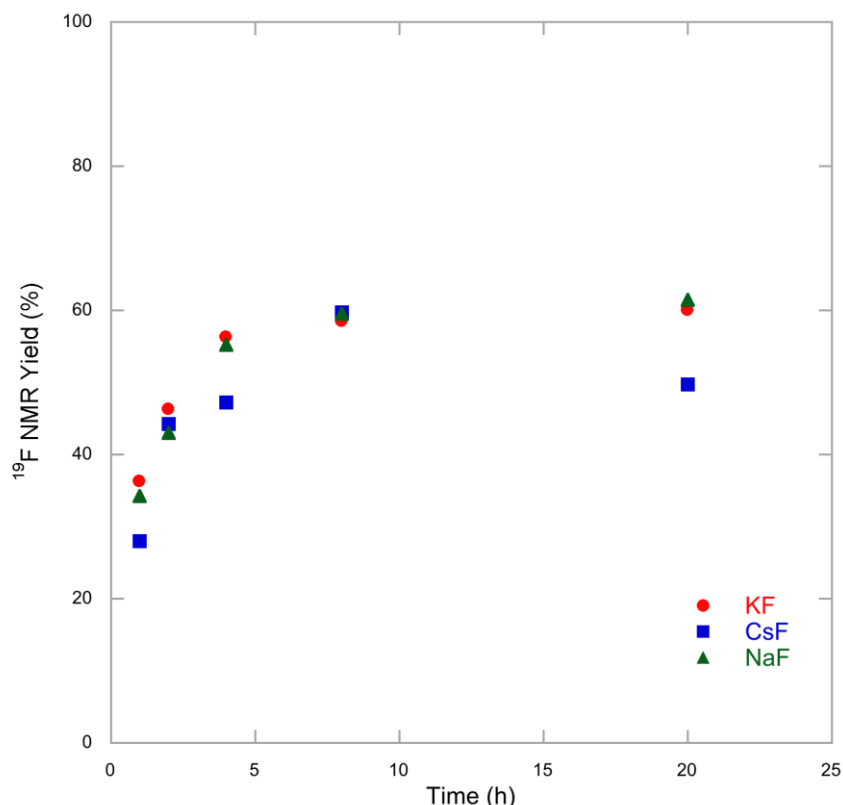
NaF, and CsF) were examined (Figure 4.1). At 60 °C, all three nucleophilic fluoride sources formed the desired product **2** in $\geq 30\%$ yield in just one hour. Reaction with CsF was slowest initially, but overall, the reaction profiles for the three alkali metal fluorides were very similar providing the highest yield of product in 8 h. For future studies, KF was chosen due to its abundance and low cost.¹⁶

Table 4.1. Copper Salts for the Nucleophilic Fluorination of **1**^a

entry	[Cu]	MF	% yield 2 ^b
1	(^t BuCN) ₂ CuOTf	AgF	<1
2	(MeCN) ₄ CuOTf	AgF	<1
3	CuF ₂	AgF	<1
4	Cu(OTf) ₂	AgF	57
5	no Cu	AgF	<1
6	Cu(OTf) ₂	KF	70
7	Cu(OTf) ₂	NaF	62
8	Cu(OTf) ₂	CsF	65

^aConditions: **1** (0.025 mmol, 1.0 equiv), [Cu] (0.1 mmol, 4.0 equiv), and MF (0.1 mmol, 4.0 equiv) in CH₃CN (0.083 M) at 60 °C for 20 h. ^bYields determined by ¹⁹F NMR spectroscopic analysis using 1,3,5-trifluorobenzene as standard.

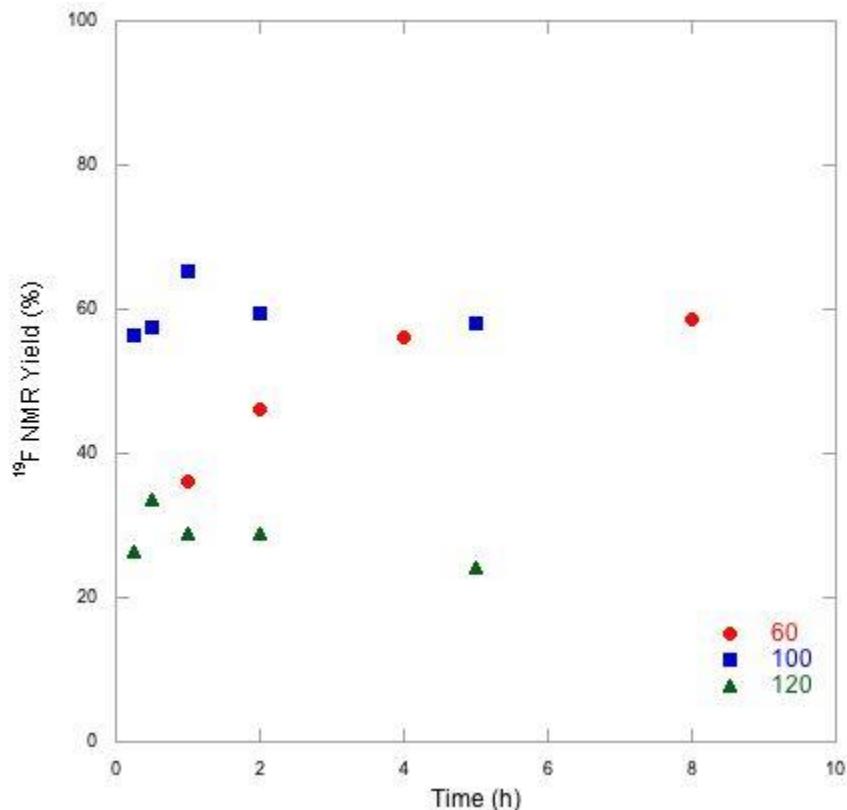
Figure 4.1. Reaction Profiles for the Fluorination of **1** with Alkali Metal Fluorides^a



^aConditions: **1** (0.025 mmol, 1.0 equiv), Cu(OTf)₂ (0.1 mmol, 4.0 equiv), and MF (0.1 mmol, 4.0 equiv) in CH₃CN (0.083 M) at 60 °C for the given time. Yields determined by ¹⁹F NMR spectroscopic analysis using 1,3,5-trifluorobenzene as standard.

Time studies at various temperatures were examined. Ideally fast reactions are better for applications such as positron emission tomography (PET) due to the short half-life of ¹⁸F (109.8 minutes).^{5,17} To affect a faster transformation, higher temperatures were investigated to promote the reaction (Figure 4.2). At 100 °C, the reaction of **1** with KF proceeded to 57% in just 30 min. Over longer times at 100 °C, the yield remained comparable to the yield obtained at 60 °C. Higher temperatures (120 °C) proved to be detrimental to the reaction; lower yields were obtained initially, and after 5 h, only 24% of **2** was obtained. The lower yields might be attributed to competitive side reactions (*vide infra*). Overall, by increasing the temperature of the reaction to 100 °C, high yields of the desired fluorinated product **2** were afforded in fast reaction times.

Figure 4.2. Reaction Profiles for the Fluorination of **1** at Various Temperatures^a



^aConditions: **1** (0.025 mmol, 1.0 equiv), Cu(OTf)₂ (0.1 mmol, 4.0 equiv), and KF (0.1 mmol, 4.0 equiv) in CH₃CN (0.083 M) at the given temperature for the given time. Yields determined by ¹⁹F NMR spectroscopic analysis using 1,3,5-trifluorobenzene as standard.

Fier and Hartwig previously reported that the use of copper complexes with –OTf and –SbF₆ counterions gave higher yields of nucleophilic fluorination reactions of aryl iodides with AgF.⁹ As such, the effect of changing the counterion associated with the copper(II) salt was explored (Table 4.2). Several copper(II) salts were synthesized with noncoordinating counterions. These copper salts were synthesized by combining CuCl₂ and excess silver salt in acetonitrile.¹⁸ Removal of AgCl and solvent gave the desired copper(II) salt. For comparison purposes, Cu(OTf)₂ was synthesized in the same manner. Under our previously determined fluorination conditions, the use of synthesized Cu(OTf)₂ provided 50% of the desired fluorinated product **2** (entry 2). The use of other copper(II) salts gave varied results. Use of Cu(SbF₆)₂ provided the highest yields of **2** (67%). Cu(BF₄)₂ and Cu(NTf₂)₂ provided modest yields of the desired product (entries 7 and 9). However, when commercial Cu(BF₄)₂ • xH₂O was used, the fluorination reaction of **1**

proceeded to only 8% yield of **2** potentially because of the presence of water associated with the copper salt. Importantly, without the presence of KF, no fluorinated product was observed indicating that the exogenous fluoride was important and fluorine did not come from the counterion of the copper(II) salt. No other copper(II) salts with noncoordinating counterions provided the desired fluorinated product. To rationalize the trend that was observed for the counterion effect on the fluorination reaction, the pKa of the conjugate acids were examined.¹⁹ However, no trend was observable for the effect of counterion on the fluorination reaction.

Table 4.2. Effect of Copper Counterion on the Fluorination of **1**^a

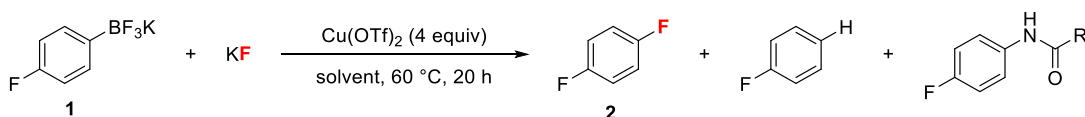
entry	Cu	% yield 2 ^b	pKa (H ₂ O)
1	Cu(SbF ₆) ₂	67	-25
2	Cu(OTf) ₂	50	-14
3	Cu(PF ₆) ₂	<1	-8
4	Cu(ONs) ₃	<1	-4
5	Cu(OTs) ₂	<1	-2.8
6	Cu(OMs) ₂	<1	-2.6
7	Cu(NTf ₂) ₂	32	-2
8	Cu(NO ₃) ₂	<1	-1.4
9	Cu(BF ₄) ₂	38	-0.4

^aConditions: **1** (0.025 mmol, 1.0 equiv), [Cu] (0.1 mmol, 4.0 equiv), and KF (0.1 mmol, 4.0 equiv) in CH₃CN (0.083 M) at 60 °C for 20 h. ^bYields determined by ¹⁹F NMR spectroscopic analysis using 1,3,5-trifluorobenzene as standard.

Other solvents were explored for this copper-mediated fluorination reaction (Table 4.3). CH₃CN worked well for the fluorination reaction of **1**, providing 70% yield of **2**. However, some side products were formed during the reaction (entry 1). One side product was fluorobenzene, formed via protodeborylation potentially from reaction with adventitious water.³ Another side product that was formed during the reaction is an amide product formed through reaction with CH₃CN. To avoid formation of this side product, non-nitrile solvents were evaluated but all provided very low yields of the desired product (entries 2–4).

Based on the formation of the amide side product, it was hypothesized that CH₃CN could act as a ligand for the active copper species in solution. To this end, Fier and Hartwig report the importance of nitrile ligand choice to affect the fluorination of aryl iodides with Cu^I salts.⁹ The use of nitrile solvents was explored to affect the desired fluorination reaction and minimize the production of the amide side product (Table 4.3, entries 5–9). The use of either propionitrile (EtCN) and *isobutyronitrile* (*i*PrCN) provided no detectable amide product but only modest yields of the desired fluorinated product (entries 5–6). When the fluorination reaction was conducted in other nitrile solvents such as trimethylacetoneitrile (*t*BuCN) and benzonitrile (PhCN), the desired fluorination occurred only in low yields and amide formation and protodeborylation were prominent (entries 7–8). The use of CH₃CN for the fluorination of aryl trifluoroborates was the most promising solvent as the highest yields of fluorinated product were obtained with only a minimum amount of side products.

Table 4.3. Solvents for the Cu(OTf)₂-Mediated Fluorination of **1**^a



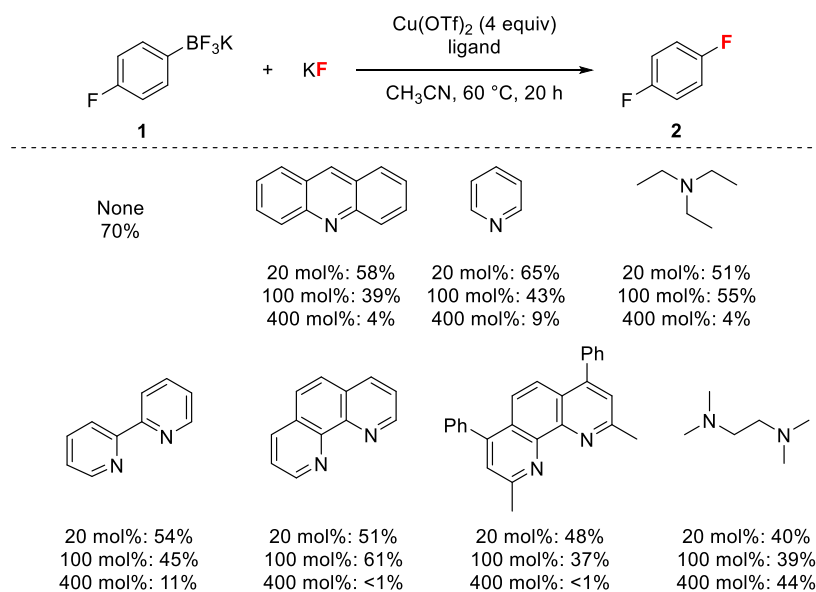
entry	solvent	% yield 2 ^b	% yield arene ^b	% yield amide ^b
1	CH ₃ CN	70	2	8
2	DMF	10	4	<1
3	DMSO	11	4	<1
4	toluene	11	3	<1
5	EtCN	57	5	<1
6	<i>i</i> PrCN	38	10	<1
7	<i>t</i> BuCN	6	6	23
8	PhCN	9	33	22
9	Adiponitrile	22	24	<1

^aConditions: **1** (0.025 mmol, 1.0 equiv), Cu(OTf)₂ (0.1 mmol, 4.0 equiv), and KF (0.1 mmol, 4.0 equiv) in solvent (0.083 M) at 60 °C for 20 h. ^bYields determined by ¹⁹F NMR spectroscopic analysis using 1,3,5-trifluorobenzene as standard.

Another approach for minimizing the amount of the amide product that is formed is to add an exogenous ligand for copper. Nitrogen ligands were examined due to their demonstrated utility for stabilizing active copper species.²⁰ Monodentate nitrogen ligands were initially examined, and it was found that at low ligand loadings (20 mol %), the

fluorination reaction was inhibited slightly but modest yields of **2** were still obtained (Figure 4.3). Furthermore, protodeborylation was more prevalent than in ligand-free reactions. Upon increasing the amount of ligand, a dramatic decrease in yield of **2** was observed; with 400 mol % of added ligand (1:1 ratio of ligand to copper), the fluorination product was obtained in less than 10% yield with monodentate nitrogen ligands.

Figure 4.3. Ligands for the Cu(OTf)₂-Mediated Fluorination of **1**^a



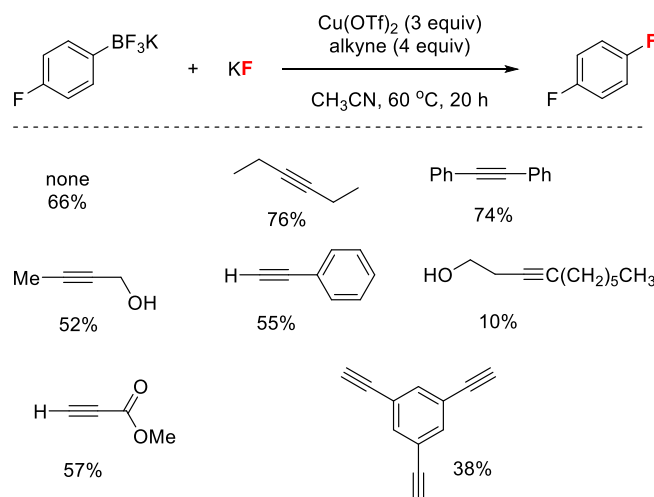
^aConditions: **1** (0.025 mmol, 1.0 equiv), Cu(OTf)₂ (0.1 mmol, 4.0 equiv), KF (0.1 mmol, 4.0 equiv) and ligand (20–400 mol %) in CH₃CN (0.083 M) at 60 °C for 20 h. Yields determined by ¹⁹F NMR spectroscopic analysis using 1,3,5-trifluorobenzene as standard.

Bidentate nitrogen ligands were next examined to affect the copper-mediated fluorination of **1** with KF (Figure 4.3). As with monodentate ligands, the yield of **2** was only modestly decreased with the addition of 20 mol % ligand in most cases. Further increase in the amount of ligand was detrimental to the reaction. One exception to this is *N,N,N',N'*-tetramethylethylenediamine (TMEDA); while the fluorination reaction was inhibited by the presence of TMEDA, increasing the amount in solution had negligible effect on the overall yield of the reaction.²¹ Additionally, with TMEDA there was no significant amount of increase in the amount of protodeborylation. While the addition of ligands to the copper-mediated fluorination reaction was detrimental, for all ligands examined, lower amounts of amide side product were produced. This supports the hypothesis that CH₃CN may act

as a ligand to stabilize the active copper species; in the presence of other ligands, binding of CH_3CN becomes less prevalent, and the side reaction with solvent was minimized. However, the amount of protodeborylation increased with the use of all ligands examined. While one unproductive reaction was shut down by the addition of ligands, another was enhanced.

Another set of ligands that have been reported to enhance the reactivity of oxidative coupling reactions involving copper are alkynes and alkenes.²² Alkynes can act as π -Lewis acids to copper and therefore as a supporting ligand to improve stability of the active copper species and prevent decomposition.²³ Alternatively, in Cu^{II} -mediated or -catalyzed processes, alkynes may complex Cu^{I} byproducts that are formed during the reaction minimizing undesired side reactions.²⁴ Merlic and coworkers demonstrated the use of 3-hexyne as a ligand to improve copper-mediated oxidative coupling reactions between dienyl boronate esters and alcohols.²² As such, 3-hexyne was explored in the $\text{Cu}(\text{OTf})_2$ -mediated fluorination reaction of **1**. While the addition of 4 equiv of 3-hexyne lead to diminished yields of **2** (60% with 3-hexyne vs. 70%), reducing the copper loading to 3 equiv in concert with the addition of 3-hexyne improved the reaction (Figure 4.4). Other alkynes were examined for the copper-mediated fluorination; internal alkynes proved best for this reaction, providing higher yields than using 3 equiv of $\text{Cu}(\text{OTf})_2$ without ligand. In addition to improving the yield of the fluorination reaction, the addition of 3-hexyne minimized the side products that were formed during the reaction in an analogous manner as the nitrogen ligands.

Figure 4.4. Alkyne Ligands for the Cu(OTf)₂-Mediated Fluorination of **1**^a



^aConditions: **1** (0.025 mmol, 1.0 equiv), Cu(OTf)₂ (0.075 mmol, 3.0 equiv), KF (0.1 mmol, 4.0 equiv) and ligand (0.1 mmol, 4.0 equiv) in CH₃CN (0.083 M) at 60 °C for 20 h. Yields determined by ¹⁹F NMR spectroscopic analysis using 1,3,5-trifluorobenzene as standard.

After examining several different parameters to optimize the nucleophilic fluorination reaction with aryl trifluoroborate **1**, the robustness of the reaction was examined (Table 4.4). The fluorination reaction is typically set up in a nitrogen-filled drybox; under these conditions, the fluorination reaction proceeded to 70% of **2**, with about 2% of fluorobenzene formed (entry 1). The use of wet solvent (stored on the benchtop) lead to a decrease in the yield of **2** (51%, entry 2). For a more systematic study, the effect of water and oxygen on the fluorination reaction of aryl trifluoroborate **1** was examined. The addition of 5–10 µL of water lead to lower yields of the desired fluorinated product **2** and an increase in the amount of fluorobenzene produced (entries 3–4). The effect of O₂ on the reaction was less dramatic; the presence of an oxygen atmosphere reduced the yield to 57% (entry 5). Overall, while the yields of **2** were reduced in the presence of oxygen and water, the reaction was not completely shut down. This offers an advantage over other fluorination reactions, where the reactions are dramatically affected by the presence of even trace water.^{3,9}

Table 4.4. Effect of Ambient Conditions on the Cu(OTf)₂-Mediated Fluorination of **1**^a

entry	conditions	% yield 2 ^b	% yield arene ^b
1	anhydrous	70	2
2	wet CH ₃ CN ^c	51	4
3	5 μ L H ₂ O	41	4
4	10 μ L H ₂ O	23	20
5	under O ₂	57	1
6	5 μ L H ₂ O, under O ₂	35	3

^aConditions: In a drybox, substrate **1** (0.5 mmol, 1.0 equiv), Cu(OTf)₂ (2.0 mmol, 4.0 equiv) and KF (2.0 mmol, 4.0 equiv) were weighed into a 20 mL vial. CH₃CN (6.0 mL) was added, and the vial was sealed with a rubber septum. The reaction vials were taken out of the drybox. Through the rubber septum, water and/or oxygen via balloon were added. Very quickly, the rubber septum was removed, and the vial was resealed with a Teflon-lined cap. The reaction mixture stirred at 60 °C for 20 h. ^bYields determined by ¹⁹F NMR spectroscopic analysis using 1,3,5-trifluorobenzene as standard. ^cCH₃CN was added outside of the drybox.

4.3. Substrate Scope^B

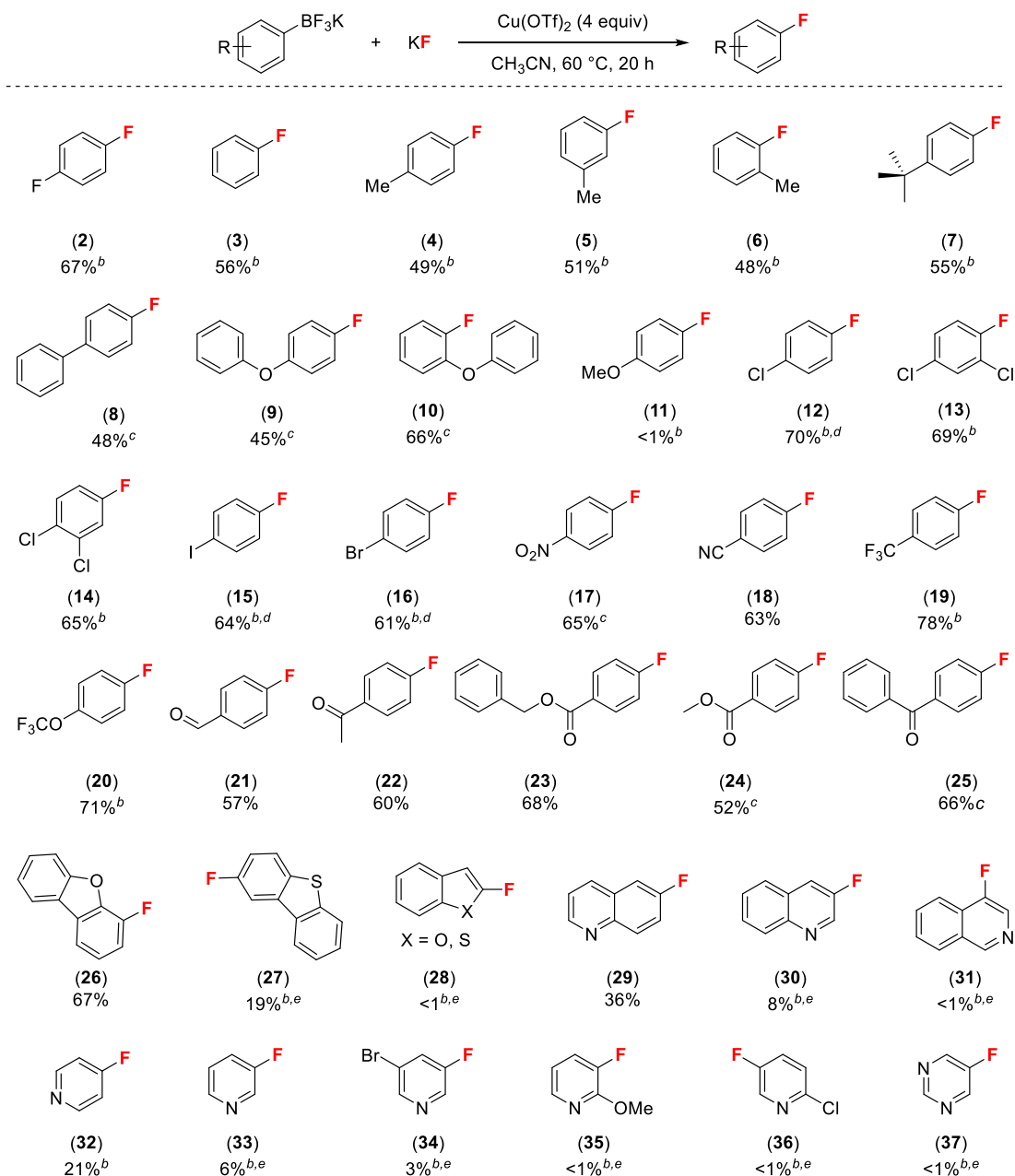
With optimized conditions in hand, the scope of the fluorination reaction was explored (Figure 4.5). While our initial optimizations were conducted on a 0.025 mmol scale, the fluorination of **1** with KF also proceeded in comparable yield (67%) on a 0.5 mmol scale. The Cu(OTf)₂-promoted fluorination with KF was applicable to both electron-deficient and electron-rich aryl trifluoroborates producing the desired fluorinated products in modest to good yield under mild reaction conditions. Electron-neutral and -rich substrates **3–10** reacted to provide modest yields of the desired fluorinated products. The presence of a methoxy group on the arene was not tolerated; product **11** was not produced in the fluorination reaction. The fluorination reaction was tolerant of sterically hindered substrates (substrates **6**, **10**, and **13**). Fluorinated product **8–10** were isolated in $\geq 97\%$ purity as trace protodeborylated side product were inseparable from the desired product.

^B The work in this section was done in collaboration with Dr. Yingda Ye. Most yields reported in Figure 4.5 represent the average of two yields: one performed by Y.Y. and the other performed by S.D.S.

Electron-poor substrates **12–25** reacted with KF and Cu(OTf)₂ to provide modest to good yields of the desired fluorinated product. This reaction shows good compatibility with carbonyl functional groups including aldehydes, ketones, and esters (**21–25**). In a few cases (**17**, **24**, **25**) the protodeborylated product could not be fully separated from the desired fluorinated product. However, significantly lower quantities of protodeborylated products were observed in this Cu-mediated fluorination method using nucleophilic fluoride compared to similar methods using electrophilic fluorinating reagents.^{2,3} One limitation of this method is that halide-containing substrates are susceptible to competing halodeboration under the reaction conditions. For example, 4-chlorophenyltrifluoroborate reacted to form the desired fluorinated product **12** in 70% yield along with 4% of 1,4-dichlorobenzene (as determined by GCMS analysis of the crude reaction mixture).

The fluorination reaction was also applied to heterocyclic compounds (**26–37**). Benzofuran and benzothiophene derivatives **28** did not provide any of the desired fluorinated product. Quinoline substrate **29** provided modest yields of the desired fluorinated product. However, installation of the fluorine on the nitrogen-containing ring of a quinoline substrate was unsuccessful (**30** and **31**). 4-Fluoropyridine **32** was obtained in relatively low yields (21%) under the standard fluorination conditions. However, by increasing the amount of Cu(OTf)₂ from 4 equiv to 10 equiv the yield of **32** increased to 49%. Other attempts at optimizing this reaction (higher temperature, use of ligands, different fluoride sources) were made but all manipulations lead to lower yields of **32**. The use of other pyridine substrates **33–37** provided very low yields of the fluorinated product or no detected product.

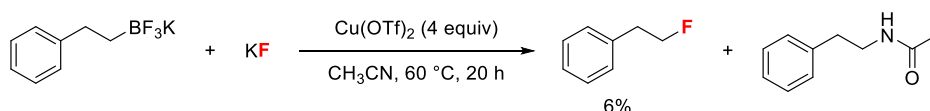
Figure 4.5. Substrate Scope of Cu(OTf)₂-Mediated Fluorination of Aryl Trifluoroborates with Potassium Fluoride^a



^aConditions: Potassium aryl trifluoroborate (0.5 mmol, 1.0 equiv), Cu(OTf)₂ (2.0 mmol, 4.0 equiv), and KF (2.0 mmol, 4.0 equiv) in CH₃CN (0.083 M) at 60 °C for 20 h. Unless otherwise noted, isolated yields are reported. ^bYield determined by ¹⁹F NMR spectroscopy with 1,3,5-trifluorobenzene as standard. ^cIsolated product was ≥ 97% pure but contained traces of inseparable protodeborylated side products. ^dDihalogenated product observed by GCMS as a side product. ^eReaction preformed using 0.025 mmol of potassium aryl trifluoroborate.

The optimized conditions were extended to the fluorination of alkyl trifluoroborates (Scheme 4.6). Using potassium phenethyltrifluoroborate, direct translation of the conditions that were developed for aryl trifluoroborates (4 equiv KF and 4 equiv Cu(OTf)₂ in CH₃CN (0.083 M) at 60 °C) resulted in only 6% of the desired fluorinated product **29**. The primary side product of this reaction as determined by GCMS was addition of the solvent to form the amide. Attempts to optimize this reaction in different solvents lead to no observed product.

Scheme 4.6. Cu-Mediated Fluorination of Alkyl Trifluoroborates with KF^a

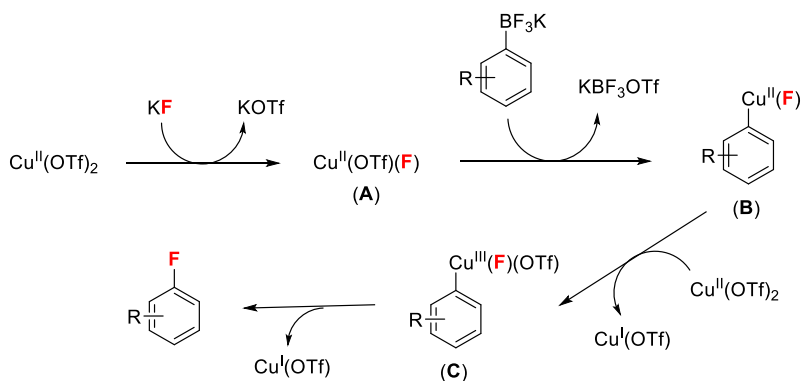


^aConditions: Potassium phenethyltrifluoroborate (0.025 mmol, 1.0 equiv), Cu(OTf)₂ (0.1 mmol, 4 equiv), and KF (0.1 mmol, 4.0 equiv) in CH₃CN (0.083 M) at 60 °C for 20 h. Yield determined by ¹⁹F NMR spectroscopy with 1,3,5-trifluorobenzene as standard.

4.4. Proposed Mechanism and Attempts at Copper-Catalyzed Fluorination of Aryl Trifluoroborates

A possible mechanism for this transformation is proposed in Scheme 4.7. In this mechanism, Cu(OTf)₂ plays a dual role in the reaction, acting as both a promoter for C–F bond formation and as an oxidant. The mild conditions employed in this reaction suggest that C–F coupling has a low activation barrier, suggesting that this step occurs via a highly reactive Cu^{III} intermediate (like **C**).^{2,3,7} It is proposed that the Cu^{III} species may form by disproportionation in which 1 equivalent of a Cu^{II} aryl intermediate **B** is oxidized by 1 equivalent of Cu(OTf)₂. Consistent with the proposed mechanism and the proposed dual role of copper is the need for excess copper to achieve high yields of the fluorinated product; with just 1 equiv of Cu(OTf)₂, the yield of **2** falls to 15% under otherwise identical conditions.

Scheme 4.7. Proposed Mechanism for the Cu(OTf)₂-Mediated Fluorination



It was hypothesized that the reaction could be rendered catalytic in Cu(OTf)₂ with the right choice in oxidant for the fluorination reaction. A series of oxidants were examined for this transformation (Table 4.5). For these reactions, the amount of Cu(OTf)₂ was reduced from 4 equiv to 2 equiv. When the fluorination reaction is conducted with just 2 equiv of Cu(OTf)₂ and no additional oxidant, the yield of **2** was reduced to 35% (entry 1). Other common oxidants including Ce(SO₄)₂, H₂O₂, NaNO₃, and benzoquinone resulted in reduced yields of **2** compared to the reaction with just 2 equiv of Cu(OTf)₂ (entries 2–5). The use of silver salts as oxidants gave comparable yields of **2** and did not improve the reaction (entries 6–7). The use of other oxidants gave very low yields of the desired fluorinated product (K₂S₂O₈, Ce(OTf)₂, FcBF₄, NaBO₃, hypervalent iodide reagents, NaNO₂, Ag₂CO₃, other copper salts).

Table 4.5. Oxidants for the Cu(OTf)₂-Mediated Fluorination of **1**^a

Reaction scheme: **1** (4-fluorophenyl trifluoroborate potassium salt) + **KF** $\xrightarrow[\text{CH}_3\text{CN, 60 } ^\circ\text{C, 20 h}]{\text{Cu(OTf)}_2 \text{ (2 equiv), oxidant (2 equiv)}}$ **2** (1,4-difluorobenzene)

entry	oxidant	% yield 2 ^b	% remaining 1 ^b
1	none	35	44
2	Ce(SO ₄) ₂	21	<1
3	H ₂ O ₂	30	23
4	benzoquinone	23	65
5	NaNO ₃	19	<1
6	V ₂ O ₅	41	31
7	AgOTf	41	48
8	AgF	39	27
9	CuF ₂	47	35
10	CeF ₄	62	<1
11	MnF ₃	56	<1
12	FeF ₃ • H ₂ O	48	42

^aConditions: **1** (0.025 mmol, 1.0 equiv), Cu(OTf)₂ (0.05 mmol, 2.0 equiv), KF (0.1 mmol, 4.0 equiv), and oxidant (0.05 mmol, 2.0 equiv) in CH₃CN (0.083 M) at 60 °C for 20 h.

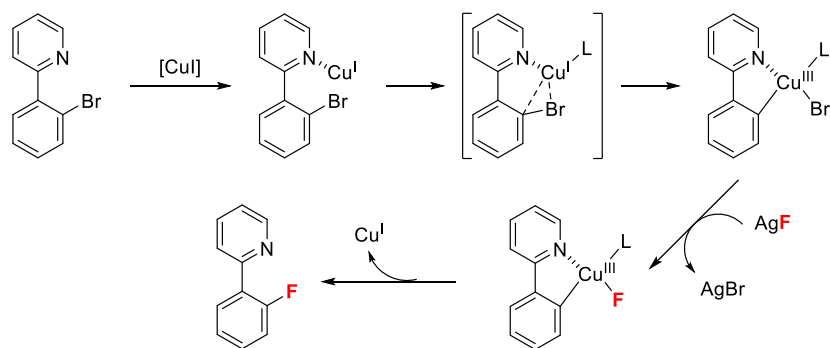
^bYields determined by ¹⁹F NMR spectroscopic analysis using 1,3,5-trifluorobenzene as standard.

The use of metal fluorides as oxidants for the copper-mediated fluorination reaction of aryl trifluoroborates proved to be promising (Table 4.5, entries 9–12). In particular, the fluorination reaction with 2 equiv of CeF₄ and 2 equiv of Cu(OTf)₂ proceeded in comparable yields to the reaction with 4 equiv of Cu(OTf)₂ (entry 10). Both KF and Cu(OTf)₂ were necessary for the fluorination reaction to proceed in high yield; without KF, the yield of **2** was only 9% and without Cu(OTf)₂, none of the desired fluorinated product was formed. However, when the amount of Cu(OTf)₂ was reduced to 20 mol % with CeF₄ as an oxidant, no detectable product was produced. These same results were seen when other promising oxidants (CuF₂ and MnF₃) were used in the presence of catalytic Cu(OTf)₂. With the understanding that the translation of the copper-mediated fluorination reaction of aryl trifluoroborates may not be straightforward to render catalytic, a different approach was sought to achieve copper-catalyzed fluorination.

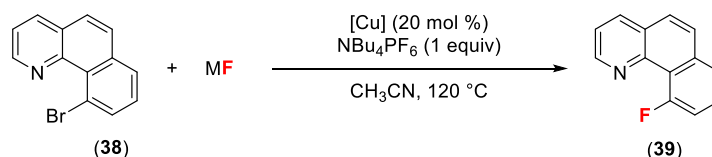
4.5. Copper-Catalyzed Fluorination of Aryl Halides via a Directed Approach

Having limited success with the copper-catalyzed fluorination of aryl trifluoroborates, focus was shifted to develop better methods for the directed copper-catalyzed fluorination of aryl halides. Inspiration was drawn from the work of Liu and coworkers, who used 2-pyridyl aryl bromides as substrates for Cu^I-catalyzed fluorination with AgF.¹⁴ The use of the directing group helped to both direct the oxidative addition and stabilize the Cu^I species preventing its oxidation by AgF (Scheme 4.8). One drawback of this method is the requirement for AgF; the authors demonstrated that the use of CsF lead to significantly reduced yields. It was hypothesized that this initial finding could be elaborated on to improve the system using inexpensive fluoride sources, less harsh conditions, and to expand the substrate scope.

Scheme 4.8. Mechanism Proposed for the Cu-Catalyzed Directed Fluorination



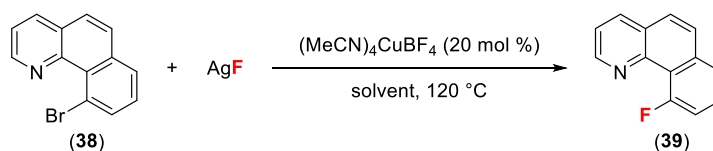
As a model substrate, halo-substituted benzo[*h*]quinoline were chosen. Liu and coworkers demonstrated the Cu^I-catalyzed fluorination of 10-bromobenzo[*h*]quinoline **38** with AgF provided the desired fluorinated product in 58% yield (Table 4.6, entry 1). In our hands, the fluorination reaction of substrate **38** proceeded in 36% yield (entry 2). The use of all other metal fluoride salts resulted in no fluorination (entries 3–6). Other Cu salts were also examined for this fluorination reaction with AgF. Use of both (MeCN)₄CuBF₄ and Cu(OTf)₂ provided higher yields of **39**; furthermore, the phase transfer reagent NBu₄X was not necessary to provide high yields of product (entries 7–8).

Table 4.6. Cu-Catalyzed Fluorination of **38^a**

entry	MF	[Cu]	% yield 39 ^b
1 ^c	AgF	(MeCN) ₄ CuPF ₆	58
2	AgF	(MeCN) ₄ CuPF ₆	36
3	KF	(MeCN) ₄ CuPF ₆	<1
4	NaF	(MeCN) ₄ CuPF ₆	<1
5	CsF	(MeCN) ₄ CuPF ₆	<1
6	NMe ₄ F	(MeCN) ₄ CuPF ₆	<1
7	AgF	(MeCN) ₄ CuBF ₄ ^d	54
8	AgF	Cu(OTf) ₂ ^d	48

^aConditions: **38** (0.05 mmol, 1.0 equiv), MF (0.1 mmol, 2.0 equiv), [Cu] (0.01 mmol, 20 mol %), and NBu₄PF₆ (0.05 mmol, 1.0 equiv) in CH₃CN (0.2 M) at 120 °C for 16 h. ^bYields determined by ¹⁹F NMR spectroscopy with 1,3,5-trifluorobenzene as standard. ^cYield reported in reference 14. ^dNBu₄PF₆ was excluded from the reaction.

Having identified improved reactivity with (MeCN)₄CuBF₄, the use of AgF in other solvents was next examined (Table 4.7). In particular, higher boiling point solvents were investigated that demonstrate higher stability towards basic fluoride salts.²⁵ Trimethylacetone nitrile (tBuCN) as a solvent gave diminished yields of **39** (entry 2); it is possible that this solvent displaced the acetonitrile ligands on the Cu^I catalyst and this lead to the lower reactivity.⁹ Benzonitrile (PhCN) as solvent gave comparable yields to that of CH₃CN (entry 3), and it has the potential to be a more suitable solvent for copper-catalyzed fluorination with other nucleophilic fluoride sources because of its increased stability to basic conditions. Amide solvents such as DMF and NMP provided modest to good yields of **39** (entries 4–6); however, in the absence of copper, the fluorination reaction proceeded in trace yields in the case of DMF, which has been used as a solvent for the uncatalyzed S_NAr fluorination reaction of aryl halides previously.²⁶ Nonpolar solvents were not suitable for this reaction (entry 7), likely due to the low solubility of AgF in nonpolar media.²⁷

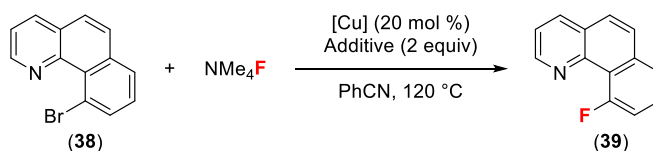
Table 4.7. Solvents for the Cu-Catalyzed Fluorination of **38** with AgF^a

entry	solvent	% yield 39 ^b	no [Cu]
1	CH ₃ CN	54	<1
2	^t BuCN	13	<1
3	PhCN	60	<1
4	DMF	12	2
5	NMP	45	<1
6	DMPU	<1	<1
7	toluene	<1	<1

^aConditions: **38** (0.05 mmol, 1.0 equiv), AgF (0.1 mmol, 2.0 equiv), and (MeCN)₄CuBF₄ (0.01 mmol, 20 mol %) in solvent (0.2 M) at 120 °C for 16 h. ^bYields determined by ¹⁹F NMR spectroscopy with 1,3,5-trifluorobenzene as standard.

When the use of other fluoride sources was examined in PhCN, anhydrous tetramethylammonium fluoride (NMe₄F) provided low yields of **39** (15%, Table 4.8 entry 1). All other alkali metal fluorides salts failed to produce the fluorinated product (<1%). Although the yield was quite low, this result demonstrated the possibility of using inexpensive fluoride sources for Cu-catalyzed fluorination. Attempts to optimize this transformation included increasing the reaction time, increasing the copper or NMe₄F loading, the use of added ligands, and lowering the temperature; however, any manipulation from the conditions in Table 4.8 entry 1 with NMe₄F lead to lower yields of the desired fluorinated product.

Given that the use of other copper salts provided some of the desired fluorinated product with AgF, we reexamined different Cu^I and Cu^{II} salts for the copper-catalyzed fluorination using NMe₄F in PhCN (Table 4.8). Additionally, the use of phase transfer reagents as an additive to help solubilize the fluoride was revisited. Under otherwise identical conditions, the reaction of **38** with NMe₄F improved with addition of the phase transfer reagent NBu₄BF₄ (entry 2). The use of (MeCN)₄CuPF₆, which was reported by Liu as the best catalyst for their system, resulted in reduced yields relative to those obtained with (MeCN)₄CuBF₄ (entries 3–4). Cu(OTf)₂ was an effective catalyst for the directed fluorination using NMe₄F in the absence of NBu₄OTf (entry 5); with the addition of the phase transfer reagent, the yield decreased (entry 6).

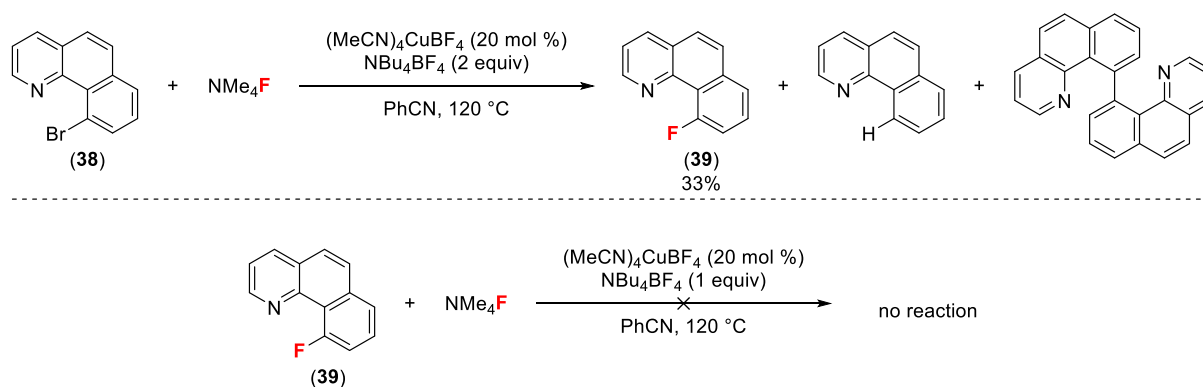
Table 4.8. Copper and Additive Screen for the Cu-Catalyzed Fluorination with NMe₄F^a

entry	[Cu]	Additive	% yield 39 ^b
1	(MeCN) ₄ CuBF ₄	none	15
2	(MeCN) ₄ CuBF ₄	NBu ₄ BF ₄	33
3	(MeCN) ₄ CuPF ₆	none	17
4	(MeCN) ₄ CuPF ₆	NBu ₄ PF ₆	26
5	Cu(OTf) ₂	none	26
6	Cu(OTf) ₂	NBu ₄ OTf	21

^aConditions: **38** (0.05 mmol, 1.0 equiv), NMe₄F (0.1 mmol, 2.0 equiv), [Cu] (0.01 mmol, 20 mol %), and additive (0.1 mmol, 2.0 equiv) in PhCN (0.2 M) at 120 °C for 16 h. ^bYields determined by ¹⁹F NMR spectroscopy with 1,3,5-trifluorobenzene as standard.

GCMS analysis of the crude reaction mixture indicates that the mass balance of the (MeCN)₄CuBF₄-catalyzed fluorination reaction is unreacted starting material, benzo[*h*]quinoline (from protodebromination), and a benzo[*h*]quinoline dimer (Scheme 4.9). To determine the source of the homocoupled product, the fluorinated product **39** was subjected to the reaction conditions to see if it formed the dimer (Scheme 4.9). Subjecting the fluorinated product to the reaction conditions resulted in unreacted starting material; no dimerization was observed, suggesting that the starting material produces the dimerized product. This is consistent with the literature of Ullmann reactions, whereby an aryl halide such as an aryl bromide or aryl chloride forms the diaryl via copper-catalysis.²⁸

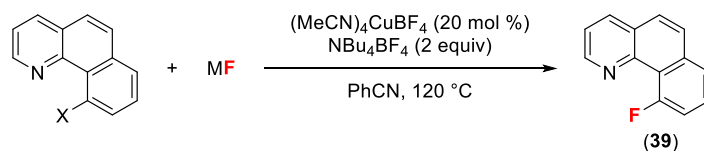
Scheme 4.9. Mass Balance of Cu-Catalyzed Fluorination with NMe₄F^a



^aConditions: **38** or **39** (0.05 mmol, 1.0 equiv), NMe₄F (0.1 mmol, 2.0 equiv), (MeCN)₄CuBF₄ (0.01 mmol, 20 mol%), and NBu₄BF₄ (0.1 mmol, 2.0 equiv) in PhCN (0.2 M) at 120 °C for 16 h. Reactions analyzed by ¹⁹F NMR spectroscopic analysis and GCMS. Yields determined by ¹⁹F NMR spectroscopy with 1,3,5-trifluorobenzene as standard.

Knowing the side products of the Cu-catalyzed fluorination reaction, attempts were made to optimize the reaction for the desired product while minimizing side product formation. Changing reaction parameters such as concentration, equivalents of NMe₄F, and equivalents of [Cu] had no positive effect on the reaction.

With little success with aryl bromide **38**, other aryl halides and pseudohalides were explored for the Cu-catalyzed fluorination (Table 4.9). When 10-chlorobenzo[*h*]quinoline was used as a substrate for the Cu-catalyzed fluorination reaction, very low yields (<5%) of the desired fluorinated product were detected by ¹⁹F NMR spectroscopic analysis of the crude reaction mixture under our optimized conditions (entries 3–4). When 10-iodobenzo[*h*]quinoline was used, the yields were comparable to that of the aryl bromide substrate (entries 5–6). However, like the use of the bromide substrate, the fluorination reaction with aryl iodides could not be improved by manipulation of the reaction parameters. When benzo[*h*]quinolin-10-yl trifluoromethanesulfonate was employed as the substrate, no product was detected (entry 7).

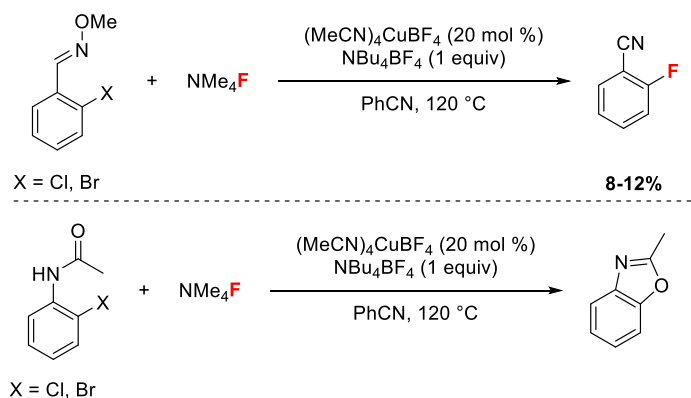
Table 4.9. Aryl Halides for Cu-Catalyzed Fluorination^a

entry	X =	MF	% yield 39 ^b
1 ^c	Br	AgF	60
2	Br	NMe ₄ F	33
3 ^c	Cl	AgF	<1
4	Cl	NMe ₄ F	<1
5 ^c	I	AgF	44
6	I	NMe ₄ F	35
7 ^d	OTf	AgF	<1

^aConditions: Substrate (0.05 mmol, 1.0 equiv), MF (0.1 mmol, 2.0 equiv), (MeCN)₄CuBF₄ (0.01 mmol, 20 mol %), and NBu₄BF₄ (0.1 mmol, 2.0 equiv) in PhCN (0.2 M) at 120 °C for 16 h. ^bYields determined by ¹⁹F NMR spectroscopy with 1,3,5-trifluorobenzene as standard. ^cNBu₄BF₄ was not included in reaction. ^dReaction was performed in CH₃CN.

Having little success with benzo[*h*]quinoline substrates, other substrates were examined for the Cu-catalyzed fluorination using the same directed approach (Scheme 4.10). The use of aryl halides with an oxime ether directing group under the optimized reaction conditions provided 2-fluorobenzonitrile in low yields. Further examination of this reaction demonstrated that copper was not necessary for this reaction and the same product was obtained without copper. It is possible that conversion of the oxime ether to 2-halobenzonitrile occurs first and subsequent S_NAr fluorination affords the fluorinated product.²⁶ *N*-(2-Halophenyl)acetamides were also poor substrates for the fluorination reaction. 2-Methylbenzoxazole was formed under the optimized fluorination conditions. The reaction of *N*-(2-halophenyl)acetamides to form benzoxazoles is a known copper-catalyzed reaction.²⁹

Scheme 4.10. Substrates for Cu-Catalyzed Fluorination^a



^aConditions: Substrate (0.05 mmol, 1.0 equiv), NMe4F (0.1 mmol, 2.0 equiv), (MeCN)4CuBF4 (0.01 mmol, 20 mol %), and NBu4BF4 (0.05 mmol, 1.0 equiv) in PhCN (0.2 M) at $120\text{ }^{\circ}\text{C}$ for 16 h. Yields determined by ^{19}F NMR spectroscopy with 1,3,5-trifluorobenzene as standard.

In conclusion, attempts at directed copper-catalyzed fluorination proved to be low yielding and challenging to optimize. It was established that when AgF was used for the fluorination, a phase transfer additive was not necessary depending on the counterion associated with the Cu^I salt. Importantly, when high boiling point solvents were used that were more stable to basic fluoride salts, fluorination could be achieved on 10-bromobenzo[*h*]quinoline in low yields using NMe4F demonstrating the feasibility of using an inexpensive F⁻ source. Additionally, the presence of a phase transfer reagent increased the reactivity likely due to improved solubility. However, attempts to optimize this reaction proved fruitless; changing the reaction temperature, Cu salt, concentration, equivalents of reagents, or use of a ligand all had either a detrimental effect or no effect on the outcome of the reaction. While our initial attempts were unsuccessful, Cu-catalyzed fluorination of aryl halides is highly desirable and further work in the field is warranted.

4.6. Conclusion

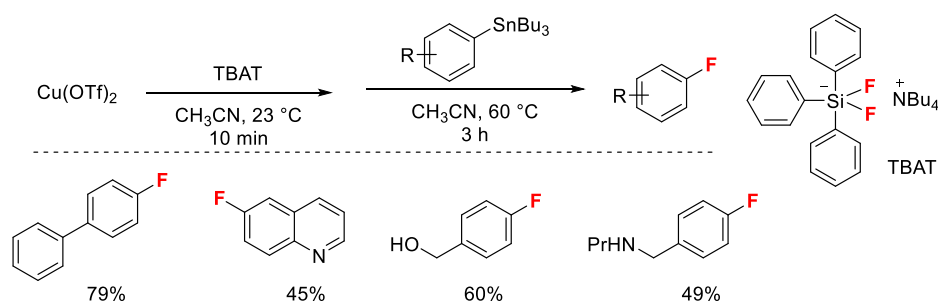
In conclusion, this chapter describes the Cu(OTf)2-mediated fluorination of aryl trifluoroborates with KF. This reaction can be applied to simple arene substrates to provide modest yields of the fluorinated product but suffers from limited applicability to heteroarenes. Attempts were made to render the reaction catalytic in Cu(OTf)2 but any

perturbation to the reaction conditions resulted in reduced yields. A different approach was taken for copper-catalyzed fluorination, namely the use of a directing group to stabilize an active copper species. However, this copper-catalyzed reaction was very low yielding when fluoride sources other than AgF were used. Overall, the results in this chapter demonstrate the difficulties associated with the development of copper-catalyzed fluorination reactions.

4.7. Outlook

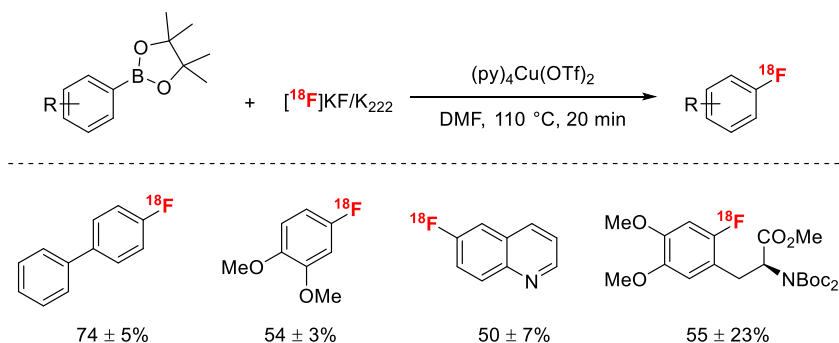
Since our report on the $\text{Cu}(\text{OTf})_2$ -mediated fluorination of aryl trifluoroborates,³⁰ there have been several reports that extrapolate from our described conditions to apply to different systems and applications. In 2016, Murphy and coworkers described the Cu-mediated fluorination of aryl stannanes with nucleophilic fluoride (Figure 4.6).³¹ The Murphy group found that by prestirring $\text{Cu}(\text{OTf})_2$ and a nucleophilic fluoride source (in this case, tetrabutylammonium difluorotriphenylsilicate (TBAT)), the amount of copper required for the fluorination could be decreased to just 2 equiv. The reaction was demonstrated on a variety of electronically diverse aryl stannanes which were converted to the aryl fluoride in modest to good yields (Figure 4.6). While this chemistry improves upon our initial findings by demonstrating that the amount of $\text{Cu}(\text{OTf})_2$ used in the fluorination reaction can be reduced, it still suffers from the need for excess copper. Furthermore, the starting aryl stannanes are not an ideal starting material for large-scale processes due to their toxicity.³²

Figure 4.6. Cu-Mediated Fluorination of Aryl Stannanes



There have been more advances in Cu-mediated fluorination since our initial publication, especially with regard application to PET chemistry. The first report by Gouverneur and coworkers demonstrated the nucleophilic ^{18}F fluorination of aryl boronate esters (Figure 4.7).³³ The Gouverneur group demonstrates that the combination of (hetero)aryl boronate pinacol esters, $(\text{py})_4\text{Cu}(\text{OTf})_2$ (py = pyridine), and $[^{18}\text{F}]\text{KF}$ provided the desired ^{18}F fluorinated arene in modest to good radiochemical conversions (RCC). Furthermore, they demonstrated the utility of this radiochemical transformation on biologically relevant arenes, including $[^{18}\text{F}]\text{F-DOPA}$, a radiotracer that can be used to measure dopamine levels in the brain.³⁴

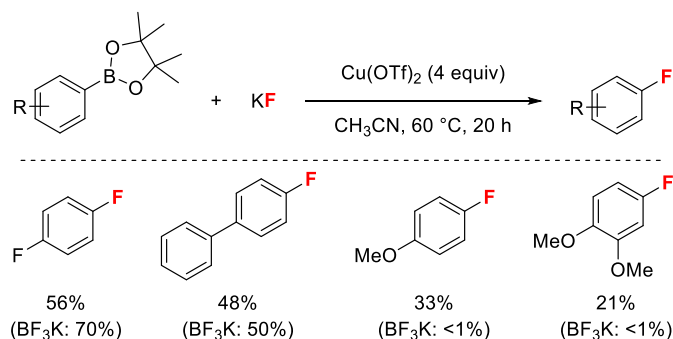
Figure 4.7. Cu-Mediated Radiofluorination of Aryl Boronate Esters



Inspired by the work of Gouverneur and coworkers, the conditions that they described were applied to Cu-mediated cold fluorination. The use of $(\text{py})_4\text{Cu}(\text{OTf})_2$ as the copper salt to mediate the fluorination reaction did not provide any of the desired fluorinated product. This is consistent with the ligand studies that were undertaken; the addition of ligands to the reaction significantly impeded the desired fluorination reaction. When aryl boronate esters were used as substrates for the Cu-mediated fluorination reaction under our standard conditions, the boronate ester analog of **1** provided 56% of the desired product (Figure 4.8). Gouverneur applied the radiofluorination conditions to many electron-rich substrates that under our Cu-mediated fluorination conditions failed. However, when the corresponding aryl boronate ester substrate was used, the desired fluorinated product was obtained in low to modest yields (Figure 4.8). Through the work of Gouverneur, it was demonstrated that the Cu-mediated fluorination reaction could be

applied to electron-rich substrates when a different aryl boronate starting substrate was used.

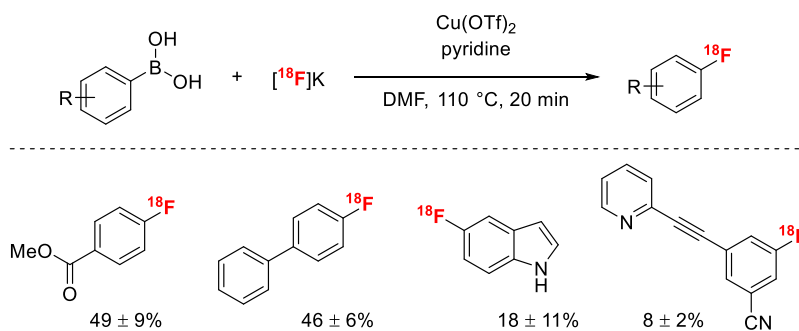
Figure 4.8. Cu-Mediated Fluorination of Aryl Boronate Esters^a



^aConditions: Substrate (0.025 mmol, 1.0 equiv), KF (0.1 mmol, 4.0 equiv), and $\text{Cu}(\text{OTf})_2$ (0.1 mmol, 4.0 equiv) in CH_3CN (0.083 M) at $60\text{ }^\circ\text{C}$ for 20 h. Yields determined by ^{19}F NMR spectroscopic analysis using 1,3,5-trifluorobenzene as standard.

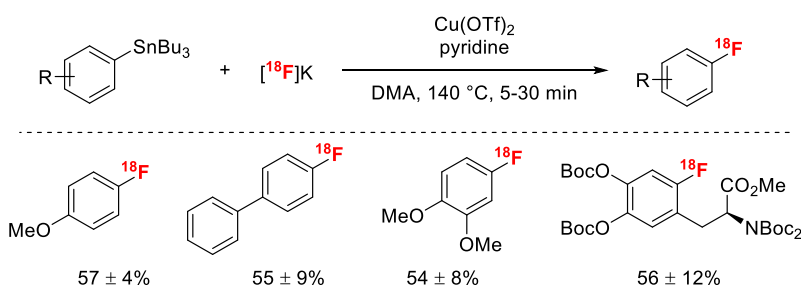
The Sanford lab in collaboration with Dr. Peter Scott at the University of Michigan Department of Radiology has developed a few methods for the radiofluorination of arenes using conditions similar to those developed for the fluorination of aryl trifluoroborates. First, the Sanford and Scott groups reported the Cu-mediated radiofluorination of aryl boronic acids (Figure 4.9).³⁵ The use of aryl trifluoroborates as substrates for the radiofluorination was found to be inefficient, likely due to isotopic exchange between ^{18}F and ^{19}F of the trifluoroborate. The use of pyridine as a ligand was found to improve the reactivity of the copper species and to improve the yields. The radiofluorination was demonstrated on electronically diverse aryl boronic acids in modest to good radiochemical conversions (RCC). Furthermore, the methodology was applied to the synthesis of $[^{18}\text{F}]\text{F-PEB}$, a radiotracer used for the quantification of metabotropic glutamate 5 receptors.³⁶

Figure 4.9. Cu-Mediated Radiofluorination of Aryl Boronic Acids



Concomitant with the work of Murphy, the Sanford and Scott collaboration disclosed the Cu-mediated radiofluorination of aryl stannanes (Figure 4.10).³⁷ The conditions used for the radiofluorination of aryl stannanes was very similar to that developed for the radiofluorination of aryl boronic acids; DMA as a solvent as well as a higher temperature (140 °C instead of 110 °C) was found to give higher yields with aryl stannanes. Aryl stannanes were converted to the radiolabeled fluorinated products in modest to good yields. Furthermore, this methodology could be applied to the radiofluorination of complex, biologically relevant molecules including [¹⁸F]F-DOPA.

Figure 4.10. Cu-Mediated Radiofluorination of Aryl Stannanes



While much progress has been made in the field of Cu-mediated fluorination, especially with regard to application to radiolabeling, there has not been a significant amount of work towards the development of copper-catalyzed fluorination reactions. Our group and others have identified that there are some significant obstacles that need to be overcome to develop methods for copper-catalyzed fluorination using inexpensive

nucleophilic fluoride sources to produce aryl fluorides. Further work is warranted in this field as the potential implications of such a methodology would be far-reaching.

4.8. Experimental Details and Characterization

4.8.1. General Information

NMR spectra were obtained on a 400 MHz (400.52 MHz for ^1H ; 376.87 MHz for ^{19}F ; 100.71 MHz for ^{13}C), a 500 MHz (500.01 MHz for ^1H ; 125.75 MHz for ^{13}C ; 470.56 MHz for ^{19}F), a 700 MHz (699.76 MHz for ^1H ; 175.95 MHz for ^{13}C), or a 500 MHz (499.90 MHz for ^1H ; 125.70 for ^{13}C) NMR spectrometer. ^1H and ^{13}C chemical shifts are reported in parts per million (ppm) relative to residual solvent peaks (CDCl_3 ; ^1H δ 7.26 ppm; ^{13}C δ 77.16 ppm). ^{19}F NMR spectra are referenced based on the internal standard 1,3,5-trifluorobenzene, which appears at -108.33 ppm, or 4-fluoroanisole, which appears at -125.55 ppm. Multiplicities are reported as follows: singlet (s), doublet (d), triplet (t), quartet (q), multiplet (m), doublet of doublets (dd), doublet of triplets (dt). Coupling constants (J) are reported in Hz. For GCMS analysis, the products were separated on a crossbond 5% diphenyl-95% dimethyl polysiloxane column (30 m length by 0.25 mm ID, 0.25 μm df). Helium was employed as the carrier gas, with a constant column flow of 1.5 mL/min. The injector temperature was held constant at 250 $^\circ\text{C}$. The GC oven temperature program for low molecular weight compounds was as follows: 32 $^\circ\text{C}$ hold 5 min, ramp 15 $^\circ\text{C}/\text{min}$ to 250 $^\circ\text{C}$, and hold for 1.5 min. The GC oven temperature program for medium molecular weight compounds was as follows: 60 $^\circ\text{C}$, hold for 4 minutes, ramp 15 $^\circ\text{C}/\text{min}$ to 250 $^\circ\text{C}$. Melting points are uncorrected. High-resolution mass spectra were recorded on a Magnetic Sector mass spectrometer.

4.8.2. Materials and Methods

Commercial reagents were used as received unless otherwise noted. Boronic acids, potassium (4-fluorophenyl)trifluoroborate, potassium phenethyltrifluoroborate, potassium pyridine-4-trifluoroborate, and potassium pyridine-3-trifluoroborate were purchased from Frontier Scientific. Potassium 4-*tert*-butylphenyltrifluoroborate, spray dried potassium fluoride, anhydrous benzonitrile (PhCN), adiponitrile, diphenylacetylene, tetrakisacetonitrile copper (I) triflate ((MeCN) $_4\text{CuOTf}$), silver nitrate, methyl propiolate,

cerium (IV) sulfate, vanadium (V) oxide, iron (III) fluoride trihydrate, tetrabutylammonium hexafluorophosphate (NBu_4PF_6), tetrabutylammonium triflate (NBu_4OTf), tetrabutylammonium tetrafluoroborate (NBu_4BF_4), anhydrous tetramethylammonium fluoride (NMe_4F), 1,3-dimethyltetrahydropyrimidin-2(1*H*)-one (DMPU), pinacol, 2-bromoaniline, and benzoquinone were purchased from Sigma Aldrich. Potassium bifluoride, acetonitrile (anhydrous), silver (I) fluoride, silver (I) tosylate, *N,N*-dimethylformamide (DMF) (anhydrous), dimethyl sulfoxide (DMSO) (anhydrous), trimethylacetonitrile ($t\text{BuCN}$), acridine, triethylamine, phenanthroline, bathocuproine, 1,3,5-triethynylbenzene, *N*-bromosuccinimide, *N*-methyl-2-pyrrolidone (NMP), 1,3-diaminopropane, methoxylamine hydrochloride, and manganese (III) fluoride were purchased from Alfa Aesar. Methanol, acetone, sodium fluoride, sodium iodide, acetic anhydride, toluene, pyridine, hexanes, ethyl acetate, pentane, diethyl ether, dichloromethane, and hydrogen peroxide (30%) were purchased from Fisher Scientific. Silver (I) tetrafluoroborate and triflic anhydride were purchased from Oakwood Chemicals. Copper (II) triflate, copper (II) fluoride, silver (I) triflate, silver (I) hexafluorophosphate, silver (I) bis(trifluoromethanesulfonyl)imide, tetrakisacetonitrile copper (I) hexafluorophosphate ($(\text{MeCN})_4\text{CuPF}_6$), copper (I) iodide, and cerium (IV) fluoride were purchased from Strem. Cesium fluoride was purchased from Chemetall. Silver (I) hexafluoroantimonate, propionitrile (EtCN), *isobutyronitrile* ($i\text{PrCN}$), 2,2'-bipyridine, *N,N,N',N'*-tetramethylethylenediamine (TMEDA), 3-hexyne, phenylacetylene, 2-butyne-1-ol, *N*-chlorosuccinimide, dioxane, 2-chloroaniline, and sodium nitrate were purchased from Acros. 3-Decyn-1-ol, 2-chlorobenzaldehyde, and benzo[*h*]quinoline were purchased from TCI America. Palladium (II) acetate was purchased from Pressure Chemicals. 2-Bromobenzaldehyde was purchased from Chem Imprex International.

Aryl trifluoroborates were synthesized according to the literature procedure³⁸ and dried under vacuum over P_2O_5 prior to use. Aryl boronate esters were synthesized per the literature procedure.³ $(t\text{BuCN})_4\text{CuOTf}$ was synthesized according to the literature procedure.⁹ 10-Chlorobenzo[*h*]quinoline and 10-bromobenzo[*h*]quinoline were synthesized according to the literature procedure.³⁹ Benzo[*h*]quinolin-10-yl trifluoromethanesulfonate was synthesized per the literature procedure.⁴⁰ 10-Iodobenzo[*h*]quinoline was synthesized according to the literature procedure from 10-

bromobenzo[*h*]quinoline.⁴¹ Oxime ethers were synthesized according to the literature procedure.⁴² *N*-(2-Halophenyl)acetamides were synthesized according to the literature procedure.⁴³

Silica gel (6A, 40–63 μm particle size) for flash chromatography was purchased from Silicycle. Diatomaceous earth was purchased from Aqua Solutions. Magnesium sulfate (anhydrous, powder) was purchased from Avantor Performance Materials. Thin layer chromatography (TLC) was performed on Macherey-Nagel GmbH & Co. pre-coated TLC-plates SIL G-25 UV₂₅₄ (0.25 mm silica gel with fluorescent indicator UV₂₅₄).

4.8.3. General Procedure for Copper-Mediated and -Catalyzed Fluorination

Experimental Details for Copper and Fluoride Screen in Table 4.1. In a drybox, substrate **1** (5.1 mg, 0.025 mmol, 1.0 equiv), copper salt (0.1 mmol, 4.0 equiv), and MF (0.1 mmol, 4.0 equiv) were weighed into a 4 mL vial. CH₃CN (0.3 mL) was added, and the vial was sealed with a Teflon-lined cap. The reaction mixture was stirred at 60 °C for 20 h. The resulting solution was cooled to room temperature and diluted with CH₃CN (1.0 mL). 1,3,5-Trifluorobenzene was added as an internal standard, and the crude reaction was analyzed by ¹⁹F NMR spectroscopy.

Experimental Details for the Reaction Profiles with Different Metal Fluorides Reported in Figure 4.1. In a drybox, substrate **1** (5.1 mg, 0.025 mmol, 1.0 equiv), Cu(OTf)₂ (36.2 mg, 0.1 mmol, 4.0 equiv), and MF (0.1 mmol, 4.0 equiv) were weighed into a 4 mL vial. CH₃CN (0.3 mL) was added, and the vial was sealed with a Teflon-lined cap. The reaction mixture was stirred at 60 °C for the given time. The resulting solution was cooled to room temperature and diluted with CH₃CN (1.0 mL). 1,3,5-Trifluorobenzene was added as an internal standard, and the crude reaction was analyzed by ¹⁹F NMR spectroscopy.

Experimental Details for the Reaction Profiles at Different Temperatures Reported in Figure 4.2. In a drybox, substrate **1** (5.1 mg, 0.025 mmol, 1.0 equiv), Cu(OTf)₂ (36.2 mg, 0.1 mmol, 4.0 equiv), and KF (5.8 mg, 0.1 mmol, 4.0 equiv) were weighed into a 4 mL vial. CH₃CN (0.3 mL) was added, and the vial was sealed with a Teflon-lined cap. The reaction mixture was stirred at the given temperature for the given time. The resulting

solution was cooled to room temperature and diluted with CH₃CN (1.0 mL). 1,3,5-Trifluorobenzene was added as an internal standard, and the crude reaction was analyzed by ¹⁹F NMR spectroscopy.

Experimental Details for the Copper Screen in Table 4.2. Synthesis of Cu^{II} salts with noncoordinating anions:¹⁸ In a drybox, CuCl₂ (1.0 mmol, 1.0 equiv) and AgX (4.0 mmol, 4.0 equiv) were combined in a 4 mL vial equipped with a magnetic stir bar. CH₃CN (0.5 mL) was added and the reaction was stirred at room temperature overnight. The resulting solution was filtered through a plug of Celite to remove AgCl. The reaction solution was concentrated and dried under vacuum at 80 °C for 8 h. When using these synthesized copper salts in fluorination reactions, the molecular weight of the complexes was determined by taking into account the presence of 2 equiv of unreacted AgX. The presence of AgX was determined to not be detrimental to the reaction. Accounting for excess AgX, the reactions were more reproducible.

For the fluorination reactions: In a drybox, substrate **1** (5.1 mg, 0.025 mmol, 1.0 equiv), copper salt (0.1 mmol, 4.0 equiv), and KF (5.8 mg, 0.1 mmol, 4.0 equiv) were weighed into a 4 mL vial. CH₃CN (0.3 mL) was added, and the vial was sealed with a Teflon-lined cap. The reaction mixture was stirred at 60 °C for 20 h. The resulting solution was cooled to room temperature and diluted with CH₃CN (1.0 mL). 1,3,5-Trifluorobenzene was added as an internal standard, and the crude reaction was analyzed by ¹⁹F NMR spectroscopy. For the reaction with Cu(SbF₆)₂, the reaction mixture was separated between water and pentane prior to ¹⁹F NMR spectroscopic analysis because the Sb–F peaks overlap with the starting material and products.

Experimental Details for the Solvent Screen in Table 4.3. In a drybox, substrate **1** (5.1 mg, 0.025 mmol, 1.0 equiv), Cu(OTf)₂ (36.2 mg, 0.1 mmol, 4.0 equiv), and KF (5.8 mg, 0.1 mmol, 4.0 equiv) were weighed into a 4 mL vial. Solvent (0.3 mL) was added, and the vial was sealed with a Teflon-lined cap. The reaction mixture was stirred at 60 °C for 20 h. The resulting solution was cooled to room temperature and diluted with CH₃CN (1.0 mL). 1,3,5-Trifluorobenzene was added as an internal standard, and the crude reaction was analyzed by ¹⁹F NMR spectroscopy and GCMS.

Experimental Details for the Ligand Screen in Figures 4.3 and 4.4. In a drybox, substrate **1** (5.1 mg, 0.025 mmol, 1.0 equiv), Cu(OTf)₂ (36.2 mg, 0.1 mmol, 4.0 equiv), KF (5.8 mg, 0.1 mmol, 4.0 equiv), and ligand (0.005-0.1 mmol, 20–400 mol %) were weighed into a 4 mL vial. CH₃CN (0.3 mL) was added, and the vial was sealed with a Teflon-lined cap. The reaction mixture was stirred at 60 °C for 20 h. The resulting solution was cooled to room temperature and diluted with CH₃CN (1.0 mL). 1,3,5-Trifluorobenzene was added as an internal standard, and the crude reaction was analyzed by ¹⁹F NMR spectroscopy and GCMS.

Experimental Details for the Studies of the Effect of Ambient Conditions in Table 4.4. In a drybox, substrate **1** (101.0 mg, 0.5 mmol, 1.0 equiv), Cu(OTf)₂ (723.4 mg, 2.0 mmol, 4.0 equiv), and KF (116.2 mg, 2.0 mmol, 4.0 equiv) were weighed into a 20 mL vial. CH₃CN (6.0 mL) was added, and the vial was sealed with a rubber septum. The reaction vials were taken out of the drybox. Through the rubber septum, water (2.5–5.0 mmol, 5–10 equiv) and/or oxygen (via balloon) were added. Very quickly, the rubber septum was removed, and the vial was resealed with a Teflon-lined cap. The reaction mixture stirred at 60 °C for 20 h. The resulting solution was cooled to room temperature and diluted with CH₃CN (3.0 mL). 1,3,5-Trifluorobenzene was added as an internal standard, and the reaction was analyzed by ¹⁹F NMR spectroscopy and GCMS.

General Procedure for Yields Reported in Figure 4.5. Unless otherwise noted, in a drybox, Cu(OTf)₂ (723.4 mg, 2.0 mmol, 4.0 equiv), KF (116.2 mg, 2.0 mmol, 4.0 equiv), and aryl trifluoroborate (0.5 mmol, 1 equiv) were weighed into a 20 mL vial equipped with a magnetic stir bar. CH₃CN (6.0 mL) was added, and the reaction vial was sealed with a Teflon-lined cap, removed from the drybox and stirred at 60 °C for 20 h. The resulting solution was cooled to room temperature and diluted with CH₃CN (3.0 mL). 1,3,5-Trifluorobenzene was added as an internal standard, and the reaction was analyzed by ¹⁹F NMR spectroscopy and GCMS. For isolated products, the reaction mixture was diluted with diethyl ether (10 mL), and the resulting mixture was washed with water (15 mL x 2) and then dried over MgSO₄. The solvent was removed by rotary evaporation at 0 °C, and

the product was purified by column chromatography on silica gel using gradients of pentane/diethyl ether.

Procedure for Fluorination of Potassium Phenethyltrifluoroborate in Scheme 4.6. In a drybox, Cu(OTf)₂ (36.1 mg, 0.1 mmol, 4.0 equiv), KF (5.8 mg, 0.1 mmol, 4.0 equiv), and potassium phenethyltrifluoroborate (5.3 mg, 0.025 mmol, 1.0 equiv) were weighed into a 4 mL vial equipped with a magnetic stir bar. CH₃CN (0.3 mL) was added, and the vial was sealed with a Teflon-lined cap, removed from the drybox, and stirred at 60 °C for 20 h. The resulting solution was cooled to room temperature and diluted with CH₃CN (1.0 mL). 1,3,5-Trifluorobenzene was added as an internal standard, and the crude reaction was analyzed by ¹⁹F NMR spectroscopy and GCMS. The product was obtained in 6% yield as determined by ¹⁹F NMR spectroscopic analysis of the crude reaction mixture. The product showed a ¹⁹F NMR signals at –217.0 (1F) ppm in CH₃CN (lit. –216.0 (1F) ppm in CH₂Cl₂).⁴⁴

Experimental Details for the Oxidant Screen in Table 4.5. In a drybox, substrate **1** (5.1 mg, 0.025 mmol, 1.0 equiv), Cu(OTf)₂ (18.1 mg, 0.05 mmol, 2.0 equiv), KF (5.8 mg, 0.1 mmol, 4.0 equiv), and oxidant (0.05 mmol, 2.0 equiv) were weighed into a 4 mL vial. CH₃CN (0.3 mL) was added, and the vial was sealed with a Teflon-lined cap. The reaction mixture was stirred at 60 °C for 20 h. The resulting solution was cooled to room temperature and diluted with CH₃CN (1.0 mL). 1,3,5-Trifluorobenzene was added as an internal standard, and the crude reaction was analyzed by ¹⁹F NMR spectroscopy and GCMS.

Experimental Details for the Copper and Fluoride Screen in Table 4.6. In a drybox, substrate **38** (12.9 mg, 0.05 mmol, 1.0 equiv), [Cu] (0.01 mmol, 20 mol %), metal fluoride (0.1 mmol, 2.0 equiv), and NBu₄PF₆ (19.4 mg, 0.05 mmol, 1.0 equiv) were weighed into a 4 mL vial. CH₃CN (0.25 mL) was added, and the vial was sealed with a Teflon-lined cap. The reaction mixture was stirred at 120 °C for 16 h. The resulting solution was cooled to room temperature and diluted with CH₃CN (1.0 mL). 1,3,5-Trifluorobenzene was added

as an internal standard, and the crude reaction was analyzed by ^{19}F NMR spectroscopy and GCMS.

Experimental Details for the Solvent Screen in Table 4.7. In a drybox, substrate **38** (12.9 mg, 0.05 mmol, 1.0 equiv), $(\text{MeCN})_4\text{CuBF}_4$ (3.2 mg, 0.01 mmol, 20 mol %), and AgF (12.7 mg, 0.1 mmol, 2.0 equiv) were weighed into a 4 mL vial. Solvent (0.25 mL) was added, and the vial was sealed with a Teflon-lined cap. The reaction mixture was stirred at 120 °C for 16 h. The resulting solution was cooled to room temperature and diluted with CH_3CN (1.0 mL). 1,3,5-Trifluorobenzene was added as an internal standard, and the crude reaction was analyzed by ^{19}F NMR spectroscopy and GCMS.

A control reaction without $(\text{MeCN})_4\text{CuBF}_4$ was run under otherwise identical conditions for each solvent.

Experimental Details for the Copper and Additive Screen in Table 4.8. In a drybox, substrate **38** (12.9 mg, 0.05 mmol, 1.0 equiv), $[\text{Cu}]$ (0.01 mmol, 20 mol %), tetrabutylammonium salt (0.1 mmol, 2.0 equiv), and NMe_4F (9.3 mg, 0.1 mmol, 2.0 equiv) were weighed into a 4 mL vial. PhCN (0.25 mL) was added, and the vial was sealed with a Teflon-lined cap. The reaction mixture was stirred at 120 °C for 16 h. The resulting solution was cooled to room temperature and diluted with CH_3CN (1.0 mL). 1,3,5-Trifluorobenzene was added as an internal standard, and the crude reaction was analyzed by ^{19}F NMR spectroscopy and GCMS.

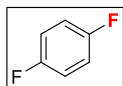
Experimental Details for the Optimized Reaction Conditions in Scheme 4.9. In a drybox, substrate **38** (12.9 mg, 0.05 mmol, 1.0 equiv), $(\text{MeCN})_4\text{CuBF}_4$ (3.2 mg, 0.01 mmol, 20 mol%), NBu_4BF_4 (32.9 mg, 0.1 mmol, 2.0 equiv) and NMe_4F (9.3 mg, 0.1 mmol, 2.0 equiv) were weighed into a 4 mL vial. PhCN (0.25 mL) was added, and the vial was sealed with a Teflon-lined cap. The reaction mixture was stirred at 120 °C for 16 h. The resulting solution was cooled to room temperature and diluted with CH_3CN (1.0 mL). 1,3,5-Trifluorobenzene was added as an internal standard, and the crude reaction was analyzed by ^{19}F NMR spectroscopy and GCMS.

Experimental Details for the Cu-Catalyzed Fluorination of Aryl Halides in Table 4.9. In a drybox, substrate (0.05 mmol, 1.0 equiv), (MeCN)₄CuBF₄ (3.2 mg, 0.01 mmol, 20 mol%), NBu₄BF₄ (32.9 mg, 0.1 mmol, 2.0 equiv), and MF (0.1 mmol, 2.0 equiv) were weighed into a 4 mL vial. PhCN (0.25 mL) was added, and the vial was sealed with a Teflon-lined cap. The reaction mixture was stirred at 120 °C for 16 h. The resulting solution was cooled to room temperature and diluted with CH₃CN (1.0 mL). 1,3,5-Trifluorobenzene was added as an internal standard, and the crude reaction was analyzed by ¹⁹F NMR spectroscopy and GCMS.

Experimental Details for the Substrate Scope in Scheme 4.10. In a drybox, substrate (0.05 mmol, 1.0 equiv), (MeCN)₄CuBF₄ (3.2 mg, 0.01 mmol, 20 mol%), NBu₄BF₄ (32.9 mg, 0.1 mmol, 2.0 equiv), and NMe₄F (9.3 mg, 0.1 mmol, 2.0 equiv) were weighed into a 4 mL vial. PhCN (0.25 mL) was added, and the vial was sealed with a Teflon-lined cap. The reaction mixture was stirred at 120 °C for 16 h. The resulting solution was cooled to room temperature and diluted with CH₃CN (1.0 mL). 1,3,5-Trifluorobenzene was added as an internal standard, and the crude reaction was analyzed by ¹⁹F NMR spectroscopy and GCMS.

Experimental Details for the Cu-Mediated Fluorination of Aryl Boronate Esters in Figure 4.8. In a drybox, substrate (0.025 mmol, 1.0 equiv), Cu(OTf)₂ (36.1 mg, 0.05 mmol, 2.0 equiv), and KF (5.8 mg, 0.1 mmol, 4.0 equiv) were weighed into a 4 mL vial. CH₃CN (0.3 mL) was added, and the vial was sealed with a Teflon-lined cap. The reaction mixture was stirred at 60 °C for 20 h. The resulting solution was cooled to room temperature and diluted with CH₃CN (1.0 mL). 1,3,5-Trifluorobenzene was added as an internal standard, and the crude reaction was analyzed by ¹⁹F NMR spectroscopy and GCMS.

4.8.4. Product Synthesis and Characterization

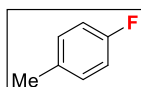


1,4-Difluorobenzene (**2**). The general procedure was followed using potassium (4-fluorophenyl)trifluoroborate (101.0 mg, 0.5 mmol, 1.0 equiv), providing **2** in 67% yield as

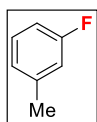
determined by ^{19}F NMR spectroscopic analysis of the crude reaction mixture. The ^{19}F NMR spectral data matched that of an authentic sample (Matrix, s, -120.26 ppm). The identity of the product was further confirmed by GCMS analysis ($m/z = 114$). The yield reported in Figure 4.5 represents a single run.



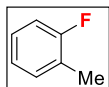
Fluorobenzene (**3**). The general procedure was followed using potassium phenyltrifluoroborate (92.0 mg, 0.5 mmol, 1.0 equiv), providing **3** in 56% yield as determined by ^{19}F NMR spectroscopic analysis of the crude reaction mixture. The ^{19}F NMR spectral data matched that of an authentic sample (Matrix, s, -113.99 ppm). The yield in reported Figure 4.5 represents a single run.



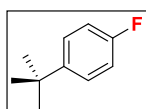
4-Fluorotoluene (**4**). The general procedure was followed using potassium (4-methylphenyl)trifluoroborate (99.0 mg, 0.5 mmol, 1.0 equiv), providing **4** in 49% yield as determined by ^{19}F NMR spectroscopic analysis of the crude reaction mixture. The ^{19}F NMR spectral data matched that of an authentic sample (Matrix, s, -119.40 ppm). The yield reported in Figure 4.5 represents a single run.



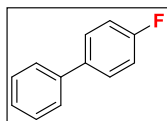
3-Fluorotoluene (**5**). The general procedure was followed using potassium (3-methylphenyl)trifluoroborate (99.0 mg, 0.5 mmol, 1.0 equiv), providing **5** in 51% yield as determined by ^{19}F NMR spectroscopic analysis of the crude reaction mixture. The ^{19}F NMR spectral data matched that of an authentic sample (Matrix, s, -115.09 ppm). The yield reported in Figure 4.5 represents a single run.



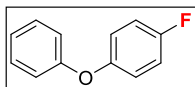
2-Fluorotoluene (**6**). The general procedure was followed using potassium (2-methylphenyl)trifluoroborate (99.0 mg, 0.5 mmol, 1.0 equiv), providing **6** in 42% yield as determined by ^{19}F NMR spectroscopic analysis of the crude reaction mixture. The ^{19}F NMR spectral data matched that of an authentic sample (Acros Organics, m, -118.63 ppm). The identity of the product was further confirmed by GCMS analysis ($m/z = 109$). The yield reported in Figure 4.5 (48%) represents an average of two runs [53% and 42%].



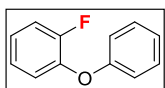
1-(*Tert*-butyl)-4-fluorobenzene (**7**). The general procedure was followed using potassium (4-*tert*-butylphenyl)trifluoroborate (120.0 mg, 0.5 mmol, 1.0 equiv), providing product **7** in 55% yield as determined by ^{19}F NMR spectroscopic analysis of the crude reaction mixture. The product showed a ^{19}F NMR signal at -120.30 ppm in CH_3CN (lit. -119.00 ppm in CDCl_3).⁴⁵ The identity of the product was further confirmed by GCMS analysis ($m/z = 152$). The yield reported in Figure 4.5 (55%) represents an average of two runs [55% and 54%].



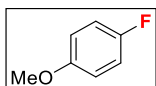
4-Fluoro-1,1'-biphenyl (**8**). The general procedure was followed using potassium trifluoro(4-phenylphenyl)borate (130.0 mg, 0.5 mmol, 1.0 equiv), providing **8** as a white crystalline solid (41.0 mg, 47% yield, $R_f = 0.35$ in pentane). The isolated product was 98% pure, and contained 2% of the corresponding protodeboronation byproduct, which was not easily separable by chromatography on silica gel. ^1H , $^{13}\text{C}\{^1\text{H}\}$, and ^{19}F NMR spectroscopic data were identical to that reported previously in the literature.⁴⁶ HRMS EI (m/z): $[\text{M}]^+$ calcd for $\text{C}_{12}\text{H}_9\text{F}$, 172.0688; measured, 172.0689. The isolated yield reported in Figure 4.5 (48%) represents an average of two runs [47% and 49%].



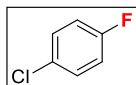
4-Phenoxyfluorobenzene (**9**). The general procedure was followed using potassium trifluoro(4-phenoxyphenyl)borate (138.0 mg, 0.5 mmol, 1 equiv), providing **9** as a colorless liquid (46.0 mg, 49% yield, $R_f = 0.25$ in pentane). The isolated product was 98% pure, and contained 2% of the corresponding protodeboronation byproduct, which was not easily separable by chromatography on silica gel. ^1H , $^{13}\text{C}\{^1\text{H}\}$, and ^{19}F NMR spectroscopic data were identical to that reported previously in the literature.⁴⁷ HRMS EI (m/z): $[\text{M}]^+$ calcd for $\text{C}_{12}\text{H}_9\text{FO}$, 188.0637; measured, 188.0630. The isolated yield reported in Figure 4.5 (45%) represents an average of two runs [49% and 41%].



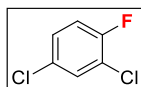
2-Phenoxyfluorobenzene (**10**). The general procedure was followed using potassium trifluoro(2-phenoxyphenyl)borate (138.0 mg, 0.5 mmol, 1 equiv), providing **10** as a colorless oil (66.0 mg, 70% yield, $R_f = 0.48$ in pentane). The isolated product was 97% pure, and contained 3% of the corresponding protodeboronation byproduct, which was not easily separable by chromatography on silica gel. ^1H , $^{13}\text{C}\{^1\text{H}\}$, and ^{19}F NMR spectroscopic data were identical to that reported previously in the literature.⁴⁸ HRMS EI (m/z): $[\text{M}]^+$ calcd for $\text{C}_{12}\text{H}_9\text{FO}$, 188.0637; measured, 188.0631. The isolated yield reported in Figure 4.5 (66%) represents an average of two runs [70% and 62%].



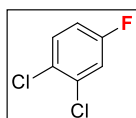
4-Fluoroanisole (**11**). The general procedure was followed using potassium (4-methoxyphenyl)trifluoroborate (107.0 mg, 0.5 mmol, 1.0 equiv), providing none of the desired product as determined by ^{19}F NMR spectroscopic analysis and GCMS.



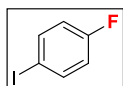
4-Fluoro-1-chlorobenzene (**12**). The general procedure was followed using potassium (4-chlorophenyl)trifluoroborate (109.0 mg, 0.5 mmol, 1.0 equiv), providing **12** in 73% yield as determined by ^{19}F NMR spectroscopic analysis of the crude reaction mixture. The ^{19}F NMR spectral data matched that of an authentic sample (Oakwood Products, m, -116.83 ppm). The identity of the product was further confirmed by GCMS analysis ($m/z = 130$). 1,4-Dichlorobenzene was also observed as a side product. The yield reported in Figure 4.5 (70%) represents an average of two runs [73% and 66%].



2,4-Dichloro-1-fluorobenzene (**13**). The general procedure was followed using potassium (2,4-dichlorophenyl)trifluoroborate (126.0 mg, 0.5 mmol, 1.0 equiv), providing **13** in 69% yield as determined by ^{19}F NMR spectroscopic analysis of the crude reaction mixture. The product showed a ^{19}F NMR signal at -118.8 ppm in CH_3CN (lit. -117.6 ppm in CDCl_3).⁴⁹ The yield reported in Figure 4.5 represents a single run.

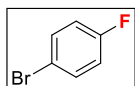


3,4-Dichloro-1-fluorobenzene (**14**). The general procedure was followed using potassium (3,4-dichlorophenyl)trifluoroborate (126.0 mg, 0.5 mmol, 1.0 equiv), providing **14** in 65% yield as determined by ^{19}F NMR spectroscopic analysis of the crude reaction mixture. The ^{19}F NMR spectral data matched that of an authentic sample (Oakwood Products, s, -113.82 ppm). The identity of the product was further confirmed by GCMS analysis ($m/z = 164$). The yield reported in Figure 4.5 represents a single run.

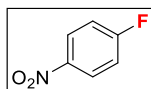


1-Fluoro-4-iodobenzene (**15**). The general procedure was followed using potassium (4-iodophenyl)trifluoroborate (155.0 mg, 0.5 mmol, 1.0 equiv), providing **15** in 61% yield as

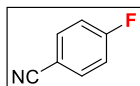
determined by ^{19}F NMR spectroscopic analysis of the crude reaction mixture. The ^{19}F NMR spectral data matched that of an authentic sample (Oakwood Products, s, -115.27 ppm). The identity of the product was further confirmed by GCMS analysis ($m/z = 222$). 1,4-Diiodobenzene was observed as a side product by GCMS. The yield reported in Figure 4.5 represents an average of two runs [61% and 66%].



1-Bromo-4-fluorobenzene (**16**). The general procedure was followed using potassium (4-bromophenyl)trifluoroborate (131.0 mg, 0.5 mmol, 1.0 equiv), providing **16** in 61% yield as determined by ^{19}F NMR spectroscopic analysis of the crude reaction mixture. The ^{19}F NMR spectral data matched that of an authentic sample (Alfa Aesar, s, -116.06 ppm). The identity of the product was further confirmed by GCMS analysis ($m/z = 174$). 1,4-Dibromobenzene was observed as a side product by GCMS. The yield reported in Figure 4.5 represents a single run.

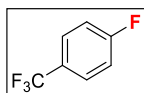


4-Fluoro-1-nitrobenzene (**17**). The general procedure was followed using potassium (4-nitrophenyl)trifluoroborate (114.5 mg, 0.5 mmol, 1.0 equiv), providing **17** as a light-yellow oil (46.0 mg, 65% yield, $R_f = 0.53$ in 3% diethyl ether in pentane). The isolated product was 97% pure, and contained 3% of the corresponding protodeboronation byproduct, which was not easily separable by chromatography on silica gel. ^1H , $^{13}\text{C}\{^1\text{H}\}$, and ^{19}F NMR spectroscopic data were identical to that of an authentic sample (Sigma Aldrich). HRMS EI (m/z): $[\text{M}]^+$ calcd for $\text{C}_6\text{H}_4\text{FNO}_2$, 141.0226; measured, 141.0226. The isolated yield reported in Figure 4.5 (65%) represents an average of two runs [65% and 65%].

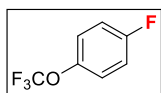


4-Fluorobenzonitrile (**18**). The general procedure was followed using potassium (4-cyanophenyl)trifluoroborate (104.5 mg, 0.5 mmol, 1.0 equiv), providing **18** as a white

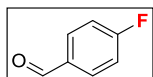
crystalline solid (42.0 mg, 69% yield, mp = 32.1–33.0 °C, R_f = 0.37 in 3% diethyl ether in pentane). ^1H , $^{13}\text{C}\{^1\text{H}\}$, and ^{19}F NMR spectroscopic data were identical to that reported previously in the literature.⁵⁰ HRMS EI (m/z): $[\text{M}]^+$ calcd for $\text{C}_7\text{H}_4\text{FN}$, 121.0328; measured, 121.0328. The isolated yield reported in Figure 4.5 (63%) represents an average of two runs [69% and 57%].



4-Fluorobenzotrifluoride (**19**). The general procedure was followed using potassium (4-trifluoromethylphenyl)trifluoroborate (126.0 mg, 0.5 mmol, 1.0 equiv), providing **19** in 78% yield as determined by ^{19}F NMR spectroscopic analysis of the crude reaction mixture. The ^{19}F NMR spectral data matched that of an authentic sample (Oakwood Products, 61.82 (3F), –108.77 (1F) ppm). The yield reported in Figure 4.5 represents a single run.

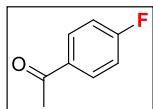


4-(Trifluoromethoxy)-1-fluorobenzene (**20**). The general procedure was followed using potassium (4-(trifluoromethoxy)phenyl)trifluoroborate (134.0 mg, 0.5 mmol, 1.0 equiv), providing **20** in 74% yield as determined by ^{19}F NMR spectroscopic analysis of the crude reaction mixture. The ^{19}F NMR spectral data matched that of an authentic sample (Oakwood Products, s, 3F, –58.94 ppm; m, 1F, –116.16 ppm). The identity of the product was further confirmed by GCMS analysis (m/z = 180). The yield reported in Figure 4.5 (71%) represents an average of two runs [74% and 68%].

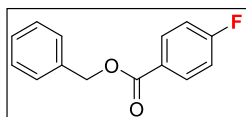


4-Fluorobenzaldehyde (**21**). The general procedure was followed using potassium (4-formylphenyl)trifluoroborate (106.0 mg, 0.5 mmol, 1 equiv), providing **21** as a colorless oil (38.0 mg, 61% yield, R_f = 0.19 in 2% diethyl ether in pentane). ^1H , $^{13}\text{C}\{^1\text{H}\}$, and ^{19}F NMR spectroscopic data were identical to that reported previously in the literature.⁵¹ HRMS EI

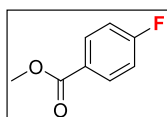
(*m/z*): [M]⁺ calcd for C₇H₅FO, 124.0324; measured, 124.0322. The isolated yield reported in Figure 4.5 (57%) represents an average of two runs [61% and 53%].



4-Fluoroacetophenone (**22**). The general procedure was followed using potassium (4-acetylphenyl)trifluoroborate (113.0 mg, 0.5 mmol, 1 equiv), providing **22** as a colorless oil (42.0 mg, 61% yield, *R*_f = 0.25 in 5% diethyl ether in pentane). ¹H, ¹³C{¹H}, and ¹⁹F NMR spectroscopic data were identical to that reported previously in the literature.⁵² HRMS EI (*m/z*): [M]⁺ calcd for C₈H₇FO, 138.0481; measured, 138.0481. The isolated yield reported in Figure 4.5 (60%) represents an average of two runs [61% and 59%].

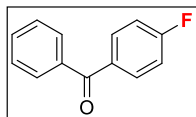


Benzyl 4-fluorobenzoate (**23**). The general procedure was followed using potassium (4-benzyloxycarbonylphenyl)-trifluoroborate (159.0 mg, 0.5 mmol, 1.0 equiv), providing **23** as a colorless oil (79.0 mg, 69% yield, *R*_f = 0.16 in 2% diethyl ether in pentane). ¹H and ¹³C{¹H} NMR spectroscopic data were identical to that reported previously in the literature.⁵³ ¹⁹F NMR (376 MHz, CDCl₃): δ -105.56 (m, 1F). HRMS EI (*m/z*): [M]⁺ calcd for C₁₄H₁₁FO₂, 230.0743; measured, 230.0744. The isolated yield reported in Figure 4.5 (68%) represents an average of two runs [69% and 67%].

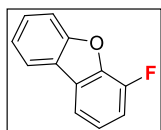


Methyl 4-fluorobenzoate (**24**). The general procedure was followed using potassium (4-methoxycarbonylphenyl)trifluoroborate (121.0 mg, 0.5 mmol, 1.0 equiv), providing **24** as a colorless oil (39.8 mg, 52%, *R*_f = 0.25 in pentane). The isolated product was 98% pure, and contained 2% of the corresponding protodeboronation byproduct, which was not easily separable by chromatography on silica gel. ¹H and ¹⁹F NMR spectroscopic data

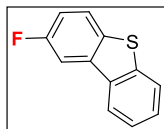
were identical to that reported previously in the literature.⁵¹ The yield reported in Figure 4.5 represents a single run.



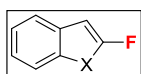
4-Fluorobenzophenone (**25**). The general procedure was followed using potassium (4-benzoylphenyl)trifluoroborate (144.0 mg, 0.5 mmol, 1.0 equiv), providing **25** as a white crystalline solid (67.0 mg, 67% yield, R_f = 0.30 in 2% diethyl ether in pentane). The isolated product was 97% pure, and contained 3% of the corresponding protodeboronation byproduct, which was not easily separable by chromatography on silica gel. ^1H , $^{13}\text{C}\{^1\text{H}\}$, and ^{19}F NMR spectroscopic data were identical to that reported previously in the literature.⁴⁶ HRMS EI (m/z): $[\text{M}]^+$ calcd for $\text{C}_{13}\text{H}_9\text{FO}$, 200.0637; measured, 200.0640. The isolated yield reported in Figure 4.5 (66%) represents an average of two runs [67% and 65%].



4-Fluorodibenzo[*b,d*]furan (**26**). The general procedure was followed using potassium dibenzofuran-4-trifluoroborate (138.0 mg, 0.5 mmol, 1.0 equiv), providing **26** as a white solid (65.0 mg, 70% yield, mp = 52.4–53.3 °C, R_f = 0.60 in pentane). ^1H NMR (600 MHz, CDCl_3): δ 7.95 (d, J = 7.7 Hz, 1H), 7.72 (d, J = 7.7 Hz, 1H), 7.63 (d, J = 8.4 Hz, 1H), 7.51 (dd, J = 7.7, 7.7 Hz, 1H), 7.38 (dd, J = 7.7, 7.7 Hz, 1H), 7.27 (ddd, J = 7.7, 7.7, 4.3 Hz, 1H), 7.21 (dd, J = 10.5, 8.4 Hz, 1H). ^{13}C NMR (176 MHz, CDCl_3): δ 156.59, 148.39 (d, J = 249.4 Hz), 143.12 (d, J = 11.5 Hz), 127.97, 127.89 (d, J = 3.1 Hz), 123.95 (d, J = 2.6 Hz), 123.44 (d, J = 6.0 Hz), 123.35, 121.05, 116.28 (d, J = 3.7 Hz), 113.68 (d, J = 16.5 Hz), 112.18. ^{19}F NMR (376 MHz, CDCl_3): δ -136.75 (m, 1F). HRMS EI (m/z): $[\text{M}]^+$ calcd for $\text{C}_{12}\text{H}_7\text{FO}$, 186.0481; measured, 186.0483. The isolated yield reported in Figure 4.5 (67%) represents an average of two runs [70% and 64%].

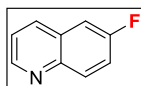


2-Fluorodibenzo[*b,d*]thiophene (**27**). The general procedure was followed using potassium dibenzothiophene-2-trifluoroborate (145.0 mg, 0.5 mmol, 1.0 equiv), providing **27** in 19% yield as determined by ^{19}F NMR spectroscopic analysis of the crude reaction mixture (s, -104.1 ppm). The identity of the product was not confirmed by GCMS. The yield reported in Figure 4.5 represents a single run.



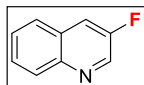
2-Fluorobenzofuran (X = O) (**28**). The general procedure was followed using potassium benzofuran-2-trifluoroborate (5.6 mg, 0.025 mmol, 1.0 equiv), $\text{Cu}(\text{OTf})_2$ (36.1 mg, 0.1 mmol, 4.0 equiv), and KF (5.8 mg, 0.1 mmol, 4.0 equiv) in CH_3CN (0.3 mL). None of the desired fluorinated product was observed by ^{19}F NMR spectroscopic analysis of the crude reaction mixture.

2-Fluorobenzothiophene (X = S) (**28**). The general procedure was followed using potassium benzothiophene-2-trifluoroborate (6.0 mg, 0.025 mmol, 1.0 equiv), $\text{Cu}(\text{OTf})_2$ (36.1 mg, 0.1 mmol, 4.0 equiv), and KF (5.8 mg, 0.1 mmol, 4.0 equiv) in CH_3CN (0.3 mL). None of the desired fluorinated product was observed by ^{19}F NMR spectroscopic analysis of the crude reaction mixture.

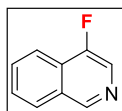


6-Fluoroquinoline (**29**). The general procedure was followed using potassium quinoline-6-trifluoroborate (117.5 mg, 0.5 mmol, 1.0 equiv). After diluting with CH_3CN at the end of the reaction time, poly(4-vinylpyridine) (1.0 g) was added to the reaction mixture, and the suspension was stirred at room temperature for 12 h. After work up, **29** was obtained as a colorless oil (29.0 mg, 39% yield, $R_f = 0.31$ in 40% diethyl ether in pentane). ^1H , $^{13}\text{C}\{^1\text{H}\}$, and ^{19}F NMR spectroscopic data were identical to that reported previously in the literature.⁵⁴ HRMS ESI⁺ (m/z): $[\text{M}+\text{H}]^+$ calcd for $\text{C}_9\text{H}_6\text{FN}$, 148.0557; measured, 148.0555.

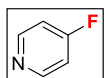
The isolated yield reported in Figure 4.5 (36%) represents an average of two runs [39% and 33%].



3-Fluoroquinoline (**30**). The general procedure was followed using potassium quinolin-3-trifluoroborate (5.9 mg, 0.025 mmol, 1.0 equiv), Cu(OTf)₂ (36.1 mg, 0.1 mmol, 4.0 equiv), and KF (5.8 mg, 0.1 mmol, 4.0 equiv) in CH₃CN (0.3 mL). After diluting with CH₃CN at the end of the reaction time, poly(4-vinylpyridine) (150.0 mg) was added to the reaction mixture and the suspension was stirred at room temperature for 12 h. Product **30** was observed in 10% yield as determined by ¹⁹F NMR spectroscopic analysis of the crude reaction mixture (−129.2 ppm, d, 1F). The identity of the product was further confirmed by GCMS analysis (*m/z* = 147). The yield reported in Figure 4.5 represents a single run.

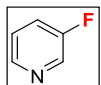


4-Fluoroisoquinoline (**31**). The general procedure was followed using potassium isoquinolin-4-trifluoroborate (5.9 mg, 0.025 mmol, 1.0 equiv), Cu(OTf)₂ (36.1 mg, 0.1 mmol, 4.0 equiv), and KF (5.8 mg, 0.1 mmol, 4.0 equiv) in CH₃CN (0.3 mL). After diluting with CH₃CN at the end of the reaction time, poly(4-vinylpyridine) (150.0 mg) was added to the reaction mixture and the suspension was stirred at room temperature for 12 h. No product was observed by ¹⁹F NMR spectroscopic analysis of the crude reaction mixture.

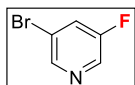


4-Fluoropyridine (**32**). The general procedure was followed using potassium pyridine-4-trifluoroborate (92.0 mg, 0.5 mmol, 1.0 equiv). After diluting with CH₃CN at the end of the reaction time, poly(4-vinylpyridine) (1.0 mg) was added to the reaction mixture and the suspension was stirred at room temperature for 12 h. After work up, **32** was formed in 24% yield as determined by ¹⁹F NMR spectroscopic analysis of the crude reaction mixture. The product showed a ¹⁹F NMR signal at −104.11 ppm in CH₃CN (lit. −106.2

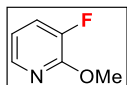
ppm in CDCl₃).⁴⁶ The identity of the product was further confirmed by GCMS analysis ($m/z = 97$). The yield reported in Figure 4.5 (21%) represents an average of two runs [24% and 18%].



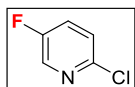
3-Fluoropyridine (**33**). The general procedure was followed using potassium pyridine-3-trifluoroborate (4.6 mg, 0.025 mmol, 1.0 equiv), Cu(OTf)₂ (36.1 mg, 0.1 mmol, 4.0 equiv), and KF (5.8 mg, 0.1 mmol, 4.0 equiv) in CH₃CN (0.3 mL). After diluting with CH₃CN at the end of the reaction time, poly(4-vinylpyridine) (150.0 mg) was added to the reaction mixture and the suspension was stirred at room temperature for 12 h. Product **33** was observed in 6% yield as determined by ¹⁹F NMR spectroscopic analysis of the crude reaction mixture. The ¹⁹F NMR spectral data matched that of an authentic sample (Oakwood Products, s, −127.45 ppm). The identity of the product was further confirmed by GCMS analysis ($m/z = 97$). The yield reported in Figure 4.5 represents a single run.



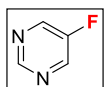
3-Bromo-5-fluoropyridine (**34**). The general procedure was followed using potassium (5-bromo-3-pyridinyl)trifluoroborate (6.6 mg, 0.025 mmol, 1.0 equiv), Cu(OTf)₂ (36.1 mg, 0.1 mmol, 4.0 equiv), and KF (5.8 mg, 0.1 mmol, 4.0 equiv) in CH₃CN (0.3 mL). After diluting with CH₃CN at the end of the reaction time, poly(4-vinylpyridine) (150.0 mg) was added to the reaction mixture and the suspension was stirred at room temperature for 12 h. Product **34** was observed in 3% yield as determined by ¹⁹F NMR spectroscopic analysis of the crude reaction mixture (−124.66 ppm, d, 1F). The identity of the product was further confirmed by GCMS analysis ($m/z = 175$). The yield reported in Figure 4.5 represents a single run.



3-Fluoro-2-methoxypyridine (**35**). The general procedure was followed using potassium (2-methoxy-3-pyridinyl)trifluoroborate (5.4 mg, 0.025 mmol, 1.0 equiv), Cu(OTf)₂ (36.1 mg, 0.1 mmol, 4.0 equiv), and KF (5.8 mg, 0.1 mmol, 4.0 equiv) in CH₃CN (0.3 mL). After diluting with CH₃CN at the end of the reaction time, poly(4-vinylpyridine) (150.0 mg) was added to the reaction mixture and the suspension was stirred at room temperature for 12 h. No product was observed by ¹⁹F NMR spectroscopic analysis of the crude reaction mixture.



2-Chloro-5-fluoropyridine (**36**). The general procedure was followed using potassium (2-chloro-5-pyridinyl)trifluoroborate (5.5 mg, 0.025 mmol, 1.0 equiv), Cu(OTf)₂ (36.1 mg, 0.1 mmol, 4.0 equiv), and KF (5.8 mg, 0.1 mmol, 4.0 equiv) in CH₃CN (0.3 mL). After diluting with CH₃CN at the end of the reaction time, poly(4-vinylpyridine) (150.0 mg) was added to the reaction mixture and the suspension was stirred at room temperature for 12 h. No product was observed by ¹⁹F NMR spectroscopic analysis of the crude reaction mixture.



5-Fluoropyrimidine (**37**). The general procedure was followed using potassium (5-pyrimidinyl)trifluoroborate (4.7 mg, 0.025 mmol, 1.0 equiv), Cu(OTf)₂ (36.1 mg, 0.1 mmol, 4.0 equiv), and KF (5.8 mg, 0.1 mmol, 4.0 equiv) in CH₃CN (0.3 mL). After diluting with CH₃CN at the end of the reaction time, poly(4-vinylpyridine) (150.0 mg) was added to the reaction mixture and the suspension was stirred at room temperature for 12 h. No product was observed by ¹⁹F NMR spectroscopic analysis of the crude reaction mixture.

4.9. References

- (1) A portion of this chapter has been adapted with permission from Ye, Y.; Schimler, S. D.; Hanley, P. S.; Sanford, M. S. *J. Am. Chem. Soc.* **2013**, *135*, 16292–16295. © American Chemical Society
- (2) Ye, Y.; Sanford, M. S. *J. Am. Chem. Soc.* **2013**, *135*, 4648–4651.
- (3) Fier, P. S.; Luo, J.; Hartwig, J. F. *J. Am. Chem. Soc.* **2013**, *135*, 2552–2559.
- (4) Based on the largest available quantity from Sigma Aldrich, 1-fluoro-2,4,6-trimethylpyridinium triflate (NFTPT) is \$34,854.63/mol and Selectfluor is \$1,030.90/mol (March 14, 2017).
- (5) Ametamey, S. M.; Honer, M.; Schubiger, P. A. *Chem. Rev.* **2008**, *108*, 1501–1516.
- (6) (a) Bergman, J.; Solin, O. *Nucl. Med. Biol.* **1997**, *24*, 677–683. (b) Campbell, M. G.; Ritter, T. *Chem. Rev.* **2015**, *115*, 612–633
- (7) Casitas, A.; Canta, M.; Solà, M.; Ribas, X. *J. Am. Chem. Soc.* **2011**, *133*, 19386–19392.
- (8) Yao, B.; Wang, Z.-L.; Zhang, H.; Wang, D.-X.; Zhao, L.; Wang, M.-X. *J. Org. Chem.* **2012**, *77*, 3336–3340.
- (9) Fier, P. S.; Hartwig, J. F. *J. Am. Chem. Soc.* **2012**, *134*, 10795–10798.
- (10) Based on the largest available quantity from Sigma Aldrich, silver (I) fluoride ($\geq 99.9\%$, trace metals basis) is \$2,440.98/mol (March 14, 2017).
- (11) Subramanian, M. A.; Manzer, L. E. *Science*, **2002**, *297*, 1665.
- (12) Grushin, V. V. Process for preparing fluoroarenes from haloarenes. US Patent 7202388, April 10, 2007.
- (13) Truong, T.; Klimovica, K.; Daugulis, O. *J. Am. Chem. Soc.* **2013**, *135*, 9342–9345.
- (14) Mu, X.; Zhang, H.; Chen, P.; Liu, G. *Chem. Sci.* **2014**, *5*, 275–280.
- (15) (a) Casitas, A.; Ribas, X. *Chem. Sci.* **2013**, *4*, 2301–2318. (b) Hickman, A. J.; Sanford, M. S. *Nature* **2012**, *484*, 177–185.
- (16) Based on the largest available quantity from Sigma Aldrich, potassium fluoride (ACS reagent, $\geq 99.0\%$) is \$4.33/mol (March 4, 2017).
- (17) Brooks, A. F.; Topczewski, J. J.; Ichiishi, N.; Sanford, M. S.; Scott, P. J. H. *Chem. Sci.* **2014**, *5*, 4545–4553.
- (18) Evans, D. A.; Murry, J. A.; von Matt, P.; Norcross, R. D.; Miller, S. J. *Angew. Chem. Int., Ed. Engl.* **1995**, *34*, 798–800.
- (19) Olah, G. A.; Prakash, G. K. S.; Sommer, J.; Molnar, A. *Superacid Chemistry*. John Wiley & Sons, Inc.: Hoboken, NJ, 2009.
- (20) (a) Morimoto, H.; Tsubogo, T.; Litvinas, N. D.; Hartwig, J. F. *Angew. Chem. Int. Ed.* **2011**, *50*, 3793–3798. (b) Liu, Y.; Chen, C.; Li, H.; Huang, K.-W.; Tan, J.; Weng, Z. *Organometallics* **2013**, *32*, 6587–6592.
- (21) TMEDA has been used as a ligand for CuF₂-catalyzed fluorination of aryl bromides and aryl iodides. See ref 12.
- (22) Winterheimer, D. J.; Merlic, C. A. *Org. Lett.* **2010**, *12*, 2508–2510.
- (23) Johnson, J. B.; Rovis, T. *Angew. Chem., Int. Ed.* **2008**, *47*, 840–871.
- (24) (a) Baker, M. V.; Brown, D. H.; Somers, N.; White, A. H. *Organometallics* **2001**, *20*, 2161–2166. (b) Lang, H.; Köhler, K.; Rheinwald, G.; Zsolnai, L.; Büchner, M.; Driess, A.; Huttner, G.; Stähle, J. *Organometallics* **1999**, *18*, 598–605.

- (25) Acetonitrile is unstable to anhydrous tetramethylammonium fluoride (NMe₄F): Christe, K. O.; Wilson, W. W.; Wilson, R. D.; Bau, R.; Feng, J. *J. Am. Chem. Soc.* **1990**, *112*, 7619–7625.
- (26) Adams, D. J.; Clark, J. H. *Chem. Soc. Rev.* **1999**, *28*, 225–231.
- (27) For the solubility of alkali metal fluorides in organic solvents: Wynn, D. A.; Roth, M. M.; Pollard, B. D. *Talanta* **1984**, *31*, 1036–1040.
- (28) (a) Monnier, F.; Taillefer, M. *Angew. Chem. Int. Ed.* **2009**, *48*, 6954–6971. (b) Beletskaya, I. P.; Cheprakov, A. V. *Coord. Chem. Rev.* **2004**, *248*, 2337–2364. (c) Ley, S. V.; Thomas, A. W. *Angew. Chem. Int. Ed.* **2003**, *42*, 5400–5449.
- (29) (a) Naidu, A. B.; Sekar, G. *Synthesis* **2010**, *4*, 579–586. (b) Saha, P.; Ramana, T.; Purkait, N.; Ali, M. A.; Paul, R.; Punniyamurthy, T. *J. Org. Chem.* **2009**, *74*, 8719–8725. (c) Evindar, G.; Batey, R. A. *J. Org. Chem.* **2006**, *71*, 1802–1808. (d) Wu, F.; Zhang, J.; Wei, Q.; Liu, P.; Xie, J.; Jiang, H.; Dai, B. *Org. Biomol. Chem.* **2014**, *12*, 9696–9701.
- (30) Ye, Y.; Schimmler, S. D.; Hanley, P. S.; Sanford, M. S. *J. Am. Chem. Soc.* **2013**, *135*, 16292–16295.
- (31) Gamache, R. F.; Waldmann, C.; Murphy, J. M. *Org. Lett.* **2016**, *18*, 4522–4525.
- (32) Tsangaris, J. M.; Williams, D. R. *Appl. Organomet. Chem.* **1992**, *6*, 3–18.
- (33) Tredwell, M.; Preshlock, S. M.; Taylor, N. J.; Gruber, S.; Huiban, M.; Passchier, J.; Mercier, J.; Génicot, C.; Gouverneur, V. *Angew. Chem. Int. Ed.* **2014**, *53*, 7751–7755.
- (34) (a) Garnett, E. S.; Firnau, G.; Chan, P. K. H.; Sood, S.; Belbeck, L. W. *Proc. Natl. Acad. Sci. U.S.A.* **1978**, *75*, 464–467. (b) Garnett, E. S.; Firnau, G.; Nahmias, C. *Nature* **1983**, *305*, 137–138.
- (35) Mossine, A. V.; Brooks, A. F.; Makaravage, K. J.; Miller, J. M.; Ichiishi, N.; Sanford, M. S.; Scott, P. J. H. *Org. Lett.* **2015**, *17*, 5780–5783.
- (36) (a) Hamill, T. G.; Krause, S.; Ryan, C.; Bonnefous, C.; Govek, S.; Seiders, T. J.; Cosford, N. D.; Roppe, J.; Kamenecka, T.; Patel, S.; Gibson, R. E.; Sanabria, S.; Riffel, K.; Eng, W.; King, C.; Yang, X.; Green, M. D.; O'Malley, S. S.; Hargreaves, R.; Burns, H. D. *Synapse* **2005**, *56*, 205–216. (b) Wang, J.-Q.; Tueckmantel, W.; Zhu, A.; Pellegrino, D.; Brownell, A.-L. *Synapse* **2007**, *61*, 951–961. (c) Lim, K.; Labaree, D.; Li, S.; Huang, Y. *Appl. Radiat. Isot.* **2014**, *94*, 349–354. (d) Liang, S. H.; Yokell, D. L.; Jackson, R. N.; Rice, P. A.; Callahan, R.; Johnson, K.; Alagille, D.; Tamagnan, G.; Collier, T. L.; Vasdev, N. *MedChemComm* **2014**, *5*, 432–435. (e) Stephenson, N. A.; Holland, J. P.; Kassenbrock, A.; Yokell, D. L.; Livni, E.; Liang, S. H.; Vasdev, N. *J. Nucl. Med.* **2015**, *56*, 489–492.
- (37) Makaravage, K. J.; Brooks, A. F.; Mossine, A. V.; Sanford, M. S.; Scott, P. J. H. *Org. Lett.* **2016**, *18*, 5440–5443.
- (38) (a) Vedejs, E.; Chapman, R. W.; Fields, S. C.; Lin, S.; Schrimpf, M. R. *J. Org. Chem.* **1995**, *60*, 3020–3027. (b) Molander, G. A.; Biolatto, B. *Org. Lett.* **2002**, *4*, 1867–1870.
- (39) Kalyani, D.; Dick, A. R.; Anani, W. Q.; Sanford, M. S. *Tetrahedron* **2006**, *62*, 11483–11498.
- (40) Szadkowska, A.; Gstrein, X.; Burtscher, D.; Jarzembska, K.; Woźniak, K.; Slugovc, C.; Grela, K. *Organometallics* **2010**, *29*, 117–124.
- (41) Klapars, A.; Buchwald, S. L. *J. Am. Chem. Soc.* **2002**, *124*, 14844–14845.

- (42) Booth, S. E.; Jenkins, P. R.; Swain, C. J.; Sweeney, J. B. *J. Chem. Soc., Perkins Trans. 1* **1994**, 3499–3508.
- (43) Cho, G. Y.; Rémy, P.; Jansson, J.; Moessner, C.; Bolm, C. *Org. Lett.* **2004**, 6, 3293–3296.
- (44) Weigert, F. J. *J. Org. Chem.* **1980**, 45, 3476–3483.
- (45) (a) Lothian, A. P.; Ramsden, C. A.; Shaw, M. M.; Smith, R. G. *Tetrahedron* **2011**, 67, 2788–2793. (b) Lohre, C.; Dröge, T.; Wang, C.; Glorius, F. *Chem. Eur. J.* **2011**, 17, 6052–6055.
- (46) Tang, P.; Wang, W.; Ritter, T. *J. Am. Chem. Soc.* **2011**, 133, 11482–11484.
- (47) Kim, H. J.; Kim, M.; Chang, S. *Org. Lett.* **2011**, 13, 2368–2371.
- (48) Jalalian, N.; Ishikawa, E. E.; Silva, L. F.; Olofsson, B. *Org. Lett.* **2011**, 13, 1552–1555.
- (49) Katircioglu, H.; Logoglu, E.; Tilki, T.; Oktemer, A. *Med. Chem. Res.* **2007**, 16, 205–212.
- (50) (a) Suzuki, Y.; Moriyama, K.; Togo, H. *Tetrahedron* **2011**, 67, 7956–7962. (b) Enthaler, S.; Weidauer, M. *Catal. Lett.* **2011**, 141, 1079–1085.
- (51) Furuya, T.; Ritter, T. *Org. Lett.* **2009**, 11, 2860–2863.
- (52) Tang, P.; Ritter, T. *Tetrahedron* **2011**, 67, 4449–4454.
- (53) Zhao, J.; Mück-Lichtenfeld, C.; Studer, A. *Adv. Synth. Catal.* **2013**, 355, 1098–1106.
- (54) Watson, D. A.; Su, M.; Teverovskiy, G.; Zhang, Y.; García-Fortanet, J.; Kinzel, T.; Buchwald, S. L. *Science* **2009**, 325, 1661–1664.

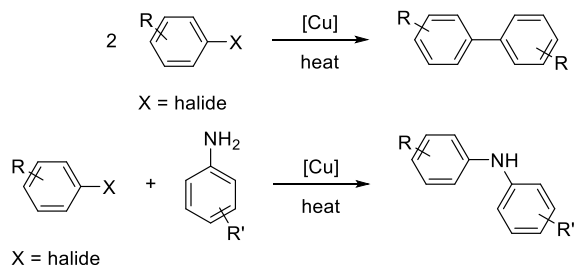
CHAPTER 5

Copper-Mediated Functionalization of Aryl Trifluoroborates¹

5.1. Background

Coupling reactions utilizing copper as the transition metal mediator have emerged in recent years as efficient and less expensive alternatives to palladium-catalyzed cross coupling reactions.^{2,3} Traditional copper-mediated cross coupling of aryl halides, such as Ullmann coupling reactions (Scheme 5.1), require high temperatures to achieve the desired transformation in low to modest yield.² Many times, the reactions are not tolerant of ambient conditions or require specialized nucleophiles to induce the desired transformations.

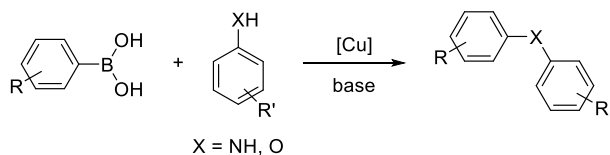
Scheme 5.1. Cu-Mediated Ullmann Coupling



Chan-Evans-Lam coupling, the coupling of an aryl boron reagent with nitrogen or oxygen nucleophiles, revolutionized the field, as it demonstrated the feasibility of using milder reaction conditions, achieving greater functional group tolerance, and accessing a wider variety of products beyond simple biaryls (Scheme 5.2).^{2,3,4} Despite progress in this field, there are still many limitations to current methods. Strong nucleophiles such as phenoxides and amines are often required, which limits the products that can be produced

by this coupling method. Furthermore, the use of heteroaryl boron nucleophiles is rare, and often these substrates are not generalized to a wide array of coupling partners.

Scheme 5.2. Chan-Lam-Evans Cu-Catalyzed Coupling Reaction



More recently, continued effort has been dedicated to developing milder, safer, and more general copper-mediated transformations starting from aryl halides and aryl boron reagents. Despite recent advances, there is not a unifying method by which one substrate can be functionalized using a variety of different nucleophiles, thus forming new C–O, C–N, and C–halide bonds, with the same copper precatalyst.⁵

Building on previous work in copper-mediated nucleophilic fluorination (Chapter 4), we sought to expand the scope of nucleophiles that could serve as coupling partners in Cu(OTf)₂-mediated functionalization of aryl trifluoroborates. In particular, a process that works for weaker nucleophiles (carboxylates, halides, sulfonates, and azides) and that proceeds under mild conditions with diverse (hetero)aryl boron partners was desired. The primary advantage of this methodology over previously reported methodologies is that the same copper salt (without any additives) can create C–O, C–N, and C–halide bonds in high yields from a common substrate (potassium aryl trifluoroborates) under identical conditions. Furthermore, the transformation uses readily available and inexpensive tetraalkylammonium and alkali metal salts and proceeds rapidly under mild reaction conditions. Such a method could be valuable for the assembly of a series of analogs in a combinatorial chemistry context.

In this chapter, the development, nucleophile scope, and substrate scope of a mild copper-mediated functionalization method of aryl trifluoroborates is discussed. Additionally, preliminary studies into the nature of the active copper species were conducted.

5.2. Reaction Optimization

Initial efforts focused on using $\text{Cu}(\text{OTf})_2$ to couple potassium (4-fluorophenyl)trifluoroborate (**1**) with potassium trifluoroacetate (KOTFA) to form ester **2** (Table 5.1). This transformation was chosen for initial screening due to the limited number of copper-mediated couplings of aryl boron reagents with carboxylate salts,^{6,7} particularly with weakly nucleophilic derivatives such as trifluoroacetate. Analogous conditions to the recently disclosed $\text{Cu}(\text{OTf})_2$ -mediated fluorination of aryl trifluoroborates⁸ were chosen as a starting point for reaction development. The combination of **1**, $\text{Cu}(\text{OTf})_2$ (4 equiv), and KOTFA (4 equiv) in CH_3CN under N_2 at 60 °C afforded ester **2** in 43% yield (Table 5.1, entry 1). When the reaction was set up on the benchtop rather than under inert conditions, a comparable yield of **2** (46%) was obtained (entry 2). Reducing the temperature to room temperature (25 °C) resulted in a significantly lower yield (18%, entry 3). However, when the coupling partner was switched to NaOTFA, the reaction proceeded to 51% yield of product **2** under otherwise analogous conditions (entry 4). There was a slight improvement in yield (55%) upon heating the reaction of **1** with NaOTFA to 60 °C (entry 5). When $\text{Cu}(\text{OTFA})_2$ was used as the nucleophilic source of $^-\text{OTFA}$, only 25% of the ester product **2** was observed, and no improvement was seen when elevated temperature was used (entry 6). As a control, when $\text{Cu}(\text{OTFA})_2$ was used in place of $\text{Cu}(\text{OTf})_2$ ($\text{Cu}(\text{OTFA})_2$ as both active copper species and $^-\text{OTFA}$ source), no product was observed at either 60 °C or 25 °C (entry 7).

Table 5.1. Copper-Mediated Trifluoroacetoxylation of **1** to Form **2**^a

entry	M	temperature (°C)	% yield 2 ^b
1 ^c	K	60	43
2	K	60	46
3	K	25	18
4	Na	25	51
5	Na	60	55
6	Cu	25	25
7 ^d	Cu	25 or 60	<1

^aConditions: Substrate **1** (0.025 mmol, 1.0 equiv), Cu(OTf)₂ (0.1 mmol, 4.0 equiv), and MOTFA (0.1 mmol, 4.0 equiv) in CH₃CN (0.083 M) for 16 h. Reactions were set up on the benchtop without the exclusion of air. ^bYields were determined by ¹⁹F NMR spectroscopy using 1,3,5-trifluorobenzene as standard. ^cReaction set up in N₂-filled drybox. ^dCu(OTf)₂ excluded from the reaction.

Most Chan-Lam-Evans copper-mediated and -catalyzed coupling reactions utilize aryl boronic acids as substrates.⁴ Under the optimized conditions (4 equiv Cu(OTf)₂, 4 equiv NaOTFA, CH₃CN (0.083 M) under ambient conditions for 16 h), several aryl boron reagents were examined for reactivity (Table 5.2). The corresponding aryl boronic acid afforded a similar yield to **1** under the optimized conditions (entry 2). Boronate esters and MIDA-protected boronate esters were poor substrates for this transformation (entries 3–4). For the rest of the studies, organotrifluoroborates were used as the substrate of choice due to the slightly higher yields and enhanced stability of these organoboron reagents.⁹

Table 5.2. Scope of Aryl Boron Reagents for Cu-Mediated Trifluoroacetoxylation^a

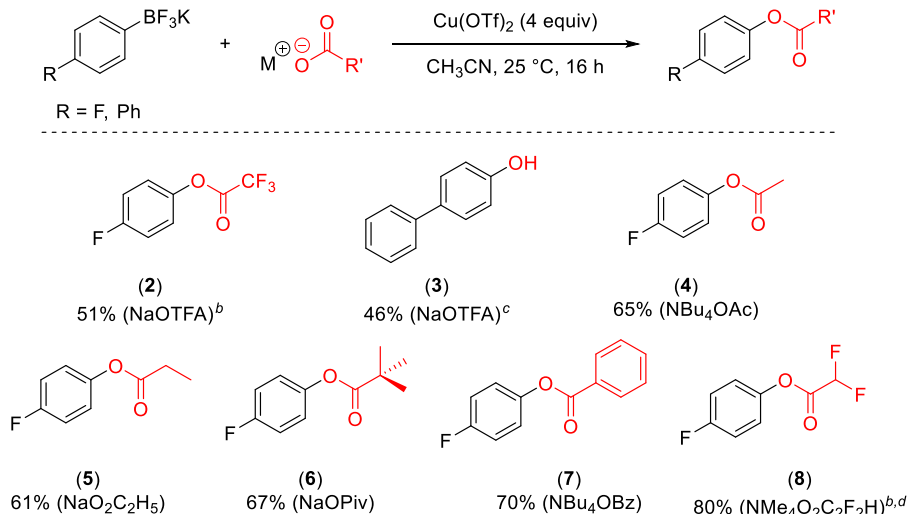
entry	substrate	% yield 2 ^b
1		51
2		50
3 ^c		2
4		<1

^aConditions: Aryl boron reagent (0.025 mmol, 1.0 equiv), Cu(OTf)₂ (0.1 mmol, 4.0 equiv), and NaOTFA (0.1 mmol, 4.0 equiv) in CH₃CN (0.083 M) at 25 °C for 16 h. ^bYields were determined by ¹⁹F NMR spectroscopy using 1,3,5-trifluorobenzene as standard. ^cKF (1.5 mg, 0.025 mmol, 1 equiv) was added to the reaction.

5.3. Nucleophile and Substrate Scope

The scope of carboxylate nucleophiles was next examined, using either potassium (4-fluorophenyl)trifluoroborate **1** or potassium (4-biphenyl)trifluoroborate as the aryl boron substrate (Figure 5.1). A variety of alkyl and aryl carboxylates participate in the Cu(OTf)₂-mediated coupling reaction, including acetate, propionate, pivalate, benzoate, and difluoroacetate salts (**4–8**). Importantly, when Cu(OAc)₂ was used in place of Cu(OTf)₂ with no excess acetate, none of the desired product **4** was observed. Trifluoroacetoxylated product **2** was not stable to work up conditions and underwent hydrolysis to 4-fluorophenol. Therefore, 4-trifluoroacetoxybiphenyl was synthesized and intentionally hydrolyzed to 4-phenylphenol for isolation. This procedure afforded the phenol in 46% yield over two steps. Overall, the mild conditions of the reaction (room temperature, no additives) compare favorably with previous reports of copper-mediated couplings between aryl/alkenyl boron reagents and carboxylate salts.⁶

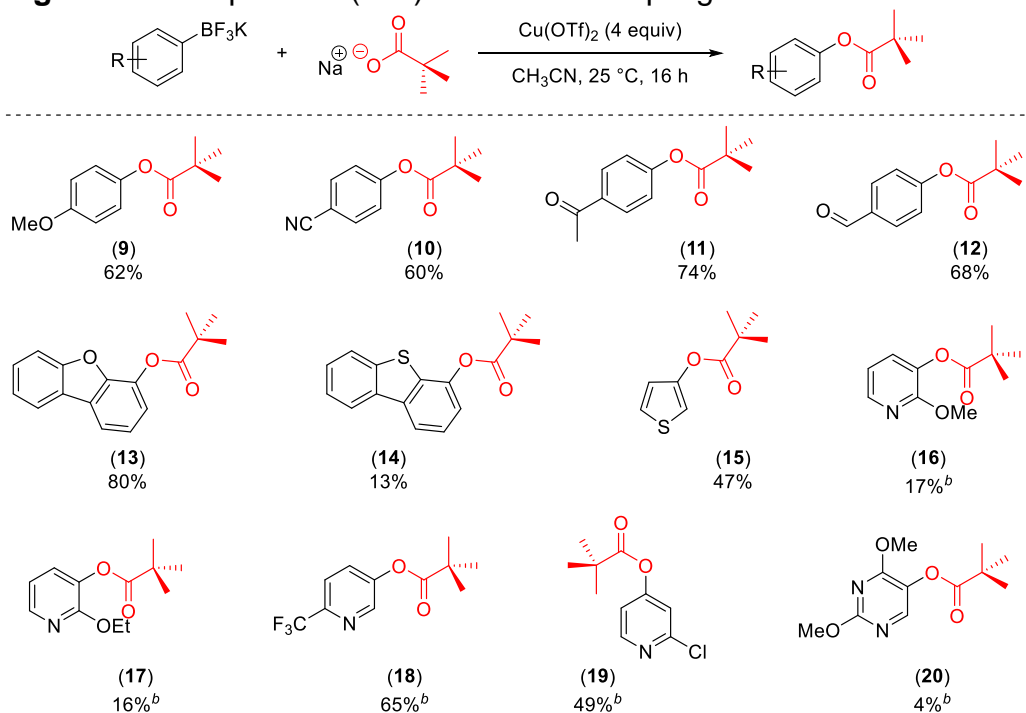
Figure 5.1. Scope of Cu(OTf)₂-Mediated Coupling with Carboxylate Nucleophiles^a



^aConditions: Potassium aryl trifluoroborate (0.5 mmol, 1.0 equiv), $Cu(OTf)_2$ (2.0 mmol, 4.0 equiv), and nucleophile (2.0 mmol, 4.0 equiv) in CH_3CN (0.083 M) at 25 °C for 16 h. Unless otherwise noted, isolated yields are reported. ^bYields were determined by ^{19}F NMR spectroscopy using 1,3,5-trifluorobenzene as standard. ^cProduct was obtained from hydrolysis of the trifluoroacetic ester. ^dReaction performed on 0.025 mmol scale.

Using NaOPiv as a representative carboxylate coupling partner, the $Cu(OTf)_2$ -mediated functionalization was demonstrated on a number of potassium (hetero)aryl trifluoroborates (Figure 5.2). Substrates bearing both electron-withdrawing and electron-donating substituents react to afford the corresponding ester in modest yields (**9–14**). Heteroaryl trifluoroborates are also compatible with the $Cu(OTf)_2$ -mediated reaction, although higher temperatures were generally required (60 °C), and the yields were modest in most cases (**15–20**). Pyridine substrates with electron-donating substituents afforded particularly low yields (**16**, **17**, and **20**), and unreacted potassium heteroaryl trifluoroborate starting material remained at the end of the reaction. Competing coordination of pyridine to the copper center may lead to reduced yields, as this would impede the productive reaction.

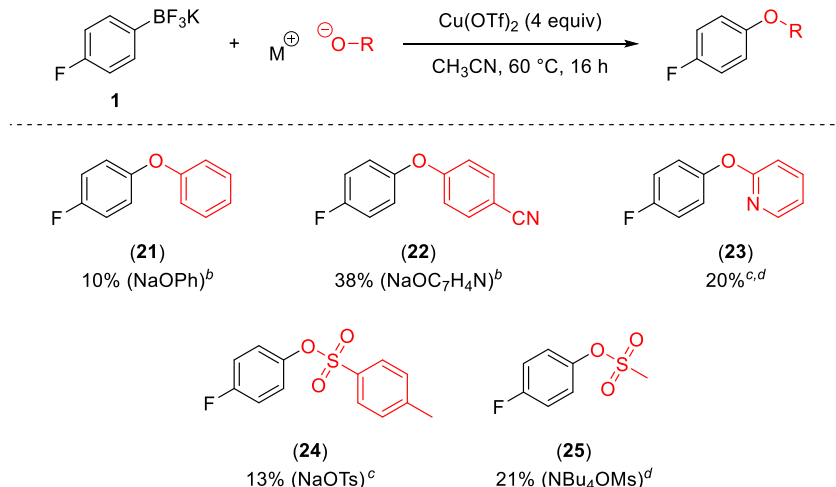
Figure 5.2. Scope of Cu(OTf)₂-Mediated Coupling with Sodium Pivalate^a



^aConditions: Potassium aryl trifluoroborate (0.5 mmol, 1.0 equiv), Cu(OTf)₂ (2.0 mmol, 4.0 equiv), and NaOPiv (2.0 mmol, 4.0 equiv) in CH₃CN (0.083 M) at 25 °C for 16 h. Isolated yields are reported. ^bReaction was performed at 60 °C.

Other oxygen-based nucleophiles were examined for Cu(OTf)₂-mediated coupling reaction with **1** (Figure 5.3). Phenoxides, common nucleophiles for Chan-Lam-Evans couplings,⁴ afforded low yields of product even at elevated temperatures (**21–23**). Furthermore, the sensitivity of these nucleophiles to water required the reactions to be set up under inert conditions. Importantly, when the corresponding phenols were used in these reactions (in the absence of base), none of the desired product was observed. Protodeborylation was prevalent when phenols were used in the copper-mediated coupling reactions. Weakly nucleophilic tosylate and mesylate undergo Cu(OTf)₂-mediated coupling with potassium (4-fluorophenyl)trifluoroborate **1** (**24–25**). The reaction with NaOTs afforded **24** in low yield and required elevated temperatures (60 °C). Despite the low yield, this is a rare example of the use of TsO⁻ as a nucleophile for a metal-mediated coupling.^{10,11} The reaction with NBu₄OMs afforded **25** in low yield, and no improvement in the reaction was observed at elevated temperatures.

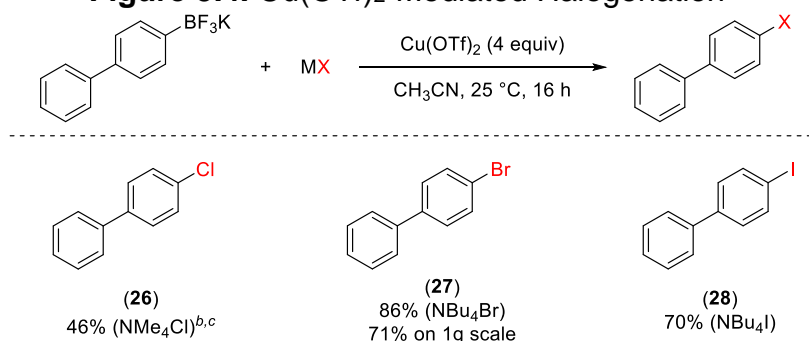
Figure 5.3. Scope of Oxygen Nucleophiles for Cu(OTf)₂-Mediated Coupling with **1**^a



^aConditions: Substrate **1** (0.025 mmol, 1.0 equiv), Cu(OTf)₂ (1.0 mmol, 4.0 equiv), and nucleophile (1.0 mmol, 4.0 equiv) in CH₃CN (0.083 M) at 60 °C for 16 h. Yields were determined by ¹⁹F NMR spectroscopy using 1,3,5-trifluorobenzene as standard. ^bReaction was set up in N₂-filled drybox. ^cReaction was performed on 0.5 mmol scale and isolated yield is reported. ^dReaction was performed at 25 °C.

The use of halide nucleophiles was next explored for the Cu(OTf)₂-mediated coupling of potassium (4-biphenyl)trifluoroborate (Figure 5.4). This substrate reacts with tetraalkylammonium halide salts under the standard conditions (4 equiv Cu(OTf)₂ and 4 equiv nucleophile in CH₃CN at room temperature for 16 h) to provide the corresponding bromo-,¹² iodo-,^{5,13} and chloroarene¹⁴ in modest to excellent yield (**26–28**). The chlorination reaction to form **26** was found to be moisture sensitive; therefore, this reaction was set up in an N₂-filled drybox. The reaction of potassium (4-biphenyl)trifluoroborate with NBu₄Br was conducted on a gram (3.9 mmol) scale, affording the brominated product **27** in 71% yield. Overall, these reaction conditions are milder than most previously reported examples of Cu-mediated halogenation of aryl boron reagents, which typically require temperatures ≥ 80 °C to achieve high yields.^{12,13,14} Hartwig and coworkers have previously reported the chlorination^{12g} and bromination^{12g} of aryl boronate esters using stoichiometric CuCl₂ and CuBr₂. When CuCl₂ and CuBr₂ were used in place of both Cu(OTf)₂ and exogenous nucleophile, **1** reacts with the copper salt to produce 33% of the chlorinated product and 65% of the brominated product, respectively, under the described conditions. Overall, the conditions described here offer higher yields when Cu(OTf)₂ and nucleophile are combined to give the desired products.

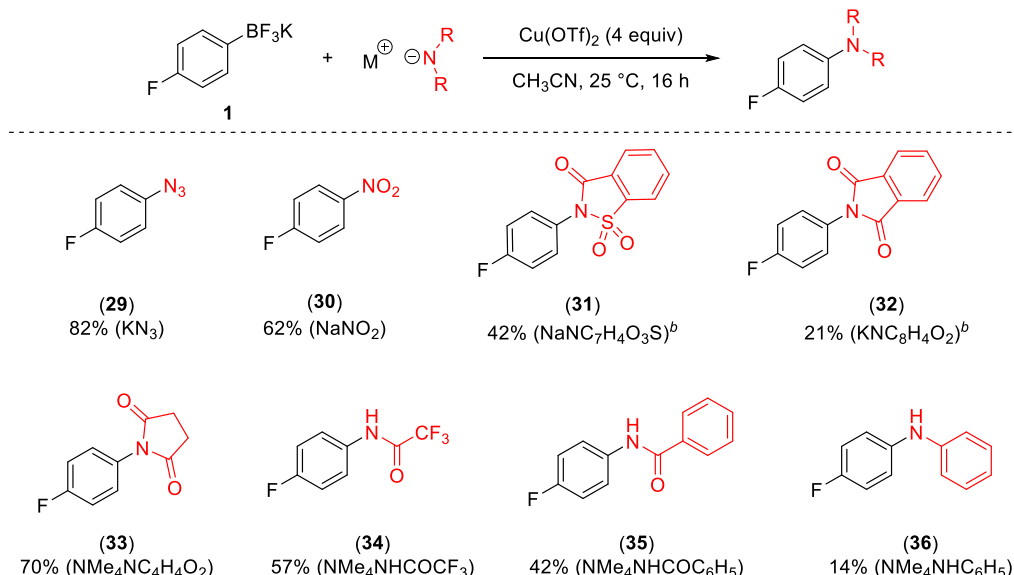
Figure 5.4. Cu(OTf)₂-Mediated Halogenation^a



^aConditions: Potassium aryl trifluoroborate (0.5 mmol, 1.0 equiv), Cu(OTf)₂ (2.0 mmol, 4.0 equiv), and nucleophile (2.0 mmol, 4.0 equiv) in CH₃CN (0.083 M) at 25 °C for 16 h. Isolated yields are reported. ^bReaction was performed at 60 °C. ^cReaction was set up in N₂-filled drybox.

Nitrogen nucleophiles were next examined as coupling partners for this Cu(OTf)₂-mediated reaction. Nitrogen nucleophiles such as amides, sulfamides, and anilines are common coupling partners for Chan-Lam-Evans reactions.^{2,3,4} Under the standard conditions, a variety of nitrogen nucleophiles provided coupled product in modest to good yields (Figure 5.5). Azidation with KN₃ proceeded efficiently under the standard conditions to afford **29** in good yield. NaN₃ provided lower yields of the desired product (58%). Nitration with NaNO₂ provided product **30** in modest yields; however, the reaction was not very clean and isolation of the desired product was challenging. Use of a sulfonamide nucleophile provided product **31** in low yield; again, a complex mixture was observed and isolation was challenging. Imide nucleophiles afforded modest to good yields of the C–N coupled product (**32–33**). Amide nucleophiles provided modest yields of the coupled product under the standard conditions (**34–35**). Reaction with an aniline salt provided low yields of product **36**. Overall, C–N coupling under the standard conditions provided only modest yields of the desired products. Furthermore, many of these reactions resulted in complex mixtures that made isolation of the desired product challenging. Often, a precipitate would form under the reaction conditions. It is believed that this precipitate is a Cu(Nuc)₂ complex that is insoluble in CH₃CN and ineffective for the coupling reaction.

Figure 5.5. Nitrogen Nucleophiles for the Cu(OTf)₂-Mediated Functionalization^a

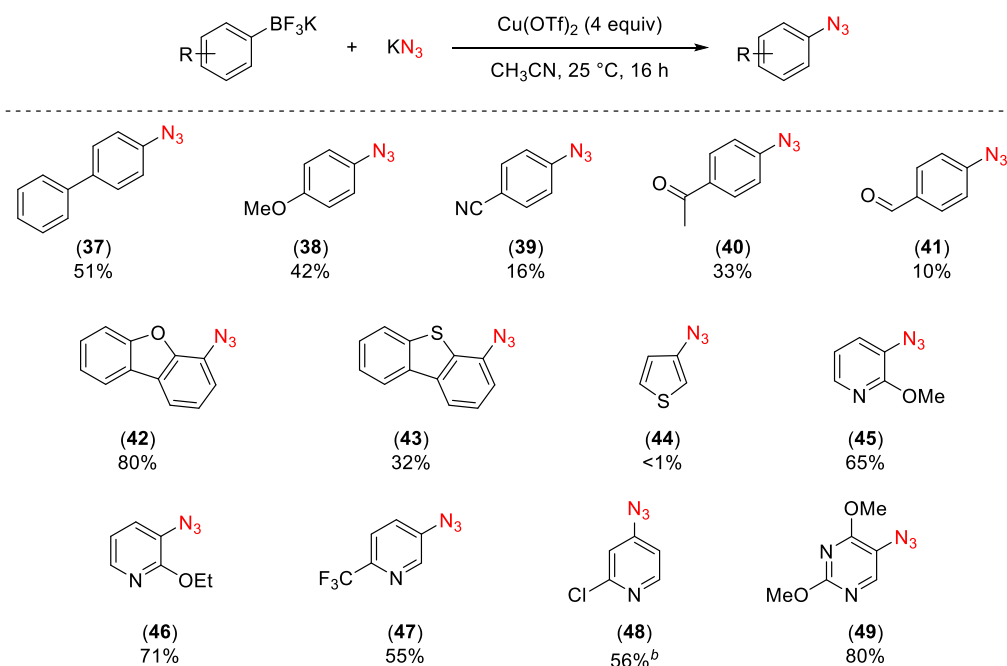


^aConditions: Substrate **1** (0.025 mmol, 1.0 equiv), Cu(OTf)₂ (1.0 mmol, 4.0 equiv), and nucleophile (1.0 mmol, 4.0 equiv) in CH₃CN (0.083 M) at 25 °C for 16 h. Yields were determined by ¹⁹F NMR spectroscopy using 1,3,5-trifluorobenzene as standard.

^bReaction was performed at 0.5 mmol scale and isolated yield is reported.

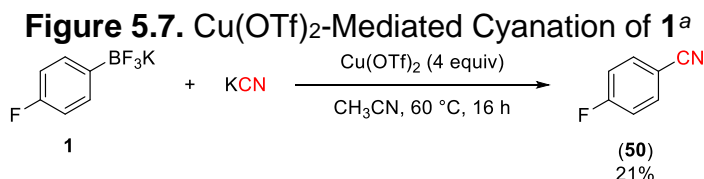
Potassium azide (KN₃) was pursued as a nucleophile to examine the substrate scope of this reaction. The aryl azide products are valuable as photoaffinity labels, substrates for Cu-catalyzed azide/alkyne cycloaddition, and as synthetic building blocks for other important transformations.¹⁵ Many existing methods for coupling aryl boron reagents and N₃⁻ suffer from the need for high reaction temperatures (>60 °C) or have limited applicability to heteroaryl substrates.¹⁶ The azidation proceeded efficiently under the standard reaction conditions (4 equiv of Cu(OTf)₂ and 4 equiv of nucleophile in CH₃CN at room temperature for 16 h) to afford a diverse array of (hetero)aryl azide products (Figure 5.6). Azidation of simple arene substrates provided modest yields of the desired products (**37–43**). Unlike the reaction with NaOPiv as the nucleophile (Figure 5.2), the reaction of potassium thiophene-3-trifluoroborate with KN₃ provided no detectable product **44**. Modest to good yields were obtained with pyridine and pyrimidine substrates bearing electron-withdrawing and electron-donating groups (**45–49**). This is in stark contrast to the corresponding carboxylation reactions with NaOPiv (Figure 5.2). It is hypothesized that the better coordinating ability of N₃⁻ versus RCO₂⁻ to copper may impede unproductive pyridine binding in this transformation.

Figure 5.6. Cu(OTf)₂-Mediated Azidation of (Hetero)Aryl Trifluoroborates^a



^aConditions: Potassium aryl trifluoroborate (0.5 mmol, 1.0 equiv), Cu(OTf)₂ (2.0 mmol, 4.0 equiv), and KN₃ (2.0 mmol, 4.0 equiv) in CH₃CN (0.083 M) at 25 °C for 16 h. Isolated yields are reported. ^bReaction was performed at 60 °C.

Carbon nucleophiles were also examined in this reaction. Sources of CF₃[−] (TMSCF₃ and TESCF₃) did not afford the trifluoromethylated product under the standard reaction conditions or at elevated temperatures. The use of KCN provided low yield (21%) of the desired product **50** when elevated temperatures (60 °C) were employed (Figure 5.7).



^aConditions: Substrate **1** (0.025 mmol, 1.0 equiv), Cu(OTf)₂ (1.0 mmol, 4.0 equiv), and KCN (1.0 mmol, 4.0 equiv) in CH₃CN (0.083 M) at 60 °C for 16 h. Yields were determined by ¹⁹F NMR spectroscopy using 1,3,5-trifluorobenzene as standard.

5.4. Mechanistic Considerations

To gain preliminary insight into the nature of the active Cu species in this Cu(OTf)₂-mediated coupling reaction, a series of different Cu^{II} salt mediators were examined (Table

5.3). These studies were explored for the reactions of both KN_3 and NaOPiv with potassium (4-fluorophenyl)trifluoroborate **1**. $\text{Cu}(\text{OTf})_2$ provided the highest yield in both the carboxylation and azidation reactions (82% and 80% respectively, entry 1). Significantly lower yields of product were obtained when $\text{Cu}(\text{OTf})_2$ was replaced with $\text{Cu}(\text{OMs})_2$ (entry 2), while $\text{Cu}(\text{OTs})_2$ afforded none of the desired product with either nucleophile (entry 3). With the use of these copper(II) salts, no incorporation of TsO^- or MsO^- was observed, and the mass balance of the reactions was unreacted starting material with traces of the protodeborylated product fluorobenzene. Cu^{II} salts with noncoordinating counterions (BF_4^- and NO_3^-) provided modest yields of both the azidation and pivalation products (entries 4–5). No functionalization was observed with the more coordinating sulfate (SO_4^{2-}) or acetate (AcO^-) Cu^{II} salts (entries 6–7). These data suggest that Cu^{II} salts with noncoordinating anions are important for the copper-mediated reaction and that lability of the counterion is imperative for the reactivity.

Table 5.3. Cu^{II} Salts for Azidation and Pivalation^a

Reaction scheme: Substrate **1** (4-fluorophenyl trifluoroborate potassium salt) reacts with $[\text{Cu}]$ (4 equiv) and KN_3 or NaOPiv (4 equiv) in CH_3CN at $25\text{ }^\circ\text{C}$ for 16 h to yield product **29** (X = N_3) or **6** (X = OPiv).

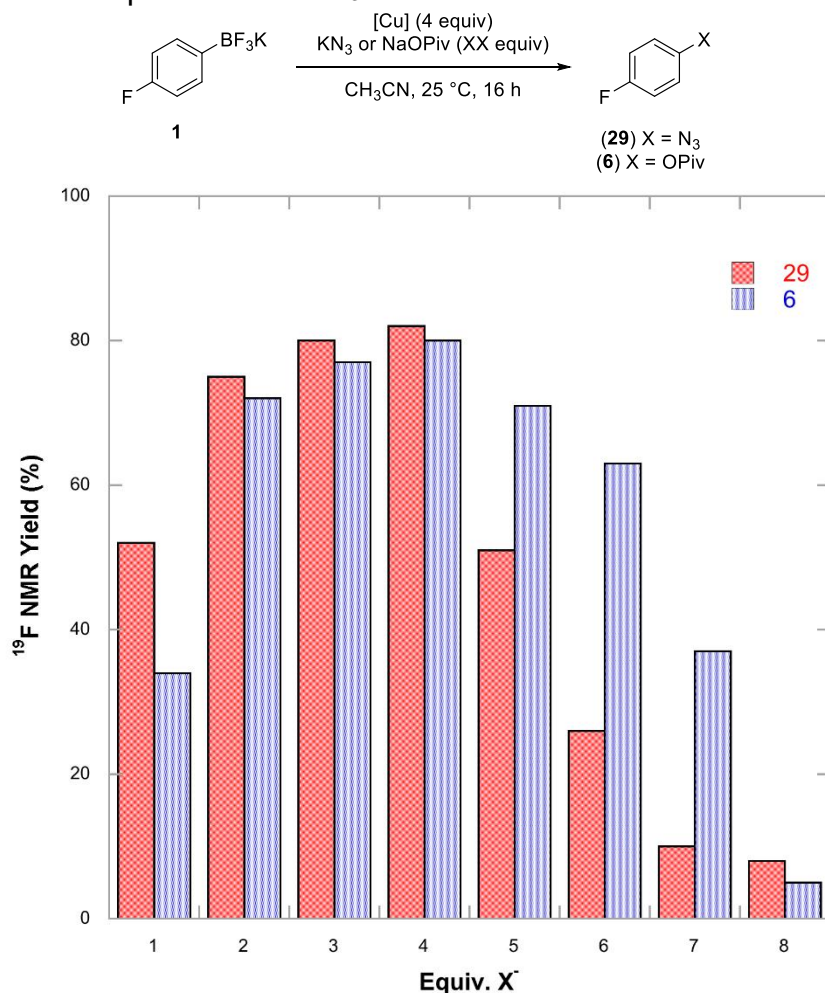
entry	$[\text{Cu}]$	% yield 29 ^b	% yield 6 ^b
1	$\text{Cu}(\text{OTf})_2$	82	80
2	$\text{Cu}(\text{OMs})_2$	11	28
3	$\text{Cu}(\text{OTs})_2$	<1	<1
4	$\text{Cu}(\text{NO}_3)_2$	52	35
5	$\text{Cu}(\text{BF}_4)_2$	40	61
6	CuSO_4	<1	<1
7	$\text{Cu}(\text{OAc})_2$	<1	<1

^aConditions: Substrate **1** (0.025 mmol, 1.0 equiv), $[\text{Cu}]$ (0.1 mmol, 4.0 equiv), and KN_3 or NaOPiv (0.1 mmol, 4.0 equiv) in CH_3CN (0.083 M) at $25\text{ }^\circ\text{C}$ for 16 h. ^bYields were determined by ^{19}F NMR spectroscopy using 1,3,5-trifluorobenzene as standard.

The effect of varying the amount of azide or pivalate nucleophile on the reaction of **1** and KN_3 or NaOPiv was next examined (Figure 5.8). For the reaction between **1** and KN_3 , the highest yield of product **29** was obtained with 4 equiv of KN_3 , which represents a 1:1 ratio of $\text{Cu}(\text{OTf})_2$ to N_3^- . Increasing the amount of KN_3 beyond 4 equiv had a detrimental effect on the reaction yield; with 8 equiv of KN_3 , the yield of **29** was <10% and

unreacted starting material remained at the end of the reaction. An analogous trend was seen when varying the amount of NaOPiv in the reaction (Figure 5.8). The maximum yield of **6** was observed with 4 equiv of NaOPiv, while <5% yield of **6** was observed with 8 equiv of NaOPiv. Additionally, if the reaction was performed with Cu(OPiv)₂ in place of Cu(OTf)₂, <14% yield of **6** was detected, with or without exogenous NaOPiv. It is hypothesized that the decrease in yield with excess nucleophile relative to Cu(OTf)₂ is due to the coordination of two nucleophiles as ligands to the Cu center, which reduces the reactivity of the Cu complex.

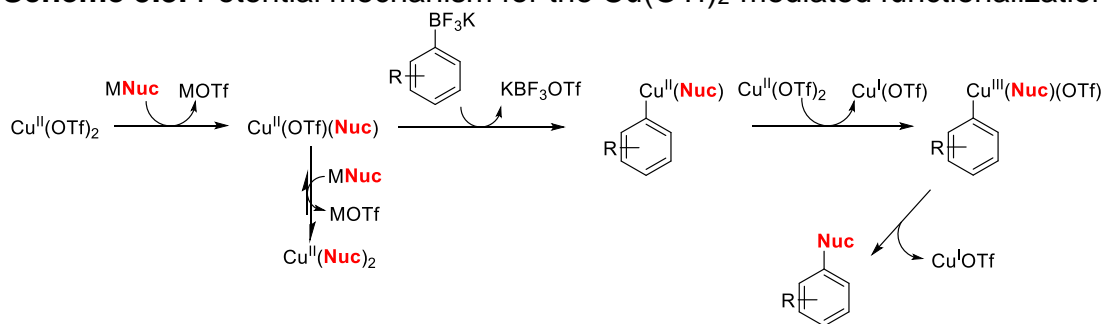
Figure 5.8. Equivalents of KN₃ and NaOPiv versus Yield of **29** and **6**^a



^aConditions: Substrate **1** (0.025 mmol, 1.0 equiv), Cu(OTf)₂ (0.1 mmol, 4.0 equiv), and KN₃ or NaOPiv (1.0–8.0 equiv) in CH₃CN (0.083 M) at 25 °C for 16 h. Yields were determined by ¹⁹F NMR spectroscopy using 1,3,5-trifluorobenzene as standard.

Given the above results regarding copper(II) sources and equivalents of nucleophile, it is hypothesized that Cu^{II} plays a dual role in the reaction: it acts as an oxidant to access a reactive Cu^{III} species and it serves as a promoter of the key C–Nuc coupling event (Scheme 5.3).¹⁷ The strongly electrophilic $\text{Cu}(\text{OTf})_2$ is hypothesized to be particularly important for the oxidation event. The addition of excess nucleophile is anticipated to deplete $\text{Cu}(\text{OTf})_2$ via ligand substitution, and thereby reduce the reactivity of the active Cu^{II} species. This proposal is consistent with the observation that low yields of product are observed when ≥ 8 equiv of nucleophile are used in the reaction. This stoichiometry should lead to essentially complete conversion of $\text{Cu}(\text{OTf})_2$ to $\text{Cu}(\text{Nuc})_2$ (Scheme 5.3).

Scheme 5.3. Potential mechanism for the $\text{Cu}(\text{OTf})_2$ -mediated functionalization



5.5. Conclusions and Outlook

This chapter demonstrates the $\text{Cu}(\text{OTf})_2$ -mediated functionalization of potassium (hetero)aryltrifluoroborates with various nucleophiles to form C–O, C–halide, and C–N bonds. This transformation enables the formation of diverse carbon-heteroatom bonds under an analogous set of conditions. These conditions are milder than most previous reports (room temperature) and do not require additives (base, ligand, etc.) to achieve high yields of the functionalized product. The use of superstoichiometric $\text{Cu}(\text{OTf})_2$ is critical for the success of the reaction. It is hypothesized that $\text{Cu}(\text{OTf})_2$ acts as both an oxidant and a mediator for the C–heteroatom coupling step. When copper(II) salts with coordinating anions (such as AcO^- and SO_4^{2-}) or excess nucleophile (>4 equiv) is used, the reaction is impeded, implicating the necessity of $\text{Cu}(\text{OTf})_2$ to be the active copper species in these transformations. More studies will be necessary to determine the

mechanism of this reaction, but preliminary investigations demonstrate the importance of the active Cu^{II} species.

The efficient and rapid derivatization of aromatic molecules into a variety of related analogues is common practice in medicinal chemistry,¹⁸ and it is anticipated that this transformation could provide valuable application in this regard. The utility of this reaction lies in the use of a single copper(II) source to induce the transformation under nearly identical conditions with a variety of nucleophiles. It overcomes shortcomings of previous examples in that the conditions are mild (potential to tolerate diverse functional groups) and do not require additives to induce the transformation. From a single starting material and copper source, one has the ability to obtain many different products.

5.6. Experimental Details and Characterization

5.6.1. General Procedures

NMR spectra were obtained on a Varian MR400 (400.52 MHz for ¹H; 376.87 MHz for ¹⁹F; 100.71 MHz for ¹³C), a Varian vnmrs 500 (500.01 MHz for ¹H; 125.75 MHz for ¹³C, and 470.56 MHz for ¹⁹F), a Varian vnmrs 700 (699.76 MHz for ¹H; 175.95 MHz for ¹³C), or a Varian Inova 500 (499.90 MHz for ¹H; 125.70 for ¹³C) spectrometer. ¹H and ¹³C chemical shifts are reported in parts per million (ppm) with the residual solvent peak used as an internal reference (CDCl₃: ¹H: δ = 7.26 ppm, ¹³C: δ = 77.16 ppm). ¹⁹F NMR spectra are referenced based on the internal standard 1,3,5-trifluorobenzene, which appears at –108.33 ppm. ¹H and ¹⁹F multiplicities are reported as follows: singlet (s), doublet (d), triplet (t), quartet (q), multiplet (m), doublet of doublets (dd), doublet of triplets (dt). Coupling constants (*J*) are reported in Hz. GCMS analysis was performed on a Shimadzu GCMS-QP2010 gas chromatograph mass spectrometer. The products were separated on a 30 m length by 0.25 mm id RESTEK XTI-5 column coated with a 0.25 μm film. Helium was employed as the carrier gas, with a constant column flow of 1.5 mL/min. The injector temperature was held constant at 250 °C. The GC oven temperature program was as follows: 32 °C hold 5 min, ramp 15 °C/min to 250 °C, and hold for 1.5 min. Melting points were determined with a Thomas Hoover Uni-Melt 6427-H10 capillary melting point apparatus and are uncorrected. High-resolution mass spectra were recorded on a Micromass AutoSpec Ultima Magnetic Sector mass spectrometer. Infrared spectroscopy

was performed on a Perkin-Elmer Spectrum BX FT-IR spectrometer, and peaks are reported in cm^{-1} .

5.6.2. Materials and Methods

Commercial reagents were used as received unless otherwise noted. Aryl trifluoroborate potassium salts were prepared using literature procedures.^{19,20} Aryl boronic acids were obtained from Frontier Scientific, Sigma Aldrich, or Boron Molecular. Potassium (4-fluorophenyl)trifluoroborate was purchased from Frontier Scientific. $\text{Cu}(\text{OTf})_2$ was obtained from Strem Chemicals, Oakwood Products, or TCI America. Anhydrous acetonitrile (CH_3CN) was obtained from Sigma Aldrich or Alfa Aesar. Ethyl acetate, hexanes, pentane, and diethyl ether for column chromatography were purchased from Fisher Scientific. 1,3,5-Trifluorobenzene, sodium trifluoroacetate (NaOTFA), and difluoroacetic acid were obtained from Oakwood Products. Tetrabutylammonium bromide (NBu_4Br), sodium tosylate (NaOTs), potassium azide (KN_3), potassium trifluoroacetate (KOTFA), pinacol, sodium hydroxide, lithium hydroxide, 2-hydroxypyridine, 4-cyanophenol, tetrabutylammonium methanesulfonate (NBu_4OMs), sodium nitrite (NaNO_2), trifluoroacetamide, benzamide, toluenesulfonic acid, and tetrabutylammonium benzoate (NBu_4OBz) were purchased from Sigma Aldrich. Tetrabutylammonium iodide (NBu_4I) was purchased from Eastman Chemical. Tetrabutylammonium acetate (NBu_4OAc) was purchased from TCI America, dried under vacuum at $60\text{ }^\circ\text{C}$ overnight, and stored in an N_2 -filled drybox. Succinimide was purchased from Pfaltz and Bauer. Sodium pivalate (NaOPiv), phenol, aniline, methanesulfonic acid, and tetramethylammonium chloride (NMe_4Cl) were purchased from Acros. NMe_4Cl was dried under vacuum at $60\text{ }^\circ\text{C}$ overnight and stored in an N_2 -filled drybox. Potassium phthalimide, copper(II) trifluoroacetate ($\text{Cu}(\text{OTFA})_2$), tetramethylammonium hydroxide (25% w/w, aqueous solution), copper(II) nitrate ($\text{Cu}(\text{NO}_3)_2$), and *o*-benzoic sulfimide sodium salt were purchased from Alfa Aesar. Copper(II) chloride (CuCl_2), copper(II) bromide (CuBr_2), copper(II) tetrafluoroborate ($\text{Cu}(\text{BF}_4)_2 \cdot x\text{H}_2\text{O}$), copper(II) acetate ($\text{Cu}(\text{OAc})_2$), copper(II) sulfate (CuSO_4), and copper(II) carbonate (CuCO_3) were purchased from Strem Chemicals. CDCl_3 was purchased from Cambridge Isotope Laboratories, Inc. Tetrahydrofuran (THF) was purchased from VWR International and

purified by an Innovative Technologies solvent purification system consisting of a copper catalyst, activated alumina, and molecular sieves.

Silica gel for flash column chromatography was purchased from Dynamic Adsorbents. Diatomaceous earth was purchased from Aqua Solutions. Magnesium sulfate (anhydrous, powder) was purchased from Avantor Performance Materials. Thin layer chromatography (TLC) was performed on Merck TLC plates pre-coated with silica gel 60 F₂₅₄.

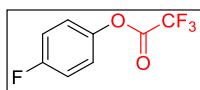
Potassium pyridone was prepared using a literature procedure.²¹ 4-Fluorophenylboronic acid pinacol ester²² and MIDA ester²³ were prepared according to literature procedures. Copper(II) tosylate (Cu(OTs)₂) and copper(II) mesylate (Cu(OMs)₂) were prepared according to the literature procedure.²⁴ Tetramethylammonium salts were synthesized according to the literature procedure.²⁵

5.6.3. General Procedure for Copper-Mediated Functionalization of Aryl Trifluoroborates

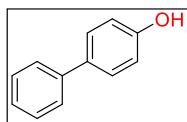
Experimental Details for Optimization of Trifluoroacetoxylation with 1 Reported in Table 5.1. In a N₂-filled drybox or on the benchtop, potassium (4-fluorophenyl)trifluoroborate **1** (5.1 mg, 0.025 mmol, 1.0 equiv), Cu(OTf)₂ (36.1 mg, 0.1 mmol, 4.0 equiv), and MOTFA (0.1 mmol, 4.0 equiv) were weighed into a 4 mL vial equipped with a magnetic stir bar. CH₃CN (0.3 mL) was added, and the vial was sealed with a Teflon-lined cap. The reaction mixture was allowed to stir at 60 °C or room temperature for 16 h. The solution was then cooled to room temperature and diluted with CH₃CN. 1,3,5-trifluorobenzene was added as an internal standard, and the reaction was analyzed by ¹⁹F NMR spectroscopy.

Experimental Details for the Aryl Boron Reagent Screen Reported in Table 5.2. On the benchtop, *p*-FC₆H₅BX₂ (0.025 mmol, 1.0 equiv), Cu(OTf)₂ (36.1 mg, 0.1 mmol, 4.0 equiv), and NaOTFA (13.6 mg, 0.1 mmol, 4.0 equiv) were weighed into a 4 mL vial equipped with a magnetic stir bar. CH₃CN (0.3 mL) was added, and the vial was sealed with a Teflon-lined cap. The reaction mixture was allowed to stir at room temperature for 16 h. The solution was then diluted with CH₃CN. 1,3,5-trifluorobenzene was added as an internal standard, and the reaction was analyzed by ¹⁹F NMR spectroscopy.

Experimental Details for the Carboxylate Nucleophile Scope in Figure 5.1. Potassium (4-fluorophenyl)trifluoroborate (**1**) (101.0 mg, 0.5 mmol, 1.0 equiv) or potassium (4-biphenyl)trifluoroborate (130.0 mg, 0.5 mmol, 1.0 equiv), Cu(OTf)₂ (723.0 mg, 2.0 mmol, 4.0 equiv), and tetraalkylammonium or alkali carboxylate salt (2.0 mmol, 4.0 equiv) were weighed into a 20 mL vial equipped with a magnetic stir bar. CH₃CN (6.0 mL) was added, and the vial was sealed with a Teflon-lined cap. The reaction mixture was allowed to stir at room temperature for 16 h. For products that were isolated, the reactions were diluted with diethyl ether or pentane (10 mL), and this solution was washed with water (3 x 10 mL). The organic layer was dried over MgSO₄, filtered, and concentrated under vacuum. The products were purified by column chromatography on silica gel using gradients of pentane/diethyl ether or hexanes/ethyl acetate. For product yields determined by ¹⁹F NMR spectroscopy, the crude reaction mixture was diluted with CH₃CN, 1,3,5-trifluorobenzene was added as an internal standard, and the reaction was analyzed by ¹⁹F NMR spectroscopy and GCMS.

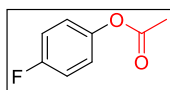


The reaction was performed with **1** according to the standard conditions with sodium trifluoroacetate (NaOTFA) as the nucleophile. Product **2** was formed in 45% yield as determined by ¹⁹F NMR spectroscopic analysis of the crude reaction mixture. The ¹⁹F NMR spectrum matched that reported previously in the literature.²⁶ The identity of the product was further confirmed by GCMS analysis, where the product peak was observed at 8.48 min (*m/z* = 208). The yield reported in Figure 5.1 (51%) represents an average of two runs [45% and 56%].

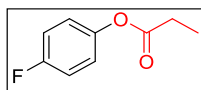


The reaction was performed with potassium (4-biphenyl)trifluoroborate according to the standard conditions with sodium trifluoroacetate (NaOTFA) as the nucleophile. The reaction mixture was then diluted with diethyl ether (10 mL), and the resulting mixture was washed with water (3 x 15 mL) and dried over MgSO₄. The solvent was removed by rotary

evaporation at 30 °C. The conversion of the trifluoroacetate to the phenol was carried out according to a literature procedure as follows.²⁷ The crude product was dissolved in THF (3.0 mL) and cooled to 0 °C. A solution of LiOH (24.0 mg, 0.5 mmol, 1.0 equiv) in water (3.0 mL) was added dropwise to the THF solution. The reaction was allowed to stir at room temperature for 3 h. The reaction mixture was quenched with 2% HCl. The resulting mixture was then extracted between water (10 mL) and diethyl ether (10 mL), and the organic extracts were dried over MgSO₄. The product **3** was obtained as a tan solid (39.0 mg, 46% yield, mp = 163–164 °C, R_f = 0.22 in 9:1 hexanes/ethyl acetate). The ¹H NMR spectrum (CDCl₃) and ¹³C{¹H} NMR spectrum (CDCl₃) matched those previously reported in the literature.²⁸ HRMS electrospray (*m/z*): [M]⁺ calcd for C₁₂H₁₀O, 170.0732; measured, 170.0729. The isolated yield reported in Figure 5.1 (46%) represents an average of two runs [46% and 46%].

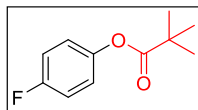


The reaction was performed with **1** according to the standard procedure with tetrabutylammonium acetate (NBu₄OAc) as the nucleophile. Product **4** was obtained as a clear liquid (50.0 mg, 65% yield, R_f = 0.46 in 9:1 pentane/diethyl ether). The ¹H NMR spectrum (CDCl₃) and ¹³C{¹H} NMR spectrum (CDCl₃) matched that previously reported in the literature.²⁹ ¹⁹F NMR (470 MHz, CDCl₃): δ –117.09 (m, 1F). IR (cm^{–1}): 1760, 1593, 1500, 1345, 1210, 1178, 1150, 1011, 906, 853, 823, 768, 749. HRMS electrospray (*m/z*): [M]⁺ calcd for C₈H₇FO₂, 154.0430; measured, 154.0437. The isolated yield reported in Figure 5.1 (65%) represents an average of two runs [65% and 64%].

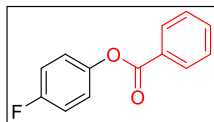


The reaction was performed with **1** according to the standard conditions with sodium propionate as the nucleophile. Product **5** was obtained as a clear liquid (48.0 mg, 57% yield, R_f = 0.5 in 95:5 pentane/diethyl ether). The ¹³C{¹H} NMR (CDCl₃) matched that previously reported in the literature.³⁰ ¹H NMR (500 MHz, CDCl₃): δ 7.09–7.05 (multiple peaks, 4H), 2.58 (q, 2H), 1.26 (t, 3H). ¹⁹F NMR (470 MHz, CDCl₃): δ –117.29 ppm (m,

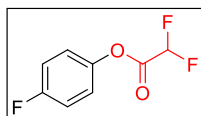
1F). IR (cm⁻¹): 1757, 1653, 1501, 1354, 1182, 1133, 1075, 981, 887, 823, 760. HRMS electrospray (*m/z*): [M]⁺ calcd for C₉H₉FO₂, 168.0587; measured, 168.0583. The isolated yield reported in Figure 5.1 (61%) represents an average of two runs [57% and 64%].



The reaction was performed with **1** according to the standard conditions with sodium pivalate (NaOPiv) as the nucleophile. Product **6** was obtained as a clear liquid (66.0 mg, 68% yield, *R*_f = 0.58 in 98:2 pentane/diethyl ether). ¹H NMR (CDCl₃): δ 7.07–6.99 (multiple peaks, 4H), 1.35 (s, 9H). ¹⁹F NMR (CDCl₃): δ –117.51 (m, 1F). ¹³C NMR (CDCl₃): δ 177.11, 161.07 (*J* = 501 Hz), 146.91 (*J* = 5.2 Hz), 122.89 (*J* = 18.2 Hz), 116.05 (*J* = 49.4 Hz), 39.04, 27.09. IR (cm⁻¹) 1749, 1503, 1481, 1276, 1182, 1107, 1028, 891, 831, 796, 755. HRMS electrospray (*m/z*): [M]⁺ calcd for C₁₁H₁₃FO₂, 196.0899; measured, 196.0899. The isolated yield reported in Figure 5.1 (67%) represents an average of two runs [68% and 65%].



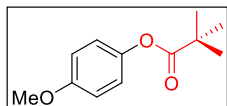
The reaction was performed with **1** according to the standard conditions with tetrabutylammonium benzoate (NBu₄OBz) as the nucleophile for 4 h. Product **7** was obtained as a white solid (80.0 mg, 74% yield, mp = 57–59 °C, *R*_f = 0.64 in 9:1 pentane/diethyl ether). The ¹H NMR (CDCl₃), ¹⁹F NMR (CDCl₃), and ¹³C{¹H} NMR (CDCl₃) spectra matched those previously reported in the literature.³¹ HRMS EI (*m/z*): [M]⁺ calcd for C₁₃H₉FO₂, 216.0587; measured, 216.0585. The isolated yield reported in Figure 5.1 (70%) represents an average of two runs [74% and 66%].



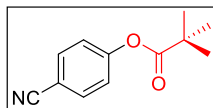
The reaction was performed with substrate **1** according to the standard conditions with tetramethylammonium difluoroacetate as the nucleophile. Product **8** was formed in 83%

yield as determined by ^{19}F NMR spectroscopic analysis of the crude reaction mixture (-116.3 ppm (m, 1F), -128.1 ppm (d, $J = 14$ Hz, 2F)). The identity of the product was further confirmed by GCMS analysis, where the product peak was observed at 9.9 min ($m/z = 190$). The yield reported in Figure 5.1 (80%) represents an average of two runs [83% and 77%].

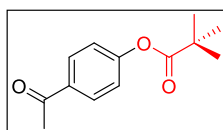
Experimental Details for the Substrate Scope with NaOPiv in Figure 5.2. The aryl trifluoroborate substrate (0.5 mmol, 1.0 equiv), $\text{Cu}(\text{OTf})_2$ (723.0 mg, 2.0 mmol, 4.0 equiv), and NaOPiv (248.0 mg, 2.0 mmol, 4.0 equiv) were weighed into a 20 mL vial equipped with a magnetic stir bar. CH_3CN (6.0 mL) was added, and the vial was sealed with a Teflon-lined cap. The reaction mixture was allowed to stir at room temperature for 16 h. For pyridine substrates, after 16 h, 1.0 g of poly(4-vinylpyridine) was added to the solution, and the resulting mixture was stirred for an additional 12 h at room temperature. The resulting solution was diluted with diethyl ether (10 mL), and the organic layer was extracted with water (3 x 10 mL) and with 1.0 M aq. NH_4OH solution, saturated with EDTA (10 mL). The organic layer was dried over MgSO_4 , filtered, and concentrated under pressure. The products were purified by column chromatography on silica using gradients of pentane/diethyl ether or hexanes/ethyl acetate.



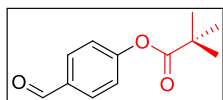
The reaction was performed using potassium (4-methoxyphenyl)trifluoroborate (107.0 mg, 0.5 mmol, 1.0 equiv) according to the standard procedure. Product **9** was obtained as a colorless oil (66.0 mg, 63% yield, $R_f = 0.38$ in 95:5 pentane/diethyl ether). The ^1H NMR (CDCl_3) and $^{13}\text{C}\{^1\text{H}\}$ NMR (CDCl_3) spectra matched those previously reported in the literature.³² HRMS electrospray (m/z): $[\text{M}+\text{H}]^+$ calcd for $\text{C}_{12}\text{H}_{16}\text{O}_3$, 209.1172; measured, 209.1173. The isolated yield reported in Figure 5.2 (62%) represents an average of two runs [63% and 61%].



The reaction was performed using potassium (4-cyanophenyl)trifluoroborate (105.0 mg, 0.5 mmol, 1.0 equiv) according to the standard procedure. Product **10** was obtained as a colorless oil (57.0 mg, 56% yield, R_f = 0.3 in 95:5 pentane/diethyl ether). ^1H NMR (500 MHz, CDCl_3): δ 7.67 (d, J = 8.5 Hz, 2H), 7.18 (d, J = 8.5 Hz, 2H), 1.35 (s, 9H). $^{13}\text{C}\{^1\text{H}\}$ NMR (125 MHz, CDCl_3): δ 176.21, 154.45, 133.59, 122.71, 118.29, 109.48, 39.23, 26.98. IR (cm^{-1}): 2230, 1750, 1699, 1653, 1601, 1505, 1480, 1397, 1274, 1205, 1166, 1095, 1028, 895, 854. HRMS electrospray (m/z): $[\text{M}+\text{H}]^+$ calcd for $\text{C}_{12}\text{H}_{14}\text{NO}_2$, 204.1019; measured 204.1012. This isolated yield reported in Figure 5.2 (60%) represents an average of two runs [56% and 63%].

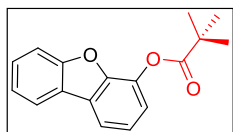


The reaction was performed using potassium (4-acetylphenyl)trifluoroborate (113.0 mg, 0.5 mmol, 1.0 equiv) according to the standard procedure. Product **11** was obtained as a white solid (86.0 mg, 78% yield, mp = 49–52 °C, R_f = 0.46 in 4:1 hexanes/ethyl acetate). The ^1H NMR (CDCl_3) and $^{13}\text{C}\{^1\text{H}\}$ NMR (CDCl_3) spectra matched those previously reported in the literature.³³ HRMS electrospray (m/z): $[\text{M}+\text{H}]^+$ calcd for $\text{C}_{13}\text{H}_{17}\text{O}_3$, 221.1172; measured, 221.1167. This isolated yield reported in Figure 5.2 (74%) represents an average of two runs [78% and 69%].

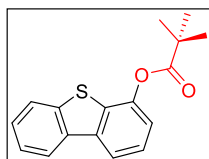


The reaction was performed using potassium (4-formylphenyl)trifluoroborate (106.0 mg, 0.5 mmol, 1.0 equiv) according to the standard procedure. Product **12** was obtained as a colorless oil (71.0 mg, 68% yield, R_f = 0.62 in 85:15 pentane/diethyl ether). The ^1H NMR (CDCl_3) and $^{13}\text{C}\{^1\text{H}\}$ NMR (CDCl_3) spectra matched those previously reported in the literature.³⁴ HRMS electrospray (m/z): $[\text{M}+\text{H}]^+$ calcd for $\text{C}_{12}\text{H}_{15}\text{O}_3$, 207.1016; measured,

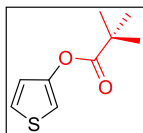
207.1013. The isolated yield reported in Figure 5.2 (68%) represents an average of two runs [68% and 68%].



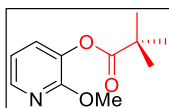
The reaction was performed using potassium dibenzofuran-4-trifluoroborate (138.0 mg, 0.5 mmol, 1.0 equiv) according to the standard procedure. Product **13** was obtained as a colorless oil (104.0 mg, 77% yield, R_f = 0.46 in 95:5 pentane/diethyl ether). The ^1H NMR (CDCl_3) and $^{13}\text{C}\{^1\text{H}\}$ NMR (CDCl_3) spectra matched those previously reported in the literature.³⁵ HRMS electrospray (m/z): $[\text{M}+\text{H}]^+$ calcd for $\text{C}_{17}\text{H}_{16}\text{O}_3$, 269.1172; measured, 269.1172. The isolated yield reported in Figure 5.2 (80%) represents an average of two runs [77% and 82%].



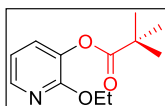
The reaction was performed using potassium dibenzothiophene-4-trifluoroborate (145.0 mg, 0.5 mmol, 1.0 equiv) according to the standard procedure. Product **14** was obtained as a yellow solid (44.0 mg, 31% yield, mp = 68–71 °C, R_f = 0.63 in 95:5 pentane/diethyl ether). ^1H NMR (500 MHz, CDCl_3): δ 8.14 (dd, J = 6, 3 Hz, 1H), 8.01 (d, J = 8 Hz, 1H), 7.83 (dd, J = 6, 3 Hz, 1H), 7.48–7.45 (m, 3H), 7.24 (s, 1H), 1.46 (s, 9H). $^{13}\text{C}\{^1\text{H}\}$ NMR (125 MHz, CDCl_3): δ 176.04, 145.89, 137.94, 135.56, 131.87, 127.09, 125.39, 124.58, 122.84, 121.94, 119.39, 118.77, 39.45, 27.25. IR (cm^{-1}): 2957, 1747, 1231, 1097, 757. HRMS electrospray (m/z): $[\text{M}+\text{H}]^+$ calcd for $\text{C}_{17}\text{H}_{17}\text{O}_2\text{S}$, 285.0944; measured, 285.0943. The isolated yield reported in Figure 5.2 (31%) represents an average of two runs [31% and 32%].



The reaction was performed using potassium thiophene-3-trifluoroborate (95.0 mg, 0.5 mmol, 1.0 equiv) according to the standard procedure. Product **15** was obtained as a colorless oil (43.0 mg, 46% yield, $R_f = 0.69$ in 95:5 pentane/diethyl ether). ^1H NMR (500 MHz, CDCl_3): δ 7.23 (dd, $J = 5.5, 3.5$ Hz, 1H), 7.09 (dd, $J = 3.5, 1$ Hz, 1H), 6.91 (dd, $J = 5.5, 1$ Hz, 1H), 1.34 (s, 9H). $^{13}\text{C}\{^1\text{H}\}$ NMR (125 MHz, CDCl_3): δ 176.00, 147.47, 123.99, 121.32, 110.49, 39.15, 27.11. IR (cm^{-1}): 2972, 1748, 1532, 1390, 1276, 1142, 1107, 763. HRMS electrospray (m/z): $[\text{M}+\text{H}]^+$ calcd for $\text{C}_9\text{H}_{13}\text{O}_2\text{S}$, 185.0631; measured, 185.0624. The isolated yield reported in Figure 5.2 (47%) represents an average of two runs [47% and 46%].

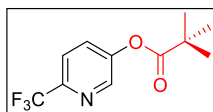


The reaction was performed using potassium (2-methoxypyridin-3-yl)trifluoroborate (108.0 mg, 0.5 mmol, 1.0 equiv) according to the standard procedure except with heating at 60 °C for 16 h. Product **16** was obtained as a white solid (18.0 mg, 17% yield, mp = 54–56 °C, $R_f = 0.39$ in 9:1 pentane/diethyl ether). ^1H NMR (500 MHz, CDCl_3): δ 8.01 (d, $J = 5$ Hz, 1H), 7.28 (d, $J = 7.5$ Hz, 1H), 6.88 (dd, $J = 7.5, 5$ Hz, 1H), 3.95 (s, 3H), 1.37 (s, 9H). $^{13}\text{C}\{^1\text{H}\}$ NMR (125 MHz, CDCl_3): δ 176.32, 156.53, 143.47, 135.28, 130.46, 116.74, 53.65, 39.07, 27.09. IR (cm^{-1}): 1754, 1602, 1559, 1474, 1455, 1413, 1318, 1262, 1173, 1099, 1016, 885, 861, 780, 751. HRMS electrospray (m/z): $[\text{M}+\text{H}]^+$ calcd for $\text{C}_{11}\text{H}_{15}\text{NO}_3$, 210.1125; measured, 210.1123. The isolated yield reported in Figure 5.2 (17%) represents an average of two runs [17% and 16%].

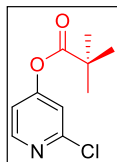


The reaction was performed using potassium (2-ethoxypyridin-3-yl)trifluoroborate (115.0 mg, 0.5 mmol, 1.0 equiv) according to the standard procedure except with heating at 60 °C for 16 h. Product **17** was obtained as a colorless oil (18.0 mg, 16% yield, $R_f = 0.44$ in

9:1 pentane/diethyl ether). ^1H NMR (500 MHz, CDCl_3): δ 7.99 (d, J = 5 Hz, 1H), 7.28 (d, J = 7.5 Hz, 1H), 6.86 (dd J = 7.5, 5 Hz, 1H), 4.36 (q, J = 7 Hz, 2H), 1.37 (s, 9H), 1.35 (t, J = 7 Hz, 3H). $^{13}\text{C}\{^1\text{H}\}$ NMR (125 MHz, CDCl_3): δ 176.29, 156.29, 143.48, 135.23, 130.35, 116.51, 62.05, 39.05, 27.13, 14.49. IR (cm^{-1}): 1754, 1699, 1653, 1602, 1558, 1540, 1506, 1474, 1455, 1385, 1319, 1260, 1178, 1102, 1029, 930, 883, 779, 750. HRMS electrospray (m/z): $[\text{M}+\text{H}]^+$ calcd for $\text{C}_{12}\text{H}_{18}\text{NO}_3$, 224.1281; measured, 224.1281. This isolated yield reported in Figure 5.2 (16%) represents an average of two runs [16% and 15%].

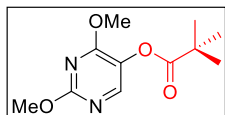


The reaction was performed using potassium (6-(trifluoromethyl)pyridine-3-yl)trifluoroborate (127.0 mg, 0.5 mmol, 1.0 equiv) according to the standard procedure except with heating at 60 °C for 16 h. Product **18** was obtained as a white solid (77.0 mg, 64% yield, mp = 53–56 °C, R_f = 0.63 in 9:1 pentane/diethyl ether). ^1H NMR (500 MHz, CDCl_3): δ 8.49 (d, J = 2 Hz, 1H), 7.73 (d, J = 8.5 Hz, 1H), 7.64 (dd, J = 8.5, 2 Hz, 1H), 1.38 (s, 9H). $^{13}\text{C}\{^1\text{H}\}$ NMR (125 MHz, CDCl_3): δ 176.06, 149.56, 145.06 (q, J = 35.3 Hz), 143.69, 122.38 (q, J = 274 Hz), 121.16 (q, J = 2.9 Hz), 39.29, 26.92. ^{19}F NMR (470 MHz, CDCl_3): δ -67.41 (s, 3F). IR (cm^{-1}): 2990, 1753, 1653, 1590, 1479, 1339, 1300, 1210, 1179, 1115, 1077, 1022, 926, 885, 862, 751, 654, 634. HRMS electrospray (m/z): $[\text{M}+\text{H}]^+$ calcd for $\text{C}_{11}\text{H}_{13}\text{F}_3\text{NO}_2$, 248.0894; measured, 248.0892. The isolated yield reported in Figure 5.2 (65%) represents an average of two runs [64% and 66%].



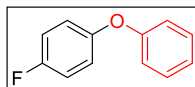
The reaction was performed using potassium (2-chloropyridin-4-yl)trifluoroborate (110.0 mg, 0.5 mmol, 1.0 equiv) according to the standard procedure except with heating at 60 °C for 16 h. Product **19** was obtained as a colorless oil (52.0 mg, 48% yield, R_f = 0.44 in 4:1 pentane/diethyl ether). ^1H NMR (500 MHz, CDCl_3): δ 8.35 (d, J = 5.5 Hz, 1H), 7.14 (d, J = 1.5 Hz, 1H), 7.03 (dd, J = 5.5, 1.5 Hz, 1H), 1.33 (s, 9H). $^{13}\text{C}\{^1\text{H}\}$ NMR (125 MHz,

CDCl₃): δ 175.29, 159.36, 152.39, 150.64, 117.40, 115.96, 39.35, 26.88. IR (cm⁻¹): 2975, 1759, 1581, 1461, 1378, 1272, 1219, 1087, 1069, 1026, 909, 890, 834, 796, 716. HRMS electrospray (m/z): [M+H]⁺ calcd for C₁₀H₁₃ClNO₂, 214.0629; measured, 214.0630. The isolated yield in Figure 5.2 (49%) represents an average of two runs [48% and 50%].

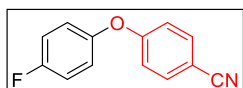


The reaction was performed using potassium (2,4-dimethoxypyrimidin-5-yl)trifluoroborate (123.0 mg, 0.5 mmol, 1.0 equiv) according to the standard procedure except with heating at 60 °C for 16 h. Product **20** was obtained as a colorless oil (5.0 mg, 4% yield, R_f = 0.38 in 4:1 diethyl ether/pentane). ¹H NMR (700 MHz, CDCl₃): δ 7.98 (s, 1H), 3.98 (two coincident s, 6H), 1.35 (s, 9H). ¹³C{¹H} NMR (176 MHz, CDCl₃): δ 176.19, 163.28, 162.25, 149.91, 129.17, 55.15, 54.37, 39.06, 27.05. IR (cm⁻¹): 1734, 1717, 1699, 1684, 1653, 1558, 1540, 1506, 1457, 1374, 1270, 1094, 782. HRMS electrospray (m/z): [M]⁺ calcd for C₁₁H₁₇N₂O₄⁺, 241.1183; measured, 241.1188. The isolated yield reported in Figure 5.2 (4%) represents an average of two runs [4% and 4%].

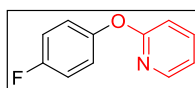
Experimental Details for the Oxygen Nucleophile Scope in Figure 5.3. Potassium (4-fluorophenyl)trifluoroborate (**1**) (101.0 mg, 0.5 mmol, 1.0 equiv) Cu(OTf)₂ (723.0 mg, 2.0 mmol, 4.0 equiv), and tetraalkylammonium or alkali salt (2.0 mmol, 4.0 equiv) were weighed into a 20 mL vial equipped with a magnetic stir bar. CH₃CN (6.0 mL) was added, and the vial was sealed with a Teflon-lined cap. The reaction mixture was allowed to stir at room temperature for 16 h. For products that were isolated, the reactions were diluted with diethyl ether (10 mL), and this solution was washed with water (3 x 10 mL). The organic layer was dried over MgSO₄, filtered, and concentrated under vacuum. The products were purified by column chromatography on silica gel using gradients of hexanes/ethyl acetate. For product yields determined by ¹⁹F NMR spectroscopy, the crude reaction mixture was diluted with CH₃CN, 1,3,5-trifluorobenzene was added as an internal standard, and the reaction was analyzed by ¹⁹F NMR spectroscopy and GCMS.



The reaction was performed with **1** (0.025 mmol) according to the standard conditions with tetramethylammonium phenoxide as the nucleophile with the exceptions that the reaction was set up in an N₂-filled drybox and the reaction was performed at 60 °C. Product **21** was formed in 13% yield as determined by ¹⁹F NMR spectroscopic analysis of the crude reaction mixture (−113.9 ppm (s, 1F)). The identity of the product was further confirmed by GCMS analysis, where the product peak was observed at 14.8 min (*m/z* = 188). The yield reported in Figure 5.3 (10%) represents an average of two runs [13% and 7%].

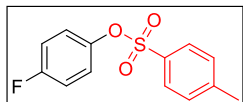


The reaction was performed with **1** (0.025 mmol) according to the standard conditions with tetramethylammonium (*p*-cyano)phenoxide as the nucleophile with the exceptions that the reaction was set up in an N₂-filled drybox and the reaction was performed at 60 °C. Product **22** was formed in 36% yield as determined by ¹⁹F NMR spectroscopic analysis of the crude reaction mixture (−119.2 ppm (s, 1F)). The identity of the product was further confirmed by GCMS analysis, where the product peak was observed at 17.7 min (*m/z* = 213). The yield reported in Figure 5.3 (38%) represents an average of two runs [36% and 40%].

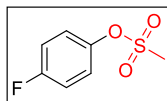


The reaction was performed according to the standard procedure with potassium pyridone as the nucleophile. Product **23** was obtained as a yellow oil (20.0 mg, 21% yield, *R_f* = 0.54 in 4:1 hexanes/ethyl acetate). The ¹H NMR (CDCl₃), ¹⁹F NMR (CDCl₃), and ¹³C{¹H} NMR (CDCl₃) spectra matched those previously reported in the literature.³⁶ IR (cm^{−1}): 1684, 1589, 2571, 1501, 1465, 1426, 1265, 1223, 1189, 1141, 1088, 883, 844, 817, 776, 733, 705. HRMS EI (*m/z*): [*M*]⁺ calcd for C₁₁H₈FNO, 189.0590; measured,

190.0664. The isolated yield reported in Figure 5.3 (20%) represents an average of two runs [21% and 19%].



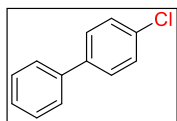
The reaction was performed according to the standard procedure with sodium tosylate (NaOTs) as the nucleophile except the reaction was heated at 60 °C for 16 h. Product **24** was obtained as a yellow oil (20.0 mg, 15% yield, R_f = 0.45 in 8:2 hexanes/ethyl acetate). The ^1H NMR (CDCl_3) and $^{13}\text{C}\{^1\text{H}\}$ NMR (CDCl_3) spectra matched those previously reported in the literature.³⁷ ^{19}F NMR (470 MHz, CDCl_3): δ -114.56 (m, 1F). IR (cm^{-1}): 1597, 1497, 1371, 1194, 1180, 1157, 1090, 869, 843, 803, 728, 691, 654. HRMS EI (m/z): $[\text{M}]^+$ calcd for $\text{C}_{13}\text{H}_{11}\text{FO}_3\text{S}$, 266.0413; measured, 266.0411. The isolated yield reported Figure 5.3 (13%) represents an average of two runs [15% and 12%].



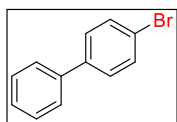
The reaction was performed with **1** (0.025 mmol) according to the standard conditions with tetrabutylammonium methanesulfonate as the nucleophile. Product **25** was formed in 36% yield as determined by ^{19}F NMR spectroscopic analysis of the crude reaction mixture (-115.4 ppm (s, 1F)). The identity of the product was further confirmed by GCMS analysis, where the product peak was observed at 14.2 min (m/z = 190). The yield reported in Figure 5.3 (21%) represents an average of two runs [20% and 23%].

Experimental Details for the Halide Scope in Figure 5.4. Potassium (4-biphenyl)trifluoroborate (130.0 mg, 0.5 mmol, 1.0 equiv), $\text{Cu}(\text{OTf})_2$ (723.0 mg, 2.0 mmol, 4.0 equiv), and the appropriate tetraalkylammonium halide salt (2.0 mmol, 4.0 equiv) were weighed into a 20 mL vial equipped with a magnetic stir bar. CH_3CN (6.0 mL) was added, and the vial was sealed with a Teflon-lined cap. The reaction mixture was allowed to stir at room temperature for 16 h. The reactions were diluted with diethyl ether or pentane (10 mL), and the organic layer was washed with water (3 x 10 mL). The organic layer was dried over MgSO_4 , filtered, and concentrated under vacuum. When necessary, the

products were purified by column chromatography on silica using gradients of pentane/diethyl ether.

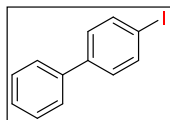


This reaction was performed according to the standard procedure with tetramethylammonium chloride (NMe_4Cl) as the nucleophile except with heating at 60 °C for 16 h. Product **26** was obtained as a white solid (43.0 mg, 46% yield, mp = 76–77 °C, R_f = 0.59 in pentane). The ^1H NMR (CDCl_3) and $^{13}\text{C}\{^1\text{H}\}$ NMR (CDCl_3) spectra matched those previously reported in the literature.³⁸ HRMS electrospray (m/z): $[\text{M}]^+$ calcd for $\text{C}_{12}\text{H}_9\text{Cl}$, 188.0393; measured, 188.0389. The isolated yield reported in Figure 5.4 (46%) represents an average of two runs [46% and 45%].



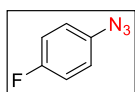
This reaction was performed according to the standard procedure with tetrabutylammonium bromide (NBu_4Br) as the nucleophile. Product **27** was obtained as a white solid after extraction with pentane (96.0 mg, 83% yield, mp = 89–90 °C). The ^1H NMR (CDCl_3) and $^{13}\text{C}\{^1\text{H}\}$ NMR (CDCl_3) spectra matched those previously reported in the literature for this compound.³⁹ HRMS electrospray (m/z): $[\text{M}]^+$ calcd for $\text{C}_{12}\text{H}_9\text{Br}$, 231.9888; measured, 231.9883. The yield reported in Figure 5.4 (86%) represents an average of two runs [83% and 88%].

This reaction was also performed on a 1.0 gram (3.85 mmol) scale according to the standard procedure. Product **27** was obtained as a white solid after extraction with pentane (636.3 mg, 71% yield).



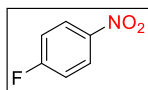
This reaction was performed according to the standard procedure with tetrabutylammonium iodide (NBu₄I) as the nucleophile. Product **28** was obtained as a white solid after extraction of the crude reaction mixture with pentane (95.0 mg, 68% yield, mp = 111–112 °C). The ¹H NMR (CDCl₃) and ¹³C{¹H} NMR (CDCl₃) spectra matched those previously reported in the literature for this compound.⁴⁰ HRMS electrospray (*m/z*): [M]⁺ calcd for C₁₂H₉I, 279.9749; measured, 279.9756. The isolated yield reported in Figure 5.4 (70%) represents an average of two runs [68% and 72%].

Experimental Details for the Nitrogen Nucleophile Scope in Figure 5.5. Potassium (4-fluorophenyl)trifluoroborate (**1**) (101.0 mg, 0.5 mmol, 1.0 equiv), Cu(OTf)₂ (723.0 mg, 2.0 mmol, 4.0 equiv), and the appropriate tetraalkylammonium or alkali salt (2.0 mmol, 4.0 equiv) were weighed into a 20 mL vial equipped with a magnetic stir bar. CH₃CN (6.0 mL) was added, and the vial was sealed with a Teflon-lined cap. The reaction mixture was allowed to stir at room temperature for 16 h. For products that were isolated, the reactions were diluted with diethyl ether or pentane (10 mL), and the organic layer was washed with water (3 x 10 mL). The organic layer was dried over MgSO₄, filtered, and concentrated under vacuum. When necessary, the products were purified by column chromatography on silica gel using gradients of hexanes/ethyl acetate. For product yields determined by ¹⁹F NMR spectroscopy, the crude reaction mixture was diluted with CH₃CN, 1,3,5-trifluorobenzene was added as an internal standard, and the reaction was analyzed by ¹⁹F NMR spectroscopy.

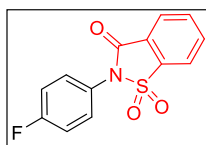


The reaction was performed with **1** (0.025 mmol) according to the standard conditions with potassium azide (KN₃) as the nucleophile. Product **29** was formed in 79% yield as determined by ¹⁹F NMR spectroscopic analysis of the crude reaction mixture (−118.3 ppm (m, 1F)). The identity of the product was further confirmed by GCMS analysis, where the

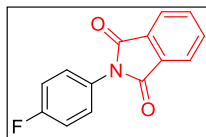
product peak was observed at 10.0 min ($m/z = 137$). The yield reported in Figure 5.5 (82%) represents an average of two runs [79% and 85%].



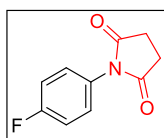
The reaction was performed with **1** (0.025 mmol) according to the standard conditions with sodium nitrite (NaNO_3) as the nucleophile. Product **30** was formed in 68% yield as determined by ^{19}F NMR spectroscopic analysis of the crude reaction mixture (-101.1 ppm (m, 1F)). The identity of the product was further confirmed by GCMS analysis, where the product peak was observed at 11.3 min ($m/z = 141$). The yield reported in Figure 5.5 (62%) represents an average of two runs [68% and 55%].



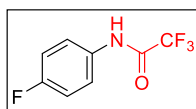
The reaction was performed according to the standard procedure with *o*-benzoic sulfimide sodium salt as the nucleophile. Product **31** was obtained as a tan solid (57.0 mg, 41% yield, mp = 152–157 °C, $R_f = 0.28$ in 4:1 hexanes/ethyl acetate). ^1H NMR (500 MHz, CDCl_3): δ 8.17 (d, $J = 9.9$ Hz, 1H), 8.02 (d, $J = 9.9$ Hz, 1H), 7.94 (td, $J = 7.5, 0.5$ Hz, 1H), 7.90 (dt, $J = 7.5$, 1 Hz, 1H), 7.53 (m, 2H), 7.28 (m, 2H). $^{13}\text{C}\{^1\text{H}\}$ NMR (125 MHz, CDCl_3): δ 164.46, 162.47, 158.41, 137.49, 135.23 ($J = 173$ Hz), 131.00 ($J = 20$ Hz), 127.03, 125.68, 124.40 ($J = 6$ Hz), 121.32, 117.19 ($J = 47$ Hz). ^{19}F NMR (470 MHz, CDCl_3): δ -109.04 (m, 1F). IR (cm^{-1}): 2360, 1735, 1684, 1699, 1653, 1558, 1506, 1457, 1312, 1227, 1183, 1090, 995, 943, 833, 801, 746, 671. HRMS EI (m/z): $[\text{M}]^+$ calcd for $\text{C}_{13}\text{H}_8\text{FNO}_3\text{S}$, 277.0209; measured, 277.0217. The isolated yield reported Figure 5.5 (42%) represents an average of two runs [41% and 43%].



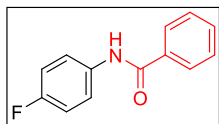
The reaction was performed according to the standard procedure with potassium phthalimide as the nucleophile. Product **32** was obtained as a tan solid (26.0 mg, 22% yield, mp = 176–178 °C, R_f = 0.38 in 8:2 hexanes/ethyl acetate). The ^1H NMR (CDCl_3), ^{19}F NMR (CDCl_3), and $^{13}\text{C}\{^1\text{H}\}$ NMR (CDCl_3) spectra matched those previously reported in the literature.⁴¹ IR (cm^{-1}): 2360, 2337, 1733, 1716, 1699, 1684, 1653, 1558, 1540, 1506, 1457, 1394, 1228, 1110, 828, 714. HRMS EI (m/z): $[\text{M}]^+$ calcd for $\text{C}_{14}\text{H}_8\text{FNO}_2$, 241.0539; measured, 242.0612. The isolated yield reported in Figure 5.5 (21%) represents an average of two runs [22% and 20%].



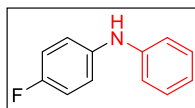
The reaction was performed with **1** (0.025 mmol) according to the standard conditions with tetramethylammonium succinimide as the nucleophile. Product **33** was formed in 68% yield as determined by ^{19}F NMR spectroscopic analysis of the crude reaction mixture (−118.0 ppm (s, 1F)). The yield reported in Figure 5.5 (70%) represents an average of two runs [68% and 71%].



The reaction was performed with **1** (0.025 mmol) according to the standard conditions with tetramethylammonium trifluoroacetamide as the nucleophile. Product **34** was formed in 57% yield as determined by ^{19}F NMR spectroscopic analysis of the crude reaction mixture (74.7 ppm (s, 3F), −115.4 ppm (m, 1F)). The identity of the product was further confirmed by GCMS analysis, where the product peak was observed at 8.5 min (m/z = 208). The yield reported in Figure 5.5 (57%) represents an average of two runs [57% and 56%].

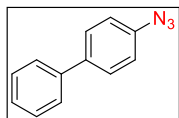


The reaction was performed with **1** (0.025 mmol) according to the standard conditions with tetramethylammonium benzoate as the nucleophile. Product **35** was formed in 39% yield as determined by ^{19}F NMR spectroscopic analysis of the crude reaction mixture (-117.8 ppm (m, 1F)). The identity of the product was further confirmed by GCMS analysis, where the product peak was observed at 16.9 min ($m/z = 216$). The yield reported in Figure 5.5 (42%) represents an average of two runs [39% and 44%].

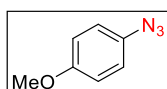


The reaction was performed with **1** (0.025 mmol) according to the standard conditions with tetramethylammonium aniline as the nucleophile. Product **36** was formed in 16% yield as determined by ^{19}F NMR spectroscopic analysis of the crude reaction mixture (-111.0 ppm (m, 1F)). The yield reported in Figure 5.5 (14%) represents an average of two runs [16% and 12%].

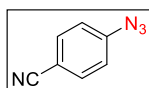
Experimental Details for the Substrate Scope with KN_3 in Figure 5.6. The aryl trifluoroborate substrate (0.5 mmol, 1.0 equiv), $\text{Cu}(\text{OTf})_2$ (723.0 mg, 2.0 mmol, 4.0 equiv), and KN_3 (162.0 mg, 2.0 mmol, 4.0 equiv) were weighed into a 20 mL vial equipped with a magnetic stir bar. CH_3CN (6.0 mL) was added, and the vial was sealed with a Teflon-lined cap. The reaction mixture was allowed to stir at room temperature for 12 h. For pyridine substrates, after 12 h, 1.0 g of poly(4-vinylpyridine) was added to the solution, and the resulting mixture was stirred for 12 h at room temperature. The resulting solution was diluted with diethyl ether (10 mL), and the organic layer was extracted with water (3 x 10 mL). The organic layer was dried over MgSO_4 , filtered, and concentrated under reduced pressure. The products were purified by column chromatography on silica with gradients of hexanes/ethyl acetate.



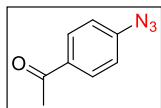
The reaction was performed using potassium (4-biphenyl)trifluoroborate (130.0 mg, 0.5 mmol, 1.0 equiv) according to the standard procedure with potassium azide (KN₃) as the nucleophile for 16 h. Product **37** was obtained as a yellow solid (48.0 mg, 49% yield, mp = 71–73 °C, R_f = 0.4 in hexanes). The ¹H NMR (CDCl₃) and ¹³C{¹H} NMR (CDCl₃) spectra matched those previously reported in the literature.^{16e} HRMS EI (*m/z*): [M]⁺ calcd for C₁₂H₉N₃, 195.0796; measured, 195.0800. The isolated yield reported in Figure 5.6 (51%) represents an average of two runs [49% and 53%].



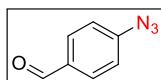
The reaction was performed using potassium (4-methoxyphenyl)trifluoroborate (107.0 mg, 0.5 mmol, 1.0 equiv) according to the standard procedure. Product **38** was obtained as a yellow oil (30.0 mg, 40% yield, R_f = 0.15 in hexanes). The ¹H NMR (CDCl₃) and ¹³C{¹H} NMR (CDCl₃) spectra matched those previously reported in the literature.^{16e} HRMS electrospray (*m/z*): [M]⁺ calcd for C₇H₇N₃O, 149.0589; measured, 149.0593. The isolated yield reported in Figure 5.6 (42%) represents an average of two runs [40% and 43%].



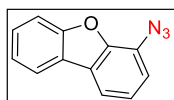
The reaction was performed using potassium (4-cyanophenyl)trifluoroborate (105.0 mg, 0.5 mmol, 1.0 equiv) according to the standard procedure. Product **39** was obtained as a tan solid (13.0 mg, 17% yield, mp = 62–64 °C, R_f = 0.56 in 4:1 hexanes/ethyl acetate). The ¹H NMR (CDCl₃) and ¹³C{¹H} NMR (CDCl₃) spectra matched those previously reported in the literature.^{16e} HRMS electrospray (*m/z*): [M+H]⁺ calcd for C₇H₄N₄, 144.0436; measured 144.0434. The isolated yield reported in Figure 5.6 (16%) represents an average of two runs [17% and 14%].



The reaction was performed using potassium (4-acetylphenyl)trifluoroborate (113.0 mg, 0.5 mmol, 1.0 equiv) according to the standard procedure. Product **40** was obtained as a brown solid (26.0 mg, 32% yield, mp = 42–45 °C, R_f = 0.27 in 9:1 hexanes/ethyl acetate). The ^1H NMR (CDCl_3) and $^{13}\text{C}\{^1\text{H}\}$ NMR (CDCl_3) spectra matched those previously reported in the literature.^{16e} HRMS electrospray (m/z): $[\text{M}]^+$ calcd for $\text{C}_8\text{H}_7\text{N}_3\text{O}$, 161.0589; measured, 161.0593. The isolated yield reported in Figure 5.6 (33%) represents an average of two runs [32% and 33%].

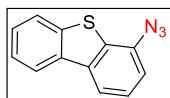


The reaction was performed using potassium (4-formylphenyl)trifluoroborate (106.0 mg, 0.5 mmol, 1.0 equiv) according to the standard procedure. Product **41** was obtained as a brown oil (7.0 mg, 10% yield, R_f = 0.40 in 90:10 hexanes/ethyl acetate). The ^1H NMR (CDCl_3) and $^{13}\text{C}\{^1\text{H}\}$ NMR (CDCl_3) spectra matched those previously reported in the literature.^{16e} HRMS electrospray (m/z): $[\text{M}+\text{H}]^+$ calcd for $\text{C}_7\text{H}_5\text{N}_3\text{O}$, 147.0433; measured, 147.0436. The isolated yield reported in Figure 5.6 (10%) represents an average of two runs [10% and 10%].



The reaction was performed using potassium dibenzofuran-4-trifluoroborate (138.0 mg, 0.5 mmol, 1.0 equiv) according to the standard procedure. Product **42** was obtained as a yellow oil (84.0 mg, 81% yield, R_f = 0.32 in hexanes). ^1H NMR (500 MHz, CDCl_3): δ 7.90 (d, J = 8 Hz, 1H), 7.66 (dd, J = 8 Hz, 1H), 7.60 (d, J = 8 Hz, 1H), 7.48 (td, J = 8, 1 Hz, 1H), 6.36 (td, J = 8, 1 Hz, 1H), 7.27 (t, J = 8 Hz, 1H), 7.10 (dd, J = 8, 1 Hz, 1H). $^{13}\text{C}\{^1\text{H}\}$ NMR (125 MHz, CDCl_3): δ 156.13, 147.45, 127.71, 126.14, 124.78, 123.69, 123.56, 123.15, 120.87, 117.05, 116.87, 112.00. IR (cm^{-1}): 2104, 1636, 1584, 1494, 1448, 1424, 1352, 1312, 1293, 1190, 1071, 915, 898, 845, 827, 787, 738. HRMS electrospray (m/z):

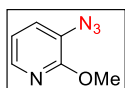
[M]⁺ calcd for C₁₂H₇N₃O, 209.0589; measured, 209.0582. The isolated yield reported in Figure 5.6 (80%) represents an average of two runs [81% and 79%].



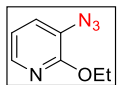
The reaction was performed using potassium dibenzothiophene-4-trifluoroborate (145.0 mg, 0.5 mmol, 1.0 equiv) according to the standard procedure. Product **43** was obtained as a yellow solid (34.0 mg, 30% yield, mp = 109–111 °C, R_f = 0.39 in hexanes). The ¹H NMR (CDCl₃) spectra matched that previously reported in the literature.⁴² ¹³C{¹H} NMR (125 MHz, CDCl₃): δ 139.53, 137.52, 135.30, 134.50, 130.50, 127.21, 125.64, 124.59, 122.99, 121.97, 117.93, 115.07. IR (cm⁻¹): 2111, 1438, 1286, 748. HRMS electrospray (*m/z*): [M]⁺ calcd for C₁₂H₇N₃S, 225.0361; measured, 225.0355. The isolated yield reported in Figure 5.6 (32%) represents an average of two runs [30% and 34%].



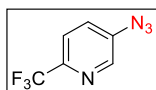
The reaction was performed using potassium thiophene-3-trifluoroborate (95.0 mg, 0.5 mmol, 1.0 equiv) according to the standard procedure. After workup and column chromatography, product **44** was not obtained as determined by GCMS and ¹H NMR spectroscopy.



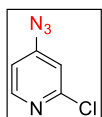
The reaction was performed using potassium (2-methoxypyridin-3-yl)trifluoroborate (108.0 mg, 0.5 mmol, 1.0 equiv) according to the standard procedure. Product **45** was obtained as a yellow oil (50.0 mg, 66% yield, R_f = 0.67 in 9:1 hexanes/ethyl acetate). The ¹H NMR (CDCl₃) NMR spectrum matched that previously reported in the literature.⁴³ ¹³C{¹H} NMR (125 MHz, CDCl₃): δ 156.59, 142.29, 127.71, 123.98, 117.22, 53.73. IR (cm⁻¹): 2115, 1585, 1470, 1449, 1410, 1308, 1236, 1096, 1012, 789, 752, 668. HRMS electrospray (*m/z*): [M]⁺ calcd for C₆H₆N₄O, 150.0542; measured, 150.0542. The isolated yield reported in Figure 5.6 (65%) represents an average of two runs [66% and 64%].



The reaction was performed using potassium (2-ethoxypyridin-3-yl)trifluoroborate (115.0 mg, 0.5 mmol, 1.0 equiv) according to the standard procedure. Product **46** was obtained as a yellow oil (59.0 mg, 71% yield, $R_f = 0.57$ in 9:1 hexanes/ethyl acetate). ^1H NMR (500 MHz, CDCl_3): δ 7.87 (dd, $J = 5, 1.5$ Hz, 1H), 7.16 (dd, $J = 7.5, 1.5$ Hz, 1H), 6.80 (dd, $J = 7.5, 5$ Hz, 1H), 4.45 (q, $J = 7$ Hz, 2H), 1.42 (t, $J = 7$ Hz, 3H). $^{13}\text{C}\{^1\text{H}\}$ NMR (125 MHz, CDCl_3): δ 156.51, 142.29, 127.82, 123.64, 116.99, 62.49, 14.34. IR (cm^{-1}): 2110, 1585, 1446, 1384, 1311, 1237, 1094, 1029, 929, 789, 752, 668. HRMS electrospray (m/z): $[\text{M}]^+$ calcd for $\text{C}_7\text{H}_8\text{N}_4\text{O}$, 164.0698; measured, 164.0702. The isolated yield reported in Figure 5.6 (71%) represents an average of two runs [71% and 71%].

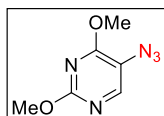


The reaction was performed using potassium (6-(trifluoromethyl)pyridine-3-yl)trifluoroborate (127.0 mg, 0.5 mmol, 1.0 equiv) according to the standard procedure. Product **47** was obtained as a yellow oil (51.0 mg, 54% yield, $R_f = 0.5$ in 9:1 hexanes/ethyl acetate). ^1H NMR (500 MHz, CDCl_3): δ 8.42 (d, $J = 2$ Hz, 1H), 7.67 (d, $J = 8.5$ Hz), 7.48 (dd, $J = 8.5, 2$ Hz, 1H). $^{13}\text{C}\{^1\text{H}\}$ NMR (125 MHz, CDCl_3): δ 144.42 (q, $J = 50.6$ Hz), 141.38, 140.05, 126.58, 122.11 (q, $J = 391.6$ Hz), 121.35 (d, $J = 1.9$ Hz). ^{19}F NMR (470 MHz, CDCl_3): δ -67.43 (s, 3F). IR (cm^{-1}): 2920, 2851, 1733, 1699, 1653, 1558, 1540, 1456, 1261, 1072, 796. HRMS electrospray (m/z): $[\text{M}]^+$ calcd for $\text{C}_6\text{H}_3\text{F}_3\text{N}_4$, 188.0310; measured, 188.0312. The isolated yield reported in Figure 5.6 (55%) represents an average of two runs [54% and 55%].



This reaction was performed using potassium (2-chloropyridin-4-yl)trifluoroborate (110.0 mg, 0.5 mmol, 1.0 equiv) according to the standard procedure except with heating at 60 $^\circ\text{C}$ for 16 h. Product **48** was obtained as a tan solid (41.0 mg, 54% yield, mp = 67–69 $^\circ\text{C}$, $R_f = 0.40$ in 9:1 hexanes/ethyl acetate). ^1H NMR (500 MHz, CDCl_3): δ 8.29 (d, $J = 5.5$ Hz,

1H), 6.96 (d, $J = 2$ Hz, 1H), 6.86 (dd, $J = 5, 2$ Hz, 1H). $^{13}\text{C}\{^1\text{H}\}$ NMR (125 MHz, CDCl_3): δ 152.81, 151.07, 150.67, 114.21, 113.09. IR (cm^{-1}): 2113, 1733, 1699, 1653, 1575, 1559, 1540, 1456, 1305, 1265, 1151, 1077, 856, 834, 740, 667. HRMS electrospray (m/z): $[\text{M}]^+$ calcd for $\text{C}_5\text{H}_3\text{ClN}_4$, 154.0046; measured, 154.0046. The isolated yield reported in Figure 5.6 (56%) represents an average of two runs [54% and 58%].



This reaction was performed using potassium (2,4-dimethoxypyrimidin-5-yl)trifluoroborate (123.0 mg, 0.5 mmol, 1.0 equiv) according to the standard procedure. Product **49** was obtained as a white solid (70.0 mg, 77% yield, mp = 47–49 °C, $R_f = 0.66$ in 4:1 hexanes/ethyl acetate). ^1H NMR (500 MHz, CDCl_3): δ 7.89 (s, 1H), 4.05 (s, 3H), 3.95 (s, 3H). $^{13}\text{C}\{^1\text{H}\}$ NMR (125 MHz, CDCl_3): δ 163.74, 161.99, 148.22, 116.99, 55.11, 54.53. IR (cm^{-1}): 2123, 1699, 1653, 1558, 1521, 1558, 1506, 1457, 1381, 1301, 1237, 1186, 1121, 1068, 997, 933, 779, 757, 667. HRMS electrospray (m/z): $[\text{M}]^+$ calcd for $\text{C}_6\text{H}_7\text{N}_5\text{O}_2$, 181.0600; measured, 181.0596. The isolated yield reported in Figure 5.6 (80%) represents an average of two runs [77% and 82%].

Experimental Details for the Cyanation of 1 in Figure 5.7. Potassium (4-fluorophenyl)trifluoroborate (**1**) (5.1 mg, 0.025 mmol, 1.0 equiv), $\text{Cu}(\text{OTf})_2$ (36.1 mg, 0.1 mmol, 4.0 equiv), and potassium cyanide (KCN) (6.5 mmol, 0.1 mmol, 4.0 equiv) were weighed into a 4 mL vial equipped with a magnetic stir bar. CH_3CN (0.3 mL) was added, and the vial was sealed with a Teflon-lined cap. The reaction mixture was allowed to stir at 60 °C temperature for 16 h. The solution was then diluted with CH_3CN . Product **50** was formed in 22% yield as determined by ^{19}F NMR spectroscopic analysis of the crude reaction mixture (–104.0 ppm (m, 1F)). The identity of the product was further confirmed by GCMS analysis, where the product peak was observed at 10.2 min ($m/z = 121$). The yield reported in Figure 5.7 (21%) represents an average of two runs [22% and 20%].

Experimental Details for the Cu^{II} Salt Study in Table 5.3. Potassium (4-fluorophenyl)trifluoroborate (**1**) (5.1 mg, 0.025 mmol, 1.0 equiv), copper salt (0.1 mmol, 4

equiv), and KN_3 (8.1 mg, 0.1 mmol, 4.0 equiv) or NaOPiv (12.4 mg, 0.1 mmol, 4.0 equiv) were weighed into a 4 mL vial equipped with a magnetic stir bar. CH_3CN (0.3 mL) was added, and the vial was sealed with a Teflon-lined cap. The reaction mixture was allowed to stir at room temperature for 16 h. The solution was then diluted with CH_3CN . 1,3,5-trifluorobenzene was added as an internal standard, and the reaction was analyzed by ^{19}F NMR spectroscopy.

Experimental Details for the Equivalents Screen in Figure 5.8. Potassium (4-fluorophenyl)trifluoroborate (**1**) (5.1 mg, 0.025 mmol, 1.0 equiv), $\text{Cu}(\text{OTf})_2$ (36.1 mg, 0.1 mmol, 4.0 equiv), and KN_3 or NaOPiv (1.0–8.0 equiv) were weighed into a 4 mL vial equipped with a magnetic stir bar. CH_3CN (0.3 mL) was added, and the vial was sealed with a Teflon-lined cap. The reaction mixture was allowed to stir at room temperature for 16 h. The solution was then diluted with CH_3CN . 1,3,5-trifluorobenzene was added as an internal standard, and the reaction was analyzed by ^{19}F NMR spectroscopy.

5.7. References

- (1) A portion of this chapter has been adapted with permission from Schimler, S. D.; Sanford, M. S. *Synlett* **2016**, 27, 2279–2284. ©Thieme
- (2) (a) Monnier, F.; Taillefer, M. *Angew. Chem. Int. Ed.* **2009**, 48, 6954–6971. (b) Beletskaya, I. P.; Cheprakov, A. V. *Coord. Chem. Rev.* **2004**, 248, 2337–2364. (c) Ley, S. V.; Thomas, A. W. *Angew. Chem. Int. Ed.* **2003**, 42, 5400–5449.
- (3) Qiao, J. X.; Lam, P. Y. S. *Synthesis* **2011**, 6, 829–856.
- (4) (a) Chan, D. M. T.; Monaco, K. L.; Wang, R.-P.; Winters, M. P. *Tetrahedron Lett.* **1998**, 39, 2933–2937. (b) Evans, D. A.; Katz, J. L.; West, T. R. *Tetrahedron Lett.* **1998**, 39, 2937–2940. (c) Lam, P. Y. S.; Clark, C. G.; Saubern, S.; Adams, J.; Winters, M. P.; Chan, D. M. T.; Combs, A. *Tetrahedron Lett.* **1998**, 39, 2941–2944.
- (5) Yang, H.; Li, Y.; Jiang, M.; Wang, J.; Fu, H. *Chem. Eur. J.* **2011**, 17, 5652–5660.
- (6) (a) Zhang, L.; Zhang, G.; Zhang, M.; Cheng, J. *J. Org. Chem.* **2010**, 75, 7472–7474. (b) Dai, J.-J.; Liu, J.-H.; Luo, D.-F.; Liu, L. *Chem. Commun.* **2011**, 47, 677–679. (c) Huang, F.; Quach, T. D.; Batey, R. A. *Org. Lett.* **2013**, 15, 3150–3153.
- (7) Notably, many Chan-Lam-Evans coupling reactions employ Cu^{II} carboxylate salts as catalysts; however, aryl–OC(O)R side products are rarely reported.
- (8) Ye, Y.; Schimler, S. D.; Hanley, P. S.; Sanford, M. S. *J. Am. Chem. Soc.* **2013**, 135, 16292–16295.
- (9) (a) *Boronic Acids: Preparation and Applications in Organic Synthesis and Medicine*, 2nd ed.; Hall, D. G., Ed.; Wiley-VCH: Weinheim, 2005. (b) Darses, S.;

- Genet, J.-P. *Chem. Rev.* **2008**, *108*, 288–325. (c) Molander, G. A.; Sandrock, D. L. *Curr. Opin. Drug Discovery Dev.* **2009**, *12*, 811–823.
- (10) For an example of C(sp³)–OTs reductive elimination from Pd^{IV}, see: Camasso, N. M.; Pérez-Temprano, M. H.; Sanford, M. S. *J. Am. Chem. Soc.* **2014**, *136*, 12771–12775.
- (11) Xu, Y.; Yan, G.; Ren, Z.; Dong, D. *Nature Chem.* **2015**, *7*, 829–834.
- (12) (a) Szumigala, R. H.; Devine, P. N.; Gauthier, D. R.; Volante, R. P. *J. Org. Chem.* **2004**, *69*, 566–569. (b) Zhang, G.; Lv, G.; Li, L.; Chen, F.; Cheng, J. *Tetrahedron Lett.* **2011**, *52*, 1993–1995. (c) Yao, M.-L.; Reddy, M. S.; Yong, L.; Walfish, I.; Blevins, D. W.; Kabalka, G. W. *Org. Lett.* **2010**, *12*, 700–703. (d) Kabalka, G. W.; Mereddy, A. R. *Organometallics* **2004**, *23*, 4519–4521. (e) Thiebes, C.; Prakash, G. K. S.; Petasis, N. A.; Olah, G. A. *Synlett* **1998**, *2*, 141–142. (f) Yao, M.-L.; Kabalka, G. W.; Blevins, D. W.; Reddy, M. S.; Yong, L. *Tetrahedron* **2012**, *68*, 3738–3743. (g) Murphy, J. M.; Liao, X.; Hartwig, J. F. *J. Am. Chem. Soc.* **2007**, *129*, 15434–15435. (h) Thompson, A. L. S.; Kabalka, G. W.; Akula, M. R.; Huffman, J. W. *Synthesis* **2005**, *4*, 547–550.
- (13) See ref 12b, 12e, 12f, 12h, and (a) Kabalka, G. W.; Mereddy, A. R. *Tetrahedron Lett.* **2004**, *45*, 343–345. (b) Ren, Y.-L.; Tian, X.-Z.; Dong, C.; Zhao, S.; Wang, J.; Yan, M.; Qi, X.; Liu, G. *Catal. Commun.* **2013**, *32*, 15–17. (c) Partridge, B. M.; Hartwig, J. F. *Org. Lett.* **2013**, *15*, 140–143. (d) Kabalka, G. W.; Gooch, E. E. *J. Org. Chem.* **1981**, *46*, 2582–2584. (e) Akula, M. R.; Yao, M.-L.; Kabalka, G. W. *Tetrahedron Lett.* **2010**, *51*, 1170–1171.
- (14) See ref 12a, 12g and (a) Wu, H.; Hynes Jr., J. *Org. Lett.* **2010**, *12*, 1192–1195. (b) Molander, G. A.; Cavalcanti, L. N. *J. Org. Chem.* **2011**, *76*, 7195–7203.
- (15) (a) Bräse, S.; Gil, C.; Knepper, K.; Zimmermann, V. *Angew. Chem. Int. Ed.* **2005**, *44*, 5188–5240. (b) Scriven, E. F. V.; Turnbull, K. *Chem. Rev.* **1988**, *88*, 297–368. (c) *Applications of Photochemistry in Probing Biological Targets*; Tometsko, A. M.; Richards, F. W. Eds.; Annals of the New York Academy of Sciences: New York, 1980.
- (16) (a) Yoshida, S.; Misawa, Y.; Hosoya, T. *Eur. J. Org. Chem.* **2014**, 3991–3995. (b) Lanke, S. R.; Bhanage, B. M. *Synth. Commun.* **2014**, *44*, 399–407. (c) Tao, C.-Z.; Cui, X.; Li, J.; Liu, A.-X.; Liu, L.; Guo, Q.-X. *Tetrahedron Lett.* **2007**, *48*, 3525–3529. (d) Li, Y.; Gao, L.-X.; Han, F.-S. *Chem. Eur. J.* **2010**, *16*, 7969–7972. (e) Grimes, K. D.; Gupte, A.; Aldrich, C. C. *Synthesis* **2010**, *9*, 1441–1448. (f) Huber, M.-L.; Pinhey, J. T. *J. Chem. Soc. Perkin Trans.* **1990**, 721–722. (g) Kumar, A. S.; Reddy, M. A.; Knorn, M.; Reiser, O.; Sreedhar, B. *Eur. J. Org. Chem.* **2013**, 4674–4680.
- (17) (a) Casitas, A.; Ribas, X. *Chem. Sci.* **2013**, *4*, 2301–2318. (b) Hickman, A. J.; Sanford, M. S. *Nature* **2012**, *484*, 177–185.
- (18) (a) Thompson, L. A.; Ellman, J. A. *Chem. Rev.* **1996**, *96*, 555–600. (b) Spandl, R. J.; Thomas, G. L.; Diaz-Gavilan, M.; O'Connell, K. M. G.; Spring, D. R. An Introduction to Diversity-Oriented Synthesis. In *Linker Strategies in Solid-Phase Organic Synthesis*; Scott, P. J. H. Ed. John Wiley & Sons, Ltd.: 2009; pp. 241–262. (c) Hajduk, P. J.; Galloway, W. R. J. D.; Spring, D. R. *Nature* **2011**, *470*, 42–43.

- (19) Vedejs, E.; Chapman, R.W.; Fields, S.C.; Lin, S.; Schrimpf, M.R. *J. Org. Chem.* **1995**, *60*, 3020–3027.
- (20) Molander, G.A.; Biolatto, B. *Org. Lett.* **2002**, *4*, 1867–1870.
- (21) Breugst, M.; Mayr, H. *J. Am. Chem. Soc.* **2010**, *132*, 15380–15389.
- (22) Fier, P. S.; Luo, J.; Hartwig, J. F. *J. Am. Chem. Soc.* **2013**, *135*, 2552–2559.
- (23) Gillis, E. P.; Burke, M. D. *J. Am. Chem. Soc.* **2007**, *129*, 6716–6717.
- (24) Deleersnyder, K.; Mehdi, H.; Horváth, I. T.; Binnemans, K.; Parac-Vogt, T. N. *Tetrahedron* **2007**, *63*, 9063–9070.
- (25) Pérez-Temprano, M. H.; Racowski, J. M.; Kampf, J. W.; Sanford, M. S. *J. Am. Chem. Soc.* **2014**, *136*, 4097–4100.
- (26) Bradamante, S.; Pagani, G. A. *J. Org. Chem.* **1980**, *45*, 114–122.
- (27) Sweeney, Z. K.; Welch, M. Non-nucleoside reverse transcriptase inhibitors. US7906540 B2, March 15, 2011.
- (28) Zeng, J.; Liu, K. M.; Duan, X. F. *Org. Lett.* **2013**, *15*, 5342–5345.
- (29) Kashyap, B.; Phukan, P. *RCS Advances* **2013**, *3*, 15327–15336.
- (30) Yamagami, C.; Takao, N.; Nishioka, T.; Fujita, T.; Takeuchi, Y. *Org. Magn. Resonance* **1984**, *22*, 439–445.
- (31) Tang, P.; Ritter, T. *Tetrahedron* **2011**, *67*, 4449–4454.
- (32) Quasdorf, K. W.; Tian, X.; Garg, N. K. *J. Am. Chem. Soc.* **2008**, *130*, 14422–14423.
- (33) Gøgsig, T.M.; Kleimark, J.; Nilsson Lill, S.O.; Korsager, S.; Lindhardt, A.T.; Norrby, P.-O.; Skrydstrup, T. *J. Am. Chem. Soc.* **2012**, *134*, 443–452.
- (34) Jiménez-González, L.; García-Muñoz, S.; Álvarez-Corral, M.; Muñoz-Dorado, M.; Rodríguez-García, I. *Chem. Eur. J.* **2007**, *13*, 557–568.
- (35) Zarate, C.; Martin, R. *J. Am. Chem. Soc.* **2014**, *136*, 2236–2239.
- (36) Platon, M.; Cui, L.; Mom, S.; Richard, P.; Saeys, M.; Mierso, J.-C. *Adv. Synth. Catal.* **2011**, *353*, 3403–3414.
- (37) Ankner, T.; Hilmer, G. *Org. Lett.* **2009**, *11*, 503–506.
- (38) Gurung, S.K.; Thapa, S.; Vangala, A.S.; Giri, R. *Org. Lett.* **2013**, *15*, 5378–5381.
- (39) Kawamoto, T.; Sato, A.; Ryu, I. *Org. Lett.* **2014**, *16*, 2111–2113.
- (40) Cuthbertson, J.; Gray, V.J.; Wilden, J.D. *Chem. Commun.* **2014**, *50*, 2575–2578.
- (41) Shrestha, R.; Mukherjee, P.; Tan, Y.; Litman, Z.C.; Hartwig, J. F. *J. Am. Chem. Soc.* **2013**, *135*, 8480–8483.
- (42) Tye, H.; Eldred, C.; Willis, M. *J. Chem. Soc., Perkin Trans. 1* **1998**, 457.
- (43) Sawanishi, H.; Tajima, K.; Tsuchiya, T. *Chem. Pharm. Bull.* **1987**, *35*, 4101–4108.

CHAPTER 6

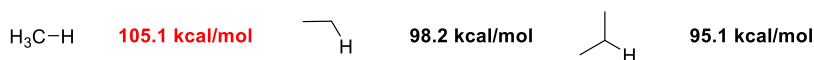
Metal-Catalyzed Selective Borylation of Methane and Ethane¹

6.1. Background

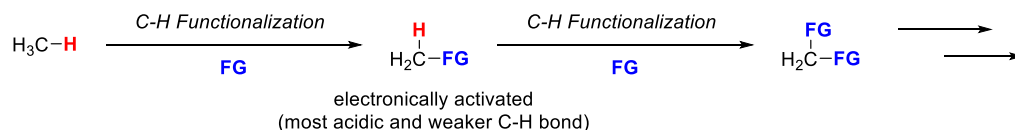
Over the past few decades, a variety of homogenous transition metal catalysts have been developed for the C–H functionalization of alkanes.^{2,3} Despite the breadth of catalysts developed for the functionalization of liquid alkanes, there are still very few methods for the selective C–H functionalization of gaseous alkanes such as methane and ethane.⁴ The limited application of these methods to methane is in large part due to particular challenges associated with functionalization of the C–H bonds in methane (Figure 6.1). The C–H bonds of methane are stronger than those of other alkanes (for example, the H₃C–H bond dissociation energy is 105.1 kcal/mol versus 98.2 kcal/mol for ethane).⁵ As such, C–H bond cleavage is much more difficult than for other alkanes with many catalysts. Furthermore, the C–H bonds of methane have low polarity due to the similar electronegativities of carbon and hydrogen ($\chi_{\text{C}} = 2.55$, $\chi_{\text{H}} = 2.20$).⁶ Additionally, overfunctionalization is often an issue for methane functionalization. The C–H bonds of the initial functionalized product (CH₃X) are often more reactive because they are weaker and more acidic than those of methane. Finally, due to the gaseous nature of methane, a solvent must be used to solubilize methane in order for it to react. A solvent that is inert, compatible with the reaction conditions, and that solubilizes methane without itself getting functionalized must therefore be identified.

Figure 6.1. Challenges Associated with the C–H Functionalization of Methane

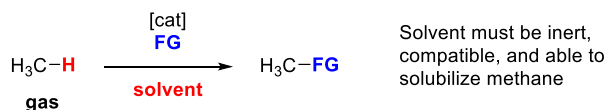
Bond Strength (BDE)



Overfunctionalization

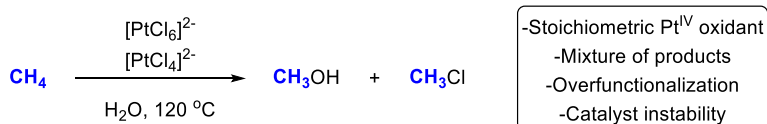


Solvent Compatibility



Despite the challenges of C–H functionalization of methane, a number of methods have been developed. In the 1970s, Shilov reported the Pt^{II} -catalyzed conversion of methane to a mixture of functionalized products: methanol and chloromethane (Scheme 6.1).⁷ This method uses stoichiometric Pt^{IV} salts as oxidants for the electrophilic activation of methane. While this method was a promising first step in methane functionalization, there are many issues with this system. Conversions are generally low, due to the low stability of the platinum catalyst, which decomposes rapidly to form platinum black (Pt^0). A mixture of products is typically produced and overfunctionalization of the initial product of methane functionalization cannot be avoided. Furthermore, the use of stoichiometric Pt^{IV} oxidants cannot be applied to large scale processes due to cost and availability limitations, and limited success has been achieved in using more economically viable oxidants for this transformation.

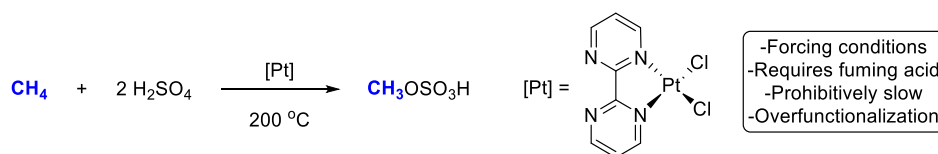
Scheme 6.1. Shilov Electrophilic Activation of Methane with Pt^{II} Catalyst



Twenty years after Shilov's initial results, Periana *et al.* reported the conversion of methane to a protected methanol derivative ($\text{CH}_3\text{OSO}_3\text{H}$) using a Pt^{II} catalyst stabilized

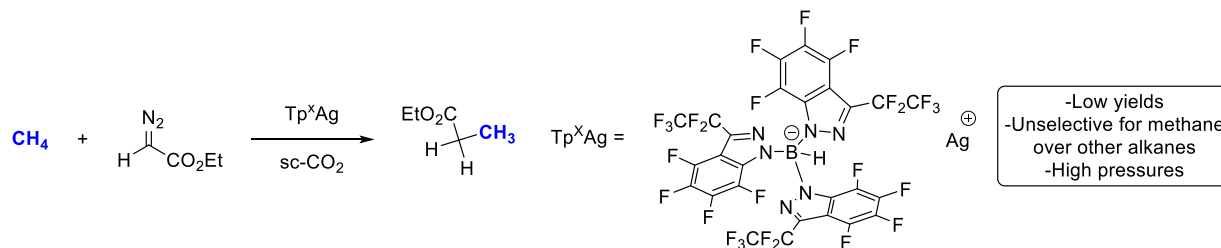
by a bipyrimidine (bpym) ligand (Scheme 6.2).⁸ Periana attributes the high reactivity of the Pt^{II} catalyst to the bpym ligand, which stabilizes Pt from decomposing Pt⁰. The methyl ester product of the functionalization reaction is chemically protected from over-oxidation, enabling high yields of the mono-oxygenated product.⁹ However, forcing conditions are necessary to achieve high yields of the desired product (200 °C, fuming sulfuric acid). The selectivity of the reaction is reasonable, but over-oxidation products are still observed in low amounts. Furthermore, the reaction is too slow for application to industrial processes.

Scheme 6.2. Pt-Catalyzed Conversion of Methane to Protected Methyl Ester



Caballero *et al.* took a different approach to methane C–H functionalization by pursuing electrophilic carbene atom insertion into a methane C–H bond.¹⁰ Their method forms a C–C bond between methane and a carbene using a Ag catalyst (Scheme 6.3). This reaction relies on the use of supercritical CO₂ as the reaction medium (which is inert toward functionalization and solubilizes methane), the silver catalyst, and ethyl diazoacetate (the carbene precursor). While Caballero *et al.* did not observe overfunctionalization of the product, the reaction was very low yielding (<20%), required high pressures (250 bar), and was not selective for methane over other alkanes.

Scheme 6.3. Ag-Catalyzed C–C Bond Formation Between Methane and Carbene



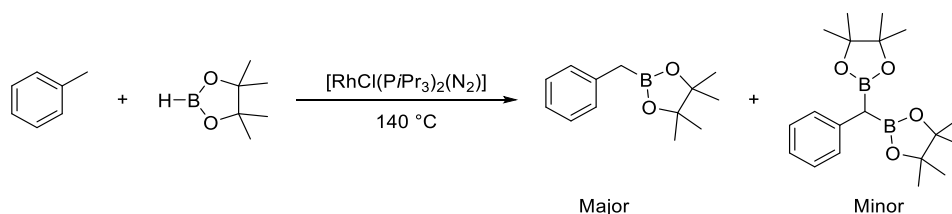
Despite the above advances in C–H functionalization of methane, there is still much room for improvement. Current methodologies suffer from overfunctionalization, inefficient catalysts, harsh conditions, and the formation of a mixture of products. As such, we sought to identify a methane C–H functionalization process that limits overfunctionalization and competing functionalization of solvent. We identified the transition metal catalyzed C–H borylation of liquid alkanes (Scheme 6.4) as an attractive platform for potentially meeting these objectives.^{11,12} A number of transition metal catalysts have been reported for liquid alkane C–H borylation, typically by employing neat reaction conditions (liquid alkane substrate as solvent) and bis(pinacolato)diboron (B_2pin_2) or pinacolborane (HBpin) as the borylating reagent. The selectivity of these reactions is dictated by sterics, with terminal $C(sp^3)$ –H bonds undergoing selective functionalization relative to secondary and tertiary C–H bonds.¹³

Scheme 6.4. Transition Metal Catalyzed C–H Borylation of Alkanes



The introduction of a Bpin substituent has been shown to electronically activate adjacent sp^3 -C–H bonds towards further C–H borylation by making them more acidic.^{14,15,16} One such example is in benzylic borylation, in which the C–H borylation of primary benzylic C–H bonds is often slower than that of the secondary C–H bond alpha to the boryl substituent of the product.^{14,15} For example, Marder and coworkers reported the borylation of toluene using a Rh catalyst (Scheme 6.5).¹⁴ A combination of benzylic monoborylation and diborylation were observed. Based on the concentrations of toluene and the monoborylated product, the yield observed for diborylated product indicated that the first borylation activated the remaining benzylic C–H bonds for further functionalization. However, there are few examples in the literature that examine the interplay between electronics and sterics in C–H borylation reactions, especially in regard to the identity of the transition metal catalyst.

Scheme 6.5. Benzylic C–H Borylation of Toluene

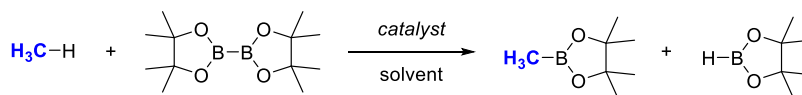


In 2005, Hall and Hartwig reported an experimental and computational study on the mechanism of sp^3 -C–H borylation of alkanes using a rhodium catalyst ($Cp^*Rh(\eta^6-C_6Me_6)$).¹⁷ For the computational portion, they used methane as the model substrate. These DFT computations suggested that the Rh catalyst should be capable of catalyzing the C–H borylation of methane, but no experimental work was conducted to support this proposal.

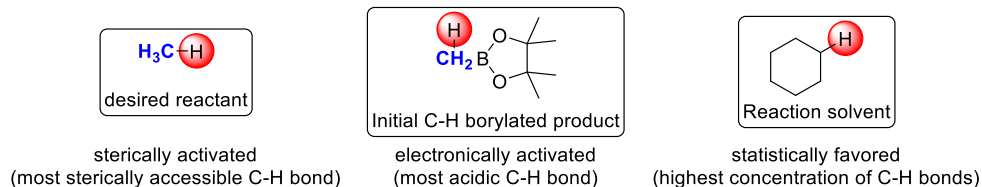
We sought to develop a methodology for the transition metal catalyzed C–H borylation of methane (Figure 6.2). A number of challenges were identified with respect to controlling the selectivity of the reaction. Conditions were sought to selectively functionalize the C–H bonds of methane (sterically most accessible) over the more reactive C–H bonds of the initial borylated product (most acidic) and the statistically favored C–H bonds of solvent (highest concentration). It was hypothesized that the selectivity of the reaction could be tuned by modifying the transition metal catalyst or the boron reagent. This design would allow for a better understanding of the interplay between sterics and electronics in governing C–H borylation reactions.

Figure 6.2. Reactivity and Selectivity Challenges of Methane C–H Borylation

Desired selective C–H borylation of methane:



Selectivity challenges:

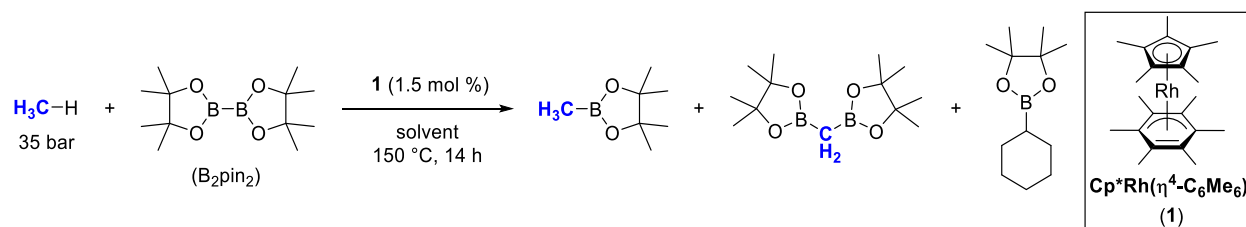


This chapter discusses the development of a method for the C–H borylation of gaseous alkanes, specifically methane and ethane. Reactivity and selectivity as a function of transition metal catalysts and boron reagents were explored. A ruthenium dimer was identified to be relatively reactive, and this catalyst also provided the highest selectivity for mono-borylation of methane. Finally, a pinene-derived diboron reagent was found to be as selective and reactive as B₂pin₂ for the C–H borylation reaction when the ruthenium dimer was employed as the catalyst.

6.2. Initial Studies and Optimization with Cp^{*}Rh(η⁴-C₆Me₆)^A

For initial investigations, Cp^{*}Rh(η⁴-C₆Me₆) (**1**)¹² was selected for methane C–H borylation, based on the computational studies of Hall and Hartwig.¹⁷ The initial reactions were conducted in a Parr high-pressure batch reactor (45 mL total volume) at 150 °C using 1.5 mol % of **1** at 35.0 bar of methane with bis(pinacolato)diboron (B₂pin₂) as the limiting reagent (0.89 mmol). The choice of solvent for the methane borylation reaction was particularly important; any C–H bonds in the solvent need to be less reactive towards C–H activation with **1** than those of CH₄ (Table 6.1). Furthermore, the solvent must be able to solubilize both **1** and CH₄ for productive reactivity. Initial studies focused on the use of perfluorinated solvents, where competing C–H functionalization of solvent would be mitigated; furthermore, methane is highly soluble in perfluorinated solvents.¹⁸ However, perfluorohexane (PFH), perfluoromethyl cyclohexane (PFMCH), and hexafluorobenzene (C₆F₆) provided only modest yields of methane borylation products (entries 1–3), likely due to the low solubility of Rh catalyst **1** in these solvents.

^A Part of the work in this section was done in collaboration with Dr. Amanda Cook. Dr. Cook's contributions include determination of experimental set up and optimizations of catalyst **1** in Table 6.1. All yields and ratios reported in Tables 6.1 and 6.2 represent data collected by Sydonie Schimler.

Table 6.1. Solvent for Methane C–H Borylation Catalyzed by **1**^a

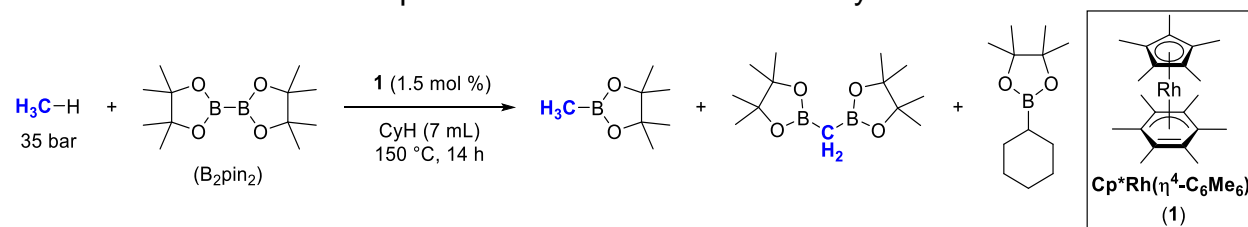
entry	solvent	% yield ^b CH_3Bpin	$\text{CH}_3\text{Bpin}:\text{solventBpin}^b$	$\text{CH}_3\text{Bpin}:\text{CH}_2(\text{Bpin})_2^b$
1	PFH	28	nd	8:1
2	PFMCH	<1	nd	nd
3	C_6F_6	4	nd	nd
4	cyclopentane	70	8:1	9:1
5	cyclohexane (CyH)	69	50:1	10:1
6	hexanes	10	1:1	nd
7	THF	<1	nd	nd
8	NMP	<1	nd	nd
9	2.5:1 PFH/CyH	48	80:1	6:1

^aConditions: B_2pin_2 (0.89 mmol, 1.00 equiv), **1** (0.027 mmol, 0.015 equiv), 35.0 bar methane, and solvent (7.0 mL) in a reactor at 150 °C for 14 h. ^bYields and ratios of all product were determined by gas chromatography-flame ionization detector (GC-FID) and are based on B_2pin_2 as the limiting reagent.

Cycloalkanes were next examined as solvents, as the sterically congested secondary C–H bonds are poor substrates for C–H borylation.¹⁹ Cyclopentane provided high yields of C–H borylated methane but solvent borylation was a major side reaction (entry 4). Cyclohexane (CyH) proved to be a more optimal solvent, affording CH_3Bpin in 70% yield with only traces of solvent borylation (~2%) (entry 5). With CyH as solvent, high selectivity was observed for monoborylation of methane relative to diborylation. Linear alkanes such as hexanes were poor solvents for methane borylation, as solvent borylation was a competitive process (entry 6).¹² Other solvents such as THF and NMP²⁰ provided none of the desired C–H borylated product, and at the end of these reactions, the mass balance was primarily unreacted B_2pin_2 (entries 7–8). To try to reduce the amount of solvent borylation further, solvent mixtures of CyH and PFH were examined for the C–H borylation reaction, but this afforded lower yields of CH_3Bpin (entry 9).

With cyclohexane identified as the ideal solvent for the C–H borylation of methane, further optimization of this transformation with catalyst **1** was investigated (Table 6.2). Lowering the catalyst loading to 0.75 mol % resulted in decreased yield relative to the

standard conditions but a slight improvement in the selectivity for monoborylation over diborylation (entry 2). Increasing the loading of **1** to 3.0 mol % resulted in higher yield of CH₃Bpin (99%) while maintaining excellent selectivity for methane borylation over both solvent borylation (59:1) and diborylation (9:1) (entry 3). Changing the concentration had minimal effect on the yield of CH₃Bpin but did have an impact on the selectivity of the reaction. Increasing the concentration of the reaction resulted in poor selectivity for monoborylation versus diborylation (4:1; entry 4). Diluting the reaction afforded comparable yields of CH₃Bpin, while significantly improving the selectivity of the reaction for CH₃Bpin over CH₂(Bpin)₂ (20:1, entry 5). Changing the temperature (to 130 °C or 170 °C) resulted in lower yields of methane borylation while maintaining the same selectivity that is observed at 150 °C (entries 6 and 7). Increasing the pressure of methane has a marked effect on the overall borylation reaction (entry 8). At 50.0 bar CH₄, the reaction proceeded to 82% yield of CH₃Bpin, with excellent selectivity for methane over solvent (82:1) and diborylation (15:1). Decreasing the methane pressure to 25.0 bar had a detrimental impact on both the yield and selectivity of the reaction (entry 9). For subsequent studies, the conditions in entry 3 of Table 6.2 using 3.0 mol % of **1** were chosen, as they consistently provided the most reproducible results.

Table 6.2. Optimization of Methane C–H Borylation with **1**^a

entry	conditions	% yield ^b CH_3Bpin	$\text{CH}_3\text{Bpin}:\text{solventBpin}^b$	$\text{CH}_3\text{Bpin}:\text{CH}_2(\text{Bpin})_2^b$
1	no change	69	50:1	10:1
2	0.75 mol % 1	55	39:1	12:1
3	3.0 mol % 1	96	57:1	5:1
4	3.5 mL CyH	53	41:1	4:1
5	14.0 mL CyH	71	45:1	20:1
6	130 °C	52	64:1	10:1
7	170 °C	68	28:1	9:1
8	50 bar CH_4	82	68:1	15:1
9	25 bar CH_4	62	27:1	7:1

^aConditions: B_2pin_2 (0.89 mmol, 1.00 equiv), **1**, methane, and CyH in a reactor for 14 h.

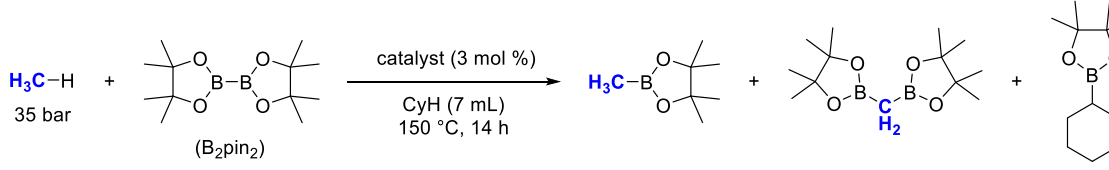
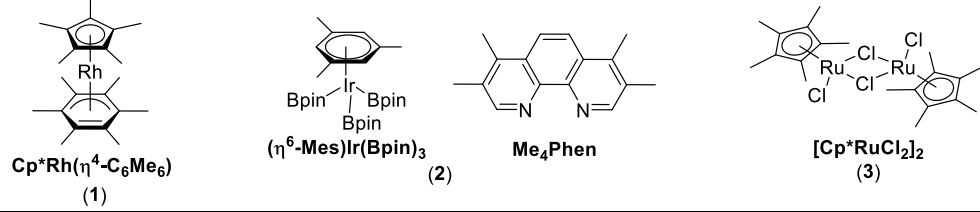
^bYields and ratios of all product were determined by gas chromatography-flame ionization detector (GC-FID) and are based on B_2pin_2 as the limiting reagent.

6.3. Evaluation of Catalysts^B

Other catalysts were examined for the C–H borylation of methane. Initial studies focused on the combination of $(\eta^6\text{-Mes})\text{Ir}(\text{Bpin})_3$ and 3,4,7,8-tetramethyl-1,10-phenanthroline (Me_4Phen) (catalyst **2**) as well as $[\text{Cp}^*\text{RuCl}_2]_2$ (**3**), both of which are known catalysts for the C–H borylation of liquid alkanes.^{21,22} Under the optimal conditions for catalyst **1** (3.0 mol %), Ir catalyst **2** provided modest yield of CH_3Bpin but very poor selectivity for methane over solvent borylation and borylation of CH_3Bpin (Table 6.3, entry 2). The C–H borylation of cyclohexane has previously been reported with this catalyst,¹⁹ and while the yields were modest, it is possible that in this system, the C–H bonds of cyclohexane could reactive competitively to the desired functionalization of the C–H bonds of methane. Ru catalyst **3** provided good yields of CH_3Bpin as well as improved selectivity relative to Rh catalyst **1** (entry 3).

^B Part of the work in this section was done in collaboration with Dr. Amanda Cook. Dr. Cook's contributions include optimizations with catalyst **1–3** with B_2pin_2 and reactivity with ethane. All yields and ratios in Table 6.3 represent data collected by Sydonie Schimler.

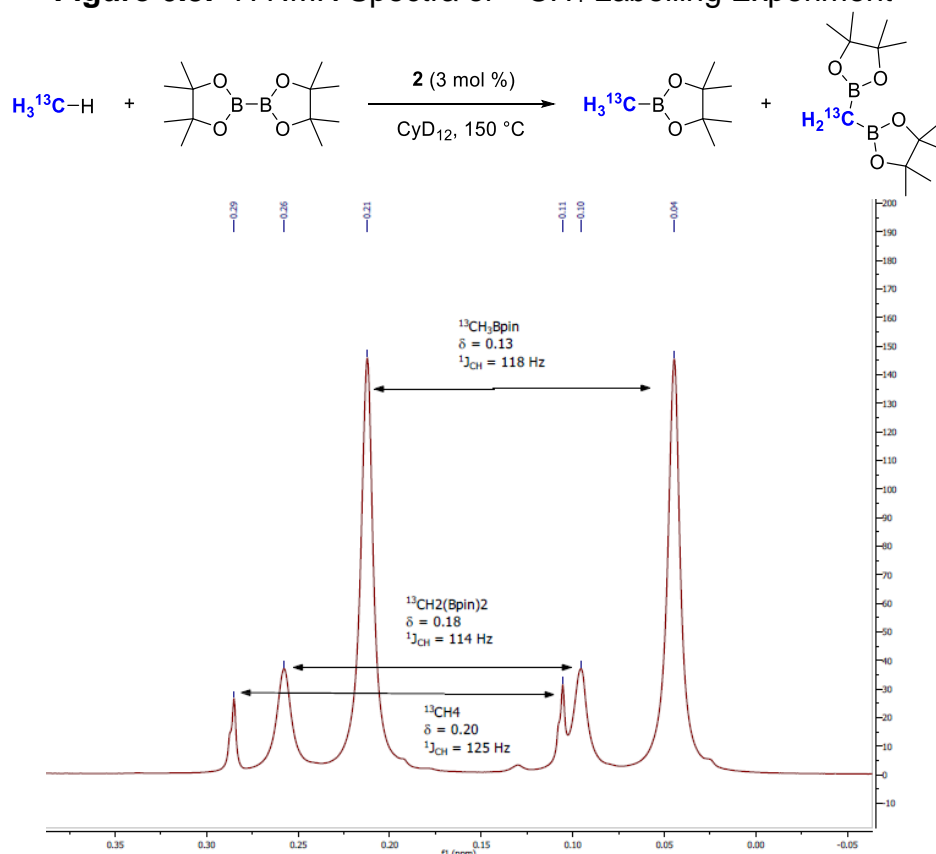
Table 6.3. Impact of Catalyst Choice on the Yield and Selectivity of Methane Borylation^a

				
				
entry	catalyst	% yield ^b CH ₃ Bpin	CH ₃ Bpin:solventBpin ^b	CH ₃ Bpin:CH ₂ (Bpin) ₂ ^b
1	1	96	57:1	9:1
2	2	46	3:1	2:1
3	3	63	85:1	16:1

^aConditions: B₂pin₂ (0.89 mmol, 1.00 equiv), catalyst (3.0 mol % with respect to metal), methane (35.0 bar), and CyH (7.0 mL) in a reactor at 150 °C for 14 h. ^bYields and ratios of all product were determined by gas chromatography-flame ionization detector (GC-FID) and are based on B₂pin₂ as the limiting reagent.

To unambiguously determine the source of the diborylated product (CH₂(Bpin)₂), ¹³CH₄ was used as the substrate for C–H borylation with Ir catalyst **2**. When ¹³CH₄ was used as the substrate under otherwise identical conditions, 33% of ¹³CH₃Bpin was produced. The diborylated product ¹³CH₂(Bpin)₂ was produced in 18% yield and was labelled with carbon-13. Products were verified by ¹H NMR spectroscopy (Figure 6.3). This suggests that the source of the diborylated product is methane and that it is not a result of decomposition of B₂pin₂.²³

Figure 6.3. ^1H NMR Spectra of $^{13}\text{CH}_4$ Labelling Experiment^a



^aConditions: B_2Pin_2 (0.890 mmol, 1.00 equiv), catalyst **2** (3 mol%), $^{13}\text{CH}_4$ (27.6 bar), and C_6D_{12} (7 mL) in a reactor at 150°C for 14 h. The crude reaction mixture was analyzed by ^1H NMR spectroscopy.

Next, the reactivity of catalysts **1–3** with other simple alkanes as well as with the other components of the methane borylation reaction (namely, cyclohexane and CH_3Bpin) were examined (Table 6.4). The borylation of ethane (C_2H_6) under conditions identical to those of the borylation of methane proceeded in modest to high yields with catalysts **1–3** (entries 1–3).^c Ru catalyst **3** provided very low yields of $\text{H}_3\text{C}-\text{CH}_2\text{Bpin}$ (20%). Not surprisingly, all three catalysts were very efficient at the borylation of hexanes (entries 4–6). This is consistent with the extensive literature on the borylation reactions of liquid straight-chain alkanes.^{12,21,22} Cyclohexane was a poor substrate for the borylation reactions with catalysts **1–3**; this is consistent with the literature on the difficulty of functionalizing secondary $\text{sp}^3\text{-C-H}$ bonds due to sterics.¹⁹ Catalysts **1** and **2** reacted with

^c Data for the borylation of ethane was collected by Dr. Amanda Cook.

CH₃Bpin to produce the diborylated product CH₂(Bpin)₂ in modest yield (entries 10 and 11). The moderate reactivity of this substrate is presumably due to the acidity of the C–H bonds which are more activated in comparison to the C–H bonds of methane. Catalyst **3** was a poor catalyst for this borylation of CH₃Bpin, affording only 28% of the borylated product (entry 12). This is consistent with the selectivity that is observed in the methane borylation reactions, where **3** is considerably more selective for methane than **2** and **3** (Table 6.3).

Table 6.4. C–H Borylation of Alkanes with Catalysts **1–3**

$\text{R-H} + \text{B}_2\text{pin}_2 \xrightarrow[\text{CyH, 150 } ^\circ\text{C}]{\text{catalyst (3 mol \%)}} \text{R-Bpin}$				
entry	substrate	product	catalyst	% yield R-Bpin ^d
1	ethane ^a		1	78
2	(C ₂ H ₆)		2	48
3			3	20
4	hexanes ^b		1	76
5	(C ₆ H ₁₄)		2	88
6			3	73
7	cyclohexane ^b		1	9
8	(c-C ₆ H ₁₂)		2	8
9			3	2
10	CH ₃ Bpin ^c		1	54
11			2	53
12			3	28

^aConditions: B₂pin₂ (0.89 mmol, 1.00 equiv), catalyst (3.0 mol % with respect to metal), ethane (35.0 bar), and CyH (7.0 mL) at 150 °C for 14 h. ^bConditions: B₂pin₂ (0.166 mmol, 1.00 equiv), catalyst (3.0 mol % with respect to metal), and cyclohexane or hexane (1.3 mL) in a Schlenk tube at 150 °C for 14 h. ^cConditions: B₂pin₂ (0.166 mmol, 1.00 equiv), catalyst (3.0 mol % with respect to metal), CH₃Bpin (0.166 mmol, 1.00 equiv), and cyclohexane (1.3 mL) in a Schlenk tube at 150 °C for 14 h. ^dYields of all product were determined by gas chromatography-flame ionization detector (GC-FID) and are based on B₂pin₂ as the limiting reagent.

The relative reactivity between methane and ethane is also important to study, given that ethane is the second most abundant component of natural gas. However, this relative reactivity is rarely addressed in C–H functionalization reactions.¹⁰ Moreover, in most reported studies, ethane is found to be more reactive than methane.²⁴ To probe the selectivity of catalysts **1–3** for methane versus ethane, known molar quantities of each

gas were added to a high-pressure reactor.^D After 14 h reaction time, the ratio of CH₃Bpin to CH₃CH₂Bpin was determined for each catalyst. The ratio of CH₃Bpin:CH₃CH₂Bpin was then corrected for the number of C–H bonds in each substrate (6 in CH₃CH₃ to 4 in CH₄) as well as the relative solubilities of the two gases (determined by Raman spectroscopy, see experimental section below). As shown in Table 6.5, all catalysts exhibit a ≥3.6:1 preference for the C–H borylation of methane over ethane. This finding is consistent with sterically controlled selectivity; the more accessible C–H bonds of methane are functionalized in preference to the more congested C–H bonds of ethane. The choice of catalyst influences the level of selectivity to a moderate degree. Rh catalyst **1** is most selective (6.1:1) while Ru catalyst **3** is least selective (3.6:1).

Table 6.5. Methane and Ethane One-Pot Competition^a

CH₄ + CH₃CH₃
35 bar (total)

+

→

catalyst (3 mol %)
CyH, 150 °C, 14 h

+

entry	catalyst	selectivity factor CH ₄ :CH ₃ CH ₃ ^b
1	1	6.1:1
2	2	4.2:1
3	3	3.6:1

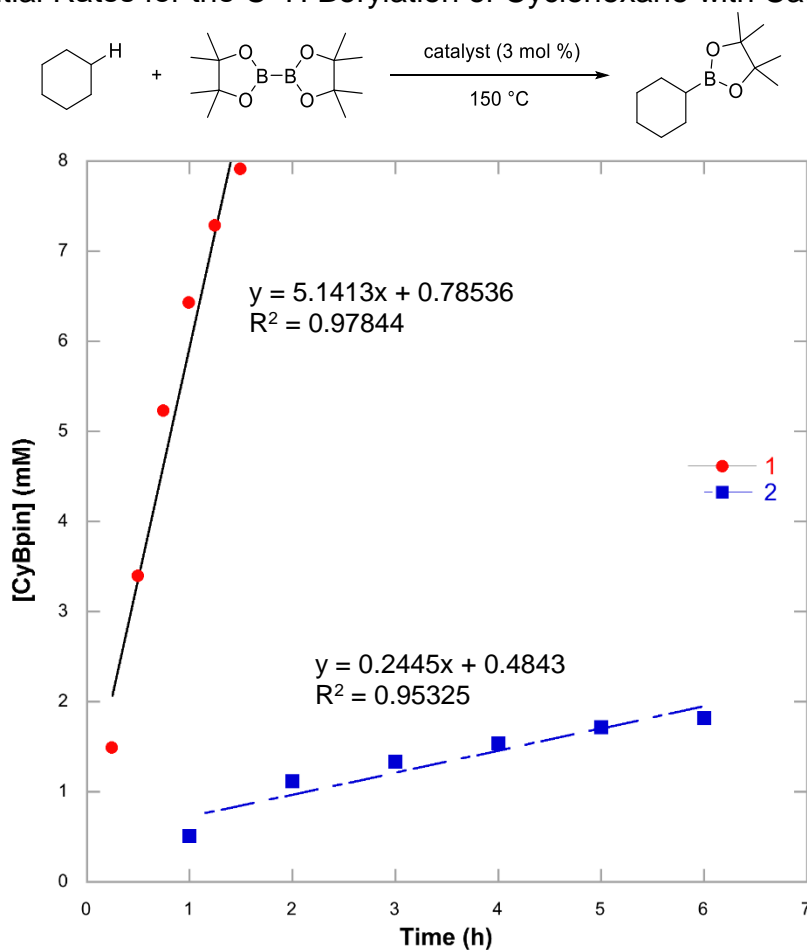
^aConditions: B₂pin₂ (0.89 mmol, 1.00 equiv), catalyst (3.0 mol % with respect to metal), methane and ethane (35.0 bar total), and CyH (7.0 mL) in a reactor at 150 °C for 14 h. Yields of all product were determined by gas chromatography-flame ionization detector (GC-FID) and are based on B₂pin₂ as the limiting reagent. ^bCorrected for solubility and statistics (see experimental section below).

The reactivity of catalysts **1** and **2** with cyclohexane and CH₃Bpin were further explored (Ru catalyst **3** was not investigated due to solubility issues). The initial rates of formation of CyBpin (Figure 6.4) and CH₂(Bpin)₂ (Figure 6.5) were examined. For both substrates, Rh catalyst **1** reacts more quickly to form the borylated product. Ir catalyst **2** reacts much slower, producing low yields of CyBpin over 6 h, while reacting faster with

^D Methane/ethane competition experiments were performed in collaboration with Dr. Amanda Cook. Dr. Cook designed the experiments. All yields in Table 6.5 represent an average of three experiments: one experiment performed by Dr. Cook and two experiments performed by Sydonie Schimler. Determination of the solubility of methane and ethane were determined by Prof. Adam Matzger with Raman data collected by Danielle Samblanet and Sydonie Schimler.

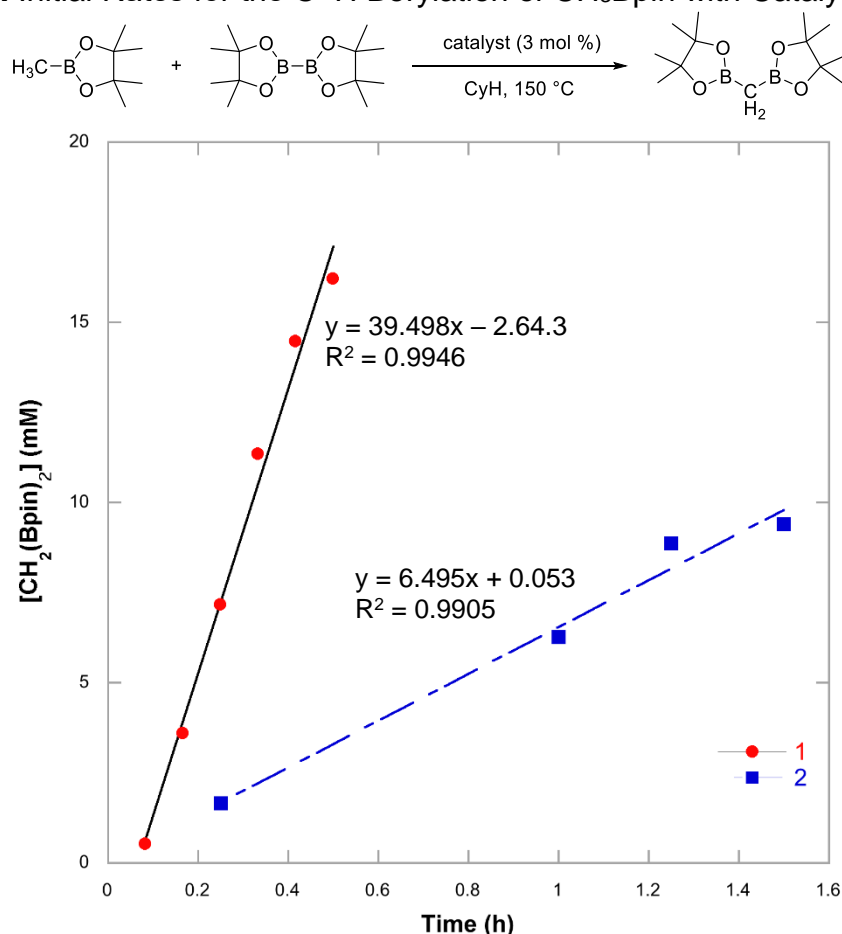
CH₃Bpin to form the diborylated product. These initial rate studies indicate that **1** is more efficient at the borylation of both cyclohexane and CH₃Bpin than **2**. However, in the context of methane C–H borylation, **1** preferentially reacts with methane to form CH₃Bpin, while reacting minimally with cyclohexane and CH₃Bpin. Catalyst **2**, on the other hand, reacts more slowly with cyclohexane and CH₃Bpin but is overall less selective for the C–H borylation of methane. Catalyst **1** reacts quickly to afford CH₃Bpin, while **2** reacts more slowly.

Figure 6.4. Initial Rates for the C–H Borylation of Cyclohexane with Catalysts **1** and **2**^a



^aConditions: B₂pin₂ (0.166 mmol, 1.00 equiv), catalyst (3.0 mol % with respect to metal), and cyclohexane (1.3 mL) in a Schlenk tube at 150 °C for the specified time.

Figure 6.5. Initial Rates for the C–H Borylation of CH₃Bpin with Catalysts **1** and **2**^a



^aConditions: B₂pin₂ (0.166 mmol, 1.00 equiv), catalyst (3.0 mol % with respect to metal), CH₃Bpin (0.166 mmol, 1.00 equiv), and cyclohexane (1.3 mL) in a Schlenk tube at 150 °C for the specified time.

With the promising results obtained with Ru catalyst **3**, other ruthenium complexes were explored to examine their capability of promoting methane C–H borylation (Table 6.6).²⁵ A number of commercially available and easily synthesized Ru complexes were examined. Ru monomers Cp^{*}Ru(pyr)Cl₂ (pyr = pyridine), Cp^{*}Ru(COD)Cl (COD = 1,5-cyclooctadiene), and Cp^{*}Ru(PPh₃)₂Cl all provided lower yields of CH₃Bpin and lower selectivities for borylation of methane (entries 2, 3, and 6). Cationic Ru complex (MeCN)₄RuCpPF₆ afforded none of the desired product (entry 5); furthermore, it was completely insoluble in cyclohexane. [Cp^{*}RuCl₂]₂ (**3**) is also insoluble in cyclohexane at room temperature and this may partly explain the induction period of this catalyst (see ref 1). It was hypothesized that Ru dimers with more solubilizing ligands might provide more active catalysts. However, both [Cp^{*}Ru(OMe)]₂ and [Cp^{*}Ru(SMe)]₂ afforded lower yields

of CH₃Bpin (entries 4 and 7). The polymeric species [Cp*RuCl]₄ afforded comparable yields to that of Ru complex **3** (entry 8). However, the selectivity for methane was reduced. While a more reactive and selective Ru catalyst for the borylation of methane has yet to be identified, it is still worthwhile to pursue other Ru complexes that may provide improved reactivity while maintaining high selectivity for CH₃Bpin.

Table 6.6. Ru Complexes for Methane C–H Borylation^a

entry	catalyst	% yield ^b CH ₃ Bpin	CH ₃ Bpin:solventBpin ^b	CH ₃ Bpin:CH ₂ (Bpin) ₂ ^b
1	[Cp*RuCl ₂] ₂	67	83:1	21:1
2	Cp*Ru(pyr)Cl ₂	25	62:1	18:1
3	Cp*Ru(COD)Cl	30	27:1	11:1
4	[Cp*Ru(SMe)] ₂	3	nd	nd
5	(MeCN) ₄ RuCpPF ₆	<1	nd	nd
6	Cp*Ru(PPh ₃) ₂ Cl	4	nd	nd
7	[Cp*Ru(OMe)] ₂	11	37:1	22:1
8	[Cp*RuCl] ₄	62	69:1	12:1

^aConditions: B₂pin₂ (0.89 mmol, 1.00 equiv), catalyst (3.0 mol % with respect to metal), methane (35.0 bar), and CyH (7.0 mL) in a reactor at 150 °C for 14 h. ^bYields and ratios of all product were determined by gas chromatography-flame ionization detector (GC-FID) and are based on B₂pin₂ as the limiting reagent.

6.4. Evaluation of Diboron Reagents

Having demonstrated the ability to modulate selectivity by changing the transition metal catalyst used for methane C–H borylation, it was of interest to examine the role of the boron reagent in selectivity. Notably, there are few examples in the literature of using

other boron reagents for C–H borylation reactions.²⁶ As such, it was of interest to expand the scope of boron reagents that might be useful for these types of transformations. Initially, the use of pinacolborane (HBpin) was examined. This reagent is more atom economical than B₂pin₂.²⁷ Under the conditions that were developed for the C–H borylation of methane using Rh catalyst **1** and B₂pin₂, the use of HBpin afforded 52% CH₃Bpin with good selectivity (Table 6.7, entry 1). Compared to the use of B₂pin₂, the yield was slightly reduced (52% versus 70%) but borylation of cyclohexane was minimal (100:1 versus 50:1) and the ratio of monoborylation to diborylation was comparable (11:1 versus 9:1). The decreased yield is comparable to literature reports of HBpin having lower reactivity than B₂pin₂.^{12,28} Increasing the catalyst loading had a detrimental effect on the C–H borylation reaction (entry 2). The concentration of the reaction had little impact on the yield of CH₃Bpin (entries 3 and 4), but when the reaction was more dilute, the selectivity for CH₃Bpin over CH₂Bpin₂ was much improved (41:1). The yields of methane C–H borylation with HBpin were modest, and it was hypothesized that the formation of H₂ during the reaction might be inhibiting the desired C–H borylation.²⁹ However, the addition of hydrogen acceptors, such as cyclohexene or norbornene, to the borylation reaction significantly impeded the desired methane C–H borylation reaction. Another possibility for the lower yields observed with HBpin is the degradation of this boron reagent to B₂pin₃, which has been reported to occur at high concentrations of HBpin.^{14,30}

Table 6.7. Methane C–H Borylation with HBpin^a

entry	conditions	% yield ^b CH ₃ Bpin	CH ₃ Bpin:solventBpin ^b	CH ₃ Bpin:CH ₂ (Bpin) ₂ ^b
1	no change	52	100:1	11:1
2	3 mol% 1	40	100:1	20:1
3	3.5 mL CyH	53	>100:1	10:1
4	14.0 mL CyH	57	>100:1	41:1

^aConditions: HBpin (0.89 mmol, 1.00 equiv), **1**, methane (35.0 bar), and CyH in a reactor at 150 °C for 14 h. ^bYields and ratios of all product were determined by gas chromatography-flame ionization detector (GC-FID) and are based on HBpin as the limiting reagent.

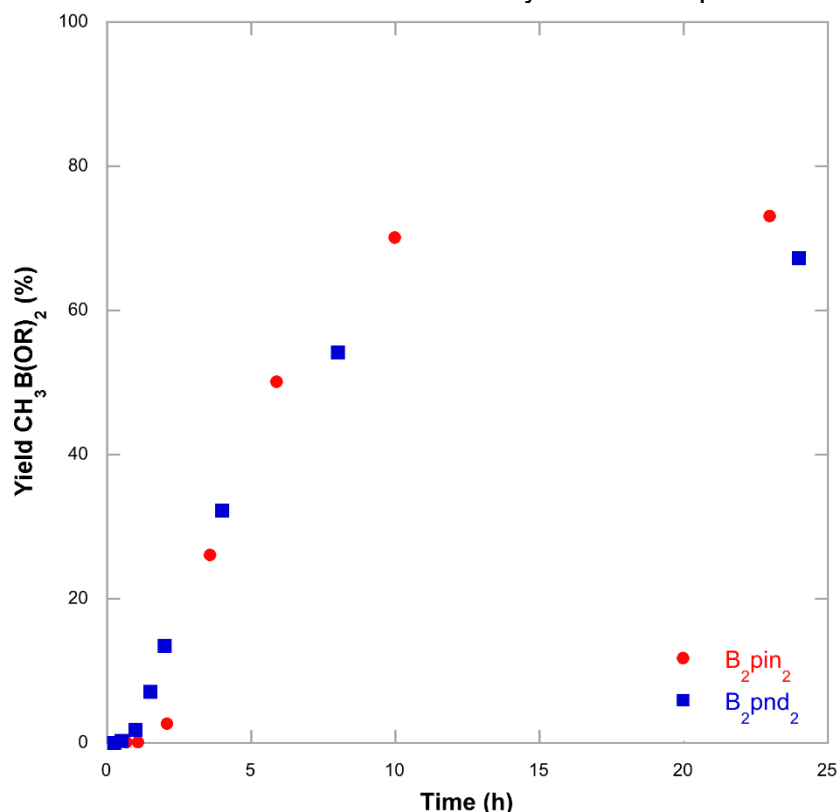
Other commercially available diboron reagents for the C–H borylation of methane were next examined (Table 6.8). The use of HBpin with catalysts **1** and **2** afforded lower yields than B₂pin₂ (entries 2 and 7), but with catalyst **3** the reaction was inhibited with HBpin (entry 12).²¹ Bis(hexylene glycolato)diboron (B₂hg₂) afforded comparable yields to HBpin (entry 3) with **1** but afforded low yields of borylated methane with either **2** or **3** (entries 8 and 13). Bis(neopentyl glycolato)diboron (B₂neo₂) was ineffective as a diboron reagent for methane C–H borylation (entries 4, 9, and 14). Diboron reagents derived from catechol (B₂cat₂) and diethyl-D-tartrate (B₂dtg₂) were inactive for the borylation of methane with all catalysts tested. Bis[(+)-pinanediolato]diboron (B₂pnd₂) as a diboron reagent afforded modest yields of methane C–H borylated product with catalysts **1** and **2** (entries 5 and 10), but with catalyst **3**, the yield of the borylated methane product was quite good (entry 15). Furthermore, the selectivity of this reaction was comparable to that of the C–H methane borylation with **3** and B₂pin₂ (i.e., CH₃Bpin : CH₂(Bpin)₂ = 21:1; see Table 6.3 above for selectivity with B₂pin₂). The reaction of Ru catalyst **3** was monitored using B₂pnd₂ and compared to the reaction with B₂pin₂ (Figure 6.6). The reaction profiles of **3** with the different diboron reagents are very similar; each profile displays an approximately 2 h induction period, followed by rapid formation of the C–H borylated product.

Table 6.8. Diboron Reagents for Methane C–H Borylation^a

$\text{H}_3\text{C}-\text{H} + \text{cat (3 mol \%)} \xrightarrow[\text{CyH (7 mL), 150 }^\circ\text{C, 14 h}]{\text{35 bar}} \text{H}_3\text{C}-\text{B}(\text{OR})_2$			
B₂Pin₂	HBpin	B₂hg₂	B₂neo₂
B₂cat₂	B₂dtg₂	B₂pnd₂	
entry	catalyst	diboron reagent	% yield ^b MeB(OR) ₂
1	1	B ₂ Pin ₂	99
2		HBpin	40
3		B ₂ hg ₂	39
4		B ₂ neo ₂	4
5		B ₂ pnd ₂	49
6	2	B ₂ Pin ₂	45
7		HBpin	23
8		B ₂ hg ₂	7
9		B ₂ neo ₂	<1
10		B ₂ pnd ₂	37
11	3	B ₂ Pin ₂	67
12		HBpin	2
13		B ₂ hg ₂	3
14		B ₂ neo ₂	2
15		B ₂ pnd ₂	52

^aConditions: Diboron reagent (0.89 mmol, 1.00 equiv), catalyst (3.0 mol % with respect to metal), methane (35.0 bar), and CyH (7.0 mL) in a reactor at 150 °C for 14 h. ^bYields and ratios of all product were determined by gas chromatography-flame ionization detector (GC-FID) and are based on boron reagent as the limiting reagent. Yields based on calibration curves of products from reaction with B₂pin₂, except for reactions with B₂pnd₂.

Figure 6.6. Reaction Profiles with Ru Catalyst **3** with B₂pin₂ and B₂pnd₂^a



^aConditions: Diboron reagent (2.67 mmol, 1.00 equiv), [Cp*RuCl₂]₂ (0.04 mmol, 1.5 mol %), methane (35.0 bar), and CyH (21.0 mL) in a reactor at 150 °C for the given time. Yields and ratios of all product were determined by gas chromatography-flame ionization detector (GC-FID) and are based on diboron reagent as the limiting reagent.

B₂pnd₂ has rarely been used for alkyl C–H borylation reactions,^{31,32} and it was of interest to extend the substrate scope of borylation reactions with this reagent to other simple alkanes (Table 6.9). Ethane was a poor substrate for C–H borylation reactions with B₂pnd₂, affording low yields of the borylated product with all three catalysts (entries 1–3). Hexane borylation proceeded in modest to good yields with B₂pnd₂ (entries 4–6). As is the case with B₂pin₂, the secondary C–H bonds are poorly reactive for C–H borylation with B₂pnd₂, with all catalysts affording low yields (entries 7–9). Overall, Rh catalyst **1** provides much lower yields for C–H borylation products with B₂pnd₂ compared to its reactivity with B₂pin₂ (see Table 6.4). Ru catalyst **3** provides comparable yields with the two different diboron reagents. These experiments suggest that the right combination of catalyst and diboron reagent is necessary to achieve high yields of the C–H borylated products.

Table 6.9. Borylation of Alkanes with Catalysts **1–3** and B₂pnd₂

entry	substrate	product	catalyst	% yield R-Bpnd ^c
1	ethane ^a		1	30
2	(C ₂ H ₆)		2	32
3			3	21
4	hexanes ^b		1	52
5	(C ₆ H ₁₄)		2	73
6			3	61
7	cyclohexane ^b		1	2
8	(c-C ₆ H ₁₂)		2	8
9			3	5

^aConditions: B₂pnd₂ (0.89 mmol, 1.00 equiv), catalyst (3.0 mol % with respect to metal), and CyH (7.0 mL) in a reactor well heated at 150 °C for 14 h. ^bConditions: B₂pnd₂ (0.166 mmol, 1.00 equiv), catalyst (3.0 mol % with respect to metal), and cyclohexane or hexanes (1.3 mL) in a Schlenk tube heated at 150 °C for 14 h. ^cYields of all product were determined by gas chromatography-flame ionization detector (GC-FID) and are based on B₂pnd₂ as the limiting reagent.

6.5. Conclusion

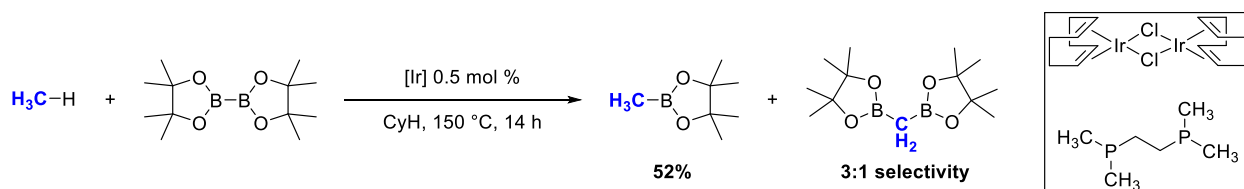
This chapter describes the development of a selective methane C–H borylation reaction. The selectivity was examined as a function of both transition metal catalyst and boron reagent. The applicability of this system to other alkanes (including ethane) was also examined. While this study supports the importance of the transition metal catalyst to induce selectivity, there is still much work to be done. A better understanding the role of both the metal center and associated ligands on the selectivity of such reactions is of high importance. Additionally, more studies into the selectivity imparted by the diboron reagent B₂pnd₂ are warranted, including the selectivity for methane versus ethane as well as the selectivity for methane versus CH₃Bpnd. Furthermore, a more systematic study of the effect of diboron reagent on the reaction could be undertaken. Examining diboron reagents with different sterics and electronics might elucidate more reactive species that can impart better selectivity.

6.6. Outlook

Concomitant with our report on methane C–H borylation, Mindiola and coworkers reported a similar system for methane C–H borylation.³³ They undertook a high-

throughput screen that identified Ir catalysts that were able to induce the methane C–H borylation reaction. Through computational analysis, Mindiola and coworkers identified phosphorus based ligands as ideal for the C–H borylation reaction (Scheme 6.6). Optimization of their conditions identified the iridium dimer $[(\text{COD})\text{Ir}(\mu\text{-Cl})]_2$ with 1,2-bis(dimethylphosphino)ethane (dmpe) as the catalyst system that provided the highest yield (52%) of the C–H borylated product. They report minimal solvent (cyclohexane) borylation but poor selectivity for monoborylation over diborylation (3:1).

Scheme 6.6. C–H Borylation of Methane Developed by Mindiola and Coworkers



6.7. Experimental Details

6.7.1. General Information

High-pressure reactors were initially pressurized using a Parr Model 5000 Multiple Reactor system or directly from the gas tank. In the cases where the Parr Model 5000 Multiple Reactor system was used, the system was operated via a 4871 process controller and SpecView version 2.5 software, and all pressures are reported from the SpecView interface at room temperature. In the cases where the gas was delivered directly from a gas tank, a gauge (0–1000 psi displayed, 0–69.0 bar) mounted on the reaction vessel was used. A description of the reaction vessels used is provided below. NMR spectra were recorded at room temperature (unless otherwise stated) on a Varian vnmrs 700 (699.76 MHz for ^1H) or a Varian MR400 (400.52 MHz for ^1H) NMR spectrometer with the residual solvent peak (CDCl_3 : ^1H : $\delta = 7.26$ ppm, C_6D_6 : ^1H : $\delta = 7.16$ ppm, DMSO-d_6 : ^1H : $\delta = 2.50$ ppm) as the internal reference unless otherwise noted. Chemical shifts are reported in parts per million (ppm, δ) relative to tetramethylsilane as an external reference at 0.00 ppm. Multiplicities are reported as follows: s (singlet), d (doublet), t (triplet), q (quartet), m (multiplet). Coupling constants (J) are reported in Hz. Gas chromatography was carried out on a Shimadzu 17A GC using a Restek Rxi®-5ms

(Crossbond® 5% diphenyl – 95% dimethyl polysiloxane; 60 m, 0.25 mm ID, 0.25 µm df) column. Yields and concentrations of product in crude reaction mixtures were determined by calibrated GC-FID analysis after the addition of an internal standard and subsequent dilution.

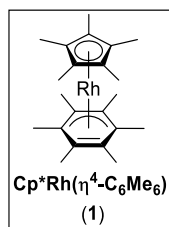
High pressure Raman data were collected using a Kaiser Optical Systems, Inc. RamanRxn1 system. *In situ* Raman analysis was performed with a NIR Immersion Sampling Optic Probe with a sapphire window and alloy C276 body (6 inch length and 0.25 inch diameter) attached to the MR Filtered Probe Head of the RamanRxn1 system. The laser source was a 400 mW Invictus operating at 785 nm. The high pressure experiments were performed in a 45 mL Parr cylinder containing a 0.3 inch center port hole with a 0.25 inch Swagelok fitting at the top. The probe was swaged into a 0.25 inch Swagelok fitting, which was then attached to the top center port hole of the reactor. Calibration was performed using cyclohexane as a wavelength standard and a white light correction for spectral intensity. Spectra were collected via the NIR Immersion Sampling Optic Probe with a range of 0–3450 cm⁻¹. Spectra were analyzed using ACD Spectrus Processor 2015 Pack 2 software.

6.7.2. Materials and Methods

All commercial reagents and solvents were used as received unless otherwise indicated. 1,5-cyclooctadiene (COD), 4,4,5,5-tetramethyl-1,3,2-dioxaborolane (HBpin; stored at –25 °C), hexamethylbenzene (C₆Me₆), hexamethyldisiloxane ((Me₃Si)₂O), 1,2,3,4,5- pentamethylcyclopentadiene (Cp*H), cyclohexane (c-C₆H₁₂; AcroSeal™), *n*-hexanes (C₆H₁₂; AcroSeal™), cyclopentane (c-C₅H₁₀), and 3,4,7,8-tetramethyl-1,10-phenanthroline (Me₄Phen) were purchased from Acros Organics. Perfluorohexane (PFH) was purchased from Apollo Scientific. 1*H*-Indene, mesitylene, *N*-methyl-2-pyrrolidone (NMP), and phosphorus pentoxide (P₂O₅) were purchased from Alfa Aesar. Methylboronic acid pinacol ester (CH₃Bpin) was purchased from Ark Pharm, Inc. CDCl₃, benzene-d₆, and dimethylsulfoxide-d₆ (DMSO-d₆) were purchased from Cambridge Isotope Laboratories. Dichloromethane (DCM), chlorobenzene (PhCl), 2-propanol (*i*-PrOH), ethyl acetate (EtOAc), acetone, and cyclohexane (c-C₆H₁₂; ACS grade) were purchased from Fisher Scientific. Methane (ultra-high purity), ethane (99.0%), and

nitrogen (pre-purified grade) were purchased from Metro Welding/Cryogenic Gases. Trifluoroacetic acid (TFA), perfluoro(methylcyclohexane) (PFMCH), bis(neopentyl glycolato)diboron (B_2neo_2), and bis(pinacolato) diboron (B_2pin_2) were purchased from Oakwood Products, Inc. $IrCl_3 \cdot XH_2O$ and $RuCl_3 \cdot 3H_2O$ were purchased from Pressure Chemical Company. Bis(catecholato)diboron (B_2cat_2) and bis(hexylene glycolato)diboron (B_2hg_2) were purchased from AK Scientific. *n*-Butyllithium (2.5 M in hexanes), cyclohexane- d_{12} , cyclopentadienyltris(acetonitrile)ruthenium(II) hexafluorophosphate ($(MeCN)_3RuCpPF_6$), bis(diethyl-D-tartrate glycolato)diboron (B_2dtg_2), and ammonium hexafluorophosphate (NH_4PF_6) were purchased from Sigma-Aldrich. $RhCl_3 \cdot XH_2O$, chloro(pentamethylcyclopentadienyl)bis(triphenylphosphine) ruthenium (II) ($Cp^*Ru(PPh_3)_2Cl$), bis(cyclopentadienyl)cobalt(II) (Cp_2Co), chloro(1,5-cyclooctadiene)(pentamethylcyclopentadienyl)ruthenium (II) ($Cp^*Ru(COD)Cl$), chloro(pentamethylcyclopentadienyl)ruthenium (II) tetramer ($[Cp^*RuCl]_4$), and dichlorobis(μ -methanethioato)bis(pentamethylcyclopentadienyl)diruthenium (II) ($[Cp^*Ru(SMe)]_2$) were purchased from Strem Chemicals, Inc. 2-Ethylboronic acid pinacol ester (CH_3CH_2Bpin), bis[(pinacolato)boryl]methane ($CH_2(Bpin)_2$), and 2,2,4,6,6-pentamethylheptane (PMH) were purchased from TCI America. Methanol (MeOH) was purchased from VWR International. Diethyl ether (Et_2O) and pentane were purchased from Fisher Scientific and either used as received (stabilized) or purified by an Innovative Technologies solvent purification system consisting of a copper catalyst, activated alumina, and molecular sieves (see details below for which was used). Tetrahydrofuran (THF) was purchased from VWR International and purified by an Innovative Technologies solvent purification system consisting of a copper catalyst, activated alumina, and molecular sieves.

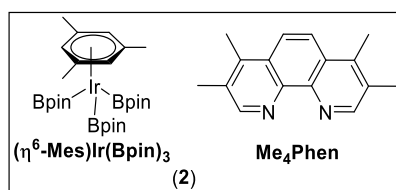
6.7.3. Catalyst Synthesis



$[\text{Cp}^*\text{RhCl}_2]_2$ was prepared according to a literature procedure,³⁴ and the ^1H NMR spectrum matched that of the commercial (Alfa Aesar) material.

$[\text{Cp}^*\text{Rh}(\eta^6\text{-C}_6\text{Me}_6)](\text{PF}_6)_2$ was prepared from $[\text{Cp}^*\text{RhCl}_2]_2$ according to a literature procedure, and the ^1H NMR spectrum matched that reported in the literature.³⁵

$[\text{Cp}^*\text{Rh}(\eta^4\text{-C}_6\text{Me}_6)]$ (**1**) was prepared from $[\text{Cp}^*\text{Rh}(\eta^6\text{-C}_6\text{Me}_6)](\text{PF}_6)_2$ according to a literature procedure,³⁶ and the ^1H NMR spectrum matched that reported in the literature.³⁷



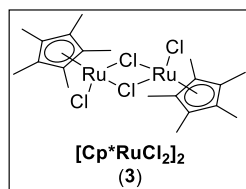
$[(\text{COD})\text{IrCl}]_2$ was synthesized according to a literature procedure,³⁸ and the ^1H NMR spectrum matched that reported in the literature.³⁹

Indenyl lithium was prepared by analogy to a literature procedure,⁴⁰ and the ^1H NMR spectrum matched that reported in the literature.⁴¹

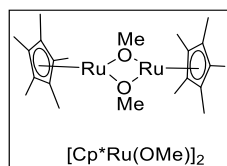
$(\text{COD})\text{Ir}(\text{Ind})$ was prepared from $[(\text{COD})\text{IrCl}]_2$ and indenyl lithium according to a literature procedure, and the ^1H NMR spectrum matched that reported in the literature.⁴²

$(\text{Mes})\text{Ir}(\text{Bpin})_3$ was prepared from $(\text{COD})\text{Ir}(\text{Ind})$ according to a literature procedure, and the ^1H NMR spectrum matched that reported in the literature.^{22c}

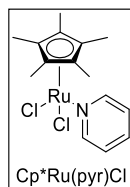
For C–H borylation reactions, catalyst **2** refers to the combination of $(\text{Mes})\text{Ir}(\text{Bpin})_3$ and Me_4phen which *in situ* forms the active catalyst.



$[(\text{Cp}^*)\text{RuCl}_2]_2$ (**3**) was prepared according to a literature procedure, with one key modification: the complex was washed with pentane (2 x 5 mL) in an N_2 -filled drybox rather than in air. The ^1H NMR spectrum matched that reported in the literature.⁴³



$[(\text{Cp}^*)\text{Ru}(\text{OMe})]_2$ was prepared from $[(\text{Cp}^*)\text{RuCl}_2]_2$ according to a literature procedure.⁴³

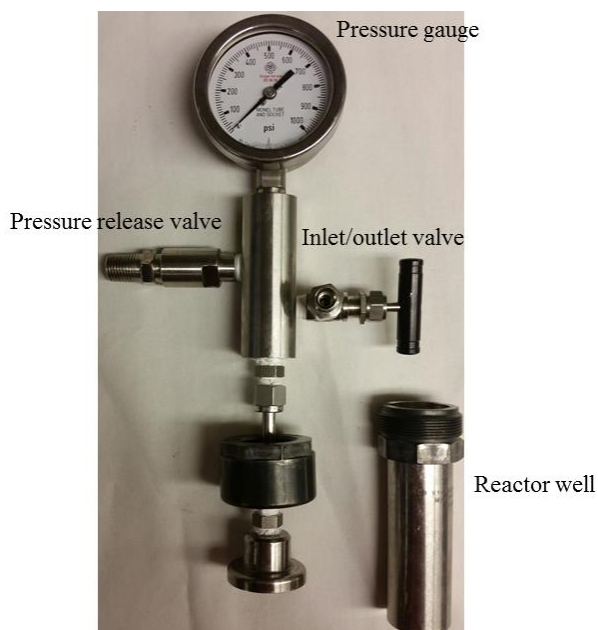


$\text{Cp}^*\text{Ru}(\text{pyr})\text{Cl}$ was prepared from $[(\text{Cp}^*)\text{RuCl}_2]_2$ according to a literature procedure.⁴⁴

6.7.4. Reactor Descriptions

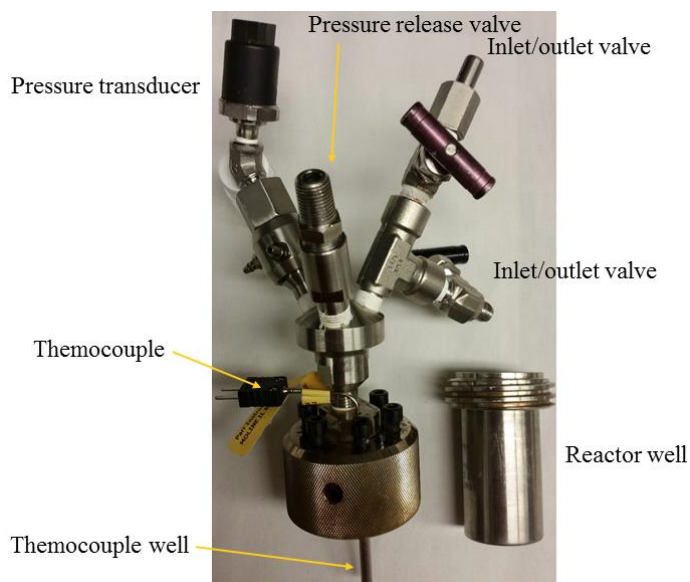
Four different types of reaction vessels were used. All are 45 mL (total volume) and are composed of a well (in which the solid and liquid reagents are charged) and a head, which contains various attachments as described below.

Image 6.1: Reactor A



Reactor A is made of Hastelloy C, and the well is 10 cm tall and has a diameter of 2.5 cm. Its head consists of a gauge (0–1000 psi displayed, 0–69.0 bar), an inlet/outlet valve for charging/discharging gases, and a safety release valve.

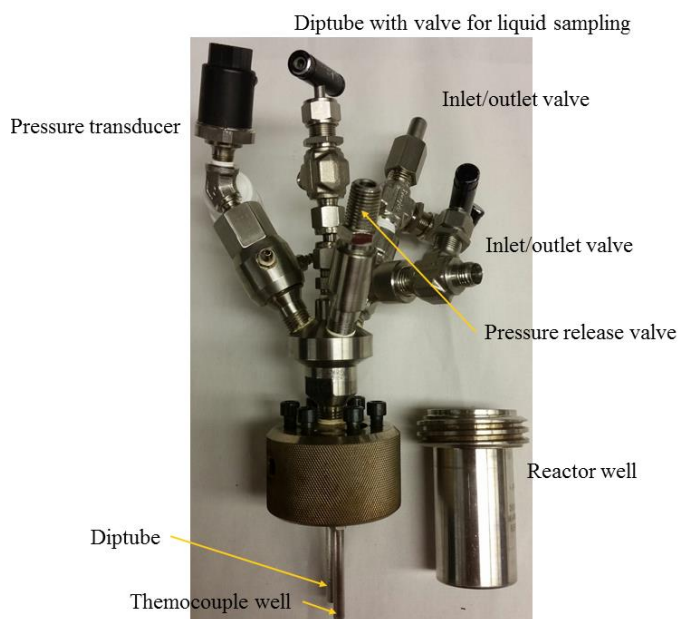
Image 6.2. Reactor B



Reactors of type B are either made of Hastelloy C or stainless steel, and the wells are 7.5 cm tall and 3 cm in diameter. The heads consist of a pressure transducer and two

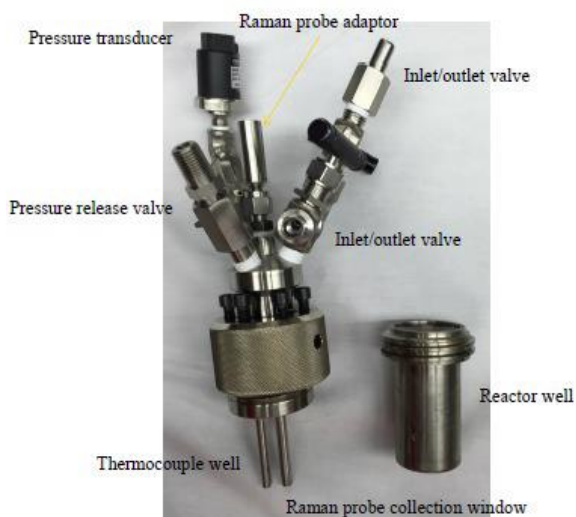
inlet/outlet valves that can connect to a Parr Model 5000 Multiple Reactor system described above, a safety release valve, and a well for a thermocouple.

Image 6.3. Reactor C



Reactor C (Hastelloy C) is identical to the type B reactors except that it has an additional attachment on the head. This attachment is a valve with a dip tube that is submerged into the well of the reactor. This attachment is used for *in situ* reaction sampling.

Image 6.4. Reactor D



Reactor D (Hastelloy C) is identical to the type B reactors except that it has an additional attachment on the head. This attachment is an adaptor for a Raman probe that is submerged into the well of the reactor. This attachment is used for *in situ* Raman spectroscopy.

6.7.5. General Procedures for C–H Borylation Reactions^E

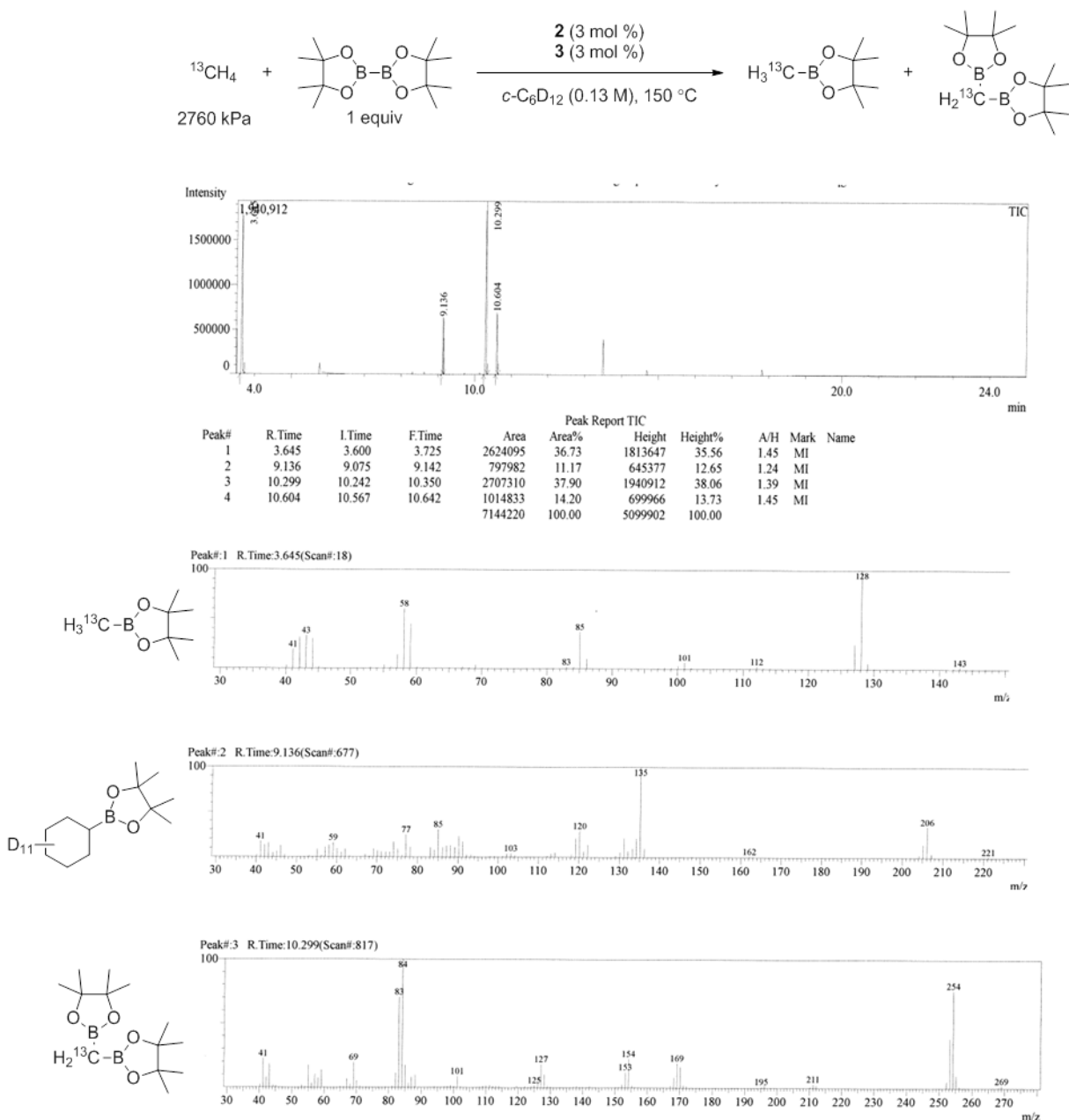
General Procedure for Methane Screening in Tables 6.1–6.3 and Table 6.6. In an N₂-filled drybox, B₂pin₂ (226.0 mg, 0.890 mmol, 1.00 equiv) and catalyst (3.0 mol % with respect to metal) were weighed into the well of the reactor (which also contained a magnetic stirbar). The solvent was measured by graduated cylinder and then added to the well of the reactor. The well was then taken outside of the drybox, and the head assembled. The headspace of the reactor was flushed 3 times with methane. To minimize the introduction of air into the reactor, the head was assembled and the reactor was flushed as quickly as possible (<2 min). The reactor was then pressurized to the desired pressure of methane. The reactor was then heated to the desired temperature in either a pre-heated oil bath or in a pre-heated aluminum heating block. To obtain the most reliable results, one reactor was set up at a time. After heating for 14 h, the reactors were flash-cooled in a liquid nitrogen bath for 5 min. The reactions were then thawed to room temperature over approximately 1 h. A standard (either PhCl or PMH) was added to the reactor well via a Hamilton gas-tight microliter syringe, and the reaction was diluted with 2 mL cyclohexane (ACS grade). An aliquot of the resulting reaction mixture was then removed and analyzed by GC-FID.

General Procedure for ¹³CH₄ Labelling Experiment in Figure 6.3. In an N₂-filled drybox, B₂Pin₂ (226.0 mg, 0.890 mmol, 1.00 equiv) and **2** (3.0 mol %) were weighed into the well of reactor C (which also contained a magnetic stirbar). *c*-C₆D₁₂ (7 mL) was measured by graduated cylinder and then added to the well of the reactor. The head was assembled, and the reactor was removed from the drybox. The reactor was pressurized to 27.6 bar of ¹³CH₄. The reactor was then heated to 150 °C in a preheated aluminum heating block.

^EReaction design and set up for screening reactions and time studies was determined by Dr. Amanda Cook.

After heating for 22 h, the reactor was flash-cooled in a liquid nitrogen bath for 5 min. The reaction was then thawed to room temperature over approximately 1 h. A standard (PhCl) was added to the reactor well via a Hamilton gastight microliter syringe, and the reaction was diluted with 2 mL cyclohexane (ACS grade). An aliquot of the resulting reaction mixture was then removed and analyzed by GCMS and NMR spectroscopy. Figure 6.7 shows the GCMS of the reaction mixture.

Figure 6.7. GCMS of $^{13}\text{CH}_4$ Labelling Experiment with Catalyst **2**



General Procedure for the C–H Borylation of Alkanes in Table 6.4. For borylation of ethane (performed by Dr. Amanda Cook): In an N₂-filled drybox, B₂pin₂ (226.0 mg, 0.890 mmol, 1.00 equiv) and catalyst (3.0 mol % with respect to metal) were weighed into the well of the reactor (which also contained a magnetic stirbar). c-C₆H₁₂ (7 mL, AcroSeal™) was measured by graduated cylinder and then added to the well of the reactor. The well was then removed from the drybox, and the head assembled. The headspace of the reactor was flushed 3 times with ethane. To minimize the introduction of air into the reactor, the head was assembled and the reactor was flushed as quickly as possible (<2 min). The reactor was then pressurized to 35.0 bar ethane. The reactor was heated to 150 °C in either a pre-heated oil bath or in a pre-heated aluminum heating block. To obtain the most reliable results, one reactor was set up at a time. After heating for 14 h, the reactors were flash-cooled in a liquid nitrogen bath for 5 min. The reactions were then thawed to room temperature over approximately 1 h. A standard (either PhCl or PMH) was added to the reactor well via a Hamilton gas-tight microliter syringe, and the reaction was diluted with 2 mL cyclohexane (ACS grade). An aliquot of the resulting reaction mixture was then removed and analyzed by GC-FID.

For borylation of *n*-hexane and cyclohexane: In an N₂-filled drybox, B₂pin₂ (42.3 mg, 0.166 mmol, 1.00 equiv) and catalyst (3.0 mol % with respect to metal) were combined in a Schlenk tube (equipped with a magnetic stirbar). Solvent (1.3 mL) was added and the tube was sealed and heated in a preheated oil bath at 150 °C for 14 h. After heating, the Schlenk tubes were flash-cooled in a liquid nitrogen bath for 5 min. The tubes were thawed to room temperature over approximately 1 h. PhCl as standard was added to the Schlenk tube via a Hamilton gas-tight microliter syringe, and the reaction was diluted with 2 mL solvent. An aliquot of the resulting reaction mixture was then removed and analyzed by GC-FID.

For borylation of CH₃Bpin: In an N₂-filled drybox, B₂pin₂ (42.3 mg, 0.166 mmol, 1.00 equiv), CH₃Bpin (23.6 mg, 0.166 mmol, 1.00 equiv), and catalyst (3.0 mol % with respect to metal) were combined in a Schlenk tube (equipped with a magnetic stirbar). Solvent (1.3 mL) was added and the tube was sealed and heated at 150 °C for 14 h. After heating for 14 h, the Schlenk tubes were flash-cooled in a liquid nitrogen bath for 5 min. The tubes

were thawed to room temperature over approximately 1 h. PhCl as standard was added to the Schlenk tube via a Hamilton gas-tight microliter syringe, and the reaction was diluted with 2 mL solvent. An aliquot of the resulting reaction mixture was then removed and analyzed by GC-FID.

General Procedure for the Methane/Ethane Competition Studies in Table 6.5. In an N₂-filled drybox, B₂pin₂ (226.0 mg, 0.890 mmol, 1.00 equiv) and catalyst (3.0 mol % with respect to metal) were weighed into the well of reactor A (which was equipped with a magnetic stirbar). Cyclohexane (7 mL, AcroSeal™) was measured by graduated cylinder and then added to the well of the reactor. The well was then taken outside of the drybox, and the head assembled. The weight of the whole apparatus was tared on a balance. The headspace of the reactor was flushed 3 times with ethane. To minimize the introduction of air into the reactor, the head was assembled and the reactor was tared and flushed as quickly as possible (<3 min). The reactor was then pressurized to ~14.0 bar of ethane, and the weight was recorded. The reactor was then pressurized with methane to a total of ~35.0 bar, and the weight was recorded. The reactor was heated to 150 °C in either a pre-heated oil bath with stirring. After heating for the desired reaction time, the reactors were cooled to room temperature over approximately 3 h. The internal standard, PMH, was added via a Hamilton gas-tight microliter syringe, and the reaction was diluted with 2 mL cyclohexane (ACS grade). An aliquot of the reaction mixture was then removed and analyzed by GC-FID. Results of these competition studies are seen in Table 6.10, and the formula used to calculate the selectivity is given below. Importantly, the yield of CH₂Bpin₂ was less than 4% in all these reactions with all catalysts. Yields in Table 6.5 represent an average of three experiments (Table 6.10) and were performed with Dr. Amanda Cook (one set of experiments) and Sydonie Schimler (reactions run in duplicate).

Table 6.10. Amounts of Methane and Ethane Added and Results of the Competition Reactions.

Entry	Cat.	Mass/mmol added		$[\text{CH}_3\text{CH}_3]/[\text{CH}_4]$	Yield		Selectivity $\text{CH}_4:\text{CH}_3\text{CH}_3$
		CH_4	CH_3CH_3		CH_3Bpin	$\text{CH}_3\text{CH}_2\text{Bpin}$	
1	2	0.90 g/ 56 mmol	1.25 g/ 42 mmol	2.4	33%	30%	4.0 : 1
	2	0.65 g/ 41 mmol	1.65 g/ 55 mmol	4.5	15%	26%	3.9 : 1
	2	0.65 g/ 41 mmol	1.60 g/ 53 mmol	4.4	7%	10%	4.6 : 1
Average=							4.2 ± 0.4 : 1
2	1	0.75 g/ 47 mmol	1.45 g/ 48 mmol	3.4	52%	46%	5.8 : 1
	1	0.70 g/ 44 mmol	1.40 g/ 47 mmol	3.5	43%	34%	6.6 : 1
	1	0.65 g/ 41 mmol	1.40 g/ 47 mmol	3.8	43%	42%	5.8 : 1
Average=							6.1 ± 0.5 : 1
3	3	0.60 g/ 37 mmol	1.40 g/ 47 mmol	4.1	18%	28%	3.9 : 1
	3	0.60 g/ 37 mmol	1.55 g/ 52 mmol	4.6	14%	27%	3.6 : 1
	3	0.70 g/ 44 mmol	1.60 g/ 53 mmol	4.1	16%	30%	3.3 : 1
Average=							3.6 ± 0.3

*See Table 6.11 for $[\text{CH}_3\text{CH}_3]/[\text{CH}_4]$ determination.

Formula for calculating selectivity in methane/ethane competition:

$$\text{Selectivity} = \left(\frac{\text{Yield } \text{CH}_3\text{Bpin}}{\text{Yield } \text{CH}_3\text{CH}_2\text{Bpin}} \right) \left(\frac{6 \text{ CH Bonds } \text{CH}_3\text{CH}_3}{4 \text{ CH Bonds } \text{CH}_4} \right) \left(\frac{[\text{CH}_3\text{CH}_3]}{[\text{CH}_4]} \right)$$

General Procedure for the Initial Rate Studies in Figure 6.4. In an N_2 -filled drybox, B_2pin_2 (42.3 mg, 0.166 mmol, 1.00 equiv) and catalyst (3.0 mol % with respect to metal) were combined in a Schlenk tube (equipped with a magnetic stirbar). Cyclohexane (1.3 mL) was added and the tube was sealed and heated in a preheated oil bath at 150 °C for the designated time. After heating, the Schlenk tubes were flash-cooled in a liquid nitrogen bath for 5 min. The tubes were thawed to room temperature over approximately 1 h. PhCl as standard was added to the Schlenk tube via a Hamilton gas-tight microliter syringe, and the reaction was diluted with 2 mL solvent. An aliquot of the resulting reaction mixture was then removed and analyzed by GC-FID.

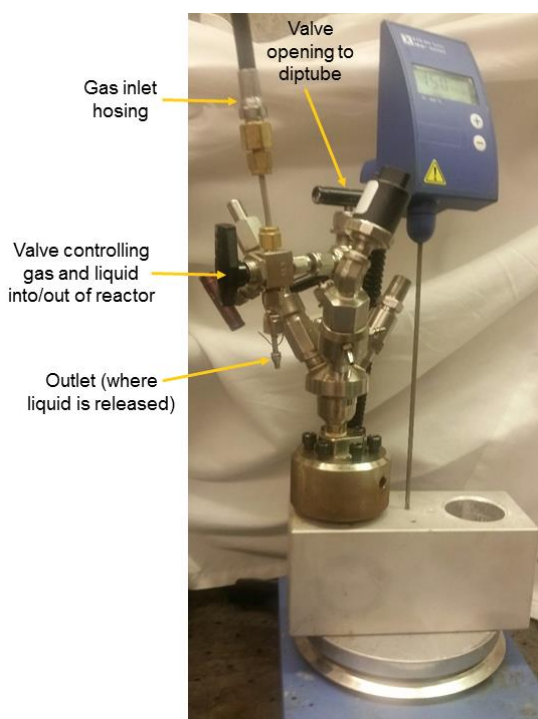
General Procedure for the Initial Rate Studies in Figure 6.5. In an N₂-filled drybox, B₂pin₂ (42.3 mg, 0.166 mmol, 1.00 equiv), CH₃Bpin (23.6 mg, 0.166 mmol, 1.00 equiv), and catalyst (3.0 mol % with respect to metal) were combined in a Schlenk tube (equipped with a magnetic stirbar). Cyclohexane (1.3 mL) was added and the tube was sealed and heated at 150 °C for the designated time. After heating, the Schlenk tubes were flash-cooled in a liquid nitrogen bath for 5 min. The tubes were thawed to room temperature over approximately 1 h. PhCl as standard was added to the Schlenk tube via a Hamilton gas-tight microliter syringe, and the reaction was diluted with 2 mL solvent. An aliquot of the resulting reaction mixture was then removed and analyzed by GC-FID.

General Procedure for the Boron Screens for C–H Borylation of Methane in Tables 6.7 and 6.8. In an N₂-filled drybox, boron reagent (0.890 mmol, 1.00 equiv) and catalyst (3.0 mol % with respect to metal) were weighed into the well of the reactor (which also contained a magnetic stirbar). Cyclohexane was measured by graduated cylinder and then added to the well of the reactor. The well was then taken outside of the drybox, and the head assembled. The headspace of the reactor was flushed 3 times with methane. To minimize the introduction of air into the reactor, the head was assembled and the reactor was flushed as quickly as possible (<2 min). The reactor was then pressurized to 35.0 bar of methane. The reactor was then heated to 150 °C in either a pre-heated oil bath or in a pre-heated aluminum heating block. To obtain the most reliable results, one reactor was set up at a time. After heating for 14 h, the reactors were flash-cooled in a liquid nitrogen bath for 5 min. The reactions were then thawed to room temperature over approximately 1 h. PhCl as a standard was added to the reactor well via a Hamilton gas-tight microliter syringe, and the reaction was diluted with 2 mL cyclohexane (ACS grade). An aliquot of the resulting reaction mixture was then removed and analyzed by GC-FID.

General Procedure for the Time Studies in Figure 6.6. In an N₂-filled drybox, diboron reagent (2.67 mmol, 1.00 equiv) and catalyst **3** (1.5 mol %) were weighed into the well of reactor C, which was equipped with a magnetic stirbar. PMH was used as the internal standard, and it was weighed into a vial and then transferred to the reaction well using the reaction solvent, cyclohexane, as the transfer medium. Additional cyclohexane (to get

to a 21 mL total volume, AcroSeal™) was then added to the well of the reactor. The well was then removed from the drybox, and the head assembled. The headspace of reactor C was then flushed 3 times with methane, and then the reactor was pressurized to 28.0 bar or methane. The reactor was then heated to 150 °C in a pre-heated aluminum heating block. Aliquots of ~0.5 mL were removed via the liquid sampling fitting, diluted to 1.5 mL with cyclohexane (ACS grade), and analyzed by GC-FID. Notably, the pressure dropped by ~3.0 bar every time an aliquot was removed; to counteract this, the reactor was immediately re-pressurized to the pressure it reaches at 150 °C (35.0 bar) after each aliquot was taken (Image 5). This re-pressurization procedure resulted in more reproducible data.

Image 6.5. Set Up for Reaction Monitoring.



General Procedure for the Borylation of Alkanes in Table 6.9. For borylation of ethane: In an N₂-filled drybox, B₂pnd₂ (0.890 mmol, 1.00 equiv) and catalyst (3.0 mol % with respect to metal) were weighed into the well of the reactor (which also contained a magnetic stirbar). c-C₆H₁₂ (7 mL, AcroSeal™) was measured by graduated cylinder and then added to the well of the reactor. The well was then removed from the drybox, and the head

assembled. The headspace of the reactor was flushed 3 times with ethane. To minimize the introduction of air into the reactor, the head was assembled and the reactor was flushed as quickly as possible (<2 min). The reactor was then pressurized to 35.0 bar ethane. The reactor was heated to 150 °C in either a pre-heated oil bath or in a pre-heated aluminum heating block. To obtain the most reliable results, one reactor was set up at a time. After heating for 14 h, the reactors were flash-cooled in a liquid nitrogen bath for 5 min. The reactions were then thawed to room temperature over approximately 1 h. PhCl as a standard was added to the reactor well via a Hamilton gas-tight microliter syringe, and the reaction was diluted with 2 mL cyclohexane (ACS grade). An aliquot of the resulting reaction mixture was then removed and analyzed by GC-FID.

For borylation of *n*-hexane and cyclohexane: In an N₂-filled drybox, B₂pnd₂ (0.166 mmol, 1.00 equiv) and catalyst (3.0 mol % with respect to metal) were combined in a Schlenk tube (equipped with a magnetic stirbar). Solvent (1.3 mL) was added and the tube was sealed and heated in a preheated oil bath at 150 °C for 14 h. After heating, the Schlenk tubes were flash-cooled in a liquid nitrogen bath for 5 min. The tubes were thawed to room temperature over approximately 1 h. PhCl as standard was added to the Schlenk tube via a Hamilton gas-tight microliter syringe, and the reaction was diluted with 2 mL solvent. An aliquot of the resulting reaction mixture was then removed and analyzed by GC-FID.

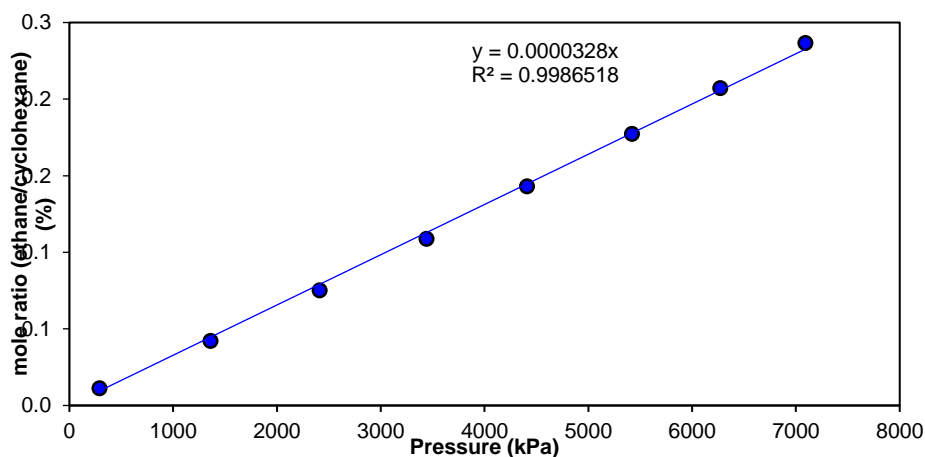
6.7.6. Determining Concentration of Methane and Ethane^F

Procedure for Determining Concentration of Methane in Cyclohexane. In an N₂-filled drybox, *c*-C₆D₁₂ (20 mL) was measured by graduated cylinder and then added to the well of reactor D (which also contained a magnetic stirbar). The head was assembled, and the reactor was removed from the drybox. The reactor was then pressurized to 78.6 bar of methane at room temperature. The Raman probe was attached via the adaptor. A dark spectrum was acquired at the onset. Raman spectra were collected for 40 exposures over a period of 30 min with collections every 3 min, at which time the concentration of methane (peak at 2905 cm⁻¹) had equilibrated. The pressure was then dropped by ~10.0 bar, and

^F Collection of Raman data was done with help from Danielle Samblanet. Calculations for the concentration of methane and ethane were performed by Professor Adam Matzger.

this process was repeated until the pressure was ~ 0.1 bar. The data were truncated to include the region between $1900\text{--}3200\text{ cm}^{-1}$. Baseline correction was applied between endpoints, and peak intensities were determined by peak picking for a reference $c\text{-C}_6\text{D}_{12}$ peak at $\sim 2105\text{ cm}^{-1}$ (search window 2100 to 2110 cm^{-1}) and for the most prominent methane peak at $\sim 2905\text{ cm}^{-1}$ (search window 2900 to 2910 cm^{-1}). The relative Raman intensities of these peaks represent the mole ratio between $c\text{-C}_6\text{D}_{12}$ and methane convoluted with the relative scattering efficiency of the two components. The relative scattering efficiency was determined by comparison to the measured solubility of methane in cyclohexane at 298 K and 1 atm ⁴⁵ which is reported as 0.00327 mole fraction (0.003281 mole ratio of methane to cyclohexane). The concentration dependence of methane in cyclohexane adheres to Henry's Law in the pressure regime tested, and therefore a linear fit to the data was employed with a zero intercept (Figure 6.8).

Figure 6.8. Mole Ratio versus Pressure at 298 K for Methane in Cyclohexane

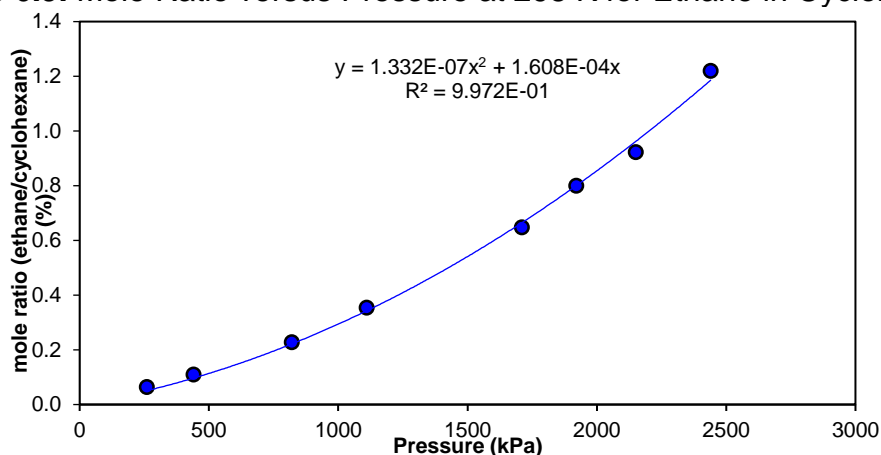


To determine the concentration of methane in $c\text{-C}_6\text{D}_{12}$ under the standard reaction conditions (35.0 bar gauge pressure at room temperature; then heated to $150\text{ }^\circ\text{C}$), a similar procedure was followed with the following modifications: reactor D was initially pressurized to a gauge pressure of 35.0 bar (actual pressure = 36.0 bar). The reactor was then heated to $150\text{ }^\circ\text{C}$ in a pre-heated aluminum heating block with stirring. Raman spectra were collected as above. The relative Raman scattering efficiency of $c\text{-C}_6\text{D}_{12}$ and methane determined above were applied to determine the mole ratio of methane:cyclohexane at $150\text{ }^\circ\text{C}$ when the pressure is allowed to rise autogenously from

a starting pressure of 36.0 bar. This mole ratio was converted to a concentration by assuming that scattering efficiency is not strongly temperature dependent. The concentration was determined to be 1.1 M. This concentration is based on the approximation that minimal volatilization of cyclohexane occurs under the reaction conditions. As such, this value is expected to slightly overestimate the relative ratio of methane compared to that of CH₃BPi during the reaction.

Procedure for Determining the Concentration of Ethane in Cyclohexane. To determine the concentration of ethane, a similar procedure was followed with the following modifications: reactor D was initially pressurized to 23.4 bar and Raman spectra were collected for 40 exposures over a period of 4 h with collections every 10 min, at which time the concentration of ethane (peak at 2942 cm⁻¹) had equilibrated. The pressure was then dropped by ~0.5 bar, and this process was repeated until the pressure was ~0.1 bar. Strong deviation from Henry's Law in the pressure regime tested necessitated measuring an experimental solubility point for ethane at pressures close to those employed in the catalysis experiments. This was carried out in reactor A. First the volume of the reactor was determined as follows: pressurizing the reactor to 13.93 bar led to a mass of ethane charged of 0.97 g. At this pressure, the density of ethane gas is 0.019038 g/mL.^{46,47} This leads to a volume for reactor A of 51.0 mL. The pressurization procedure was then repeated with 5.20 g of cyclohexane present, and a pressure of 16.13 bar was established after equilibration. The mass of the added ethane was determined to be 2.10 g. Subtracting the headspace contribution from the ethane present (51.0 mL reactor volume – 6.67 mL solvent volume) accounts for 1.00 g of ethane. Therefore, 1.10 g of ethane is dissolved, leading to a mole ratio of 0.592 ethane:cyclohexane under these conditions. Applying this solubility to the Raman data (to account for the difference in scattering efficiency of ethane and cyclohexane) yields the following solubility data in Figure 6.10. The data were fit to a second order polynomial with a forced zero intercept. The equation predicts a room temperature, 0.1 bar mole ratio of ethane to cyclohexane of 0.0174, which is in good agreement with a previous report.¹⁸

Figure 6.9. Mole Ratio versus Pressure at 298 K for Ethane in Cyclohexane



Mole Ratio of Methane and Ethane. The mole ratio of methane and ethane under conditions relevant to ethane/methane competition reactions were next measured. In an N_2 -filled drybox, $c\text{-C}_6\text{D}_{12}$ (7 mL) was measured by graduated cylinder and then added to the well of reactor D (which also contained a magnetic stirbar and a glass cylinder to displace solvent volume toward the Raman probe). The head was assembled, and the reactor was removed from the drybox. The reactor was initially pressurized to 15.7 bar (gauge pressure). Prior to pressurization with methane, the pressure had dropped to 0.99 bar due to ethane dissolving in $c\text{-C}_6\text{D}_{12}$. The reactor was then pressurized to 35.9 bar (gauge pressure) with methane. The reactor was heated in a pre-heated aluminum heating block to 150 °C, with stirring and Raman spectra were collected for 40 exposures over a period of 4 h with collections every 10 min, at which time the ethane (peak at 2942 cm^{-1}) and methane (peak at 2905 cm^{-1}) had equilibrated. Under these conditions, the ethane:methane: mole ratio was 3.18 at room temperature and decreased to 2.14 at elevated temperature. The change in solubility for methane was minor between room temperature and 150 °C⁴⁸ whereas the solubility of ethane decreases substantially. With the solubility behavior for methane and ethane elucidated under the reaction conditions, equations were solved for the partitioning of each gas into the liquid and headspace of reactor D. The partial pressure of each gas was determined from the weight of the added gas, the solubility of each gas as a function of pressure at room temperature, and the previously reported gas phase densities of ethane and methane.⁴⁹ The room temperature ratios of concentration in solution were scaled by a constant factor derived from the

change in the relative concentrations with heating to 150 °C and are reported in Table 6.10 and 6.11.

Table 6.11. Results from Determining the Methane:Ethane Concentration Ratio under the Conditions Reported in Table 6.10.

Entry	Cat.	Mass added		Mass Ratio CH ₃ CH ₃ /CH ₄	[CH ₃ CH ₃]/ [CH ₄] (298 K)	[CH ₃ CH ₃]/ [CH ₄] (423 K)*
		CH ₄	CH ₃ CH ₃			
1	2	0.90 g	1.25 g	1.4	3.6	2.4
	2	0.65 g	1.65 g	2.5	6.8	4.5
	2	0.65 g	1.60 g	2.5	6.6	4.4
2	1	0.75 g	1.45 g	1.9	5.1	3.4
	1	0.70 g	1.40 g	2.0	5.3	3.5
	1	0.65 g	1.40 g	2.2	5.6	3.8
3	3	0.60 g	1.40 g	2.3	6.1	4.1
	3	0.60 g	1.55 g	2.6	6.8	4.6
	3	0.70 g	1.60 g	2.3	6.1	4.1

* Extrapolated from 298 K

6.8. References

- (1) A portion of this chapter has been adapted with permission from Cook, A. K.; Schimler, S. D.; Matzger, A. J.; Sanford, M. S. *Science* **2016**, 351, 1421–1424. ©American Association for the Advancement of Science
- (2) Hartwig, J. F. *J. Am. Chem. Soc.* **2016**, 138, 2–24.
- (3) For examples of the following see: Dehydrogenation: Choi, J.; MacArthur, A. H. R.; Brookhart, M.; Goldman, A. S. *Chem. Rev.* **2011**, 111, 1761–1779; Oxygenation: Shilov, A. E.; Shul'pin, G. B. *Chem. Rev.* **1997**, 97, 2879–2932; Carbonylation: Sakakura, T.; Sodeyama, T.; Sasaki, K.; Wada, K.; Tanaka, M. *J. Am. Chem. Soc.* **1990**, 112, 7221–7229; C-, N-, or O-atom insertion: Mansuy, D. *Coord. Chem. Rev.* **1993**, 125, 129–141.
- (4) (a) Gunsalus, N. J.; Konnick, M. M.; Hashiguchi, B. G.; Periana, R. A. *Isr. J. Chem.* **2014**, 54, 1467–1480. (b) Cavaliere, V. N.; Mindiola, D. J. *Chem. Sci.* **2012**, 3, 3356–3365.
- (5) Blanksby, S. J.; Ellison, G. B. *Acc. Chem. Res.* **2003**, 36, 255–263.
- (6) Caballero, A.; Pérez, P. J. *Chem. Soc. Rev.* **2013**, 42, 8809–8820.
- (7) Stahl, S. S.; Labinger, J. A.; Bercaw, J. E. *Angew. Chem. Int. Ed.* **1998**, 37, 2180–2197.
- (8) Periana, R. A.; Taube, D. J.; Gamble, S.; Taube, H.; Satoh, T.; Fujii, H. *Science* **1998**, 280, 560–564.
- (9) Ahlquist, M.; Niesen, R. J.; Periana, R. A.; Goddard, W. A. *J. Am. Chem. Soc.* **2009**, 131, 17110–17115.
- (10) Caballero, A.; Despagnet-Ayoub, E.; Díaz-Requejo, M. M.; Díaz-Rodríguez, A.; González-Núñez, M. E.; Mello, R.; Muñoz, B. K.; Ojo, W.-S.; Asensio, G.; Etienne, M.; Pérez, P. J. *Science* **2011**, 332, 835–838.

- (11) (a) Waltz, K. M.; Hartwig, J. F. *Science* **1997**, *277*, 211–213. (b) Hartwig, J. F. *Chem. Soc. Rev.* **2011**, *40*, 1992–2002. (c) Hartwig, J. F. *Acc. Chem. Res.* **2012**, *45*, 864–873. (d) Mkhaliid, I. A. I.; Barnard, J. H.; Marder, T. B.; Murphy, J. M.; Hartwig, J. F. *Chem. Rev.* **2010**, *110*, 890–931. (e) Ishiyama, T.; Miyaura, N. *J. Organomet. Chem.* **2003**, *680*, 3–11.
- (12) Chen, H.; Schlecht, S.; Semple, T. C.; Hartwig, J. F. *Science* **2000**, *287*, 1995–1997.
- (13) Wei, C. S.; Jiménez-Hoyos, C. A.; Videa, M. F.; Hartwig, J. F.; Hall, M. D. *J. Am. Chem. Soc.* **2010**, *132*, 3078–3091.
- (14) Shimada, S.; Batsanov, A. S.; Howard, J. A. K.; Marder, T. B. *Angew. Chem. Int. Ed.* **2001**, *40*, 2168–2171.
- (15) Larsen, M. A.; Wilson, C. V.; Hartwig, J. F. *J. Am. Chem. Soc.* **2015**, *137*, 8633–8643.
- (16) (a) Tajuddin, H.; Harrisson, P.; Bitterlich, B.; Collings, J. C.; Sim, N.; Batsanov, A. S.; Cheung, M. S.; Kawamorita, S.; Maxwell, A. C.; Shukla, L.; Morris, J.; Lin, Z.; Marder, T. B.; Steel, P. G. *Chem. Sci.* **2012**, *3*, 3505–3515. (b) Vanchura, B. A.; Preshlock, S. M.; Roosen, P. C.; Kallepalli, V. A.; Staples, R. J.; Maleczka, R. E.; Singleton, D. A.; Smith, M. R. *Chem. Commun.* **2010**, *46*, 7724–7726.
- (17) Hartwig, J. F.; Cook, K. S.; Hapke, M.; Incarvito, C. D.; Fan, Y.; Webster, C. E.; Hall, M. B. *J. Am. Chem. Soc.* **2005**, *127*, 2538–2552.
- (18) Wilhelm, E.; Battino, R. *Chem. Rev.* **1973**, *73*, 1–9.
- (19) Liskey, C. W.; Hartwig, J. F. *J. Am. Chem. Soc.* **2012**, *134*, 12422–12425.
- (20) Preshlock, S. M.; Ghaffari, B.; Maligres, P. E.; Krska, S. W.; Maleczka, R. E.; Smith, M. R. *J. Am. Chem. Soc.* **2013**, *135*, 7572–7582.
- (21) Murphy, J. M.; Lawrence, J. D.; Kawamura, K.; Incarvito, C.; Hartwig, J. F. *J. Am. Chem. Soc.* **2006**, *128*, 13684–13685.
- (22) (a) Li, Q.; Liskey, C. W.; Hartwig, J. F. *J. Am. Chem. Soc.* **2014**, *136*, 8755–8765. (b) Boller, T. M.; Murphy, J. M.; Hapke, M.; Ishiyama, T.; Miyaura, N.; Hartwig, J. F. *J. Am. Chem. Soc.* **2005**, *127*, 14263–14278. (c) Chotana, G. A.; Vanchura, B. A.; Tse, M. K.; Staples, R. J.; Maleczka, R. E.; Smith, M. R. *Chem. Commun.* **2009**, 5731–5733.
- (23) Ghaffari, B.; Vanchura, B. A.; Chotana, G. A.; Staples, R. J.; Holmes, D.; Maleczka, R. E.; Smith, M. R. *Organometallics* **2015**, *34*, 4732–4740.
- (24) (a) Lin, M.; Hogan, T. E.; Sen, A. *J. Am. Chem. Soc.* **1996**, *118*, 4574–4580. (b) Demoulin, O.; Le Clef, B.; Navez, M.; Ruiz, P. *Appl. Catal. A Gen.* **2008**, *344*, 1–9. (c) Graf, P. O.; Mojet, B. L.; Lefferts, L. *Appl. Catal. A Gen.* **2008**, *346*, 90–95.
- (25) There are few examples of ruthenium-catalyzed C–H borylation reactions, see: ref 21 and (a) Fernández-Salas, J. A.; Manzini, S.; Piola, L.; Slawin, A. M. Z.; Nolan, S. P. *Chem. Commun.* **2014**, *50*, 6782–6784. (b) Okada, S.; Namikoshi, T.; Watanabe, S.; Murata, M. *ChemCatChem* **2015**, *7*, 1531–1534.
- (26) Liskey, C. W.; Hartwig, J. F. *Synthesis* **2013**, *45*, 1837–1842.
- (27) Murai, M.; Omura, T.; Kuninobu, Y.; Takai, K. *Chem. Commun.* **2015**, *51*, 4583–4586.
- (28) For computational analysis of B–B and B–H bond strength, see: Rablen, P. R.; Hartwig, J. F. *J. Am. Chem. Soc.* **1996**, *118*, 4648–4653.

- (29) For examples of the use of H₂ acceptors in C–H silylation reactions, see: (a) Simmons, E. M.; Hartwig, J. F. *J. Am. Chem. Soc.* **2010**, *132*, 17092–17095. (b) Li, Q.; Driess, M.; Hartwig, J. F. *Angew. Chem. Int. Ed.* **2014**, *53*, 8471–8474.
- (30) Clegg, W.; Scott, A. J.; Dai, C.; Lesley, G.; Marder, T. B.; Norman, N. C.; Farrugia, L. *Acta Crystallogr. Sect. C* **1996**, *52*, 2545–2547.
- (31) Szabó, K. J.; Olsson, V. J. *J. Org. Chem.* **2009**, *74*, 7715–7723.
- (32) For other examples of the use of B₂pnd₂, see: (a) Kurahashi, T.; Hata, T.; Masai, H.; Kitagawa, H.; Shimizu, M.; Hiyama, T. *Tetrahedron* **2002**, *58*, 6381–6395. (b) Ramachandran, P. V.; Pratihari, D.; Biswas, D.; Srivastava, A.; Reddy, M. V. R. *Org. Lett.* **2004**, *6*, 481–484.
- (33) Smith, K. T.; Berritt, S.; González-Moreiras, M.; Ahn, S.; Smith, M. R.; Baik, M.-H.; Mindiola, D. J. *Science* **2016**, *351*, 1424–1427.
- (34) White, C.; Yates, A.; Maitlis, P. M.; Heinekey, D. M. *Inorganic Synthesis*. John Wiley and Sons, **2007**, pp. 228–234.
- (35) Rybinskaya, M. I.; Kudinov, A. R.; Kaganovich, V. S. *J. Organomet. Chem.* **1983**, *246*, 279–285.
- (36) Bowyer, W. J.; Merkert, J. W.; Geiger, W. E.; Rheingold, A. L. *Organometallics* **1989**, *8*, 191–198.
- (37) Bowyer, W. J.; Geiger, W. E. *J. Am. Chem. Soc.* **1985**, *107*, 5657–5663.
- (38) Choudhury, J.; Podder, S.; Roy, S. *J. Am. Chem. Soc.* **2005**, *127*, 6162–6163.
- (39) Grobbelaar, E.; Purcell, W.; Basson, S. S. *Inorg. Chim. Acta* **2006**, *359*, 3800–3806.
- (40) Wang, H.; Wang, H.; Li, H.-W.; Xie, Z. *Organometallics* **2004**, *23*, 875–885.
- (41) Tay, B.-Y.; Wang, C.; Stubbs, L. P.; Jacob, C.; van Meurs, M. *J. Organomet. Chem.* **2011**, *696*, 3431–3435.
- (42) Merola, J. S.; Kacmarcik, R. T. *Organometallics* **1989**, *8*, 778–784.
- (43) Koelle, U.; Kossakowski, J.; Grumbine, D.; Tilley, T. D. *Inorg. Synth.* **1992**, *29*, 225–228.
- (44) Koelle, U.; Kossakowski, J. *J. Organomet. Chem.* **1989**, *362*, 383–398.
- (45) Widegren, J. A.; Finke, R. G. *J. Mol. Catal. Chem.* **2003**, *198*, 317–341.
- (46) Friend, D. G.; Ingham, H.; Fly, J. F. *J. Phys. Chem. Ref. Data* **1991**, *20*, 275–347.
- (47) Equation of state was derived from ref 44 as implemented in the National Institute of Standards and Technology (NIST) Webbook fluid properties calculator: <http://webbook.nist.gov/cgi/cbook.cgi?ID=74-84-0>.
- (48) Similar observations of methane in propylene carbonate are available in: Jou, F.-Y.; Mather, A. E.; Schmidt, K. A. G. *J. Chem. Eng. Data* **2015**, *60*, 1010–1013.
- (49) Lemmon, E. W.; McLinden, M. O.; Friend, D. G. Thermophysical Properties of Fluid Systems in *NIST Chemistry WebBook, NIST Standard Reference Database Number 69*, Linstrom, P. J.; Mallard, W. G., Eds. (National Institute of Standards and Technology, 2016); <http://webbook.nist.gov>, (retrieved February 4, 2016).